



**University of
Nottingham**

UK | CHINA | MALAYSIA

**Organic geochemical controls on the
dermal absorption of polycyclic aromatic
hydrocarbons from manufactured
gasworks soils**

By Alison Williams-Clayson, MChem (with Honours)

Thesis submitted to the University of Nottingham
for the degree of Doctor of Philosophy

November 2023

Abstract

Brownfield sites, such as former manufactured gas plants (MGPs), hold potential for urban redevelopment. However, the soils in these areas are often contaminated with a variety of organic pollutants. Among these, polycyclic aromatic hydrocarbons (PAHs) are persistently found as mixtures in soil, with several PAHs being recognized as potentially carcinogenic. Human health risk assessments (HHRAs) establish estimates on the risks posed from individual PAHs, including the potential dermal bioavailability. However, the dermal bioavailability values of PAHs currently applied in HHRAs are based on a single study that does not comprehensively represent the complexities of PAH-soil interactions. The study's singular PAH spiking approach within a single soil type failed to account for the heterogeneous interplay between diverse PAHs, soil properties and environmental factors. Consequently, this previous study potentially overestimated the PAH availability in soil and creates uncertainty in any calculated dermal bioavailability. There is a shortage of research investigating the dermal bioavailability of a large diversity of PAHs from different soil types in real-world contaminated soils (not spiked), including no knowledge of the dermal absorption behaviour of alkylated PAHs (alkyl-PAHs) and a lack of research into the organic matter (OM) fractions influencing PAH dermal bioavailability.

To address these gaps this thesis focuses on assessing the relationships between both parent and alkylated PAHs and the characterised bulk OM of real-world contaminated MGP soils. The aim is to ascertain whether characterised bulk OM contribute to variations in PAH distributions across MGP sites and industrial processes, as well as to explore their influence on *in vitro* human dermal bioavailability.

In this work, quantification of PAHs was achieved through gas chromatography tandem mass spectroscopy (GC-MS/MS), while bulk OM is characterised using Rock-Eval(6) Pyrolysis (RE). Chapter 5 describes the employment of principal component analysis (PCA) to differentiate MGP processes based on PAH distributions, with the assistance of the RE parameters. The findings reveal distinctive signatures for MGP processes with oil associations and lower temperatures, from petrogenic signatures and contributions of heavier weight

PAHs, whereas other processes were found challenging to identify. Varied quantities of alkyl-PAHs in MGP soils were identified, emphasising the need to investigate the dermal bioavailability of these compounds.

Chapter 6 reports the measured dermal absorption (quantified as dermal fluxes) of 27 parent and alkylated high molecular weight (HMW) PAHs from real-world soils. Fluxes of the receptor solution (RS) and synthetic membrane are quantified, revealing that real-world contaminated soils influenced by environmental factors, lead to lower dermal fluxes compared to previous investigations using spiked soils. The majority of available HMW PAHs were measured in the membrane, showing that the membrane acted as a sink for PAHs released from soils, resulting in delayed diffusion of HMW PAHs into the RS. Notably, fluxes decrease with increases in the PAH ring number, highlighting the potential risks associated with low ring number PAHs including one alkyl-PAH group at longer exposure timesteps, a factor currently overlooked in HHRAs.

Chapter 7 reports linear regression analysis relationships between RE parameters and RS fluxes of five MGP samples which indicated strong associations between HMW PAHs exhibiting high fluxes and specific RE parameters. However, it is important to acknowledge that these relationships were primarily driven by one sample exhibiting exceptionally high PAH concentrations and RE values. Nonetheless, RE demonstrates promise as a screening tool for characterising contaminated soil, particularly for PAHs with higher fluxes and stronger correlations estimated for the membrane fluxes. However, further investigations exploring a larger dataset of soils is recommended to verify assumptions and produce models capable of predicting the dermal bioavailability of HMW PAHs from soils.

In summary, this research advances the knowledge of dermal bioavailability by investigating the largest number of different PAHs, including previously unstudied alkyl-PAHs, and demonstrating their potential risk for dermal absorption. Additionally, certain RE parameters offer promise for estimating PAH bioavailability in soil. By elucidating the complexities of PAH-soil interactions and assessing their influence on dermal absorption, this study enriches our understanding of PAHs' dermal bioavailability from real-world

contaminated soils. This knowledge can contribute to the refinement of accurate HHRAs, particularly regarding the potential risks posed by a diverse set of PAHs in varied contaminated soil contexts.

Acknowledgements

Completion of this Doctoral research would not have been possible without the support and assistance of various people who I would like to acknowledge and thank.

Firstly, I'd like to give a big thanks to my principal supervisors Christopher Vane, Darren Beriro and Matthew Jones. Thank you for all the support and guidance you have provided throughout my PhD and the help you've provided to getting my PhD to this stage with several potential research papers. Additionally, I would like to thank my other industry supervisors Russell Thomas of WSP who continually provided me with in-depth knowledge about the MGP processes and sites, and I'd like to thank Chris Taylor of National Grid Property Holdings, for their advice and insights into the contaminated world of the gasworks industry. Additionally, I'd like to thank the people at National Grid Property Holdings and the Contractors who helped me with my field work at MGP sites. I am incredibly grateful for the funding provided by the CASE partnerships which enabled me to complete this PhD. In addition, I'd like to thank the Envision DTP for providing me with support, training and development opportunities throughout my PhD.

I was lucky enough to be hosted by both the University of Nottingham and the British Geological Survey (BGS), therefore gaining the benefits of both worlds. At the University of Nottingham, I'd like to thank Teresa Needham for her help in training me on the particle size analyser at the University. Additionally, I would like to thank George Swann whose annual reviews always made me feel better about the work I'd managed to achieve within a year, even when in a Pandemic lockdown. I would also like to thank the other PhD students at the University who always made me feel welcome, even after such long absences from the University.

For the majority of my PhD, I spent most of my time at BGS and have many people to thank from BGS. This includes the BGS Organic Geochemistry team: Alex Kim, Vicky Moss-Hayes and Raquel Alfama Lopes Dos Santos, all who have given me support, guidance and training. A special thanks goes to Alex, who provided impeccable training and support for me, who additionally helped

me developed a GC-MS/MS method and helped me to get my head around appropriate spiking values for samples. I additionally need to thank the BGS Sample Preparation team, including Mark Kalra, who helped with the initial sample preparation.

A special mention of course goes to Jack Lort who not only developed the *in vitro* dermal methodology and taught me how to undertake the method while coming out of a global pandemic. But also provided me with encouragement and a laugh for when everything was going wrong.

On a more personal level, I would like to mention my parents, Alan and Evelyn and my brother, James. Thank you for all the support you have provided, and of course for all the laughter you bring into my life. Thank you for reminding me of how far I have come. I also must thank my husband's family Jenny, Gareth, Rachel and Matt, thank you for your support including sending me flowers in a challenging work week.

Thanks go to my rabbits, Merry and Pippin. They would rather eat this thesis than read it. Lastly, but certainly not the least I would like to express my greatest gratitude to my now husband Chris. Planning a DIY wedding from scratch was never going to be easy while completing an experimental PhD during a pandemic, but with your love and support behind me, I have achieved what others dare not to think about. Thank you for all that you do including your help with R coding and for your constant belief in me, and for sharing my most utterly low and ecstatically high moments with.

This thesis is dedicated to my beloved golden retriever, Ace, who sadly passed away several days before I submitted my thesis. I wish I could celebrate with you at the end, a bittersweet ending never had such meaning.

Table of Contents

Abstract	ii
Acknowledgements	i
List of figures.....	i
List of tables	i
List of equations.....	i
Chapter 1 Introduction	2
1.1 Background to research project	2
1.2 Research aim and questions	4
1.2.1 Aim.....	4
1.2.2 Research questions	4
1.2.3 Research objectives	5
1.3 Thesis structure	6
Chapter 2 Literature Review.....	8
2.1 Introduction.....	8
2.2 Contaminated land.....	8
2.2.1 Contaminated land human health risk assessments	8
2.2.2 Brownfield land	13
2.2.3 Manufactured Gas Plant sites	14
2.2.4 Contaminant types	15
2.3 Polycyclic Aromatic Hydrocarbons.....	16
2.3.1 Types of PAHs	16
2.3.2 PAH sources, fate and transport.....	20
2.3.3 PAH mixtures and lists	21
2.3.4 Spiked soils vs field-contaminated soils.....	24
2.4 Assessing PAHs from soils.....	25
2.4.1 Quantification of PAHs in solid and aqueous matrices	25
2.4.2 Methods to assess PAH fate from soil.....	27
2.4.3 Bioavailability and bioaccessibility measurements	28
2.4.4 <i>In vitro</i> human dermal bioavailability experiments	31
2.4.5 PAH soil concentration	37
2.5 Soil characteristics	38
2.5.1 Overview of sorption and desorption of PAHs from soil.....	38
2.5.2 Organic matter and organic carbon	39
2.5.3 Dual-mode sorption mechanism.....	41

2.5.4	Types of OC	42
2.5.5	Quantification of OC.....	45
2.5.6	Quantification of bulk OM using Rock-Eval Pyrolysis	46
2.5.7	Inorganic components role	47
2.5.8	Particle and pore size	48
2.5.9	Soil moisture	48
2.5.10	Multiple linear regression analysis and highlighted literature	49
2.6	Literature summary.....	50
Chapter 3	Methodology.....	51
3.1	Introduction.....	51
3.2	Soil sampling and selection	51
3.3	Rock-Eval(6) Pyrolysis	52
3.4	Particle size analysis	52
3.5	Soil selection for PAH quantification.....	53
3.6	Soil selection for the <i>in vitro</i> dermal experiments	55
3.7	Sample preparation and PAH extraction	55
3.7.1	Soil sample preparation	57
3.7.2	Membrane and receptor solution sample preparation.....	58
3.8	Gas Chromatography Tandem Mass Spectroscopy	60
3.8.1	GC-MS/MS method development.....	60
3.8.2	GC-MS/MS method.....	61
3.8.3	GC-MS/MS calibrations	63
3.8.4	GC-MS/MS LOD and LOQ	64
3.9	<i>In vitro</i> dermal experiments	64
3.9.1	<i>In vitro</i> dermal experiment method development.....	64
3.9.2	Methodology of applied <i>in vitro</i> dermal experiment	66
3.10	Data evaluation and statistical analysis.....	69
3.11	Quality control methods	69
3.11.1	Quality control samples	69
3.11.2	Extraction efficiencies	71
3.11.3	QC methods for dermal experiments	71
Chapter 4	Quality Control Assessment	72
4.1	QC Introduction.....	72
4.2	Sample preparation and analytical QC	72
4.2.1	General methods quality assurance activities.....	72

4.2.2 Spiked solvents.....	74
4.2.3 Extraction efficiencies – Sample recoveries	76
4.2.4 GC-MS/MS detection limits	81
4.2.5 Blank samples and duplicates	82
4.2.6 Measurements of Certified Reference Materials (CRMs).....	84
4.3 QC for the <i>in vitro</i> dermal experiments	86
4.3.1 Mass balance	86
4.3.2 Dermal matrices weight checks.....	86
4.3.3 Validating dermal results by comparison to other studies	88
4.4 QC summary	90
Chapter 5 Characterisation of former Manufactured Gas Plant soils using parent and alkylated Polycyclic Aromatic Hydrocarbons and Rock-Eval(6) Pyrolysis.....	91
5.1 Abstract.....	92
5.2 Introduction.....	92
5.3 Materials and methodology.....	95
5.3.1 Sample collection and selection	95
5.3.2 Sample preparation.....	96
5.3.3 PAH concentration	96
5.3.4 Rock-Eval(6) Pyrolysis.....	97
5.3.5 Data evaluation and statistical analysis.....	98
5.4 Results and discussion	98
5.4.1 Distributions and concentrations of PAHs.....	98
5.4.2 Rock-Eval(6) Pyrolysis.....	117
5.4.3 Characteristics of gasworks processes.....	127
5.4.4 Evaluation of applied methods.....	128
5.5 Conclusions.....	129
5.6 Acknowledgements	130
Chapter 6 Dermal absorption of high molecular weight parent and alkylated Polycyclic Aromatic Hydrocarbons from Manufactured Gas Plant soils using <i>in vitro</i> assessment	131
6.1 Abstract.....	132
6.2 Introduction.....	132
6.3 Materials and methods	136
6.3.1 Sample selection.....	136
6.3.2 <i>In vitro</i> dermal absorption experiments.....	137

6.3.3 Sample analysis.....	138
6.3.4 Dermal flux	138
6.3.5 Data analysis	139
6.3.6 Quality control.....	139
6.4 Results	139
6.4.1 PAH concentrations in soils.....	139
6.4.2 Membrane flux	140
6.4.3 Receptor solution flux	146
6.4.4 Combined receptor solution and membrane flux.....	155
6.4.5 PAH Physicochemical Properties and Initial Soil Concentration Influences	155
6.4.6 Quality control.....	161
6.5 Discussion.....	162
6.5.1 HMW parent PAH dermal flux	162
6.5.2 HMW alkylated PAH dermal flux.....	164
6.5.3 PAH physicochemical properties and initial soil concentration influences.....	165
6.5.4 Comparison to other studies.....	166
6.5.5 Future work and implications.....	168
Chapter 7 Effect of bulk organic matter from Rock-Eval(6) Pyrolysis and particle size on dermal absorption of high molecular weight parent and alkylated polycyclic aromatic hydrocarbons in Manufactured Gas Plant soils.....	171
7.1 Abstract.....	172
7.2 Introduction.....	172
7.3 Methodology	179
7.3.1 Sample collection and <i>in vitro</i> dermal experiments.....	179
7.3.2 Soil properties – Rock-Eval(6) Pyrolysis and Particle Size Analysis.....	180
7.3.3 Statistical analysis.....	180
7.4 Results	181
7.4.1 Rock-Eval(6) Pyrolysis and Particle Size Analysis.....	181
7.4.2 Linear regression between PAH RS fluxes and soil properties	185
7.4.3 Soil properties potential influence on PAH membrane flux	189
7.5 Discussion.....	190
7.5.1 RS fluxes relationships with bulk OM.....	190
7.5.2 PSA influence on RS flux.....	195

7.5.3 Comparison with other MGP soils	195
7.5.4 Implications and future research	196
7.6 Conclusion	197
Chapter 8 General discussions	199
8.1 Introduction	199
8.2 Discussion of results	199
8.2.1 Review of research focus	199
8.2.2 Research key findings	200
8.2.3 Research discussion	201
8.3 Implications and future directions	214
8.3.1 Implications	214
8.3.2 Research Constraints	216
8.3.3 Future directions	217
8.4 Summary	220
Chapter 9 Conclusion	221
Chapter 10 References	224
Appendix A	247
Appendix B Chapter 5 Research Papers SI	268
Appendix C Chapter 6 Research Papers SI	268
Appendix D Chapter 7 Research Paper SI	269

List of figures

Figure 1. The framework for environment risk assessment and management, figure taken from the Green Leaves III document (Gormley et al., 2011).	9
Figure 2. Diagram showing generic contaminant source, exposure pathways and receptors in human health risk assessment of contaminants in soil.....	11
Figure 3. Figure taken from Thomas (2014) shows the MGPs production process, with black arrows showing the gas production main stages and grey arrows showing by-product stages.	15
Figure 4. Subclasses of inorganic and organic contaminants found in soil, with examples of compounds from each.	16
Figure 5. Examples of PAHs and PAC containing heteroatoms structures, note that the C2-pyrene structure is one of many isomers that comprise in the C2-pyrene alkylated homologue series.....	17
Figure 6. Number of PAHs studied in individual papers, graph produced from 60 research papers studying PAH contamination/fate in soil.	21
Figure 7. Chart of the origin of PAHs in research studies, produced from 60 research papers studying PAHs fate in soils.	24
Figure 8. A brief overview of the stages needed for PAH quantification.	26
Figure 9. a) diagram of basic skin structure and b) illustration of contaminant proportions in soil with their relation to bioaccessibility and bioavailability...	30
Figure 10. Simple set up for an in vitro method.	35
Figure 11. Desorption stages details from two- and three-compartment models.	39
Figure 12. Depicts the SOM division used within literature, the main divisions include OM, types of organic carbon (OC), humic substances (HS), chemical functional groups and OM type e.g. peat. Chart created from 40 papers.	40
Figure 13. Correlation between PAHs release to TOC with different experimental methods, created from 10/40 papers reviewed. EXT = solvent extraction, SORP. EQU. = sorption equilibrium, IN VIVO H. O = in vivo high organisms' experiments, MIN/BIO = mineralisation/biodegradation.....	41
Figure 14. Bar chart of the correlation between the different HS and the release of PAHs from soil, created from 10 papers.	44
Figure 15. Workflow diagram of the steps used to choose the soils for PAH quantification.	54
Figure 16. PCA biplot of the k-means clustering (k=5) using the ten RE parameters of 94 MGP soils.....	55
Figure 17. Alkylated PAH Peak Integrations for the CRM NIST-1944	63
Figure 18. (a) Simplified diagram of the in vitro dermal experiments, (b) soil being weighed before application to the membrane, (c) soil applied membrane placed in the glass diffusion cell, (d) soil removed from membrane after dermal experiment, (e) collection of matrices after dermal experiments (soil, membrane and RS), and (f) setup of dermal in vitro experiment in water bath.	68
Figure 19. GC-MS/MS chromatograms of RS samples, (a) A11 RS at 10-hr for BaP >LOQ, (b) A11 RS at 1-hr for BaP <LOQ, (c) the only A11 RS at 1-hr which measured BghiP >LOQ and (d) chromatogram showing A11 RS at 1-hr for Pyr	

>LOQ as a black and red filled peak represents Pyr measured in a blank dermal experiment, (e) H16 membrane at 1-hr for Pyr >LOQ and filled red peak is Pyr measured in a blank dermal experiment.	83
Figure 20. Measured CRM NIST-1944 samples in this study (red – DCRM and green – DGWS batches) compared to certified PAH concentrations (blue), errors bars are 95% CI.	85
Figure 21. Measured CRM BCR-524 samples in this study (red) compared to certified PAH concentrations (blue), errors bars are 95% CI.	85
Figure 22. Mass difference percentages between the wet-applied soil on the membrane and the collected dried soil after removal from the membrane post-experiment, a -25% was the target to account for the added moisture to the soil (dashed line on plot). Note experiments with no bar represent dermal blank experiments which did not include applied soil.	88
Figure 23. Bar chart showing the percentages of the proportions of the PAHs with different number of rings for(a) EPA16 and (b) Alkyl21.	100
Figure 24. (a) PCA biplot created using the log transformed PAH51 concentrations of all 48 gasworks soils and 2 background park soils. (b) PAH51 individual PAH contributions of all 48 gasworks soils and 2 background park soils towards PCA (c) PAH51 individual PAH PCA biplot of all 48 gasworks soils and 2 background park soils. (d) PAH51 individual PAH contributions of all gasworks soils with a \sum PAH51 concentration >100 mg/kg towards PCA. (e) PAH51 individual PAH PCA biplot of all gasworks soils with a \sum PAH51 concentration >100 mg/kg towards PCA.....	105
Figure 25. Chord diagram to show the MGP processes related to each site and an annotated PCA biplot of GWS PAH percentage contributions towards \sum PAH51, GWS with \sum PAH51 <100 mg/kg removed.....	108
Figure 26. Bar charts of the mean percentage contribution of each alkylated series towards the \sum Alkyl21% for each site.....	109
Figure 27. Alkylated PAH distributions for six gasworks soils. (a) sample A5, (b) sample A17, (c) sample D3, (d) sample E1.4, (e) sample H16, (f) sample I5, (g) sample A3 and (h) sample I7. Colour of lines: red=petrogenic, orange=pyrogenic with moderate temperature, black=pyrogenic with higher temperature.	114
Figure 28. PAH diagnostic ratio cross plots applied to gasworks soils, (a) An/An+Phen vs (C0-Ph/An)/(C0:C1-Phen/An), and (b) (Fla+Pyr)/(Fla+Pyr+C2-C4-Phen/An) vs (C1-C4-Phen/An)/(Phen/An).	117
Figure 29. S2 deconvolution fractions applied to GWS, (a) use of Sebag et al. (2016) fractions, (b) log PAH51 plotted against Sebag et al. (2016) fractions percentages, (c) use of Haeseler et al. (1999) fractions, (d) Sebag et al. (2016) I-index vs R-index plot created with 50/94 soils (soils with measured PAH concentrations).....	121
Figure 30. (a) annotated van Krevelen diagram (OI values above 250 have been removed), and (b) annotated TpkS2 vs HI plot.	126
Figure 31. Diagram illustrating the dermal experiments conducted in the control reference soil study and the five MGP samples, including which dermal matrices were measured for each sample at each timestep.	137

Figure 32. Boxplot of the initial soil concentrations of the 27 HMW PAHs in the 5 MGP soils and BCR-524. Note y-axis breaks and change in scale for the extreme PAH concentrations for E1.5.	140
Figure 33. Mean membrane fluxes for the four HMW PAHs (a) Fla, (b) Pyr, (c) BaP and (d) C1-Fla/Pyr over the timesteps 1-h, 10-h and 24-h. Data points represent mean membrane fluxes and error bars are the 95% CI. The H16 sample uses triplicate experiment results for each timestep, whereas the BCR-524 uses triplicate membranes for 24-h and one membrane measured at 1-h and 10-h. Note different y-axis scales in all plots and lines representing different samples...	142
Figure 34. Boxplots of the membrane fluxes for (a) H16 triplicate experiments at each timestep and (b) BCR-524 triplicates experiments for 24-h). Absence of boxplot indicates PAHs are <LOQ in membrane.	145
Figure 35. Mean RS fluxes for the four HMW PAHs (a) Fla, (b) Pyr, (c) BaP and (d) C1-Fla/Pyr over the timesteps 1-h, 10-h and 24-h. Data points represent mean fluxes of the triplicate experiments performed for each timestep for each MGP sample, and error bars are the 95% CI. Note different y-axis scales in all plots and lines representing different samples.....	148
Figure 36. RS flux for individual PAHs at each timestep, data based on three experiments per timestep, (a) A11, (b) E2.7 (c) I3, (d) H16 and (e) E1.5 reported as boxplots. Samples ordered by ascending soil PAH concentration, Fla and Pyr removed from larger boxplot to allow the scale of fluxes for other PAHs to be represented. Absence of boxplot indicates PAHs are <LOQ in RS.	153
Figure 37. Boxplots of the total fluxes for (a) H16 triplicate experiments at each time step and (b) BCR-524 triplicates experiments for 24-h). Absence of boxplot indicates PAHs <LOQ.	157
Figure 38. Multiple plots of the sample H16 RS flux relationship with PAH physicochemical properties. The y-axis plots the H16 RS fluxes at 24-h for triplicate experiments and the x-axis plots the PAH physicochemical properties: alkylated chain length, boiling point (°C), Henry's Law Constant, Log Kow, Molecular weight (Da), number of rings in structure, vapour pressure (Pa) and water solubility (mg/L). Physicochemical property values taken from Achten and Andersson (2015) whereby the mean physicochemical property values of individual alkyl-PAHs were used to represent the alkylated homologue series. Line of best fit calculated with locally estimated scatterplot smoothing (LOESS).	158
Figure 39. The initial soil PAH concentration (mg/kg) of the 27 HMW PAHs plotted against (a) 24-h membrane fluxes for H16 and BCR-524 and (b) 24-h RS fluxes for all samples, line produced from linear regression.....	160
Figure 40. RE parameters for the five MGP soils and BCR-524. Units for each RE parameter displayed on the y-axis are: S1 (HC mg/g), S2 (HC mg/g), TpkS2 (°C), S3 (CO ₂ mg/g), PC (%), RC (%), TOC (%), HI (mgHCg ⁻¹ TOC), OI (mgO ₂ g ⁻¹ TOC), and Sebag et al. (2016) R-index and I-index are unitless. ..	182
Figure 41. S2 pyrogram of the five MGP soils and BCR-524 sample, the temperature ramping of RE is illustrated in the upper plot corresponding to the plot displaying all samples. Samples with lower responses zoomed in for the inside plot.....	183

Figure 42. Particle size distribution triangle of the MGP soils, showing percentages of fractions determined with particles <250 μm 185

Figure 43. (a) Linear regression r^2 values between each HMW PAH RS flux at the 24-hour timestep with the soil properties and initial soil concentration for the MGP samples only (BCR-524 not included). Linear regression created using results for each of the three dermal experiment conducted for one MGP soil (e.g. 3 dermal experiments x 5 soils = 15 points). Brighter green tiles signify linear regression models with performing the best by fitting better to the data (high r^2 values), brighter red colours are associated to linear regression models not fitting with the data. * Indicates a p-value < 0.05 for the tested linear regression, this indicates that the soil property has a meaningful addition to the model. (b) Simple linear regression plots for Fla RS flux at 24-hours and the soil properties. Points represent the observation from one of the three dermal experiments undertaken for each MGP soil - triplicate dermal experiments occurred for each MGP soil (e.g. three experiments undertaken with the MGP soil H16 and each experiments observation is a point). 189

Figure 44. Linear regression r^2 values between RS flux (triplicate dermal experiment results) vs soil properties of MGP samples with the removal of sample E1.5 at the 24-hour timestep for each HMW PAH. Brighter green tiles signify higher r^2 values (higher percentage of variation explained by soil property), while brighter red tiles are associated to lower r^2 values. * Indicates significant regression with a p-value < 0.05. 192

List of tables

Table 1. Relevant pathways contributions to the total exposure calculated by CLEA software from The LQM/CIEH S4ULs for HHRAs (Nathanail et al., 2015).....	13
Table 2. Lists the research papers which have investigated different PAHs.....	23
Table 3. Papers studying dermal uptake of PAHs from soil and other materials.	32
Table 4. Papers on PAH concentration in soil affected by soil physicochemical properties.	37
Table 5. Lists the research papers who undertook MLR and PCA.....	49
Table 6. List of the materials and chemicals used in the research and the suppliers of the materials.	56
Table 7. Sample preparation and spiking values for the soil samples measured in the different experimental batches. Acronyms in the table include soil weight (wt.), PAH surrogate (Surr.) volume (vol.) and the PAH internal standards (I.S).	58
Table 8. Sample preparation and spiking values for the membrane and receptor solution samples measured in the DCRM experiments (with BCR-524) and DGWS experiments (with MGP soils). *Full volume of RS analysed.....	60
Table 9. Receptor solution formula to make 100 mL.	66
Table 10. List of quality assurance measures applied in this research.	72
Table 11. Mean, standard deviation, %RSD, and bias for DGWS sample batches using MX45 spiked solution at 0.20 pg/ μ L.	75
Table 12. Mean, standard deviation, %RSD, and bias for DGWS sample batches using MX183 spiked solution at 0.2 pg/ μ L.	76
Table 13. Surrogate recoveries for each analytical batch and each sample type	79
Table 14. LOD and LOQ for each PAH in each matrix.....	81
Table 15. The mass balance percentages for all H16 experiments and triplicate 24-hour and one 10-hour experiment for BCR-524.	87
Table 16. Comparisons of RS, membrane and total fluxes for the sample BCR-524 at 24-hours between my study and Lort (2021).....	89
Table 17. Summary of the dermal fluxes of 24-hour BaP for my samples results which were compared to other studies to validate this study's findings.....	90
Table 18. Overview of sites MGP processes and PAH concentrations.....	106
Table 19. QC regime procedures and results for study.	161
Table 20. RE parameters relation to bulk OM in soils and the potential influence these variables can have on the release and dermal bioavailability of HMW PAHs in soils based on previous studies.	176
Table 21. Parameters applied to calculate the dermal absorption fraction (ABS_d) for BaP as applied by Forsberg et al. (2021).	211

List of equations

Equation 1. Fick's First Law of Diffusion.	36
Equation 2. Calculation of OM from TOC%.	41
Equation 3. Calculation for the fine particle associated carbon (FPAC).	48
Equation 4. Calculation of %Bias.	70
Equation 5. Calculation of % relative standard deviation (%RSD).	70
Equation 6. Equation of sum of dermal matrices PAH masses (measured in ng) equalling the initial soil PAH mass at beginning of dermal experiment (0-hr). 71	
Equation 7. Calculation of Mass Balance % for dermal experiments.	71
Equation 8. Calculation of dermal fluxes in dermal experiments for membrane and RS.	139
Equation 9. Fick's Second Law of diffusion.	165
Equation 10. Calculation of ABS_{exp}	211
Equation 11. Calculation of ABS_d	211

CHAPTER 1

INTRODUCTION

1.1 Background to research project

This thesis is designed to improve societal understanding of the dermal bioavailability of a diverse set of high molecular weight polycyclic aromatic hydrocarbons (HMW PAHs), including both parent and alkylated HMW PAHs. The influence of soil properties (predominately bulk organic matter (OM)) on the dermal bioavailability of HMW PAHs from post-industrial contaminated soils was explored using Rock-Eval(6) Pyrolysis (RE), particle size analysis (PSA), *in vitro* dermal experiments and gas chromatography tandem mass spectrometry (GC-MS/MS).

The UK has numerous brownfield sites, which are derelict land perceived to have contamination problems as a result of former operations at the site (Oliver et al., 2005). Brownfield sites have the potential to undergo remediation and redevelopment to provide vital components of sustainable urban growth, curbing the need for new construction on undeveloped land (e.g. greenfield land) (Rankl, 2023, CPRE (The Countryside Charity), 2019). The remediation of brownfield sites is an effective approach to achieve one of the 17 United Nations sustainable development goals (SDGs), to provide sustainable cities and communities (Ahmad et al., 2018).

Prior to remediation of brownfield sites, risk assessments are conducted to determine potential human and environment risks posed by contaminants. Contaminated soils of post-industrial brownfield sites, such as former Manufactured Gas Plant (MGP) sites, are known for extensive quantities of PAH contamination (Thomas, 2014) (Section 2.2). Polycyclic aromatic hydrocarbons (PAHs) are a group of hazardous organic compounds, with certain PAHs known or suspected as carcinogens and mutagens to humans (Section 2.3) (International Agency for Research on Cancer, 1965-2023, Rankl, 2023). Alkylated PAHs (alkyl-PAHs) are anticipated to have equivalent or potentially greater toxicity compared to parent compounds (Meador, 2008, Richter-Brockmann and Achten, 2018), however, limited research been dedicated to

exploring alkyl-PAHs (Achten and Andersson, 2015). One component of assessing risks to human health posed by PAHs from contaminated soils is the dermal exposure pathway, whereby the dermal bioavailability is estimated which provides guidance on the appropriate actions required to make the site suitable for use (Section 2.4.3). Human dermal bioavailability (addressed as dermal bioavailability in this thesis) refers to the proportion of compound/pollutant absorbed into skin (or skin substitute such as a synthetic membrane), where it may remain or be further absorbed into the human lymphatic or circulatory systems (or surrogate such as receptor solution) (Section 2.4.3) (Beriro et al., 2016).

Current risk assessments make assumptions of the dermal bioavailability of PAHs using a single dermal study. However, Wester et al. (1990) study introduces uncertainties as it examines only one PAH in one type of soil, neglecting the potential effects of other soil properties and physicochemical characteristics of PAHs on the dermal bioavailability. Subsequent research on the dermal bioavailability of PAHs from soils has been limited (Section 2.4.4) (Beriro et al., 2016, Ruby et al., 2016, Spalt et al., 2009). Particularly there are few dermal studies investigating PAH compound mixtures in real-world contaminated soils and exploring influences of soil properties upon the dermal bioavailability (Section 2.4.3). The leading consensus from research highlights soil organic matter (OM) as the dominant soil factor controlling PAH release from soil (Section 2.5) (Yu et al., 2018, Ehlers and Loibner, 2006, Chen et al., 2007). Rock-Eval(6) Pyrolysis (RE) has previously been applied as a screening tool to characterise various types of bulk OM and former research has indicated potential associations between the OM fractions characterised by RE parameters governing PAH release behaviour (Section 2.5.6) (Poot et al., 2014, Haeseler et al., 1999, Sebag et al., 2016). However, no known research has applied RE bulk OM characterisation parameters in predicting the dermal bioavailability of PAHs from real-world contaminated soils.

This research aims to expose the complex interactions between soil properties and the dermal bioavailability of parent and alkylated HMW PAHs. These findings hold the potential to refine risk estimation and management by directing attention towards specific PAHs, thus contributing to informed decision-making

for remediation companies, landowners, consultants, and regulators. The outcome is a reduction in uncertainties inherent to HHRAs concerning chronic exposure to carcinogenic soil-based chemicals within contaminated brownfield sites.

1.2 Research aim and questions

1.2.1 Aim

To investigate the distributions of parent and alkylated PAHs and characterised bulk OM of former manufactured gas plant (MGP) contaminated soils, and to determine whether these variables contribute to differences between MGP sites/processes and human *in vitro* dermal bioavailability.

1.2.2 Research questions

Delivery of the research aim is guided by the following three research questions:

1. Can the specific MGP process associated with a soil sample be identified through the analysis of parent and alkylated PAH distributions, and/or by characterising its bulk OM properties?
2. What is the *in vitro* dermal bioavailability measured by flux (ng/cm²/h) for parent and alkylated PAHs in MGP soils, and are there trends between the two?
3. To what extent do bulk OM properties from soil exert influence on the *in vitro* dermal bioavailability of both parent and alkylated PAHs within MGP contaminated soils?

1.2.3 Research objectives

The research questions were addressed by the following eight research objectives:

1. Perform an extensive literature review to identify key knowledge gaps in dermal bioavailability studies and to determine the soil properties and methods to investigate which are most likely to influence PAH release from soil (Chapter 2).
2. Establish a GC-MS/MS method that will enable PAH analysis of parent and alkylated PAHs across a dynamic concentration range in multi-matrix samples extending from low to exceedingly high PAH concentrations (Chapter 3 and 4).
3. Extensively characterise the bulk OM and particle size of a wide range of (>90) post-industrial brownfield soil samples obtained from former MGP sites using RE and particle size analysis (PSA) (Chapter 5).
4. Use numerical statistics to group soils into clusters based on their distributions of parent and alkylated PAHs and/or shared attributes of soil bulk OM. Examine whether the generated clusters can be used to characterise soils by their MGP processes (Chapter 5).
5. Conduct *in vitro* dermal exposure simulation experiments using a three-component dermal model (soil, synthetic skin membrane and receptor solution) on a selected sub-group of the contaminated MGP soils (Chapter 6).
6. Quantify the PAH concentrations in samples using the developed GC-MS/MS method to obtain MGP soil concentrations (mg/kg) and dermal fluxes (ng/cm²/h) for parent and alkylated PAHs (Chapter 5, 6 and 7).
7. Compare the dermal fluxes between different PAHs (including parent vs alkylated PAHs) and trends between PAHs with the highest and/or lowest dermal bioavailability across a selected subset of MGP soils, to establish which PAHs pose the greatest risks to human health (Chapter 6).
8. Investigate whether bulk OM properties influence the dermal bioavailability of PAHs by evaluating and characterising the relationships between the bulk

OM of soil assessed by RE parameters and PAH dermal flux by assessing trends and differences between selected samples results (Chapter 7).

1.3 Thesis structure

The research presented in this thesis is part of the research by Envision Doctoral Training Program (DTP), University of Nottingham (UoN), British Geological Survey (BGS) and Collaborative Awards in Science and Engineering (CASE) partners WSP and National Grid Property Holdings. The main findings in this thesis are presented as three research papers in Chapters 5, 6 and 7, which have or will be submitted for publication.

Chapter 1 introduces a background into the research and provides the research aim, questions and objectives of the thesis.

Chapter 2 is linked to objective 1 and depicts the research fields explored in this PhD including contaminated soils, dermal bioavailability and soil properties impacting dermal bioavailability.

Chapter 3 describes the methods used through this thesis, these methods were used to address objectives 2,3 and 5.

Chapter 4 provides the results of the quality control in this research.

Chapter 5 addresses research objectives 2, 3, 4 and 6. The chapter investigates characterising MGP soils by their MGP process using PAH distributions and bulk OM parameters described by Rock-Eval(6) Pyrolysis (RE) and addresses research question one.

Chapter 6 addresses research objectives 5, 6 and 7. The chapter describes the *in vitro* dermal experiments performed and the dermal flux results for 27 HMW parent and alkylated PAHs, hence answering research question two.

Chapter 7 calculates linear regression between the RE parameters from Chapter 5 and the dermal fluxes from Chapter 6, an attempt to answer research question 3 by addressing objective 8.

Chapter 8 links the results of the three research papers, chapters 5, 6 and 7. For this thesis the bulk of research is presented as three research papers, chapter 5, 6

and 7. At the time of writing the papers are at various stages in the publication process and have multiple authors associated with each paper.

Chapter 9 summarises the key findings and provides a summary of the research impact.

CHAPTER 2

LITERATURE REVIEW

2.1 Introduction

The following chapter provides a literature review of previous studies investigating the research fields applied in this work. The literature review was used to address research objective 1 by identifying the key research gaps that this research can focus on addressing. The topics comprise details about soil contamination, PAHs, PAH bioavailability specifically dermal bioavailability and soil characteristics influencing PAH fate in soil. The last section of this literature review is a summary of the gaps in current literature and how this study can help fill these.

2.2 Contaminated land

2.2.1 Contaminated land human health risk assessments

Contaminants are defined as any physical, chemical, biological, or radiological substance found in air, water, soil or biological matter that can cause significant harm to receptors of organisms, such as humans and the environment (United States Environmental Protection Agency (EPA), 2012). Contaminated land is generated by the presence of contaminants in soil and groundwater (DEFRA, 2012). To help minimise the likelihood of the unacceptable risks posed by contaminated sites to human and environmental health a range of legislation, policies and guidance have been put in place to identify, assess and manage the associated risks (Riding et al., 2013). In England, the most common legal frameworks for managing the risks to human and environmental health arising from land contamination are the Town and Country Planning Act 1990 and the Environmental Protection Act 1990: Part 2A (DEFRA, 2012). The Town and Country Planning Act is used when there is a change in the land use (e.g. an old petrol station site being converted into residential houses), the land must be shown to be safe and suitable for the new use (LQM, 2020). On the other hand, the Environmental Protection Act 1990: Part 2A framework refers to the risks that can occur from contamination with the current use of a site (there is no plan to change the use of the site); to state that the site is contaminated, the land must

be proven to be associated with having ‘Significant Possibility of Significant Harm’ (SPOSH) (LQM, 2020).

Risk to human or environmental health is defined as a combination of the likelihood that harm will occur as a result of contaminants in, on or under land, and the scale and seriousness of that harm or pollution if it did occur (DEFRA, 2012). The assessment and management of environmental risks are processed using the framework in the Green Leaves III document, the document is aimed at generic risks and can be used to assess and manage land contamination. The four component framework shown in Figure 1 shows the stages for risk assessment (Gormley et al., 2011).

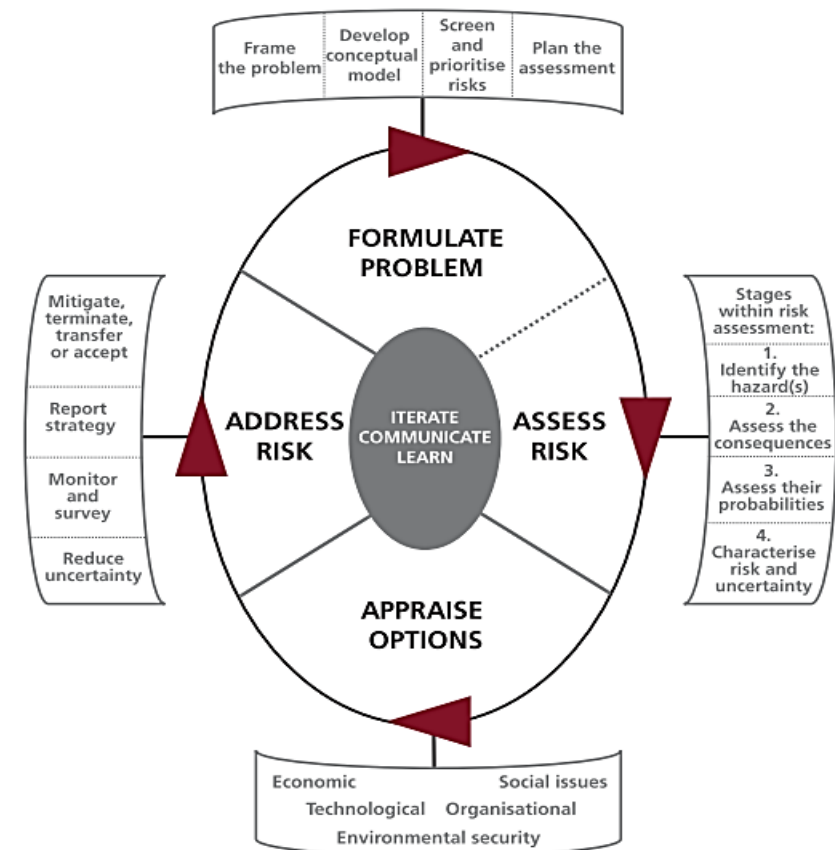


Figure 1. The framework for environment risk assessment and management, figure taken from the Green Leaves III document (Gormley et al., 2011).

Formulating the problem, involves generating questions about the risks and generating a conceptual model to represent the problems. Conceptual models are able to present the relationships between the hazards source, exposure pathways and the receptors (Gormley et al., 2011), e.g. contaminant-pathway-receptor

linkages (contaminant linkage) (DEFRA, 2012). In practice the conceptual model risks are communicated in the form of text, plans, cross sections, photographs and tables of the relevant risks. Evidence is built up in stage two of the framework by assessing the risk by using desk based studies, site visits, generic quantitative risk assessments and potentially detailed quantitative risk assessments, conditional on the contaminated site (DEFRA, 2012). The gathered evidence facilitates the generation of the possible relationships between contaminants, pathways and receptors (Environment Agency, 2009b). A summary of the collected information is then used by local authorities to determine whether the site is contaminated, and if contaminated, generate future plans to tackle the contamination (DEFRA, 2012).

The risks are estimated firstly by characterising the contaminants route, from the source > soil > exposure > intake > uptake > harm of human receptor. The exposure of a contaminant is the quantity of contaminant available for intake at a particular site of a human and can be quantified as the contaminants concentration in the medium (air, water, soil) (DEFRA and EA, 2002). The intake is the amount of contaminant entering or contacting the point of entry, such as the mouth (ingestion) and skin (dermal) (DEFRA and EA, 2002). The amount of intake is not necessarily the amount absorbed into the body, the amount of contaminant that enters the body and reaches the systemic circulation is the uptake and subsequently is the primary concern, given it has the potential to cause harm by adverse health effects (Environment Agency, 2009b).

Absorption can occur through the gastrointestinal system (ingestion), the skin (dermal) or the pulmonary system (inhalation) (DEFRA and EA, 2002). Figure 2 shows an example of contaminant linkages that might be used in a conceptual model of residential houses being built on a former contaminated site. This example shows the main pathways the contaminant can reach the receptors (in this case humans) include ingestion, dermal and inhalation. The risk evaluated from the exposure of a contaminant to a human will vary depending on the pathway the contaminant undertakes. To measure the total exposure of a contaminant, the relevant contaminant pathways need to be combined to generate a contaminant's overall exposure to a human (CL:AIRE, 2014). Each

pathway can contribute a different percentage to the total contribution depending on the contaminant and the exposure situation. To understand each pathways contribution, the pathways exposure, intake and uptake of the contaminant needs to be understood and measured to help assessments.

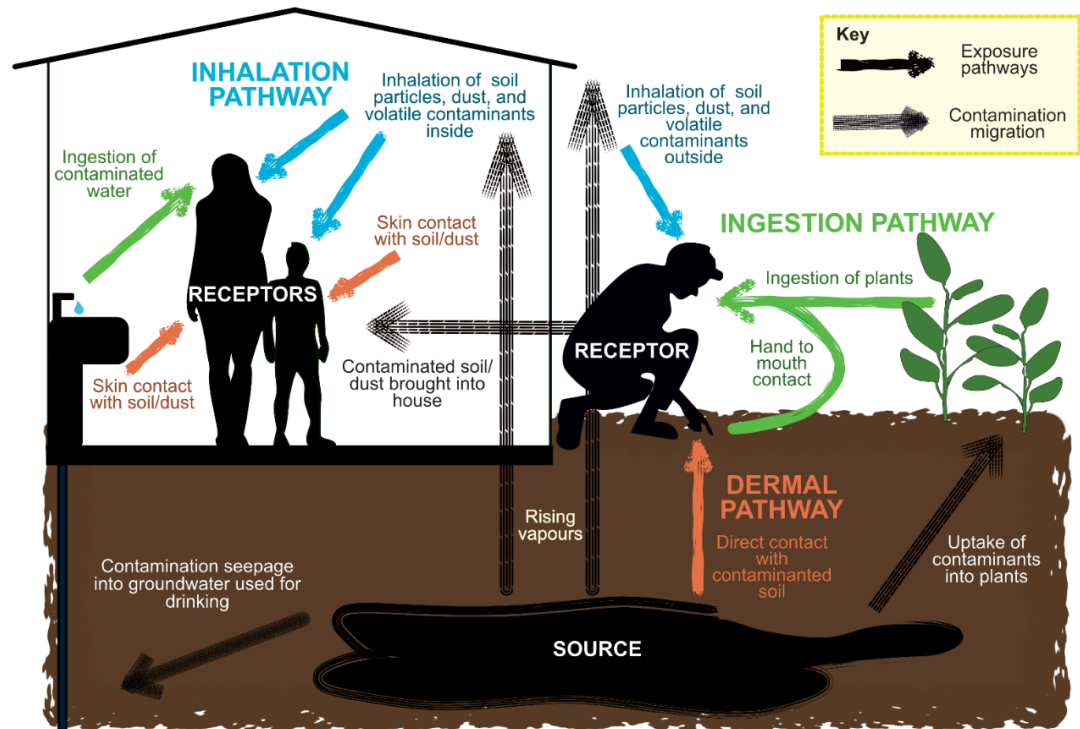


Figure 2. Diagram showing generic contaminant source, exposure pathways and receptors in human health risk assessment of contaminants in soil.

Human health risk assessments (HHRAs) of contaminated sites are most commonly used to estimate the chronic exposure and toxicology of soil contaminants. Both the exposure and chemical toxicity of the contaminant in soil are assessed as criteria to determine a measurable value to represent whether the contaminant is at an acceptable level of risk in a particular exposure scenario (CL:AIRE, 2014). For England and Wales, the Environment Agency (EA) developed the Contaminated Land Exposure Assessment (CLEA) model, which is a deterministic HHRA model software (Environment Agency, 2009a). The exposure pathways, receptors, soil types, land use and contaminant concentrations are inputted into CLEA. CLEA will use generic assumptions on the behaviour of the chemicals in the environment at different site conditions with different human behaviours, to estimate the exposures a child and adult

could potentially receive by contacting specific contaminated soil (Environment Agency, 2009b). The CLEA software derives a soil assessment criteria, either a Generic Assessment Criteria (GAC) or a Site-Specific Assessment Criteria (SSAC) developed by the EA (Cole and Jeffries, 2009). CLEA GAC are scientifically based generic assessment criteria derived as a function of a contaminant's toxicity and exposure (Cole and Jeffries, 2009). Soil concentrations at or below the GAC indicate the possibility of significant harm is unlikely (Cole and Jeffries, 2009).

In HHRAs, contaminant concentrations are compared with assessment criteria minimal risk values to assess the contamination risk. For residential use with plant uptake, BaP GAC is 5 mg/kg, concentrations above this value are considered as a potential risk to human health (CL:AIRE, 2014, Beriro et al., 2020). Contaminant specific GAC have been published by the EA, Contaminated Land: Applications in Real Environments (CL:AIRE) use derived GAC, the Land Quality Management Ltd./ Chartered Institute of Environmental Health (LQM/CIEH) use Suitable 4 Use Levels (S4ULs) (Land Quality Management Ltd, 2015). LQM/CIEH have published data sets calculated by CLEA for each pathway's percentage contribution to the total exposure by a contaminant. An example of two contaminants classed as polycyclic aromatic hydrocarbons (PAHs) are shown in Table 1. Benzo[a]pyrene (BaP) is a heavier high molecular weight (HMW) PAH compared to naphthalene (Nap) a lighter low molecular weight (LMW) PAH, pathway percentage contributions vary by contaminant and the exposure scenario (Nathanail et al., 2015).

The land use will impact the exposure scenario, for example, behaviour between a commercial use and residential one. The scenario will also impact a contaminants exposure contribution to a receptor, for example a person is more likely to spend longer periods outside touching soil (dermal receptor), undertaking activities such as gardening on a residential site compared to a commercial site. Combined with differences between the physicochemical properties of different contaminants and soil matrices, this produces different contributions to the total exposure from different pathways. The transport and

Table 1. Relevant pathways contributions to the total exposure calculated by CLEA software from The LQM/CIEH S4ULs for HHRAs (Nathanail et al., 2015).

Exposure pathway	Benzo[a]pyrene (% contribution)		Naphthalene (% contribution)	
	Commercial	Residential without home-grown produce	Commercial	Residential without home-grown produce
Total Ingestion	81.9	94.3	31.4	9.2
Total Dermal	17.6	5.5	6.7	0.5
Total Inhalation	0.6	0.2	52.8	64.7

fate (movement in the environment) of contaminants will differ, for example LMW PAHs, like naphthalene, are more volatile than the HMW PAHs, like BaP, therefore Nap inhalation pathway provides the highest contribution to the total exposure, whereas the BaP accumulates in soil rather than being lost by volatilisation and hence has higher ingestion and dermal contributions to the total possible exposure (Table 1). To provide the most realistic method of assessing the risk of a contaminant to human health, all exposure pathways and interactions with the environment and receptors must be deduced for different land uses (Semple et al., 2004, Naidu et al., 2015).

2.2.2 Brownfield land

Brownfield sites are defined by CABERNET (Concerted Action on Brownfields and Economic Regeneration Network) as “sites that have been affected by the former uses of the site and surrounding land; are derelict and underused; may have real or perceived contamination problems; are mainly in developed urban areas; and require intervention to bring them back to beneficial use” (Oliver et al., 2005). Developing on brownfield land has been proposed as a approach for sustainable urban growth, helping to achieve one of the 17 United Nations sustainable development goals (SDGs), to provide sustainable cities and communities (Ahmad et al., 2018). CPRE (The Countryside Charity) have stated that at least one million homes could be built on suitable brownfield land in the

UK (Rankl, 2023, CPRE (The Countryside Charity), 2019). Transforming brownfield land into beneficial uses can curb the need for new construction on greenfield sites, protecting the Green Belt and makes use of otherwise potentially underutilised land (CPRE (The Countryside Charity), 2019).

Before construction can begin the contamination must be fully examined to determine if the site is currently appropriate or needs remediating to make it safe and suitable for use (Ministry of Housing Communities and Local Government, 2019). Remediating strategies to remove contaminants include *in situ* treatment (treatment of contamination in subsurface) or *ex situ* treatment (treatment of excavated soil) and civil engineering methods (use of barriers or excavation) (CL:AIRE, 2015). Examples of treatment methods include chemical, biological and thermal treatments (CL:AIRE, 2015). Depending on the contamination and site, remediation can cause excessive environmental impacts to the site and be exceptionally expensive (CL:AIRE, 2015). Accurately assessing the risks posed by the contamination using HHRAs can help determining the extent of remediation required and avoid unnecessary remediations and costs, potentially leading to larger numbers of brownfield sites being redeveloped for societal use.

2.2.3 Manufactured Gas Plant sites

Former Manufactured Gas Plants (MGPs) (also known as Gasworks) are generally long-abandoned brownfield land. MGPs formerly synthesised manufactured gas consisting of hydrogen, methane and carbon monoxide by anaerobically heating coal at MGP sites in Britain between 1792 and 1981 (Thomas, 2014, Gallacher et al., 2017b). Developments to the MGP process provided improvements to the manufacturing efficiency, resulting with different MGP sites applying different processes, Section 5.2 Introduction provides details of the different MGP processes developed. The basic concept of the processes are shown in Figure 3 and includes initially externally heating coal without air in a vessel called a retort chamber, gases would be driven off to be further condensed, washed and purified to create the end product of manufactured gas (Thomas, 2014).

In addition to the synthesised manufactured gas, a variety of by-products and wastes were created from the processes. MGPs attempted to use the by-products

elsewhere, for example coal tar could be distilled into fractions creating oil and pitch (Thomas, 2014). Unfortunately this could not be undertaken all the time due to demands and product types, resulting with by-products disposed often disposed on site or in tips, leading to contaminants penetrating into soil and groundwater (Thomas, 2014). By-products and wastes included coke, coal tar, char, soot, hydrogen sulphide, ammoniacal liquor, and sulphate of ammonia and encompassed of complex mixtures of inorganic and organic substances (Thomas, 2014, Ruby et al., 2016). The extent and type of contamination at MGPs has been shown to depend on the MGP site's history, previous studies have shown coal tars from different MGP processes to produce different contaminant distributions (Gallacher et al., 2017b). In Chapter 5, I investigate the effect on the MGP process on the contamination distributions in MGP soils.

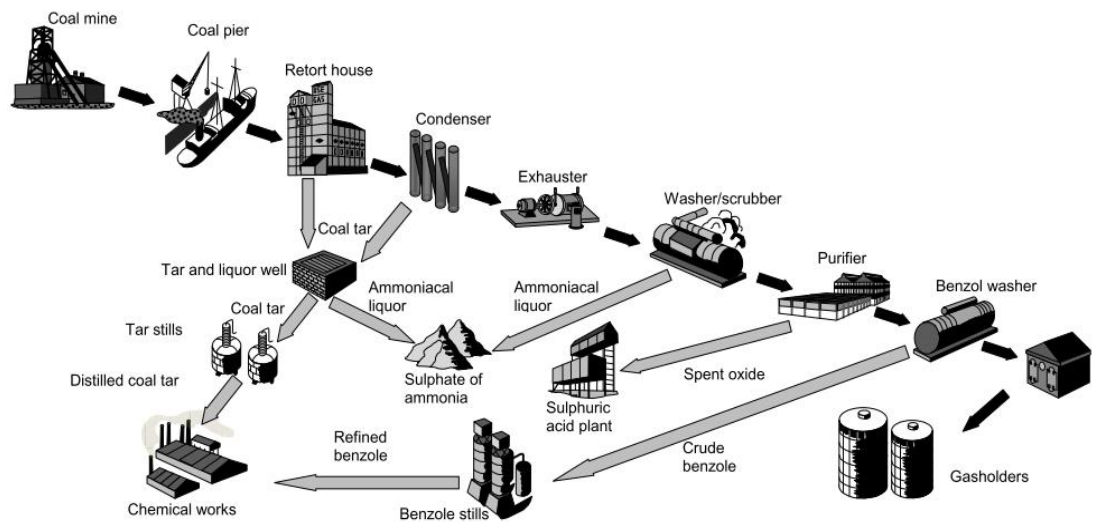


Figure 3. Figure taken from Thomas (2014) shows the MGPs production process, with black arrows showing the gas production main stages and grey arrows showing by-product stages.

2.2.4 Contaminant types

A range of different contaminant compounds can be present in soil as indicated in Figure 4, including inorganic metals such as arsenic, lead, cadmium and organic contaminants including polycyclic aromatic hydrocarbons (PAHs), pesticides, persistence organic pollutants (POPs), polychlorinated biphenyls (PCBs) and petroleum oil spills. The presence and quantity of the contaminant will depend on the contamination source, which can vary from industrial,

nonindustrial and environmental sources and the specific source material (Ruby et al., 2016).

MGP byproducts and wastes are encompassed with mixtures of contaminant compounds, such as PAHs and phenols (Ministry for the Environment New Zealand Government, 1997). PAHs are one of the major contaminants of concern in soils contaminated at former MGP sites, due to their toxicity and potential mutagenic/carcinogenic properties (Public Health England, 2017), with PAHs occurring in mixtures in coal tar, oil tar, pitch, coal, char and soot (Ruby et al., 2016).

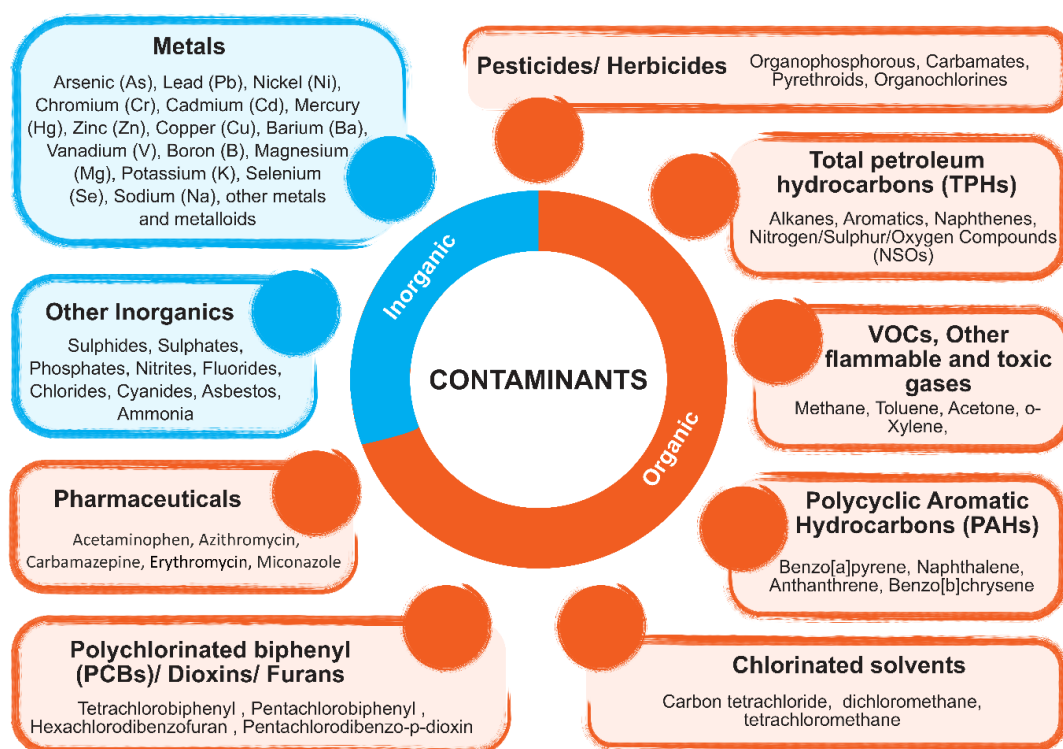


Figure 4. Subclasses of inorganic and organic contaminants found in soil, with examples of compounds from each.

2.3 Polycyclic Aromatic Hydrocarbons

2.3.1 Types of PAHs

PAHs are composed of two or more fused aromatic benzene rings (an aromatic ring of six carbons), Figure 5 illustrates several different types of PAHs. Low molecular weight (LMW) PAHs contain 2-3 fused aromatic rings and high molecular weight (HMW) PAHs have ≥ 4 fused aromatic rings. PAHs are

hydrocarbons comprising of carbon and hydrogen atoms in a conjugated ring system of alternative single and double bonds. The carbon π -electrons involved in the double bonds are delocalised (not localised to only one atom) across the ring causing the molecule to have a higher stability than predicted, based on the bond energies of other chemical structures.

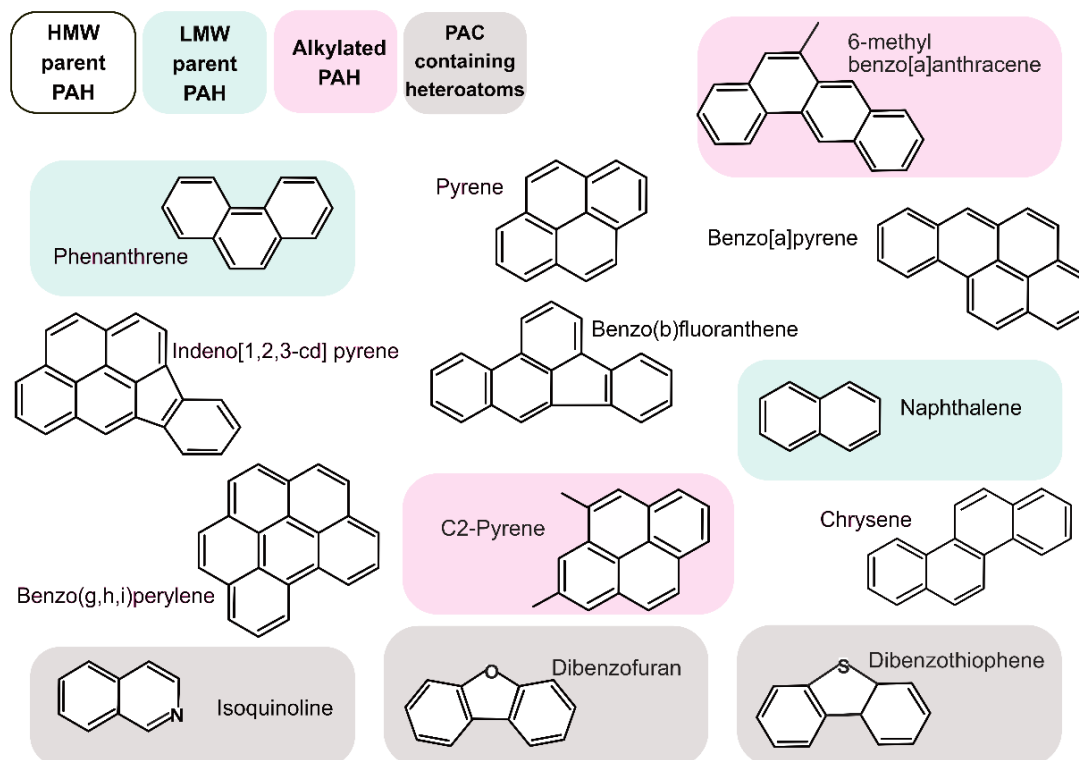


Figure 5. Examples of PAHs and PAC containing heteroatoms structures, note that the C2-pyrene structure is one of many isomers that comprise in the C2-pyrene alkylated homologue series.

PAHs are hydrophobic and lipophilic compounds favouring partitioning into lipophilic phases such as oils and fats and repel water phases. This provides PAHs with a high octanol to water partitioning factor (K_{ow}) (James et al., 2011). Each PAH will vary by their physicochemical properties, including molecular weight, solubility, charge and the types of interactions formed with a soil's matrix (Environment Agency, 2009a). As a result, PAHs exhibit different binding capacities to different soil media, subsequently affecting the PAHs release from soil and whether the PAH is classed as a risk.

HMW PAHs exhibit higher contributions to the dermal pathway than LMW PAHs, due to the assumption that volatile compounds will volatilise faster than

the occurrence of dermal uptake and the lipophilicity of HMW PAHs favouring partitioning into lipid medias such as skin (Swartjes, 2011). HMW PAHs have a high persistency in soil given they are hydrophobic compounds and have low aqueous solubility that favours partitioning into non-aqueous phases like soil (Beriro et al., 2016). In contrast, LMW PAHs have higher solubilities and a greater suitability for microbial communities to mineralise over HMW PAHs (Couling et al., 2010). These attributes along with a combination of other factors such as other PAH physio-chemical properties and their resistance to breakdown cause HMW PAHs to be highly persistent in soil compared to LMW PAHs (Nathanail et al., 2015, Kanaly and Harayama, 2000). Knowledge of a PAHs presence and exposure alone is not enough to determine their uptake into the body, which determines their potential health risk.

HMW PAHs highest contribution to the total exposure is from the ingestion pathway, making ingestion the most influential pathway and therefore the most studied pathway for HMW PAHs (Beriro et al., 2016, Duan et al., 2014). This is especially relevant to children who have a smaller body mass and who conduct a higher degree of hand-to-mouth activities, enhancing their risk *via* the ingestion pathway (James et al., 2011). The inhalation pathway is negligible for HMW PAHs. Beriro et al. (2016) and Ruby et al. (2016) have indicated uncertainties still apparent for the dermal pathway. Both identified several limitations and gaps in the dermal absorption literature including the influence of soil properties and that better analytical practices particularly at low PAH concentrations are required.

The persistency of PAHs in soil is a concern to human health due to their toxicity, with several PAHs being categorised as carcinogenic (International Agency for Research on Cancer, 2010). The toxicity of PAHs differs between compounds meaning several PAHs are classified as a higher risk to human health than other compounds. For example, the HMW PAH benzo[a]pyrene (BaP) is classified in Group 1, Group 1 compounds are known human carcinogens. The LMW PAH naphthalene (Nap) in comparison is classified into Group 2B, Group 2B, compounds that are possibly carcinogenic to humans (International Agency for Research on Cancer, 2010). Many other PAHs are unclassified which creates uncertainties to the risks they pose to humans and the environment (Andersson

and Achten, 2015). The toxicity of PAHs is generally classified by their toxic equivalency factors (TEFs). TEF represent the degree of toxicity of an individual PAH in relation to BaP, which has a TEF of 1, BaP is the chosen reference compound due to its well characterized toxicology (Richter-Brockmann and Achten, 2018). Toxic equivalents (TEQ) can be calculated by multiplying the PAHs concentration with its TEF to generate the PAHs potential toxic potency, which can help measure the risk of a PAH mixture (Richter-Brockmann and Achten, 2018).

There are hundreds of different PAH compounds with a few examples in Figure 5, including parent PAHs which have the basic ring structure, alkylated PAHs (alkyl-PAHs) which have bonded aliphatic hydrocarbon chains added to the ring structures, or polycyclic aromatic compounds (PACs) with heteroatomic substituents on or within the ring system, heteroatoms (atoms other than carbon and hydrogen) could be oxygen, nitrogen or sulphur (Geier et al., 2018). A large volume of research has been based on these parent PAHs and the most commonly studied PAHs. The 16 U.S Environmental Protection Agency (EPA) PAHs, also known as the 16 USEPA PAHs and/or “priority PAHs”, abbreviated to EPA16 (Andersson and Achten, 2015). The EPA16 are solely parent PAHs and are typically investigated due to them being relatively easy to measure, high abundance in the environment and for hundreds of studies initially investigating them (Andersson and Achten, 2015).

Alkyl-PAHs alkylated chain can vary in location on the ring and length of the alkylated chain. Alkyl-PAHs can be grouped according to the total number of carbons in the alkyl moiety, such as C1, C2, C3 and C4-Phen, whereby C2-Phen indicates either two individual alkyl chains with one carbon atom or a single chain with a length of two carbons (Meador, 2008). Alkylation of PAHs creates numerous PAH molecule possibilities in contaminated soil, however there are very few studies on their toxicities, even though alkyl-PAHs are expected to be as toxic (or more toxic) than their respective parent compounds (Meador, 2008, Richter-Brockmann and Achten, 2018). Alkyl-PAHs are difficult to study with spectroscopy analysis due to the stronger fragmentation of the alkylated chain, overlap of peaks and the limited alkyl-PAH standards available to commercially purchase (Andersson and Achten, 2015).

2.3.2 PAH sources, fate and transport

PAHs found in soil can originate from a variety of different sources, PAH sources can dictate the type and concentrations of PAHs present within the mixture. Petrogenic sources (PAHs found naturally in petroleum products of coals and oils) are enriched with alkyl-PAHs and LMW PAHs, whereas pyrogenic sources (produced *via* incomplete combustion) are rich with HMW parent PAHs compounds (Andersson and Achten, 2015). HMW parent PAHs have a higher resistance to breaking at the higher temperatures used in pyrogenic origins, due to a higher amount of strong aromatic bonds which require vast amounts of energy to break. In comparison, LMW PAHs and alkyl-PAHs have weaker bonds (single bonds within alkylated chains) and fewer bonds to break, hence these compounds declined presence in pyrogenic sources (Andersson and Achten, 2015).

Diagnostic ratios can be used to identify PAH sources, in the ratio, one PAH is more thermodynamically stable over the other PAH. For example, phenanthrene (Phen) is more thermally stable than anthracene (An), and thus a low Phen/An ratio means a pyrogenic source (Khan et al., 2008). A Phen/An ratio < 10 and fluoranthene/pyrene (Fla/Pyr) ratio > 1 typically mean that the PAHs originate from a pyrogenic source, whereas Phen/An > 15 and Fla/Pyr < 1 show that the PAHs originate from petrogenic sources (Khan et al., 2008).

In order to predict the risks PAHs pose to humans and the environment, understanding the fate and transport (movement) of PAHs after being released from the source is required (Abdel-Shafy and Mansour, 2016). The most important transport mechanisms for contaminants through soil are volatilization, leaching, and erosion or suspension of soil particles (Cachada et al., 2018). Certain structural aspects of the source will enable the source to have a higher affinity towards PAHs, which potentially can lead to entrapment of PAHs and a decrease in the release of PAHs from the source (Yu et al., 2018). Xia et al. (2016) stated that the source material had the greatest impact on PAH partitioning. Their findings showed that the amount of PAH loss decreased in the PAH source order of solvent $>$ fuel oil $>$ soot $>$ skeet. MGP soils can contain mixtures of PAHs that originate from a variety of different sources e.g. non-

aqueous phase liquids (NAPLs) such as oils and tars, solid structures like char and soot, or semi-solid states such as pitch (Yu et al., 2018, Ruby et al., 2016).

2.3.3 PAH mixtures and lists

Thousands of PAHs can be present in complex environmental mixtures which are inherently difficult to analyse from soil samples, due to thousands of different compounds present. For example, Gallacher et al. (2017b) found 16 MGP tar samples containing between 650-1568 compounds. However, from this literature research their appears to be a deficiency in analysing the fate of large numbers of PAHs in mixtures from soil. Figure 6 emphasises that many papers either use one or two PAHs or focus on the EPA16 PAHs. The fate of PAHs mixtures in soils are difficult to predict due to the vast number of different combinations and properties that can occur (Stokes et al., 2005, Cipullo et al., 2018). Analysing an MGP soil for just the presence of PAHs could result in potentially thousands detected at various concentrations.

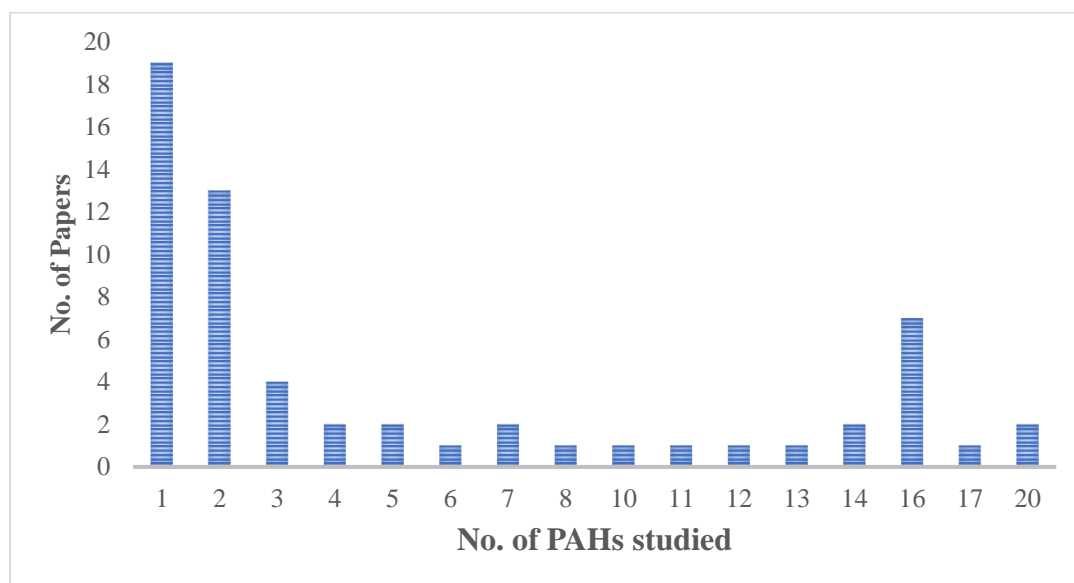


Figure 6. Number of PAHs studied in individual papers, graph produced from 60 research papers studying PAH contamination/fate in soil.

It would be unrealistic to investigate every individual PAH present in a soil sample; therefore, the development of PAH lists has been implemented to narrow the proportion of PAHs analysed. Recent studies have implied that the most used PAH list, EPA16, which was initially created to assess drinking water, neglects PAHs higher toxicities than PAHs in the EPA16 (Andersson and Achten, 2015).

Investigating contaminated soils using only the EPA16 are possibly underestimating the overall toxicity and risk of contaminated soils (Geier et al., 2018). Advantages for using the EPA16 include their commercial availability for standards, limited analytical complexity and the lower costs associated with the narrow number of PAHs being analysed (Andersson and Achten, 2015). The high usage of the EPA16 PAHs for over 40 years around the world has resulted in laboratories easily comparing data and determining concentration changes throughout time, the difficulty in changing to further or other, PAHs will lose these attributes (Andersson and Achten, 2015).

A limited number of studies have investigated extending the number of PAHs analysed other than the EPA16 (Andersson and Achten, 2015). Richter-Brockmann and Achten (2018) investigated 59 PAHs and showed that even when the non-EPA PAHs are at very low concentrations, they accounted for 69.3-95.1% of the TEQ. An additional argument has stated that several lists should be implemented depending on the purpose and site being analysed (Andersson and Achten, 2015). For example Hong et al. (2003) found that over 95% of the total PAHs present in lampblack (black soot created from incomplete combustion) were of the parent PAHs and not alkyl-PAHs. There is limited research on lists incorporating PAHs from MGP sites. Roy et al. (1998) investigated MGP tar-contaminated soils and quantitated the standard parent PAHs and two alkyl-PAHs. Gallacher et al. (2017b) established a comprehensive database of a total of 2369 unique organic compounds present in 16 MGP tar samples, with the majority (948) being aromatic compounds, 173 compounds were present within all samples. Table 2 lists the studies which explored different PAHs other than the EPA16 PAHs and highlights more toxic PAHs of concern.

Table 2. Lists the research papers which have investigated different PAHs.

Paper	PAH Numbers	Types of PAHs	Highlighted PAHs with TEF
<i>Andersson and Achten (2015)</i>	Propose list of 40 PAHs (40 EnvPAHs) Proposed list of 23 NSO-heterocycles Metabolites	US EPA 16 C2-alkyl derivatives higher molecular weight PAHs PANHs, PASHs or PAOHs PAH metabolites	dibenzo[a,l]pyrene (10 x BaP) dibenzo[a,i]pyrene (10 x BaP) dibenzo[a,h]pyrene (10 x BaP) benzo[c]fluorene (20 x BaP) 7,12dimethylbenzo[a]anthracene (2 x BaP) 6-nitrochrysene (TEF = 10) 1,6-dinitropyrene (TEF = 10)
<i>Richter-Brockmann and Achten (2018)</i>	59 PAHs		dibenzo[a,h]anthracene (TEF = 1) dibenzo[a,e]pyrene (TEF = 1) 5-methylchrysene (TEF = 1) dibenzo[a,l]pyrene (TEF = 10) dibenzo[a,j]pyrene (TEF = 10) dibenzo[a,h]pyrene (TEF = 10) 7Hbenzo[c]fluorene (TEF = 20)
<i>Hawthorne et al. (2006)</i>	34 PAHs		
<i>Geier et al. (2018)</i>	123 PAHs	Parent PAHs used as target PAHs; two alkyl-PAHs quantitated.	
<i>Roy et al. (1998)</i>	18 PAHs	MGP contaminated soil.	
<i>(Gallacher et al., 2017b)</i>	2369 unique compounds	948 aromatic compounds, 196 aliphatic compounds, 380 sulphur-containing compounds, 209 oxygen-containing compounds, 262 nitrogen-containing compounds, 15 mixed heterocycles, 359 compounds from derivatisation.	
<i>(McGregor et al., 2012)</i>	58-113 (number of PAH peaks used in statistical methods)	PAHs in coal tars from MGPs: naphthalenes, parent PAHs, alkyl-PAHs, N-PAHs, O-PAHs and parent S-PAHs.	

2.3.4 Spiked soils vs field-contaminated soils

Research on the fate of PAHs in soils can be conducted on either field-contaminated soil or spiked soil. Field-contaminated soils have been historically contaminated in a real-world situation, in comparison spiked soils are insert PAHs in soil in a laboratory. For example investigating wherever spiked radio-labelled PAHs have been mineralised by soil bacteria is one method to examine PAHs fate in the environment (Boonchan et al., 2000). Figure 7 illustrates that, of those papers reviewed, 39 studies spiked their soil samples whereas 19 used field contaminated samples. The issues arising from spiking soils in laboratory conditions not only incorporates a limited number of PAH types being studied but includes the absence of environmental impacts such as weathering, biodegradation and ageing (Barnier et al., 2014). For example, natural wetting and drying cycles on soils led to more phenanthrene remaining in soil after mineralisation than a soil with a consistent moisture content (White et al., 1997). Possibly these cycles helped compounds reach inaccessible soil sites unable to readily release PAHs (White et al., 1997). Hatzinger and Alexander (1995) found that phenanthrene had increased resistance to biodegradation with increased age.

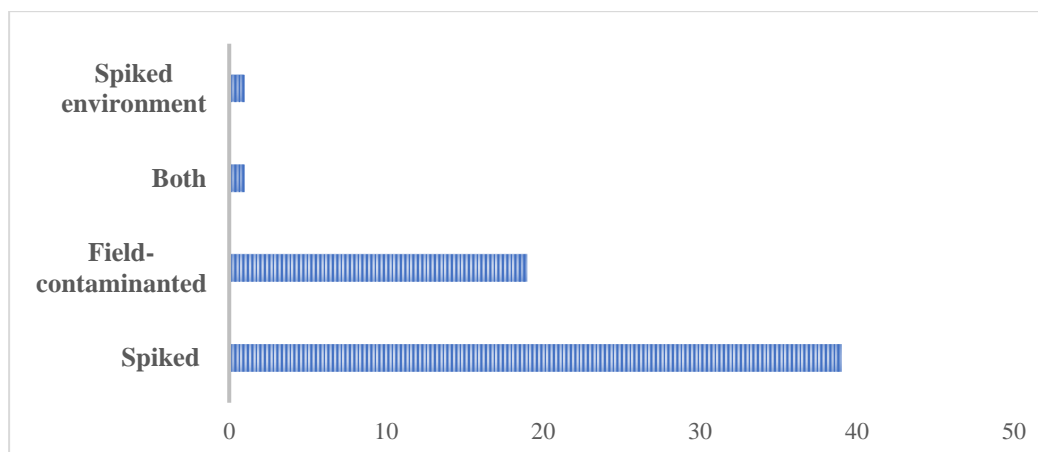


Figure 7. Chart of the origin of PAHs in research studies, produced from 60 research papers studying PAHs fate in soils.

Ageing PAHs has been shown to decrease the extractability and release of PAHs from soils (Duan et al., 2015, Chung and Alexander, 1998). Umeh et al. (2019a) showed that soils spiked and aged for 4 years in a lab released less BaP than a 500-day aged sample, indicating that a spiked soil monitored for a few days can overestimate the release of PAHs from soil compared to a real-field

contaminated site that has been aged for decades. This is particularly relevant to MGP sites that have been inactive for decades to a century, with PAHs left in the soil for these periods. Researchers believe that molecules become unavailable by the sequestration of PAHs, which is a combination of the PAHs slowly partitioning into organic matter or slowly diffusing into micropores (Kelsey et al., 1997, Kelsey and Alexander, 1997). Effects from sequestration/ageing can be seen to vary among different soils (Chung and Alexander, 1998), For example, Duan et al. (2015) tested four diverse soil types with four different extraction methods and showed that the amount of BaP extracted decreased from sandy to clayey soils.

Studies using spiked soils to understand the potential fate and risk posed by PAHs in soil are potentially providing inaccurate results when compared to field-contaminated soils. Since spiked soils investigate only a limited number of PAH types, in soils that are not aged and weathered like a real-world soil scenario and do not represent complex PAH mixtures.

2.4 Assessing PAHs from soils

2.4.1 Quantification of PAHs in solid and aqueous matrices

To assess posed risks from PAHs in soil, PAHs require to be quantified from different media, such as soil, sebum-sweat mixture, skin/artificial membranes and blood/receptor solution to measure the fate of PAHs. Several stages are required to quantify PAHs see Figure 8. The chosen sample preparation method is important, given methods such as drying and sieving can significantly change the quantity of retrieved PAHs (Beriro et al., 2014). Analytical techniques to quantify PAHs include, gas chromatography-mass spectrometry (GC-MS)(Larsson et al., 2013), gas chromatography-flame ionisation detector (GC-FID) (Thompson and Nathanail, 2003) and high-pressure liquid chromatography (HPLC) (Duan et al., 2014).

GC-MS is the most commonly used method for the quantification of PAH. The GC part of the instrument separates PAHs on the basis of the retention of a PAH to the stationary phase (affinity to solid column opposed to carrier gas) in a narrow column under carefully controlled time and temperature conditions. A compounds affinity towards the stationary phase is dictated by the PAH

properties, such as a compound's polarity and vapour pressure. When the PAH compound is released from the GC column, the mass spectroscopy stage ionizes the separated PAHs into fragmented ions, the formed ions mass-to-charge ratio (m/z) is then measured. MS provides confirmation of the GC peaks identity using unique spectrographic signatures. Increased PAH selectivity for PAH analysis can occur using gas chromatography tandem mass spectrometry (GC-MS/MS) in selected reaction monitoring (SRM) mode. GC-MS/MS works similar to GC-MS; however, GC-MS/MS incurs an additional phase during the mass spectrometry stage, whereby a precursor ion is selected and fragmented further generating daughter/product ions. The fragmentation pattern of the precursor ions and daughter ions enable GC-MS/MS to be highly selective at targeting compounds in complex mixtures (Niessen, 2017). Additionally, the high selectivity is needed to measure the alkyl-PAH compounds, alkyl-PAHs have multiple isomers (e.g. the C2-Nap group includes seven different isomers). GC-MS/MS can distinguish the alkyl-PAHs isomers over the wide retention time window, distinguishing the alkyl-PAHs from other signal noise. As a result of the above benefits GC-MS/MS was selected as the analytical method to quantify PAHs in this study.

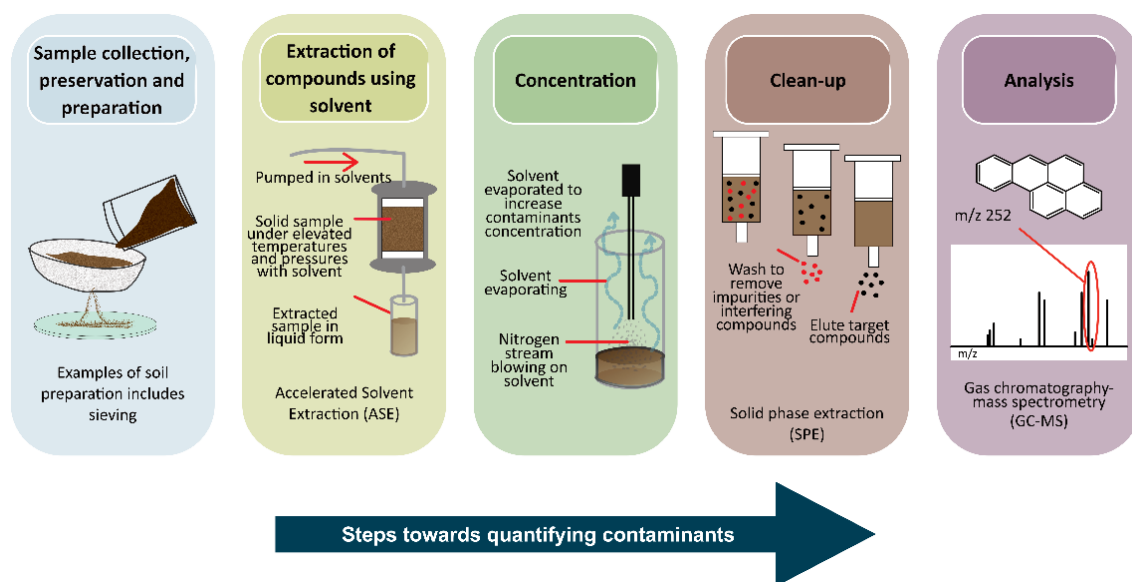


Figure 8. A brief overview of the stages needed for PAH quantification.

2.4.2 Methods to assess PAH fate from soil

Several experimental techniques have been established to measure the PAH fate from soil and can be categorised into three groups; equilibrium assays, kinetic assays and bioavailability or bioaccessibility assays (Yu et al., 2018). These experimental techniques can be described as *in vivo* or *in vitro* depending on whether the experiment uses living organisms or not. Additionally, *ex vivo* methods are used, in a dermal study this would measure an extracted organisms skin in an external environment (Beriro et al., 2016). Results of the extent of PAHs release, intake and uptake from soil will differ between experimental methods, White et al. (1997) observed differences between the amounts of PAHs extracted with solvents from soil in contrast to the uptake of PAHs by earthworms. Nevertheless, broad trends of soil and PAH properties can be observed and roughly compared to one another to help create a general knowledge of PAH behaviour and possible bioavailability.

Equilibrium and kinetic assays

Equilibrium assays determine the affinity of a contaminant to either the aqueous or solid phase, signalling whether a PAH will favour being released or sorbed (Yu et al., 2018). An example includes measuring the soil-sebum partition coefficient, which is the partitioned amount from soil to sebum (Beriro et al., 2020). Kinetic assays establish rate constants for different PAH fractions in the soil, rate constants are designated as k_{rapid} , k_{slow} and $k_{\text{very slow}}$. Luo et al. (2012) for example developed regression models describing k_{rapid} and k_{slow} desorption and its dependency on soil properties. Extractability of PAHs using different solvents is one of the major techniques used to establish PAHs release rates and expected intake/uptake, for kinetic assays the amounts extracted at different times is a measure of the total amount of PAH being released from soil. Inaccurate assumptions of PAHs fate can arise by using these extraction methods, exhaustive extractions use harsh solvents which can release PAHs which otherwise would not be released in normal environmental conditions (Duan et al., 2014, Duan et al., 2015). Instead, non-exhaustive techniques are preferred and work on the basis of PAHs mass transfer mechanisms (Rhodes et al., 2010).

Other methods used to study the PAH fate in soil use values from the mineralisation/degradation of bacteria or earthworms. Although these values directly show the influence in which PAHs cause an effect on a living organism, a bacteria/earthworm PAH uptake value cannot be used directly to predict the PAH uptake of a higher organisms. Given that the pathways and receptors of the different organisms will be very different and that these organisms belong to different ecosystems (Bogan and Sullivan, 2003).

2.4.3 Bioavailability and bioaccessibility measurements

Definitions

Incorporating the bioavailability/bioaccessibility for all pathways into risk assessments creates an effective system to demonstrate the overall harm that contaminated land can pose to human health. Bioaccessibility is the intake amount, the fraction of contaminant that is potentially available for uptake through a biological/artificial membrane but does not give a definite representation of the uptake. Bioaccessibility may therefore overestimate the amount of contaminant that could enter and cause harm *via* systematic circulation, as not all this bioaccessible amount is necessarily absorbed. The bioavailability of a contaminant is the proportion that can cross a biological/artificial membrane and pass into the systematic circulation or synthetic receptor solution, thus generating a value that is more likely to represent the amount that would cause harm.

The use of bioavailability and bioaccessibility in the literature is often ambiguous and is repeatedly poorly defined (Naidu et al., 2015, Riding et al., 2013, Semple et al., 2004, Semple et al., 2013). Especially when work is concentrated on a specific source, pathway or receptor which are often not specified (Naidu et al., 2015, Riding et al., 2013, Semple et al., 2004, Semple et al., 2013, European Centre for Ecotoxicology and Toxicology of Chemicals, 2002). There is a lack of a conventional definition for the two terms for dermal absorption, apart from in Beriro et al. (2016). Here, I have built on the definitions presented in Beriro et al. (2016) for use in my work:

Dermal bioaccessibility is the fraction of the total soil contaminant released into a biological medium where it becomes freely accessible for absorption and/or diffusion across a biological/synthetic membrane. For example, the dermal bioaccessible fraction is released from soil into a sweat-sebum mixture which then has the potential to absorb through the skin into the systemic circulation. Contaminants may also stay mobile within a sebum-sweat-soil medium on the surface of the skin and on the dead cells of the stratum corneum (skin surface layer). The dermal bioaccessible fraction includes unbound soil contaminants and temporally constrained contaminants, which can be successively released from the soil sites either over time or through portioning into different fractions.

Dermal bioavailability is the proportion of the dermal bioaccessible fraction that is absorbed into the living part of the skin where it can either remain or be absorbed into the lymphatic or blood circulatory systems. Whether within the living part of the skin or in systemic circulation the contaminant has entered the body and has the potential to cause harm to a receptor. The dermal bioavailable fraction cannot be greater than the dermal bioaccessible fraction.

Figure 9 a-b illustrates these terms in the context of the structure of human skin. A proportion of contaminants in the soil will be unable to be released from the soil matrix, due to entrapment or being strongly bound to the soil and is not dermal bioaccessible (Umeh et al., 2018). Whereas the bioaccessible fraction accounts for the proportion of contaminants that can be released from the soil matrix and therefore have the potential to cross the skins membrane to become bioavailable. However, a proportion of this bioaccessible fraction may stay within the sebum-sweat-soil medium or on the stratum corneum or will only be released from the soil with time. Bioaccessible contaminants can be released rapidly (minutes to hours), slowly (hours to days), or very slowly (days to months), depending on the soil matrix and the contaminants physicochemical properties. This has a knock-on effect on the amount of contaminants that are bioavailable at a specific time, once the contaminants within the sebum-sweat medium are released and cross the skin membranes the contaminant can be described as bioavailable. Beriro et al. (2020) proposed that the quantity of PAH released into sebum from soil was affected by both the soil type and PAH type.

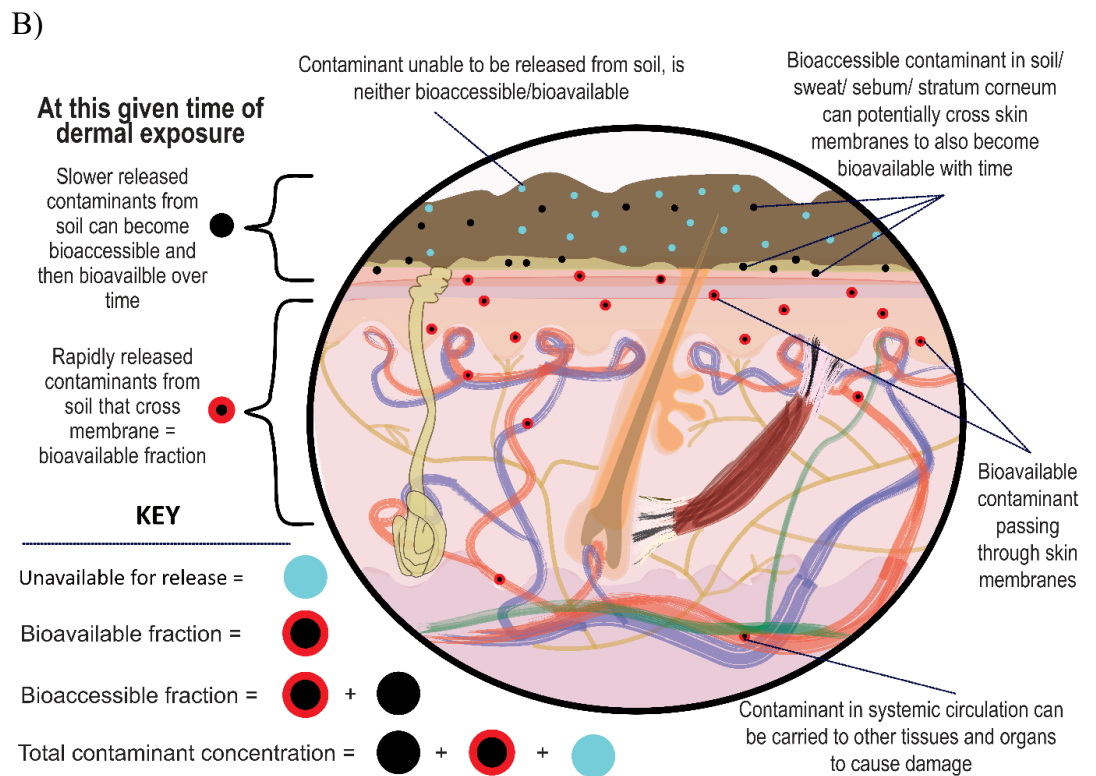
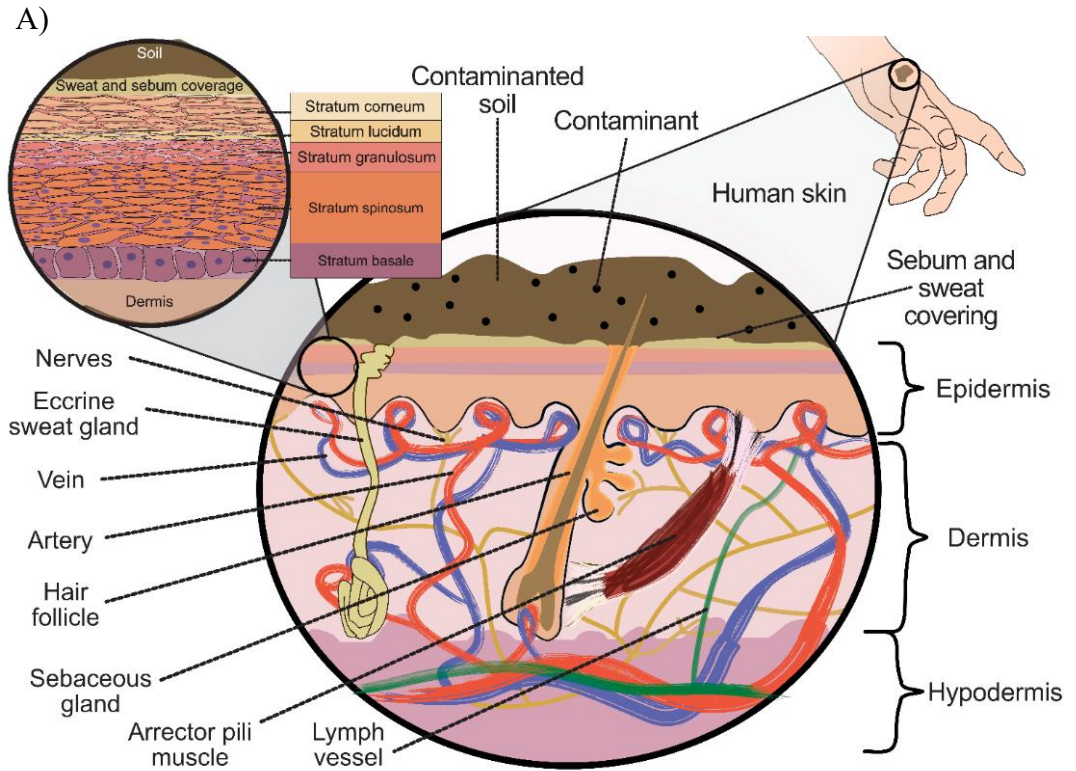


Figure 9. a) diagram of basic skin structure and b) illustration of contaminant proportions in soil with their relation to bioaccessibility and bioavailability.

Bioavailability and bioaccessibility assays

Bioavailability and bioaccessibility assays use several different *in vivo* or *in vitro* methods, including methods similar to the equilibrium and kinetic assays above and therefore have similar limitations. A key benefit to undertaking a bioavailability or bioaccessibility assay is to engineer the assay to measure a specific intake or uptake of a particular pathway. For example, studying the oral bioaccessibility of PAHs by an *in vivo* experiment involving feeding contaminated soils to rats or swine and measuring the output of PAHs in either blood, urine or faeces (Oomen et al., 2002, Duan et al., 2014, Cave et al., 2015). *In vivo* experiments have a number of issues including difficulties in experimental replication, ethical issues and costs (Umeh et al., 2019a). Leading to the development of *in vitro* methods, for an *in vitro* method to be both regulatory and scientific accepted, the *in vitro* method should be correlated to a *in vivo* method, given that results from different *in vitro* tests can vary greatly from one another with the same soil sample (Denys et al., 2012).

2.4.4 *In vitro* human dermal bioavailability experiments

The PAH dermal absorption can be described as a fraction or percentage of the applied dose (e.g. percentage absorbed of the dose applied (PADA) and the dermal absorption fraction (ABS_d)) (Moody et al., 2007, Wester et al., 1990). HHRA's make assumptions about the dermal bioavailability of PAHs from soil using the results of a single *in vivo* monkey study by Wester et al. (1990). This single study proposed 13% of BaP will be absorbed from the soil into the skin and is expressed in HHRA's as ABS_d (Environment Agency, 2009b). The default setting in CLEA assumes BaP bioavailability to be 13% for the dermal pathway (Environment Agency, 2009b, Beriro et al., 2020). This interpretation can lead to several uncertainties, given that the study only measures one PAH (BaP) in one type of soil, neglecting other soil and PAH physicochemical property effects on dermal bioavailability. Only limited research as presented in Table 3 have investigated the dermal bioavailability of PAHs, particularly studying the soil physicochemical properties affects upon dermal bioavailability (Beriro et al., 2016). The previous dermal studies generally investigated low numbers of PAHs compounds and soil types, with only three studies investigating soil properties influence on the dermal bioavailability of PAHs.

Table 3. Papers studying dermal uptake of PAHs from soil and other materials.

Paper	Experiment method	Endpoint	No. PAHs	No. Soils	Soil Type	Contamination Method	Exposure Time	Properties Investigated
<i>Wester et al. (1990)</i>	<i>In vitro</i> human skin <i>In vivo</i> monkey	Wash recovery Urine recovery	1	1	Yolo County soil sample 65-California-57-8	Spiked with ¹⁴ C-BaP	24-hr	Soil vs solvent
<i>(Yang et al., 1989)</i>	<i>In vitro</i> rat skin <i>In vivo</i> rat experiment	Radioactivity in receptor solution Radioactivity in tissues	1	1	Crude oil fortified soil	Spiked ³ H-BaP	4 timesteps 24 to 96-hr	Soil loadings and sole source crude oil vs crude oil contaminated soil
<i>Kadry et al. (1995)</i>	<i>In vivo</i> rat experiment	Plasma concentration, urine recovery	1	2	High sand and high clay soils	Spiked with ¹⁴ C-Phen	11 timesteps 1 to 48-hr	Sand, clay, organic matter
<i>Roy et al. (1998)</i>	<i>In vitro</i> pig skin	Skin recovery	1 13*	9	Former MGP soils	Spiked ³ H-BaP (surrogate for target PAHs)	10 timesteps 1 to 144-hr	MGP tar contaminated soil, soil influence

<i>Sartorelli et al. (2001)</i>	<i>In vitro</i> human skin	Receptor solution recovery	7	1	Coal dust from electric power plant	Field contaminated	4 timesteps 6 to 72-hr	Coal dust
<i>(Roy and Singh, 2001)</i>	<i>In vitro</i> human skin	Radioactivity in receptor fluid	1	1	Coal tar spiked- and coal tar/ ³ H-BaP	Coal tar spiked	8 timesteps 1 to 96-hr	Soil loading, ageing
<i>(Abdel-Rahman et al., 2002)</i>	<i>In vitro</i> human skin	Radioactivity in skin and receptor fluid	1	2	Sand and clay soil	Spiked ³ H-BaP	12 timesteps 0 to 16-hr	Ageing soil vs pure compound
<i>(Stroo et al., 2005)</i>	<i>In vitro</i> human skin	Receptor fluid	1	7	Lampblack and lampblack/soil from oil-gas MGPs	Field contaminated	5 timesteps 8 to 96-hr	Field contaminated MGP soils
<i>(Moody et al., 2007)</i>	<i>In vitro</i> human skin	Skin, receiver solution, soap wash, apparatus wash	1	1	Commercial gardening soil	Spiked ¹⁴ C-BaP	4 timesteps 6 to 24-hr & 42-hr	Soil vs solvent
<i>(Moody et al., 2011)</i>	<i>In vitro</i> human skin	“By difference” method	5	1	Coal-tar contaminated soil	Field contaminated	24-hr	Field contaminated soils

<i>Hu and Aitken (2012)</i>	Empore™ C18 extraction disk	Desorption kinetic model	14	1	Former USA MGP	Field contaminated	6 days	Soil loading, temperature and soil moisture content
<i>Xia et al. (2016)</i>	<i>In vitro</i> pig skin in evaporating dish	Skin recovery	2	12	Soils spiked with different PAH sources	Soils spiked with solvent and sources	16-hr	PAH sources: skeet, soot, fuel oil, solvent
<i>(Peckham et al., 2017)</i>	<i>In vitro</i> human skin	Skin and receptor fluid	1	4	Four soils	Spiked ¹⁴ C-BaP and aged	8-hr and 24-hr	Weathered vs unweathered soil, spiking amount, total organic carbon and black carbon
<i>(Forsberg et al., 2021)</i>	<i>In vitro</i> human skin	Tape, skin and receptor fluid	6	3	Weathered soils and target fragments from former defence sites	Field contaminated and spiked BaP	10 timesteps 1 to 72-hr	PAH concentration, field contaminated vs spiked
<i>(Lort, 2022)</i>	<i>In vitro</i> synthetic skin	Soil, membrane and receptor fluid	3	3	Two MGP soils and CRM BCR-524	Field contaminated	8 timesteps 0.5 to 48-hr	Field contaminated soils

Dermal bioavailability experiments using *in vivo* methods place contaminated soil onto the skin of an animal and analyse the PAH contamination from blood, urine or faeces (Wester et al., 1990, Kadry et al., 1995). Beriro *et al.*, (2016) provided an extensive review on *in vitro* methods and alterations to the membrane type, soil dosing and soil maturity. Most follow a simple design as shown in Figure 10. Diffusion cells place a skin membrane in-between a donor chamber and receptor solution chamber, the amount of PAH within the membrane, receptor solution and soil can be analysed to determine the bioavailability (Beriro et al., 2016). Two of the most common designs differ by the receptor solution being static in a static diffusion cell or flowing in the flow-through diffusion cell (Beriro et al., 2016). Multi-plate systems use multiple wells filled with receptor fluid upon the membrane which is placed upon a well plate of the dosed solution (Beriro et al., 2016). Fibre arrays use membrane-coated fibre which absorb organic compounds and can provide data used regression modelling (Beriro et al., 2016). Passive samplers place samplers on various skin locations, compounds are extracted from the samplers and analysed to determine the skin's exposure (Beriro et al., 2016).

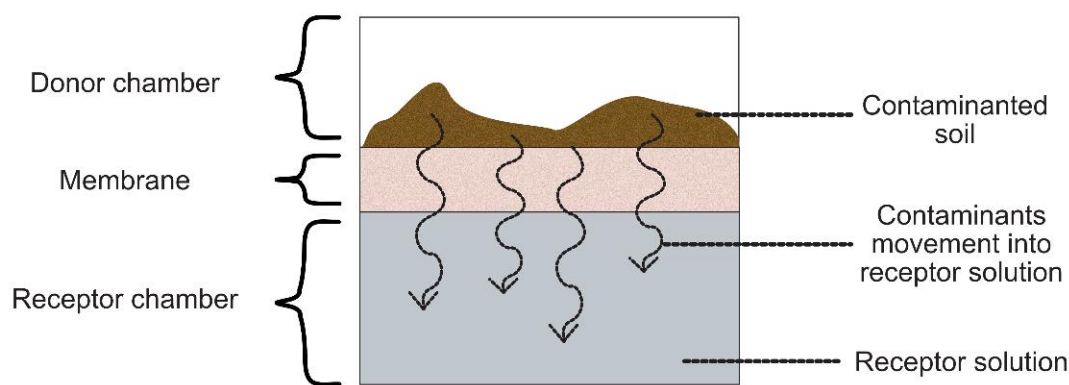


Figure 10. Simple set up for an *in vitro* method.

A dermal bioavailability study to highlight for my study is the work undertaken by Lort (2022), who researched the dermal bioavailability of three HMW PAHs (BaP, pyrene (Pyr) and dibenz[a,h]anthracene (DahA)) in two MGP soils and the certified reference material (CRM) BCR-524 soil contaminated by creosote oil. Lort (2022) developed an *in vitro* method and assessed the performance of the new method to measure the dermal absorption of PAHs from solvents and soils. Lort (2022) showed that the dermal bioavailability results measured by the *in*

in vitro dermal method using spiked solvents were within range of previous dermal studies. Indicating that the developed *in vitro* method was applicable for determining dermal bioavailability. Lort (2022) subsequently measured the dermal bioavailability of real-world MGP soils and found the results to be much lower than the dermal bioavailability used in current guidance based on the *in vivo* study by Wester et al. (1990). This agrees with other studies that suggest real-world soils have a lower dermal bioavailability than spiked soils (Forsberg et al., 2021, Roy et al., 1998). Previous studies have suggested that both PAH and soil properties have an effect on the release of PAHs from soil and the dermal bioavailability (Lort, 2022, Beriro et al., 2020).

The dermal bioavailability in the studies were compared by flux, which is not impacted by soil loading (amount of soil applied to the surface) and thus a better prediction to compare absorption studies (Frasch et al., 2014, Beriro et al., 2016). Flux (J) is the penetration rate and calculated using Fick's First Law of diffusion in Equation 1 (Beriro et al., 2016), whereby ΔC is the change in concentration (concentration gradient) and Δt is the change in time and A is the surface area. The flux of a compound expresses the maximum concentration of a compound absorbed into the skin relative to time and can help determine the dermal bioavailability of PAHs (Beriro et al., 2016). Theoretically, there should be an unlimited supply of the compound, referred as an infinite dose, so that the flux is not limited by the amount of the compound which would create a finite dose (Beriro et al., 2016). Several flux definitions include a steady state flux which is achieved after a lag phase and shown graphically as the gradient of a penetration plot before plateauing (Beriro et al., 2016), whereas a peak flux is defined as the highest flux achieved from a specified dose (Frasch et al., 2014). The peak flux provides a worst-case scenario for dermal exposure and thus determined by assessing by multiple exposure timesteps to capture the peak flux.

$$J = \frac{\Delta C}{\Delta t} A$$

Equation 1. Fick's First Law of Diffusion.

2.4.5 PAH soil concentration

MGP sites are generally over this GAC value (5 mg/kg for BaP), for example Thavamani et al. (2011) measured BaP concentrations in soils near gasworks between 58 to 738 mg/kg. In theory, the assumption that a soil with a high PAH concentration is caused by soil parameters which highly sequester or entrap PAHs making them unavailable for uptake seems feasible. The common trends observed in papers investigating the PAH concentration in relation to soil physicochemical properties observe that soils with higher amounts of condensed soil organic matter (SOM) and fine particle fractions such as silt and clay contain the highest PAHs concentrations (Talley et al., 2002, Pan et al., 2006) as shown by Table 4, these are potentially soil properties worth investigating to determine if they additionally impact PAH release from soil and dermal bioavailability values.

Table 4. Papers on PAH concentration in soil affected by soil physicochemical properties.

Paper	No. Soils	No. PAHs	PAH concentration correlation with soil parameters		
			Negative	Positive	None
<i>Barnier et al. (2014)</i>	3	16			Between PAH soil conc. and slower released PAHs
<i>James et al. (2011)</i>	8	13			OC, pH, sand, silt and clay content
<i>Ukalska-Jaruga et al. (2019)</i>	41	16		Stable SOM fractions. TOC content (r = 0.73), HN (r = 0.71) and BC (r = 0.87), especially HMW PAHs	Clay, pH
<i>Müller et al. (2000)</i>	10	20		LMW PAHs concentration: floatables > clay > silt > fine sand > coarse sand	
<i>Lorenzi et al. (2010)</i>	16	16		Smaller size fraction – finer particles	
<i>Khan et al. (2008)</i>	5	16		SOC	

<i>Lu et al. (2012)</i>	2 soils + 4 size fractions	16	clay>silt>coarse sand>fine sand
<i>Uyttebroek et al. (2006)</i>	1 soil + size fractions	1	49% Clay > 18% silt > 8% coarse sand > 7% fine sand
<i>Pernot et al. (2013)</i>	1	16	Fine silt fraction.

2.5 Soil characteristics

Soil composition will vary depending on parent materials, climate, organisms, topography and time. Components include pore spaces, filled by either air and water, and solid structures, the majority of which are minerals, and a small percentage of which are organic matter (OM) (Brady et al., 2008).

2.5.1 Overview of sorption and desorption of PAHs from soil

Sorption is the process that accumulates solutes to the surfaces and interphases of a matrix such as soil, sorption can obstruct the PAH's mobility, reducing the availability of PAHs to organisms (Huang et al., 2003). Sorption can occur by either adsorption, whereby the PAHs attach to a two-dimensional surface, or absorption which involves the PAH penetrating into a three-dimensional matrix (Ehlers and Loibner, 2006). Desorption, on the other hand, is the release and transport of PAHs from the soil matrix, released PAHs are able to interact with minerals and organic content by either sorbing to the surfaces or mobilising into pores in certain soil structures (Cipullo et al., 2018, Ehlers and Loibner, 2006). Depending on the interaction between the contaminant and the soil matrix, a number of gradations of desorption can occur (Cipullo et al., 2018).

The bioavailability of PAHs can be estimated by using results from sorption and desorption experiments. Experimental research shows that both sorption and desorption of PAHs in soil have a rapid stage that is subsequently followed by slower steps (Wu and Gschwend, 1986). Carmichael et al. (1997) determined that up to 90% of the initial PAH soil concentration was sorbed within 24 hours, with PAHs inhabiting the soil's most accessible sites. Past research on the desorption of PAHs has produced two models, either a two-compartment or three-compartment model to explain the stages of PAH release from soil (Semple et al., 2013).

Figure 11 describes the properties and sorption/desorption rates associated to each stage in both models, including which desorption mechanism controls the PAH release: release of PAHs from sorption and the diffusion of the PAHs through sorbent to water (Barnier et al., 2014, Semple et al., 2013). A desorption kinetics study on field contaminated soils conducted by Barnier et al. (2014) measured the rapid desorption stage of PAHs to occur between 0 and 15 hours, with 40% and 60% of the total amount desorbed in this time, followed by a slower stage that had not reached equilibrium after 300 hours (Barnier et al., 2014). Different mechanisms are dependent on the soil constituents, to understand the dermal bioavailability of PAHs these desorption mechanisms associated with the soil physicochemical properties must therefore be determined.

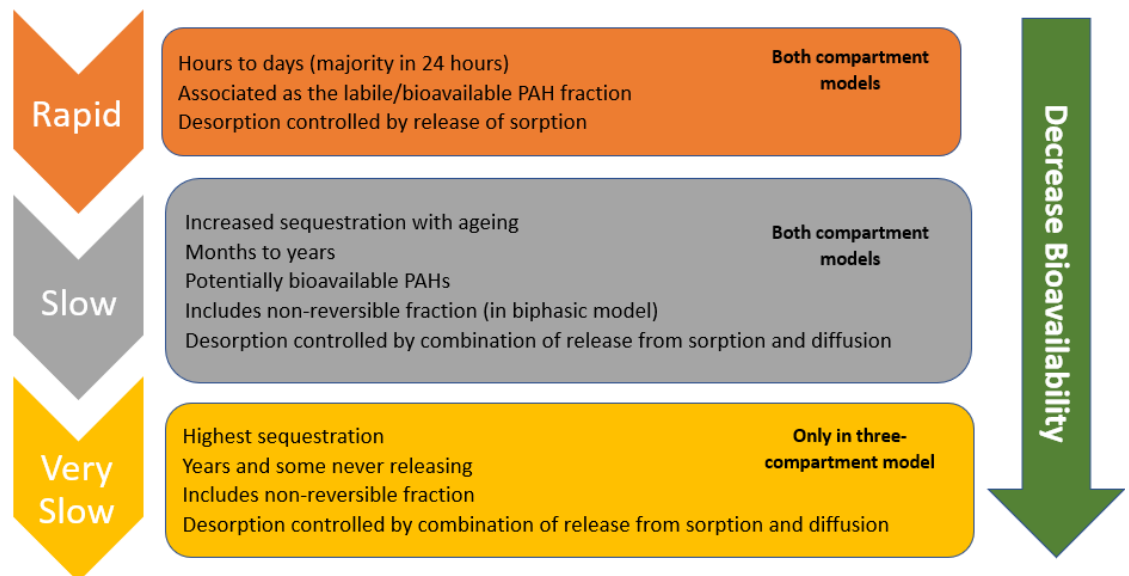


Figure 11. Desorption stages details from two- and three-compartment models.

2.5.2 Organic matter and organic carbon

Numerous studies have concluded that soil organic matter (SOM) is the dominant influential factor for PAH sequestration and consequently the release/availability of PAHs (Yu et al., 2018, Ehlers and Loibner, 2006, Chen et al., 2007). The variety of natural organic substances/structures in soil are caused by the diversity of organic components decaying to different degrees within soil to form an extensive diversity of organic structures (Yu et al., 2018, Ehlers and Loibner, 2006). Classifying and quantifying the SOM complexity is difficult and has resulted in researchers establishing a range of different terminologies to

describe aspects of SOM responsible for impacting PAH behaviour in soil. However, many of these SOM terminologies and subcategories overlap with one another and are analysed by different methods, as a result making it difficult to correlate results between different research papers (Figure 12).

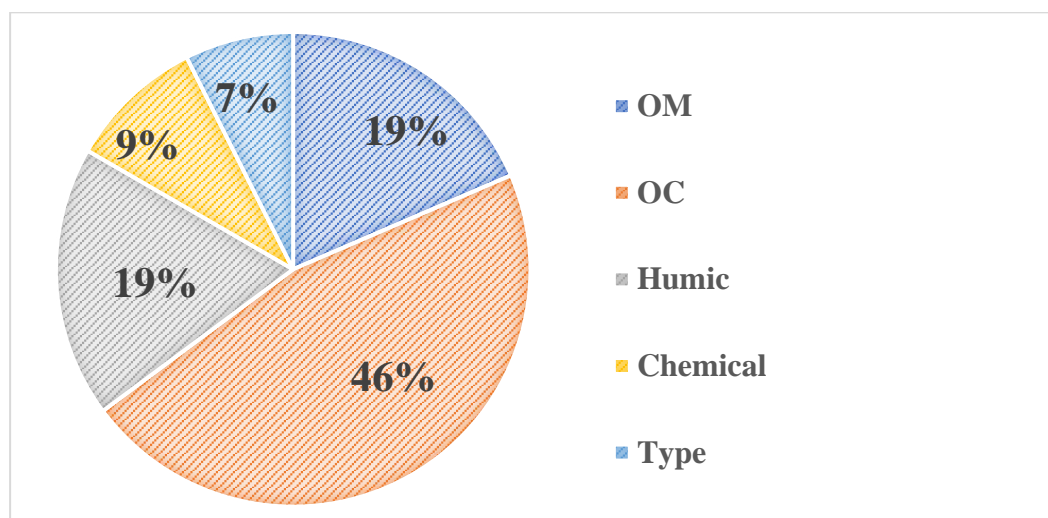


Figure 12. Depicts the SOM division used within literature, the main divisions include OM, types of organic carbon (OC), humic substances (HS), chemical functional groups and OM type e.g. peat. Chart created from 40 papers.

OM is the overall organic component of soil comprised of natural and/or anthropogenic OM, and can be divided into insoluble, particulate OM (POM), and dissolvable, dissolved organic matter (DOM) divisions. The latter of which can solubilise PAHs (Tao et al., 2006, Hwang and Cutright, 2004). OM and OC are often used interchangeably in the literature, OM includes all elements associated with organic compounds and is difficult to measure directly (Pluske et al., 2020). Commonly OM is determined by total organic carbon (TOC) shown in Equation 2, TOC is the total amount of carbon within SOM and is the most used term in the literature. TOC is useful to summarise the amount of OC within soil, however, is broad in terms of which specific organic components are present and acting as the dominant factors controlling the PAH sequestration and release. Most studies show that an increase in TOC will decrease the release of PAHs (Figure 13). Duan and Naidu (2013) showed that TOC accounted for ~68% of the variation in the sorption distribution coefficient for phenanthrene sorption. In another study, Luo et al. (2012) found that PAH extractability negatively correlated with TOC. Whereas TOC was found to be the most significant

parameter to increase sequestration and reduce biodegradation for pyrene and phenanthrene for Bogan and Sullivan (2003).

$$OM (\%) = TOC (\%) \times 1.72$$

Equation 2. Calculation of OM from TOC%.

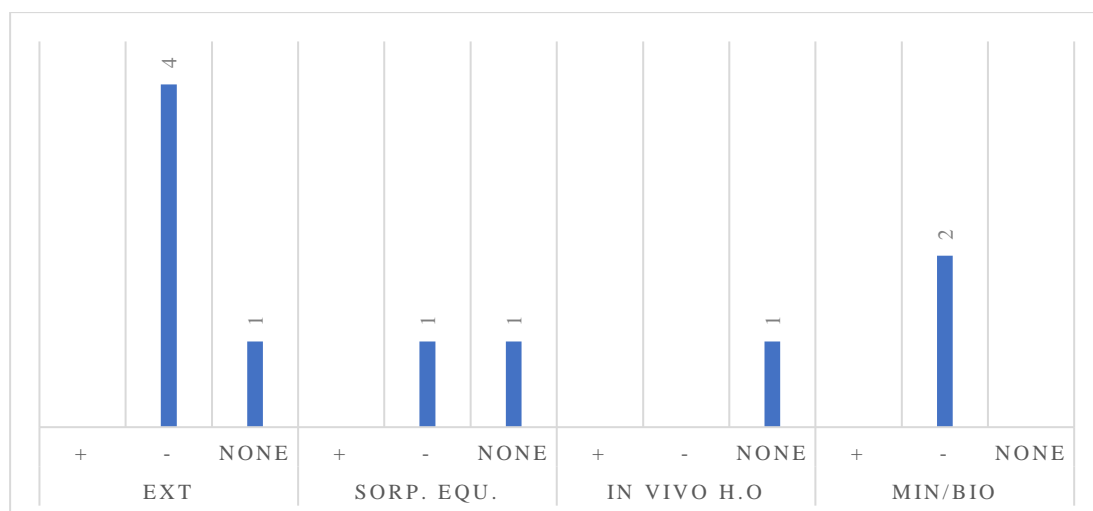


Figure 13. Correlation between PAHs release to TOC with different experimental methods, created from 10/40 papers reviewed. EXT = solvent extraction, SORP. EQU. = sorption equilibrium, IN VIVO H. O = in vivo high organisms' experiments, MIN/BIO = mineralisation/biodegradation.

2.5.3 Dual-mode sorption mechanism

Xing and Pignatello (1997) created the 'dual-mode' sorption model, which has become widely accepted among researchers to explain the non-uniform sorption potential of SOM. In this model, the sorption mechanism is determined by the type of OM (Semple et al., 2013), categorised as either a "glassy" or a "rubbery" state (Xing and Pignatello, 1997). However, other studies interchangeably describe glassy and rubbery states as OM or OC, with further relatable terms given for the rubbery state as soft OM/OC, labile OM/OC, amorphous OM (AOM), and the glassy state related with hard OM/OC, recalcitrant OM/OC, condensed OM/OC, or carbonaceous geosorbents (CGs).

Rubbery OM is described as a comparatively homogenous gel-like matrix, enriched in aliphatic carbons, including OM such as amino acids, lipids, lignins and humic and fulvic substances (Pehkonen et al., 2010, James et al., 2016,

Semple et al., 2013, Luthy et al., 1997). Sorption from the rubbery OM is seen as a rapid linear process with non-specific partitioning, which is non-competitive and reversible (Pehkonen et al., 2010, James et al., 2016, Luthy et al., 1997). In contrast, glassy OM is described as condensed OM enriched with aromatic carbons including black carbon (BC), kerogen and coke (Pehkonen et al., 2010, James et al., 2016, Luthy et al., 1997). Glassy OM sorption is slower and nonlinear, with competition for site-specific sorption sites. Both states use dissolution as a sorption mechanism, but the glassy state has the additional hole-filling mechanism, whereby PAHs can become entrapped in nanopores (Xing and Pignatello, 1997).

Both states generally occur within SOM heterogenous structures, resulting with rapid, slow, linear and nonlinear sorption and desorption occurring simultaneously in experimental studies (Semple et al., 2013). The amount of each state present in soil may potentially help dictate the PAH bioavailability. Hard OM/OC has been shown to have a high sorption and lower release of PAHs than soft OM/OC (Lueking et al., 2000, Luo et al., 2012, Umeh et al., 2018). For example, Lueking et al. (2000) showed that Lachine shale predominately containing hard carbon, had a less linear and slower PAH desorption than Michigan peat and Chelsea topsoil geosorbents containing fresher amorphous chemically oxidised soft carbon (Lueking et al., 2000).

2.5.4 Types of OC

Black carbon

Black carbon (BC) is a chemically heterogeneous carbon type, classed within the glassy/hard OC domains, produced by incomplete combustion of fossil fuels, wood and biomass and can be found ubiquitously in the environment (Semple et al., 2013). Formation involves either carbonization (charring) of OM by combustion (charcoal particles) or condensation of the gas phase (soot particles) (Andreae, 1995). BC is known as a strong sorbent for organic contaminants such as PAHs (Semple et al., 2013, Ukalska-Jaruga et al., 2019). Examples of BC include soot, unburned coal, kerogen, fly ash and charcoal, which all possess different structures and physicochemical properties (Semple et al., 2013, Huang et al., 2003). The structure of BC soot is aciniform (onion-like) whereas BC charcoal is formed of stacked aromatic planar sheets containing narrow pores

(Semple et al., 2013, Pehkonen et al., 2010, Hale et al., 2012). These narrow pores can be penetrated by PAHs which can form π - π interactions with the pore walls (Semple et al., 2013).

Semple et al. (2013) produced an insightful review on the impact of BC upon the bioaccessibility of organic contaminants in soil, determining that the majority of research has shown BC to reduce PAH bioavailability. BC has been suggested to only signify approximately 4% of soils TOC, although it can be accountable for 80% of the total sorption (Semple et al., 2013). The review also determined that types of BC and the behaviour of BC over long timescales needs further investigation, given that the physicochemical properties of BC can vary depending upon the BCs origin, combustion and weathering conditions, and mode of formation (Semple et al., 2013).

Humic substances

Humic Substances (HS) are organic substances that have remained after biomass transformation. HS have a high sorption capability due to their abundance of hydrophobic carbon domains that include macromolecular aliphatic chains, aromatic carbon components and high quantities of flexible pores (Ukalska-Jaruga et al., 2019, Ressler et al., 1999). HS can be divided by dilute base and acid solutions; fulvic acids (FA) are soluble in both acid and base solutions, humic acids (HA) are soluble in only base solutions, and humins (HN) are not soluble in alkaline solutions (Ukalska-Jaruga et al., 2019, Huang et al., 2003). HN is the least understood, but thought to comprise of unaltered and less-altered biopolymers, such as polysaccharides, lignin, mineral-bound lipids, humic acid-like materials, kerogen and BC (Huang et al., 2003). The majority of literature summarised in Figure 14 propose HN to be the most influential HS to reduce release of PAHs from soil.

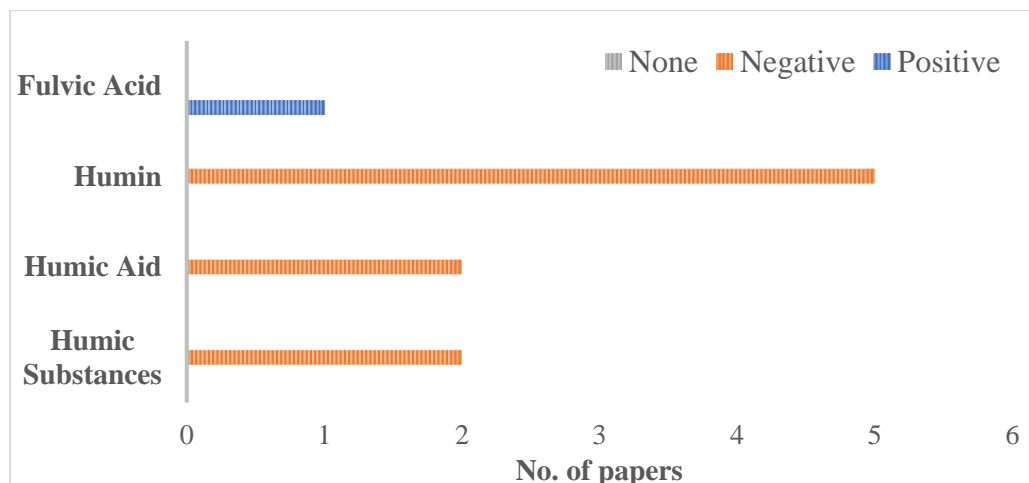


Figure 14. Bar chart of the correlation between the different HS and the release of PAHs from soil, created from 10 papers.

HS sorption ability can vary depending on other soil factors such as pH, decreasing pH has restrict PAH sorption due to protonation and coiled compact configurations which (De Melo et al., 2016, Jones and Tiller, 1999). HN has a strong affinity towards organic pollutants Pan et al. (2006) reported 55-76% of phenanthrene and 49-78% pyrene was residing in the HN fraction, with the percentages increasing with time, signifying that HN is the main fraction leading to slow sorption. HNs strong affinity to PAHs can be hindered by being bound to mineral particles and buried within the FA/HA fraction (Pan et al., 2006). Studies have separated minerals associated to HN (Chen et al., 2007) and SOM (Hwang and Cutright, 2002) to determine the impact minerals have on OM sorption to PAHs. Removal of minerals from HN increased the linearity and sorption capacity (Chen et al., 2007) and removal of clay from SOM showed a significant amount of desorption (Hwang and Cutright, 2002). Indicating that clay minerals are attributed as the PAH desorption-resistant fraction and that minerals can shield/block SOM binding sites (Hwang and Cutright, 2002).

Mineral size fractions interactions with OM

Yu et al. (2018) proposed that soil particle size can be used to distinguish SOM fractions, which avoids harsh thermal and oxidation treatments which may change OM functionality. SOM in the sand fraction are comprised mainly of fresh or slightly decomposed plant material, while the silt fraction contains partially degraded residues. Lastly, the clay-fraction SOM is highly contributed

by strongly processed OM, with aromatic and aliphatic structures which have a greater resistance to microbial degradation (Doick et al., 2005). The OC types in the silt and clay fractions are turned over more slowly than OC found in sand, and thus are more stable than sand OC and can accumulate compounds more effectively (Doick et al., 2005). A general trend in research has shown that the sorption of PAHs increases as the particle size decreases, therefore the amount of PAH release decreases in the order: sand > silt > clay. Reasoned to be due to the OM association to the size fraction.

2.5.5 Quantification of OC

To determine precisely which fraction of OM influences PAH bioavailability from soil, the quantification method and terminology used should be carefully considered. As certain terminologies can overlap with one another, such as BC is a subsection of TOC and hard OC. Additionally, studies use different classification/analytical methodologies to categorise supposedly the same OM fractions, which subsequently leads to analysis of different components being classed the same term. For example, applying harsher conditions will measure less OM as hard OC, meaning that the bioavailability results between papers carefully considered in direct comparisons. Both the sample process and OM quantification method are important factors in describing the main OC fractions impacting PAH release from soils when comparing studies.

The primary way to quantify BC is to either thermally or chemically treat the soil, or a combination of both, to obtain a BC residue. Difficulties in characterising BC sorption include BC being either modified or oxidised chemically when being isolated, or kerogen remaining in the BC (Huang et al., 2003). Comparing BC measurements between six different methods on individual samples ranged from a factor of 2 up to a factor of 571 (Schmidt et al., 2001), which demonstrates that correlating results between methods is very difficult. Increasing the intensity of the chemical attack decreased the measurable amount of BC (Schmidt et al., 2001). Another study determined that the three most commonly used methods to determine BC, including the benzene polycarboxylic acid (BPCA) method, UV/NMR method and the chemo-thermal oxidation (CTO) ¹³CNMR method, and determined that all these methods tend

to overestimate the content of BC (Gerke, 2019). Hence the PAHs bioavailability results compared to one another are subjective.

2.5.6 Quantification of bulk OM using Rock-Eval Pyrolysis

Another technique that has been applied to characterise soil OM, in this instance the bulk OM in soil is a technique called Rock-Eval Pyrolysis. Rock-Eval Pyrolysis uses temperature programmed heating under an inert atmosphere to inflict pyrolysis followed by combustion (oxidation) to a sample (Behar et al., 2001b, Lafargue et al., 1998). Both the quantity of hydrocarbons released, detected by flame ionization detector (FID) and the release of CO and CO₂ monitored by infrared (IR), are recorded in response to the increasing temperature versus time throughout the pyrolysis and oxidation stages (Lafargue et al., 1998). Use of Rock-Eval(6) Pyrolysis (RE) has shown to provide consistent and reproducible results, predominately used to assess the hydrocarbon potential, maturity and differentiation of source rocks for oil and gas exploration (Behar et al., 2001b, Lafargue et al., 1998). More recently RE is being used to investigate different types of OM in soils including contaminated soils (predominately oil spills) (Upton et al., 2018, Disnar et al., 2003, Hetényi et al., 2005, Könitzer et al., 2016, Lafargue et al., 1998).

RE advantages include the limited amount of sample preparation required, making RE relatively quicker than other methods, and a single RE measurement produces a range of parameters that can help characterise the varying hydrocarbons within samples. Descriptions of RE parameters and the associated links to the bioavailability of PAHs can be found in 5.3.4 Rock-Eval(6) Pyrolysis and 7.2 Introduction. The percentage of residual carbon (RC%) is one RE parameter, calculated using the percentage of hydrocarbons that survived the pyrolysis stage as a fraction of the TOC measured by RE. The RC% is thought to be composed of refractory OC such as soot, char, coal and kerogen. Poot et al. (2014) found BC to be approximately 7% of RC determined by RE. The study found that the RE RC% gave improved predictions of the 4-ring PAHs desorbing fractions compared to BC measured by chemo-thermal oxidation 375°C (CTO375) (Poot et al., 2014). Their study showed that increasing the RC%, increased the amount of carbonaceous material, resulting with more PAHs

residing in these domains and creating a large very slow desorbing fraction (Poot et al., 2014).

Other studies have applied RE as a screening tool to help determine the extent of PAH contamination (Wu et al., 2012, Haeseler et al., 1999, Disnar et al., 2003). To my knowledge only Haeseler et al. (1999) has detailed the characterisation of MGP contaminated soils with RE. However, their study only analysed five MGP soils with an older instrument (Rock-Eval III) which excludes several of the RE parameters that the Rock-Eval(6) instrument can measure. Furthermore, their study does not investigate the RE parameters relationship with the PAH bioavailability in MGP soils. Other studies have investigated the use of RE in studying influences with PAH desorption using Tenax extractions on sediments (Oen et al., 2006, Poot et al., 2014). However, these studies used sediments and not contaminated MGP soils which are expected to experience differences in contamination sources (OC types), environmental conditions and higher PAH concentrations. Consequently, it is predicted that the RE parameters values for MGP soils will differ to sediments and therefore produce differing relationship results between the bulk OC and PAH desorption.

2.5.7 Inorganic components role

The majority of papers have stated that the main factor dominating PAHs behaviour in soil is from the organic fraction of soil (Ehlers and Loibner, 2006). Some authors propose neglecting minerals if the OC content is >0.1% (Pan et al., 2006), particularly in water-soil systems, where water is preferred to be adsorbed compared to PAHs onto a minerals surface (Xing, 1997). Other researchers have argued that both SOM and minerals (particularly clays) are the main sorbents controlling PAH sorption and release (Hwang and Cutright, 2004). When the soil contains limited amounts of OC, measured sorption coefficients were still often higher than predicted (Mader et al., 1997, Hwang and Cutright, 2002) suggesting that the mineral phase impacts sorption activity (Mader et al., 1997).

PAHs can adsorb to inorganic surfaces by participating in linear reversible processes, where the diffusion is controlled by pore & diffusant sizes (Ehlers and

Loibner, 2006, Luthy et al., 1997). Research has suggested that minerals can bind to the aryl-C in OM (Ahangar et al., 2008), suggesting that the presence of minerals blocks the higher affinity OM divisions from binding to PAHs, which subsequently increases the PAH bioavailability. In contrast, Hwang and Cutright (2002) showed that removing either clay minerals or OM from bulk soil increased the PAH releases compared to the bulk soil, indicating that mineral-OM interactions can hinder bioavailability. Hwang and Cutright (2003) argued that OM, clay minerals and size fraction are equally as important in the sorption of PAHs.

2.5.8 Particle and pore size

Duan et al. (2014) showed that the relative bioavailability (RB) of BaP correlated negatively with the fine particle associated carbon (FPAC) value and the percentage proportion of pore sizes <6 nm. FPAC is calculated using Equation 3, the negative correlations correspond with smaller particles having higher amounts of clay and OM which can adsorb PAHs, especially HMW PAHs like BaP.

$$FPAC = (Slit + Clay)/TOC$$

Equation 3. Calculation for the fine particle associated carbon (FPAC).

However, in the oral bioavailability swine model study by James et al. (2016), no relationship between FPAC and the bioavailability of the five PAHs studied was found. Although, other work has shown that a decrease in particle size decreases PAH release (Brändli et al., 2008). The contradiction between studies needs further research to agree upon the role of particle and pore sizes, or whether the results gained were additionally affected by other soil properties.

2.5.9 Soil moisture

A few papers have studied the impact of moisture on PAH release from soil. Hu and Aitken (2012) determined that increasing the soil moisture content (SMC) decreases PAH desorption, whereby HMW PAHs showed no significant difference in desorption between a SMC of 2% and 8%, but a dramatic decrease in desorption at 20%. This occurrence could be the result of the HMW PAHs higher hydrophobicity prohibiting the release and diffusion of PAHs from soil.

2.5.10 Multiple linear regression analysis and highlighted literature

Soil is a complex system and the need to analyse multiple parameters together will enable a more accurate understanding on soils physicochemical properties effect on PAHs bioavailability. Only a limited number of studies have examined soil with multiple linear regression (MLR) and principal component analysis (PCA) as shown in Table 5, with limited numbers of PAHs behaviour examined. Slight differences between soil parameters could be the result of the different experimental methods used, however the main soil parameters affecting PAH release from the majority of studies are related to OC, the finer particle size minerals and pore fractions, which agrees with most of the literature studied. Appendix A Table S1 lists highlighted research papers which were reviewed within this literature review with interesting results between soil properties and the fate of PAHs in soil, including PAH bioavailability, biodegradation, extractability, sorption and desorption experimental values.

Table 5. Lists the research papers who undertook MLR and PCA.

Paper	Type	No. PAHs	No. Soils	Experiment	Endpoints	Key Parameters
<i>Chung and Alexander (2002)</i>	MLR	1	16	Mineralisation and extractability	% Decrease in mineralisation	OC, silt
					% Decrease in extractability	OC, clay, cationic electronic conductivity
					% Not mineralised	OC
					% Not extracted	OC, silt
<i>Luo et al. (2012)</i>	MLR	3	7	Extractability	K_{slow}	Hard OC, PF 6nm
					K_{rap}	PF 6nm, TOC
<i>Duan and Naidu (2013)</i>	MLR	1	32	Sorption partition coefficient	Modified Freundlich coefficient K'_f	TOC, clay
					$\log K_{OC}$	Log TOC, clay, log DOC, sand, clay
<i>Crampon et al. (2014)</i>	PCA	7	5	Degradation	Pearson correlation coefficients (r) for HMW PAHs	Smectite, mature geopolymers

2.6 Literature summary

In reviewing the literature, several gaps have been identified and will be investigated in this research, which fulfils research objective one from Section 1.2.3. There are several uncertainties relating to the dermal bioavailability of PAHs from soil, due to the limited amount of research on the area. The research gaps established include the lack of investigations analysing field-contaminated soil samples, compared to the number of studies using spiked soils which have been linked to overestimating PAH release from soil. Secondly, there is not enough use of diverse PAH types and mixtures, specially, there are no studies investigating the dermal bioavailability of alkyl-PAHs in MGP soils. Thirdly, there is limited research on the dermal bioavailability of PAHs from former MGPs soils. Only 4 papers investigated soils properties effects on the dermal bioavailability of PAHs with low numbers of soil properties. In addition, there is no known research using Rock-Eval Pyrolysis parameters to determine relationships between the dermal bioavailability of PAHs and the bulk OM fractions.

With these literature gaps in mind, my research focuses on determining the dermal bioavailability of PAHs from real-world contaminated soils from former MGPs. Use of such soils delivers benefits of investigating an abundance of different PAH mixtures at various concentrations, thus will provide an improved representation of a real human dermal exposure from contaminated soil. I will use an *in vitro* dermal simulation method to analyse the dermal bioavailability of several different PAH compounds (>20 PAH compounds). The selected PAHs will include the EPA16, parent PAHs with higher toxicities than BaP and alkyl-PAHs. MGP soils are expected to have elevated proportions of hydrocarbon contamination, hence the OC fraction and particle size are suspected as being dominate factors and will be investigated. These soil properties will be investigated using RE and particle size analysis (PSA). By addressing the above research gaps this thesis is expected to contribute valuable insights into the complex relationships between PAH mixtures, soil properties and the dermal bioavailability of PAHs, ultimately adding to the knowledge needed to help improve the estimation of risks posed by PAHs in contaminated soils.

CHAPTER 3

METHODOLOGY

3.1 Introduction

In this chapter the experimental and analytical methodologies used in this research are outlined in addition to the quality control (QC) methods used to assess the performance and credibility of the results. The fundamentals of the methods are described in the research papers found in Chapters 5-7, therefore, to avoid repetition this section of the thesis will provide details of the methodologies not included in the research papers. Several details from the supplementary information (SI) of the research papers (now in Appendices B-D) are placed in this chapter for the benefit of the thesis.

This chapter presents the full sample preparation methods and analytical methods for measuring PAHs *via* gas chromatography tandem mass spectroscopy (GC-MS/MS). Methods to measure the soil properties included Rock-Eval(6) Pyrolysis (RE), to measure the bulk OM, and particle size analysis (PSA). Subsequently, the method for the *in vitro* dermal experiments is presented and finally the QC methods applied throughout the research reported. For ease of reading about the different experimental batches within this research, the batches are abbreviated. All MGP soil samples analysed for PAH concentrations and RE values investigated Chapter 5 are abbreviated to GWS-CH batch, samples from the dermal *in vitro* control reference soil study using a certified reference material (CRM) BCR-524 are abbreviated as the DCRM batch and samples from the dermal *in vitro* experiments using five MGP soils are abbreviated as the DGWS batch.

3.2 Soil sampling and selection

Site access to collect MGP soil samples was provided by National Grid Property Holdings and remediation contractors. The locations of the sites are commercially sensitive and are therefore not presented here. Sample collection took place between 2016 – 2021 from 10 UK former MGP sites, including a gasholder station, and a former tar distillation plant at a chemical works of a

large city gasworks site. Sample collection occurred while the sites were under investigation or remediation by National Grid Property Holdings, which influenced where and when sampling could occur.

The temporal span of sample collection can influence the concentrations and distributions of PAHs in soils. The MGP sites have been inactive for a range of 46-99 years, making the sampling time span relatively short in comparison. The current study primarily serves as a proof-of-concept exploration, with the aim to determine the feasibility of characterising MGP soils in accordance with MGP processes. Consequently, a wide array of samples was collected from various former MGP sites, enabling a comprehensive evaluation of different MGP processes. This approach aimed to capture the realistic contamination scenarios faced by risk assessors during periods of site investigation and worker exposure. Therefore, the impact of time span and sample collection ages were not evaluated in this study but is suggested for future work. Appendix B Chapter 5 Research Papers SI Table S1-S2 present details of the site histories and MGP processes that were used at each site and the details of each sample collected.

Samples were stored in amber glass jars in chest freezers until initial sample preparation. The BGS Soil Preparation Team initially freeze-dried samples, which is a technique recommended over other drying methods when measuring PAHs (Beriro et al., 2014). Freeze dried samples were sieved through a 250 μm brass mesh and the <250 μm fraction was used in further experimental procedures (Kim et al., 2017). The sieved soils were stored into new amber glass jars in a dry, dark cool storage area until required for PAH quantification or *in vitro* dermal experiments.

3.3 Rock-Eval(6) Pyrolysis

Rock-Eval(6) Pyrolysis (RE) was used to characterise the bulk OM in the soils and was conducted by a lab technician at BGS. Full details of the RE method and the parameters measured can be found in Section 5.3.4 Rock-Eval(6) Pyrolysis.

3.4 Particle size analysis

Full details of the PSA method can be found in Section 7.3.2 Soil properties – Rock-Eval(6) Pyrolysis and Particle Size Analysis. It is noted that the Wentworth

scale applied to categorise the particle sizes traditionally includes size fractions > 250 μm , with sand fractions ranging in sizes of 62.5-2,000 μm , silt fraction ranging in sizes of 3.9-62.5 μm and clay ranging in sizes of 0.006-3.9 μm . However, this study was focusing upon the particle sizes most likely to adhere to skin. As taken from SI of Chapter 6 paper, the selection of the <250 μm fraction was based on its relevance to potential adherence to children's hands and its comparability to other *in vitro* methods for assessing both oral bioaccessibility and dermal bioavailability (Beriro et al., 2020, Lort, 2022, Forsberg et al., 2021). Moreover, previous research by Kissel et al. (1996) demonstrated that soils with larger grain sizes exhibited increased adherence when the moisture content exceeded 10%. As the soil moisture content in my study surpassed this threshold, the upper size fraction of 250 μm was chosen for my investigations.

3.5 Soil selection for PAH quantification

A subsample of MGP soils were selected for PAH quantification due to the limited availability of the GC-MS/MS instrument. To select the soils with the most diverse soil properties to explore for research objective 4 and 8, both RE and PSA values were used to cluster soils with similar soil properties. Figure 15 presents a workflow diagram of the steps used to choose the soils for PAH quantification for Chapter 5. Ten RE parameters were used in k-means clustering on the 94 soils, these ten parameters were selected from the eighteen available RE parameters. Only ten parameters were selected as several RE parameters are derived from another RE variable, hence removal of these parameters removed potential bias towards interlinked RE parameters. The ten RE variables used for the k-means clustering were S1, S2, TpkS2, S3CO, S3'CO, S3, S3', PC%, RC% and TOC%. A k value of 5 was chosen as avoided overlapping of clusters and overcomplicating the model, additionally a k=6 produced similar clusters. The resulting clusters are presented in the principal component analysis (PCA) biplot Figure 16, whereby ~88% of the samples are in clusters 1 and 5, showing that most MGP soils have similar values for the ten selected RE parameters. Subsequent k-means clustering cluster (k=2) was applied using additive log ratio transformation (ALR) values of sand/clay, to determine clusters based on particle size. Afterwards, random sampling was applied using the sample() function in R

(R Core Team, 2023) for each cluster. 50/95 soils were selected and quantified for PAHs using GC-MS/MS.

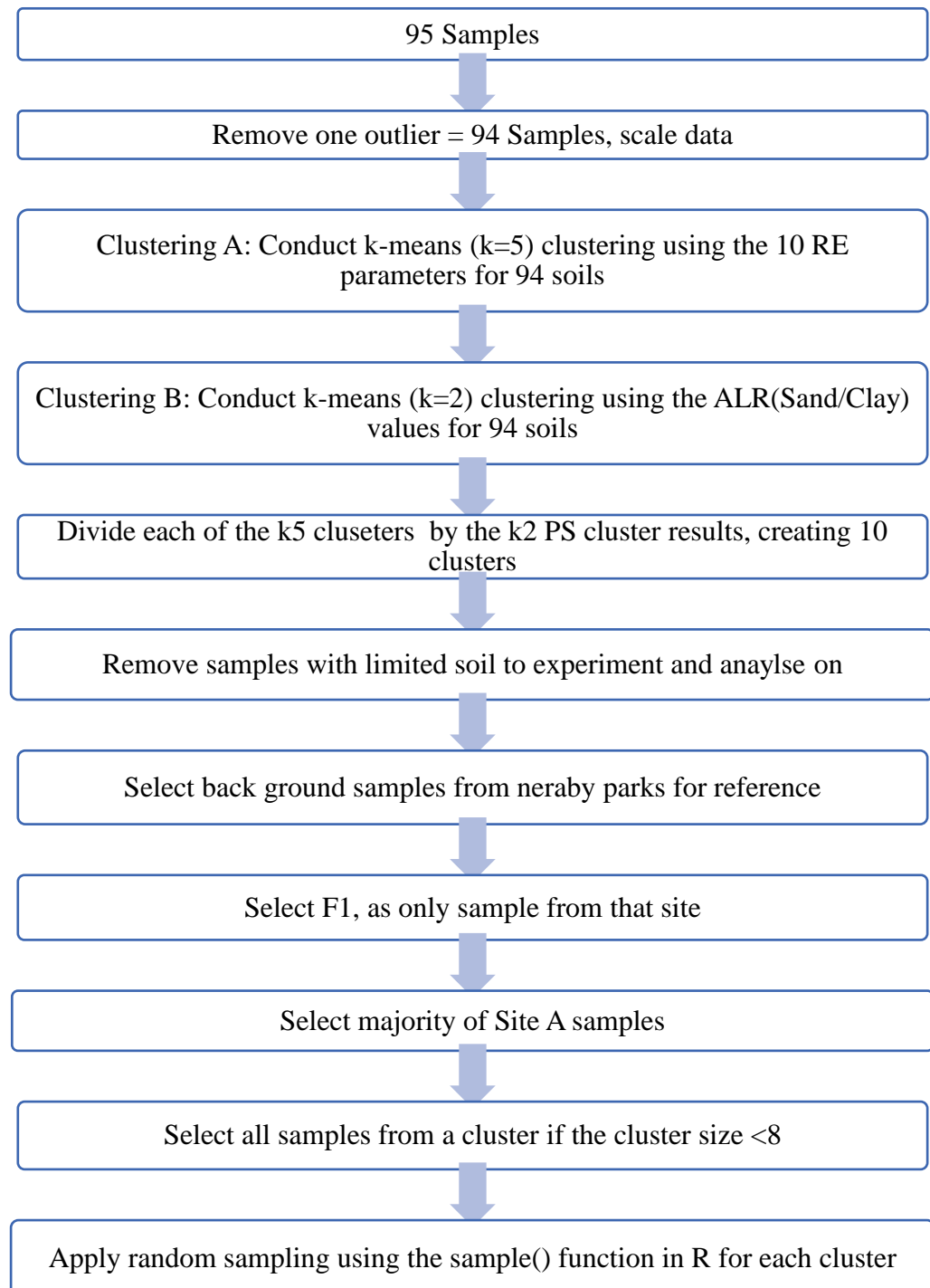


Figure 15. Workflow diagram of the steps used to choose the soils for PAH quantification.

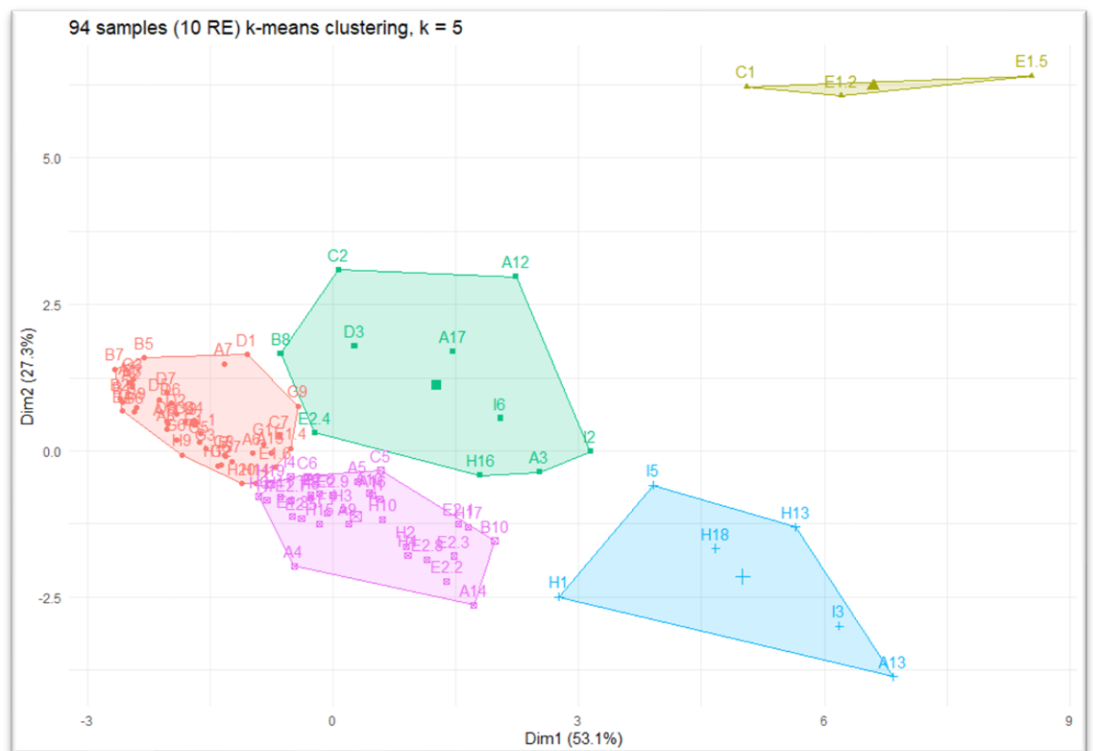


Figure 16. PCA biplot of the *k*-means clustering (*k*=5) using the ten RE parameters of 94 MGP soils.

3.6 Soil selection for the *in vitro* dermal experiments

This section was taken from the SI of Chapter 6 and describes how five MGP soils were selected from the 48 MGP soils with measured PAH concentrations. Use of the *k*-means clustering created above and shown in Figure 16 was used in soil selection for the dermal experiments. To identify the most suitable soils for the dermal experiments the selection process considered three criteria: (1) one soil was chosen from each *k*-means cluster to represent that cluster, (2) the selected soils originated from different MGP sites, and (3) the benzo[*a*]pyrene (BaP) concentration exceeded the Generic Assessment Criteria (GAC) (> 5 mg/kg) as stipulated by CL:AIRE (2014). Satisfying these conditions, the following soils were chosen for the dermal experiments: A11, E1.5, E2.7, H16 and I3.

3.7 Sample preparation and PAH extraction

This section will present the general methods used in this study for the preparation and PAH extraction of samples (soil, membrane and receptor solution (RS)). The procedures used are well-established procedures used by the

BGS Organic Geochemistry laboratory (Vane et al., 2021, Vane et al., 2020, Kim et al., 2017, Lort, 2022). The materials and chemicals used in the research are listed in Table 6 which was taken from the SI of Chapter 6. The following sections were also taken from the SI sections from Chapter 6.

Table 6. List of the materials and chemicals used in the research and the suppliers of the materials.

Use	Material/chemical
Solvents and materials used for general sample preparation	Copper 99% powder, max. 106 µm (Acros organics); Thermo Scientific ASE cellulose extraction filters; pentane ≥95%, (Fisher Scientific); hexane ≥95% (Fisher Scientific), methanol (Fisher Scientific); acetone ≥99.8% (Fisher Scientific); dichloromethane (DCM) ≥99.8% (Fisher Scientific); and toluene 99.85% (Acros Organics).
Deuterated PAHs used as surrogates and internal standards (I.S)	Purchased from QMX Laboratories Ltd which included phenanthracene-d10, pyrene-d10, benzo[b]fluoranthene-d12, benzo[a]pyrene-d12, benzo[g,h,i]perylene-d12, fluorene-d10, fluoranthene-d10, perylene-d12 and indeno[1,2,3-c,d]pyrene-d12.
PAH Mix Standards	Purchased from the supplier QMX Laboratories Ltd and contained: PAH-Mix 45, 10 µg/mL in cyclohexane: naphthalene, acenaphthylene, acenaphthene, fluorene, phenanthrene, anthracene, fluoranthene, pyrene, benz[a]anthracene, chrysene, benzo[b]fluoranthene, benzo[k]fluoranthene, benzo[e]pyrene, benzo[a]pyrene, perylene, indeno[1,2,3-c,d]pyrene, dibenz[a,h]anthracene, and benzo[g,h,i]perylene. PAH-Mix 183, 10 µg/mL in cyclohexane: 7H-benzo[c]fluorene, cyclopenta[c,d]pyrene, benz[a]anthracene, chrysene, 5-methylchrysene, benzo[b]fluoranthene, benzo[k]fluoranthene, benzo[j]fluoranthene, benzo[a]pyrene, indeno[1,2,3-c,d]pyrene, dibenz[a,h]anthracene, benzo[g,h,i]perylene, dibenzo[a,l]pyrene, dibenzo[a,e]pyrene, dibenzo[a,i]pyrene, and dibenzo[a,h]pyrene. PAH-Mix 9, 10 µg/mL in cyclohexane: naphthalene, acenaphthylene, acenaphthene, fluorene, phenanthrene, anthracene, fluoranthene, pyrene, benz[a]anthracene, chrysene, benzo[b]fluoranthene, benzo[k]fluoranthene, benzo[a]pyrene, indeno[1,2,3-c,d]pyrene, dibenz[a,h]anthracene, and benzo[g,h,i]perylene.

Dermal <i>in vitro</i> experiment components	Strat-M™ (47mm diameter) membranes were purchased from Merck Millipore (Watford, UK), Hanks' Balanced Salt Solution (HBSS) purchased from ThermoFisher Scientific (Loughborough, UK), Bovine Serum Albumin (BSA) purchased from Merck Life Science UK Ltd. (Gillingham, UK) and HEPES purchased from ThermoFisher Scientific (Loughborough, UK).
Solid phase extraction (SPE) cartridges	Strata PAH SPE cartridges (0.75g/6mL) purchased from Phenomenex Ltd (Macclesfield, UK) for receptor solution clean-up, and Agilent, Bond Elute TPH w.500 mg Na2SO4, 1g sorbent, 3 ml reservoir volume purchased from SLS (Scientific Laboratory Supplies Ltd.) (Nottingham, UK).

3.7.1 Soil sample preparation

Soil sample preparation is detailed in Section 5.3.2 and in this section, although the same techniques of accelerated solvent extraction (ASE), solid phase extraction (SPE) and GC-MS/MS were applied to all soil samples, deviations in the soil weight, ASE dilution, aliquot amount and spiking concentrations of surrogates varied due to improved estimations of the soils PAH concentrations.

This next section was taken from the SI sections from Chapter 6 and provides an overview of the soil preparation methods, which can be applied to all the soil batched processed. For soil preparation, weighed samples (0.5 g for MGP soils and 1.0 g for CRM) were spiked with deuterated PAH surrogates. To eliminate elemental sulphur from the soils, approximately 2 g of activated copper powder was added, along with approximately 5 g of clean sodium sulphate as a dispersing agent. The extraction process was performed using ASE with the Dionex ASE 350 instrument, utilising a mixture of dichloromethane (DCM) and acetone (1:1 v/v) at 100°C and 1500 psi, following the methodology described by Lort (2022). Subsequently, the ASE extracts were diluted, and an appropriate aliquot was selected based on the expected PAH concentration in the sample, Table 7 provides the spiking and volume metrics for each sample.

Table 7. Sample preparation and spiking values for the soil samples measured in the different experimental batches. Acronyms in the table include soil weight (wt.), PAH surrogate (Surr.) volume (vol.) and the PAH internal standards (I.S).

Batch	Sample	Soil Wt. (g)	Spiked Surr. (pg/ μ L)	ASE dilution vol. (mL)	Aliquot (μ L)	GC-MS Vial (mL)	Spiked I.S (pg/ μ L)
GWS-CH	NIST-1944	1.0	200	50	2000	1.0	200
	2 BG soils	1.0	200	50	2000	1.0	200
	48 MGP soils	0.5	200	50	400	1.0	200
DCRM	NIST-1944	1.0	200	50	2000	1.0	200
	BCR-524	0.5	80	50	800	1.0	200
DGWS	NIST-1944	1.0	200	20	800	1.0	200
	MGP soils (exc. E1.5)	0.5	200	20	200	1.0	200
	E1.5 MGP soil	0.5	80	50	40	1.0	200

The samples subsequently underwent solvent transfer to cyclohexane and were subsequently filtered using SPE with a Varian Bond Elute TPH cartridge (500 mg Na₂SO₄, 1 g sorbent, 3 mL reservoir volume). The SPE cartridges were conditioned with 6 mL of pentane before loading the sample. To elute the first fraction containing alkanes, 1.5 mL of pentane was used. A second fraction, containing the desired PAH fraction, was eluted with 6 mL of hexane/isopropanol (97:3 v/v), as previously applied by Vane et al. (2020). The sample subsequently underwent solvent transfer to toluene, followed by using a gentle stream of nitrogen to blow down the sample. After which deuterated PAH internal standards (I.S) were added to makeup to 1 mL before the GC-MS/MS analysis. The details of each specific soil sample preparation values for the surrogate and I.S spikes, ASE dilution and aliquots are presented in Table 7.

3.7.2 Membrane and receptor solution sample preparation

This next section was taken from the SI sections from Chapter 6 and provides an overview of the sample preparation methods used for the membrane and receptor solution (RS). The processing of membranes and RS followed procedures similar to those used by Lort (2022). Membranes air dried after dermal experimentation were spiked with surrogates and subsequently cut into fragments using cleaned

scissors to increase the surface area for extraction. These membrane pieces were combined with approximately 0.5 g of activated copper powder and approximately 5 g of clean sodium sulphate before undergoing ASE extraction with DCM:acetone (1:1 v/v) at 50°C and 1500 psi, consistent with Lort (2022) methodology. ASE membrane extractions were diluted with 50 mL, and an aliquot (2 mL for 1-hour membranes and 1 mL for 10 and 24-hour membranes) was taken for filtration through SPE, following the same method as applied to the soil samples.

Unlike the membranes, the RS did not undergo ASE. Instead, the full volume of RS (~33 mL) was spiked with deuterated PAH surrogates. The RS samples were mixed with acetonitrile (1:3 v/v) and loaded into a Strat PAH SPE cartridge (0.75 g/6 mL), pre-conditioned with 10 mL DCM, 10 mL methanol, and 20 mL deionised water. After loading the sample, the SPE cartridge was washed with 5 mL of methanol:deionised water (1:1 v/v) and dried under 10” Hg vacuum for 20 seconds before eluting the desired PAH fraction with 6 mL of DCM, in accordance with Lort (2022) procedure. To ensure the absence of water in the eluted sample, the RS extract was passed through a Pasteur pipette filled with sodium sulphate and clean glass wool. The resulting RS extract was blowdown, spiked with deuterated PAH internal standard and topped up to fill a 250 µL GC-MS insert, before being analysed by GC-MS/MS. Table 8 presents the sample preparation metrics for the membrane and RS samples for the dermal experiment batches.

Table 8. Sample preparation and spiking values for the membrane and receptor solution samples measured in the DCRM experiments (with BCR-524) and DGWS experiments (with MGP soils). *Full volume of RS analysed.

Batch	Sample Type	Timestep (hr)	Spiked Surr. (pg/ μ L)	ASE dilution vol. (mL)	Aliquot (μ l)	GC-MS Vial (mL)	Spiked I.S (pg/ μ L)
DCRM	Memb.	1	1250	50	8000	1.0	200
		10, 24	50,000	50	200	1.0	200
	RS*	1, 10, 24	80	NA	NA	0.25	20
DGWS	Memb.	1	200	50,000	2000	1.0	200
		10, 24	200	50,000	1000	1.0	200
	RS*	1, 10, 24	80	NA	NA	0.25	20
	(excl. E1.5)						
	E1.5 RS*	1, 10, 24	1600	NA	NA	0.25	80

3.8 Gas Chromatography Tandem Mass Spectroscopy

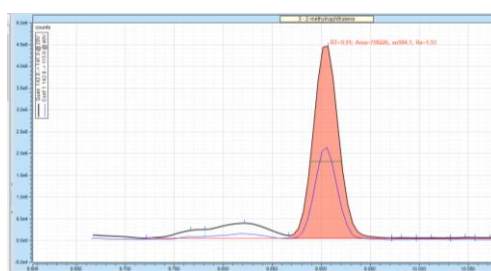
3.8.1 GC-MS/MS method development

To quantify a diversity of PAHs at varying concentration levels in all the sample types (soil, membrane and RS), a gas chromatography tandem mass spectrometry (GC-MS/MS) method utilising selected reaction monitoring (SRM) mode was developed as part of this research. Reasons for selecting this analytical method were described in Section 2.4.2. To develop this GC-MS/MS method, values for the targeted fragment ions, retention times (RT) and collision energies were collected from two literatures (Ghetu et al., 2021, Sørensen et al., 2016) and trialled on both the NIST-1944 CRM and a randomly selected MGP soil. Development of the GC-MS/MS method included comparing the full scan chromatogram peaks to the SRM chromatogram peaks for the PAH standard mixes (MX9, MX45 and MX183), the CRMs and a randomly selected MGP soil to determine the relative retention times for the method. Large RT windows were used to identify the alkyl-PAH series RT, peaks produced in these RT windows were compared to the alkyl-PAH chromatogram peaks reported in Ghetu et al. (2021) SI. Improvements to the GC-MS/MS method occurred throughout the research, including changing RT due to the instrument and column performance

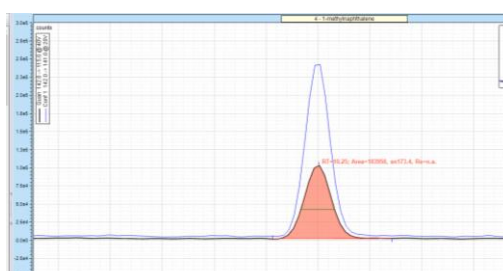
varying over time and adding additional PAH SRM parameters from uncovered literature research found later.

3.8.2 GC-MS/MS method

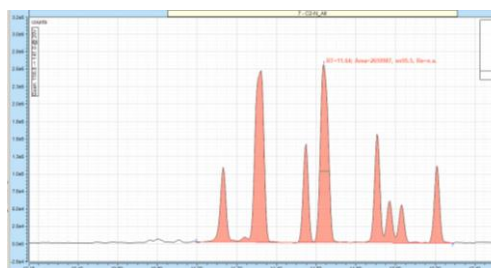
The details of the GC-MS/MS instrument parameters are detailed in Chapter 5 and Chapter 6 Methodology sections. The full list of RT, windows, quantifier precursor ions, quantifier product ions and collision energies are presented in Appendix A Table S2. Figure 17 presents examples of the peak integrations of the alkyl-PAHs for the CRM NIST-1944. Chromatogram peaks were integrated on the software Chromeleon 7.2.10 and the calibration levels of PAH mix standards were used by the software to calculate respective concentrations. These concentrations were exported to Microsoft excel where recoveries of the surrogates were applied for correction of the PAH concentrations. Lab procedurals (ASE dilutions, aliquots, weighed samples) are factorised in the concentrations to determine actual concentrations. Concentrations calculated above the >LOQ were taken as the PAH concentration for the sample.



2-methylnaphthalene



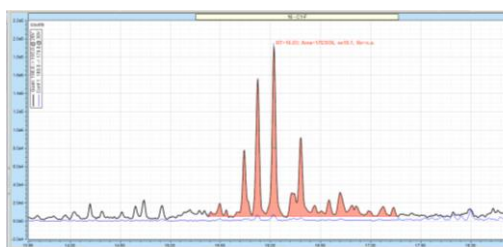
1-methylnaphthalene



C2-Nap



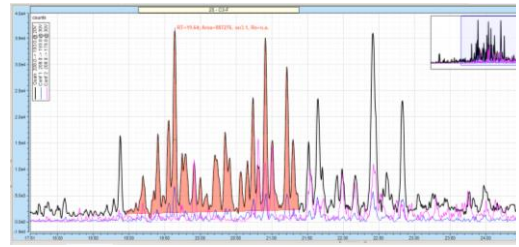
C3-Nap



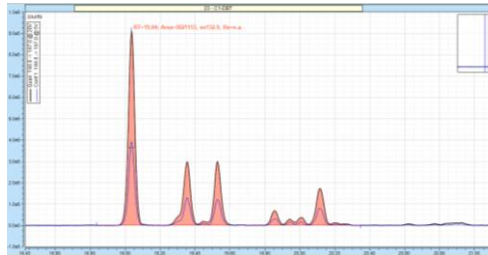
C4-Nap



C1-Flu



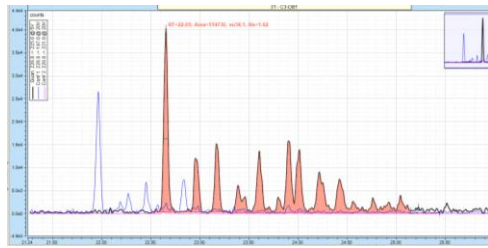
C2-Flu



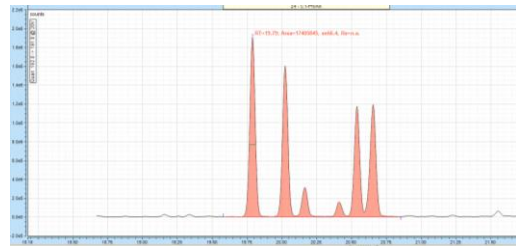
C3-Flu



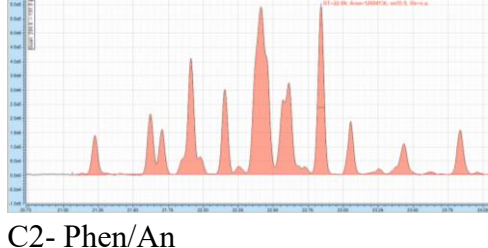
C1-DBT



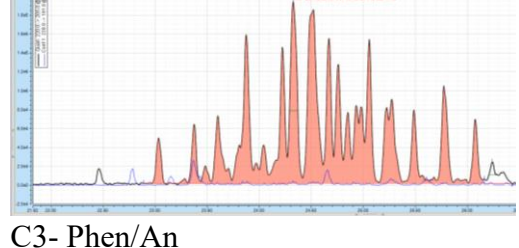
C2-DBT



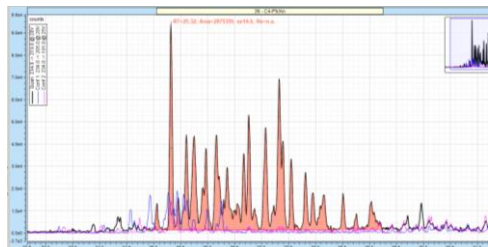
C3-DBT



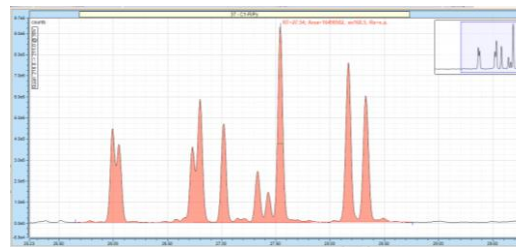
C1-Phen/An



C2-Phen/An



C3-Phen/An



C4-Phen/An



C1-Fla/Pyr



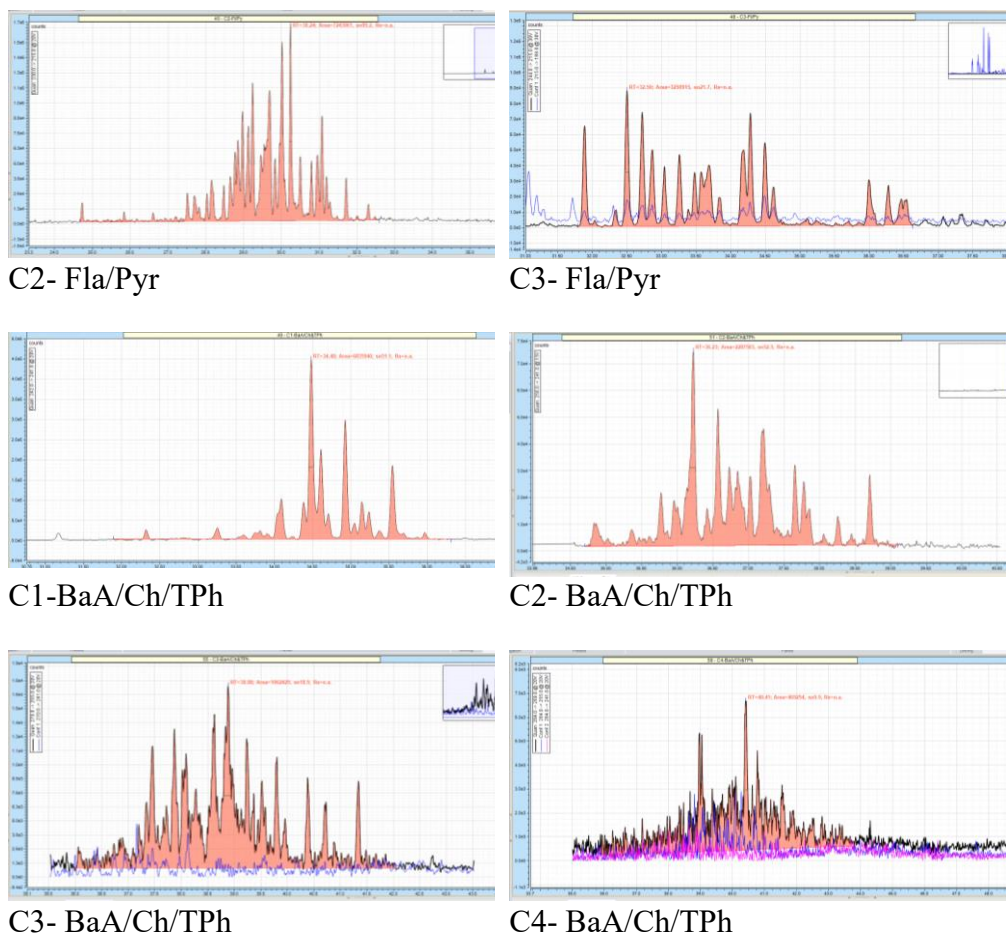


Figure 17. Alkylated PAH Peak Integrations for the CRM NIST-1944

3.8.3 GC-MS/MS calibrations

Calibrations used to quantify PAHs in this study comprised of a PAH standard mix (MX45 or MX9 or MX183), surrogates and internal standards (I.S.). Deuterated surrogates used included phenanthrene-d10, pyrene-d10, benzo[b]fluoranthene-d12, benzo[a]pyrene-d12 and benzo[g,h,i]perylene-d12. Deuterated I.S. used included fluorene-d10, fluoranthene-d10, perylene-d12 and indeno[1,2,3-cd]pyrene-d12. Six calibration levels were used, whereby the I.S. would consistently be spiked at 200 pg/ μ L and the PAH standard mix and surrogates would be spiked at increasing concentrations of: 10 pg/ μ L, 20 pg/ μ L, 80 pg/ μ L, 200 pg/ μ L, 400 pg/ μ L and 700 pg/ μ L. A large concentration range was required to capture all the varying concentrations in the MGP soils. Three replicas were run for each calibration and a linear plot generated from the results.

3.8.4 GC-MS/MS LOD and LOQ

The limit of detection (LOD) and limit of quantification (LOQ) are used to describe the smallest amounts that are measured reliably by an analytical method. The LOD and LOQ for PAHs were calculated using a signal-to-noise ratio of 3 for LOD and a signal-to-noise ratio of 10 for the LOQ, calculated using the lowest calibration level samples (10 pg/μL) (Slezakova et al., 2011, Alawi and Azeez, 2016, Baltrons et al., 2013). The calculated LOD and LOQ (pg/μL) were converted to the same units as samples by factoring the sample preparation dilutions, aliquots and weight/volumes. HMW PAHs soils had a LOD range of 0.003 – 0.257 mg/kg and a LOQ of 0.010 – 0.857 mg/kg, membranes had a LOD range of 0.006 – 0.257 μg/g and a LOQ of 0.038 - 1.71 μg/g, and RS had a LOD range between 0.0007 – 0.0312 ng/mL and a LOQ between 0.001 – 0.104 ng/mL (see Section 4.2.4 GC-MS/MS detection limits for full details).

3.9 *In vitro* dermal experiments

Investigating the dermal bioavailability of PAHs from soils in this research is part of the continuous work between the BGS and the UoN. The first project was funded by the STARS (Soils Training and Research Studentship) CDT for Lort (2022) and this second project is funded through the ENVISION DTP (Doctoral Training Partnership). This section will present the *in vitro* dermal method initially created by Lort (2022) and how this study developed this method to apply to further MGP soils and increased varieties of HMW PAHs. The next few sections about the dermal *in vitro* experiments are taken from a combination of sources of my work including the methodology section of research paper 2, the SI of Chapter 6 (paper 2) and additional information about methodology for context placed here for ease of reading.

3.9.1 *In vitro* dermal experiment method development

While Lort (2022) conducted dermal experiments on two MGP soils and the CRM soil BCR-524, measuring three PAHs (BaP, Pyr, and DahA), my study extended the investigations to five MGP soils and the same CRM BCR-524, quantifying 20 parent and 7 alkylated HMW PAHs. Lort (2022) provided a comprehensive account of the development and performance of the *in vitro* dermal experiment method. Lort (2022) assessment of the method's performance was validated by comparing the dermal fluxes generated from spiked solutions

with published data, which confirmed efficient PAH absorption using the dermal experiment method. Lort (2022) reported a favourable mass balance with the method, achieving an effective removal of the soil from the membrane and a reduced variation in PAH adsorption from soil samples compared to other studies. Given that Lort (2022) had previously reported the effectiveness of the dermal *in vitro* method with soils, my study deemed it appropriate to apply the same methodology.

In this study, I applied a lower soil moisture content (SMC) of 25% w/w compared to the 40% w/w SMC used by Lort (2022). The decision informed by analysing COSMOS UK daily hydrometeorological and soil data (2013-2019) retrieved from the UKCEH Environmental Information Data Centre (EIDC) website in February 2021. I selected eight monitoring sites located in closest proximity to the MGP sites and calculated the mean SMC as 25%, with a range of 9-40% across the selected sites. While Lort (2022) may have determined the SMC using data from all COSMOS monitoring sites, including those with higher rainfall, I opted for an SMC that closely represented real-world conditions at the MGP sites under study. The Wilcoxon signed-rank test confirmed that the differences in dermal diffusion for the three PAHs (BaP, Pyr, and DahA) between my study and Lort (2022) were not statistically significant, indicating that the variance in SMC did not significantly impact dermal absorption, thus supporting the comparability of the studies.

Both my study and Lort (2022) conducted analytical measurements on the same GC-MS instrument, but my research utilised GC-MS/MS instead of gas GC-MS to quantify PAHs. Lort (2022) operated in single ion monitoring (SIM) mode, while I used SRM mode. The adoption of GC-MS/MS offers several advantages, including heightened sensitivity and selectivity, and cost-effectiveness for analysing a multitude of targeted compounds at low concentrations (Yao et al., 2013). The use of GC-MS/MS enhances precision and accuracy through the use of SRM ion selection, minimising background noise and non-target compounds, thereby ensuring the detection of only PAH peaks. This is particularly beneficial for the lower PAH concentrations expected in the RS and for the detection of alkyl-PAHs. Detailed information regarding the quality and performance of GC-MS/MS is provided in the Section 4.2.

3.9.2 Methodology of applied *in vitro* dermal experiment

Selection of the five soils to be used for the dermal experiments was described in Section 3.6 (based on on k-means clustering of Rock-Eval (RE) parameters). The synthetic membrane employed in this study was Strat-M (Millipore), which is consistent with that used by Lort (2022). Previous studies have attested to the suitability of Strat-M as an effective alternative for skin permeation studies due to its resemblance to real skin properties studies (Haq et al., 2018, Kaur et al., 2018). The advantages of using a synthetic membrane include its consistent composition, controlled thickness (~300 μm for Strat-M), shorter preparation time, reduced storage requirements, cost-effectiveness and avoidance of ethical issues (Haq et al., 2018). Strat-M's multi-layered structure closely emulates human stratum corneum, comprising a combination of lipids, ceramides, cholesterol, and free fatty acids in proportions similar to those found in the human skin barrier (Haq et al., 2018).

The RS formula used in my study remained consistent with that employed by Lort (2022). Table 9 provides the quantities of ingredients used to prepare 100 mL of RS. The RS was comprised of Hank's Balanced Salt Solution (HBSS) at pH 7.0-7.4, Bovine Serum Albumin (BSA), the most abundant protein in blood, and the zwitterionic organic chemical buffering agent HEPES, which provided pH stability. The RS was thoroughly prepared by stirring until no visible solids were present (typically 10-24 hours stirred) and subsequently refrigerated overnight to achieve equilibrium, adhering to the same procedure as Lort (2022).

Table 9. Receptor solution formula to make 100 mL.

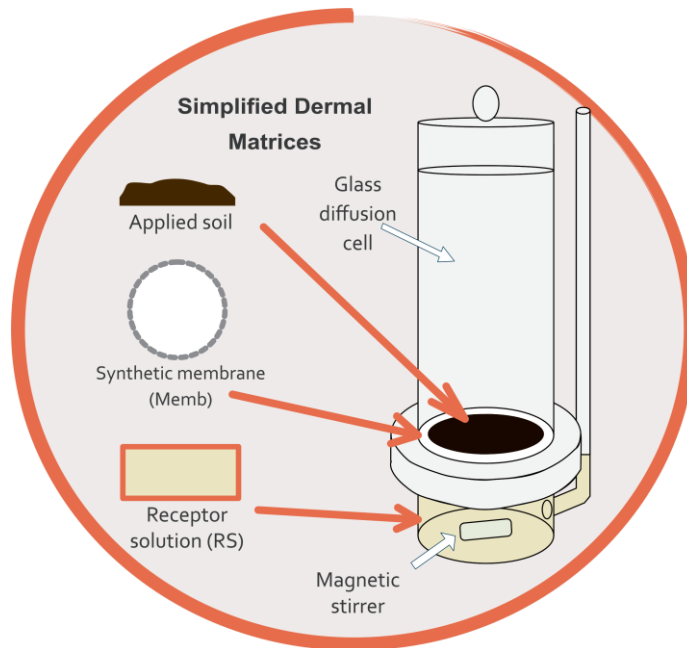
Ingredient	Quantity
HBSS	100 mL
BSA	4 g
HEPES	0.48 g

Dermal experiments were conducted in a manner consistent with Lort (2022). For each dermal experiment, 1.0 g of moistened soil (soil moisture content (SMC%) 25%) was applied at a thickness of approximately 2 mm to a synthetic membrane (Strat-M) using a brass stencil (surface area 8.55 cm^2). High soil

loadings were deliberately used to create a supermonolayer to ensure complete coverage, an infinite dose, and maximise the potential to create steady-state conditions (Frasch et al., 2014, Peckham et al., 2017). The membranes with applied soil were placed on top of the donor chamber of a Franz glass diffusion cell containing a magnetic stirrer bar and the receptor solution (RS) (~33 ml). The RS was formulated using Hank's Balanced Salt Solution (HBSS) (Thermo Fisher Scientific), Bovine Serum Albumin (BSA) (Merck Life Science UK Ltd.) and a HEPES buffering agent (Thermo Fisher Scientific). The glass diffusion cell was assembled, clamped, and placed in a water bath set to 32 °C for the specified timestep (1-hour (h), 10-h, or 24-h, timesteps selected to simulate real-world exposure time scenarios and comparison with other studies). Upon completion of the experiments, soils were gently removed from the membrane with a spatula, which was then washed with deionised water. The collected soils were freeze-dried and stored in sealed 10 mL crimp top glass vials. The membranes were air-dried on a watch glass before being stored in sealed glass containers. The full volume of RS was pipetted into 50 mL Pyrex glass vials sealed with caps. Both soils and RS were stored in a refrigerator maintained at 4 °C until further sample preparation (max. 8 weeks). RS samples from all five MGP soils were measured in triplicate at each of the three-timesteps, membrane samples were measured for H16 at all timesteps and BCR-524 at 24-h.

Modifications to Lort's method (Lort, 2022) were applied to ensure experiments provided a close representation of real-world MGP site conditions. Modifications included reducing the soil moisture content (SMC%) from 40% to 25% and applying a higher soil loading calculated based on the average particle size of dry soil. The lower SMC% was determined by calculating the mean SMC% from real-world data at eight monitoring sites closest to the MGP sites using the COSMOS UK daily hydrometeorological and soil data (2013-2019) (Stanley et al., 2021). Figure 18 provides several photos of the *in vitro* dermal experiments in action. After completion of the experiment, collected soils were stored in glass containers and freeze-dried, while membranes were left to air dry on glass watch plates before storage in glass containers. RS samples were pipetted into Pyrex glass vials and stored in the refrigerator until further sample preparation.

(a)



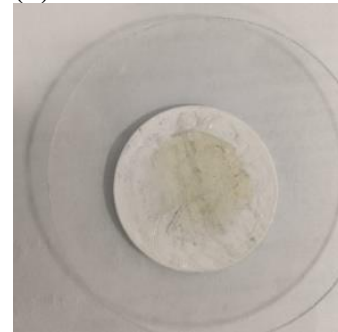
(b)



(c)



(d)



(e)



(f)

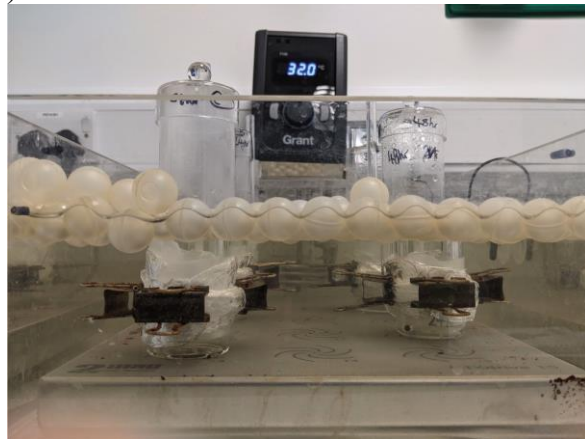


Figure 18. (a) Simplified diagram of the *in vitro* dermal experiments, (b) soil being weighed before application to the membrane, (c) soil applied membrane placed in the glass diffusion cell, (d) soil removed from membrane after dermal experiment, (e) collection of matrices after dermal experiments (soil, membrane and RS), and (f) setup of dermal *in vitro* experiment in water bath.

3.10 Data evaluation and statistical analysis

Data evaluation and statistical analyses included simple linear regression, Pearson's Correlation, principal component analysis (PCA), Shapiro-Wilk test, Levene's test, one-way ANOVA, Welch's ANOVA, and the post-hoc tests – Tukey HSD, Games-Howell and Pairwise Wilcoxon Rank Sum tests. Statistical analysis was performed using R Statistical Software (R Core Team, 2023). Details of the statistical analysis can be found in Appendix B Chapter 5 Research Papers SI Section S3.

3.11 Quality control methods

The quality control (QC) for both the analytical methods and the *in vitro* dermal experiments were assessed. Section 6.3.6 states the methods used to assess the QC for this research and the QC results and performance are found in Section 6.4.6. This next section will describe the QC conducted for this research and the QC results can be found in Chapter 4 Quality Control Assessment. As a quick summary for this section, the sample preparation and analytical method QC was assessed using spiked solvent measurements, surrogate extraction efficiencies, chromatogram verification of LOD and LOQ values and the measurements of two CRM samples. The dermal experiments QC was assessed by mass balance, weighed matrix balance checks, analysis of blank dermal experiments (no applied soil) and comparing the calculated membrane and RS fluxes in this study to other studies. This included comparing the dermal fluxes of the BCR-524 sample in this study's control reference soil study with the BCR-524 fluxes measured by Lort (2022). The following sections are taken from Chapter 6 SI to describe the applied techniques to assess the QC.

3.11.1 Quality control samples

The QC samples were used to examine the performance of the dermal experiments, the sample preparation and the GC-MS/MS method. The QC samples would be processed and analysed using the same methods as the experimental samples. QC samples included spiked solvents, procedural blanks, samples from blank dermal experiments (no soil application), duplicate samples and CRMs.

Spiked solvents contained toluene spiked with surrogates, internal standards and standard PAHs mixes (MX45, MX9 and MX183). Spiked solvents served to evaluate the analytical performance of the GC-MS/MS without the influence of complex matrices (soil, membrane, or RS) during sample batches. To assess potential contamination during the analytical runs, procedural blanks were processed and measured alongside soil sample batches. To ascertain whether additional HMW PAHs not originating from the soil were present in the RS and membrane samples for dermal experiments, blank dermal experiments were conducted, processed and analysed alongside field sample dermal matrices. To assess the analytical variability of the instrument, I utilised the relative percent difference (RPD) for side-by-side duplicate samples, aiming for an RPD value of <30% (Udesky et al., 2019).

Lastly, to establish the accuracy of my method, I measured and compared CRMs against their reported concentrations to assess the sample preparation and analytical methods. CRMs can help to determine the difference between a study's measured value and the true value, known as the bias (Environment Agency, 2018). The bias is calculated by deducting the true CRM value (CRM certified value) from the measured CRM sample and the percentage bias is calculated using Equation 4.

$$\%Bias = \frac{(measured\ CRM\ mean - reported\ true\ CRM\ value)}{reported\ true\ CRM\ value} \times 100$$

Equation 4. Calculation of %Bias.

The precision of the overall study's method was calculated as the % relative standard deviation (%RSD) and represents the distribution of repeated measurements on the sample and calculated using Equation 5 (Environment Agency, 2018).

$$\%RSD = \frac{Standard\ deviation\ of\ measured\ values}{Mean\ of\ measured\ values} \times 100$$

Equation 5. Calculation of % relative standard deviation (%RSD).

The %Bias and %RSD were also applied to the spiked soil samples to determine variance from the targeted spiked concentration.

3.11.2 Extraction efficiencies

Deuterated PAH surrogates were spiked into weighed-out samples before sample preparation, to assess extraction efficiency. Processed samples were subsequently spiked with deuterated PAH I.S before analysis on the GC-MS/MS and compared to surrogate values to calculate percentage recoveries.

3.11.3 QC methods for dermal experiments

Mass balance is a technique that can be used assess the adequacy of PAH recovery from dermal experiments and was employed in accordance with established methods (Bucks et al., 1988, Lort, 2022). The determination of mass balance involves evaluating the PAH mass from the three matrices in a dermal experiment, namely Soil PAH_T, Memb PAH_T and RS PAH_T, (PAH masses in matrices at a specified time step) in relation to the initial soil PAH mass (PAH₀) at 0 hours, as depicted in Equation 6.

$$\text{Initial soil PAH}_0 \text{ (ng)} = \text{Soil PAH}_T + \text{Memb PAH}_T + \text{RS PAH}_T$$

Equation 6. Equation of sum of dermal matrices PAH masses (measured in ng) equalling the initial soil PAH mass at beginning of dermal experiment (0-hr).

The mass balance can be expressed as a percentage by dividing the sum of PAH masses in the three matrices by the initial soil PAH mass and multiplying the result by 100, as shown in Equation 7. Weight checks were conducted for soil and membranes before and after dermal experiments to evaluate the effectiveness of soil removal from the membrane and to identify any sample loss during the procedure. Membranes should weigh the same as they started to indicate that no soil remained or membrane scrapped away, whereas soils should aim to achieve a -25% difference to the initial soil weight to account for the 25% moisture content in soils.

$$\text{Mass balance (\%)} = \frac{\text{Soil PAH}_T + \text{Memb PAH}_T + \text{RS PAH}_T}{\text{Initial soil PAH}_0} \times 100$$

Equation 7. Calculation of Mass Balance % for dermal experiments.

To validate my study's method, a control reference soil study (DCRM) was conducted using the CRM BCR-524 and compared to Lort (2022) work to ascertain the similarity of the results. The dermal fluxes for BCR-524 at 24 hours were compared for BaP, Pyr, and DahA, the only PAHs measured by Lort (2022).

CHAPTER 4

QUALITY CONTROL ASSESSMENT

4.1 QC Introduction

The basic QC results for this research are presented for the three research papers in sections 5.3.5, 6.4.6, Appendix B Chapter 5 Research Papers SI and Appendix C Chapter 6 Research Paper SI. The QC results are included here for ease of reference and to allow for this section of the thesis to go into further details than the papers. Similar to Chapter 3, to facilitate easy referencing, the control reference soil dermal experiments involving the CRM BCR-524 sample are herein denoted as the DCRM experiments, while the dermal investigations concerning MGP samples are referred to as DGWS experiments, and finally GWS-CH denotes the samples investigated in Chapter 5 by quantifying PAHs and bulk OM for MGP soils.

4.2 Sample preparation and analytical QC

4.2.1 General methods quality assurance activities

Several practices were used as quality assurance measures to achieve a high quality of work throughout this research and are presented in Table 10.

Table 10. List of quality assurance measures applied in this research.

Method Activity	QC Action
Laboratory etiquette	<ul style="list-style-type: none">• Laboratory user undertaken all health and safety procedures during research including all appropriate training.• Laboratory notebook used to record all lab activities and notebook stored securely.• Appropriate PPE worn in lab including nitrile gloves, FFP3 facemasks, eye protection and lab coat.• Laboratory activities performed in fume cupboards and HEPA filtered laminar flow cabinet when applicable.

Balance Checks	<ul style="list-style-type: none"> Balances checks were measured and recorded before each weighing batch with 0.001 g, 0.002 g, 0.005 g, 0.01 g, 0.02 g, 0.05 g, 0.1 g, 0.2 g, 0.5 g, 1 g and 2 g weights. If weight deviated from $\pm 1\%$ balance was recalibrated.
Cleaning of work area, vessels, syringes, ASE cells, GC-MS/MS and dermal apparatus	<ul style="list-style-type: none"> Work areas cleaned by solvents and deionised (DI) water before sample preparation or experiments. Glassware was cleaned using chromic acid to eradicate presence of hydrocarbon compounds and wrapped in foil to avoid contamination when not in use. Syringes were cleaned prior to use and in-between samples by rinsing full syringe volume 7 times with clean DCM or toluene. ASE extraction cells were cleaned by sonication of the disassembled cells in acetone:DCM (50:50) solution for 5 minutes, subsequently cell components were left to evaporate solvent before reassembly. ASE underwent rinse cycles prior to each batch of samples and in between samples to avoid cross contaminations in the systems. GC-MS/MS injection syringe was cleaned by rinses with toluene between each sample injection and blank toluene samples was ran through the GC-MS/MS column between every 20 samples (more frequent with membranes).
Sample storage	<ul style="list-style-type: none"> Soil samples were stored in amber glass jars in a dark cool storage space. Liquid samples stored in a fridge to avoid evaporation. PAH standards stored in tightly sealed capillary bottles in the fridge, the bottles were weighed at room temperature to monitor for any solvent evaporation occurrences, if bottle measured weight loss new batches would be used. Experimental dermal matrices collected after experimentation were stored in glass bottles and Pyrex bottles in a fridge.
Stock checks	<ul style="list-style-type: none"> All samples labelled at each stage. Batches of reagents used were recorded in the event of problems.
Reagents	<ul style="list-style-type: none"> Appropriate purity solvents (analytical grade) within expiry date were used in work. DI water was used for equipment rinsing and Milli-Q water was used as a reagent for sample preparations (provided by BGS).

4.2.2 Spiked solvents

For the DGWS batch of spiked solvents using MX45, all PAHs demonstrated acceptable %RSD (<15%) and %Bias (<30%) values, as per the Environment Agency (2018) guidance. This outcome provided confidence in the suitability of the developed analytical method for measuring a wide range of PAHs. The MX183, utilised for measuring HMW PAHs absent in MX45, exhibited %Bias values below 30%, confirming the accuracy of PAH measurements in the spiked solutions. Table 11 and Table 12 shows each PAHs %RSD and %Bias for the spiked solvents using MX45 and MX183.

Four HMW PAHs in MX183 measured %RSD values exceeding 15%, suggesting potential variability in measurements for these analytes or deviations in the spiking of samples. Notably, these variances were more pronounced for HMW PAHs with the highest LOQ and heaviest molecular weights, however they were assumed to be caused by systemic errors with the MX183 samples (such as slight errors with spiking), as good results were measured for the PAH (BghiP) present in the MX45 samples, suggesting the causation was due to the MX183 sample. Nonetheless, the %Bias remained within acceptable limits (<30%), except for the alkyl-PAH, 5-methylchrysene, where a slight deviation of 3% was observed for a single alkyl-PAH species. Alkyl-PAHs are difficult to analysis with spectroscopy due to the stronger fragmentation of the alkylated chain and the alkyl groups effect on the mass spectroscopic profiles (Andersson and Achten, 2015), therefore the slightly higher bias was accepted for this research. In conclusion, the instrumental performance with spiked PAH solutions was considered satisfactory, and variations in dermal matrices measurements were attributed to either matrix interference or sample preparation.

Table 11. Mean, standard deviation, %RSD, and bias for DGWS sample batches using MX45 spiked solution at 0.20 pg/ μ L.

	MX45					
	Mean	n	SD	%RSD	Bias	%Bias
Nap	0.19	7	0.02	9.20	-0.04	-20.78
Acy	0.19	7	0.01	6.23	-0.03	-15.44
Ace	0.19	7	0.01	5.83	-0.03	-15.71
Flu	0.20	7	0.01	4.99	-0.02	-7.89
Phen	0.21	7	0.01	2.78	0.00	1.74
An	0.20	7	0.01	3.66	0.01	4.90
Fla	0.21	7	0.01	2.44	0.00	0.62
Pyr	0.21	7	0.01	2.74	0.01	2.65
BaA	0.18	7	0.02	11.34	0.05	22.69
Chry	0.20	7	0.02	10.95	0.04	19.34
BbF	0.20	7	0.00	1.19	0.00	-0.91
BkF	0.20	7	0.00	1.93	0.00	-1.09
BeP	0.23	7	0.02	10.41	0.00	0.40
BaP	0.21	7	0.01	6.82	0.00	-1.75
Per	0.21	7	0.02	7.18	0.00	-1.14
IcdP	0.20	7	0.02	8.39	-0.02	-10.95
DahA	0.19	7	0.02	10.65	-0.03	-14.59
BghiP	0.22	7	0.03	12.07	-0.02	-9.41

Table 12. Mean, standard deviation, %RSD, and bias for DGWS sample batches using MX183 spiked solution at 0.2 pg/μl.

	MX183					
	Mean	n	SD	%RSD	Bias	%Bias
BaA	0.16	8	0.02	12.14	-0.04	-18.23
CCP	0.25	8	0.02	9.75	0.05	24.87
Chry	0.18	8	0.02	8.40	-0.02	-9.96
BbF	0.17	8	0.00	1.15	-0.03	-12.83
BkF	0.17	8	0.00	1.92	-0.03	-16.13
BjF	0.20	8	0.01	2.58	0.00	-1.76
BaP	0.18	8	0.01	6.29	-0.02	-8.32
IcdP	0.18	8	0.02	11.88	-0.02	-9.92
DahA	0.17	8	0.02	11.63	-0.03	-15.14
BghiP	0.19	8	0.03	16.31	-0.01	-5.32
DalP	0.21	8	0.03	12.77	0.01	3.77
DaeP	0.18	8	0.03	17.92	-0.02	-8.75
DaiP	0.17	8	0.04	24.70	-0.03	-15.55
DahP	0.17	8	0.04	21.79	-0.03	-14.33
BcFlu	0.21	8	0.01	6.64	0.01	5.86
5-methylchrysene	0.27	8	0.01	2.83	0.07	33.07

4.2.3 Extraction efficiencies – Sample recoveries

The surrogate recoveries for the analytical batches for each sample type for the dermal experiments are presented in Table 13, while surrogate recoveries for the MGP soils measured in Chapter 5 are shown in Appendix B Chapter 5 Research Papers SI. Spiked solvent samples exhibited high recoveries and low %RSD, with recovery values ranging between 88 – 116% (mean 101%) and %RSD ranging from 0.5-8.5% (mean 3.2%) for MX45-spiked solvents in the DGWS dermal matrices batches. Soil samples measured high recoveries, with the DGWS soil batch averaging ~80% and the DCRM batch averaging ~132%. Lower recoveries were measured for membranes and RS samples, attributed to the high affinity of PAHs to lipophilic matrices (membrane), the lower PAH concentrations and the different sample preparation procedure involved in RS analysis, which required a different SPE method and additional solvent transfer

step, potentially leading to PAH losses. The DGWS samples exhibited mean recoveries of 81.4%, 75.1% and 76.2% for soils, membranes and RS, respectively. In the DCRM batch, the mean recovery for membranes was 93%.

The CRM NIST-1944 measurements were used to assess the sample preparation and analytical methods performance in establishing the true concentration value. Assessments of which surrogates to use for concentration corrections were determined using NIST-1944 measured concentrations. The GWS-CH and DCRM batches reported lower %Bias when the surrogate BghiP-d12 was used and hence was employed for those sample calculations. Conversely, the DGWS batches used BaP-d12 recovery factors instead, as the CRM NIST-1944 samples measured with the surrogate BghiP-d12 reported higher %Bias, suggested to be caused by spiking errors with BghiP-d12. This approach ensured accurate and reliable measurements for HMW PAHs.

The DCRM RS samples (experiments for the BCR-254 sample control reference soil study) exhibited low recoveries in the range of 12-74% (mean 27%) and high %RSD (mean %RSD of 40%). Further investigation revealed that the issue of low recovery for this subset of DCRM RS samples arose due to unintended storage of the RS in the fridge for five months. This unintentional prolonged storage compromised the sample integrity, making the RS difficult to extract through SPE and led to high amounts of sample loss. However, RS samples not subjected to extended fridge storage (DGWS samples) exhibited much higher recoveries (~75%), confirming the reliability of my method and the issue caused by the prolonged RS storage. The DCRM RS samples were stored in the fridge for a prolonged period because initially 1 mL of the sample was processed and analysed, however measurements using the 1 mL of RS resulted in several HMW PAHs not being detected (<LOQ) at specific time steps.

This prompted the subsequent analysis of the full volume of RS with the prolonged fridge storage. No statistically significant differences between the two batches (1 mL and full volume RS) were observed in the Kruskal-Wallis test (p-value > 0.05 for each timestep). The full volume RS samples successfully detected various HMW PAHs >LOQ in contrast to the 1 mL RS samples, validating the requirement for the full volume of RS to be analysed to ensure

accurate measurement. This included measuring Chry, BaA, BbF, BkF, BaP, BghiP and IcdP at both 10-hour and 24-hour experiments with the full volume RS and not for the 1 mL RS. This finding highlights the impact of improper sample storage on RS samples and emphasises the quantity of RS required for detection, providing valuable insights for future studies to avoid replication of such issues. Despite the low recovery data for the DCRM RS samples, for estimation purposes the Wilcoxon signed-rank test demonstrated no statistically significant differences (p -values < 0.05) between my study and Lort (2022) BCR-524 RS fluxes using the full volume RS sample results, as seen in Section 4.3.3 Validating dermal results by comparison to other studies. Theoretically this assumes that surrogate recoveries as correction factors produced correct PAH concentrations, however due to the uncertainties associated with the low surrogate recoveries, the BCR-524 RS fluxes were not quantified in the research paper, but the presence of PAHs was.

Table 13. Surrogate recoveries for each analytical batch and each sample type

Batch	Sample Type	n	Phen-d10		Pyr-d10		BbF-d12		BaP-d12		BghiP-d12	
			Recovery (%)	%RSD								
DGWS_Soil	Spiked Solvent	6	107.9	4.0	99.3	1.2	102.3	1.7	88.5	2.3	NA	NA
DGWS_Soil	Procedural Blank	2	42.5	83.0	55.3	34.0	83.0	14.5	66.2	9.7	NA	NA
DGWS_Soil	NIST-1944	8	76.5	15.3	82.4	10.5	87.2	9.0	77.2	9.7	NA	NA
DGWS_Soil	Field sample	61	75.3	22.3	80.5	18.0	90.7	11.2	79.0	12.8	NA	NA
DGWS_M	Spiked Solvent	6	105.0	3.5	100.0	1.1	110.3	4.7	94.5	2.7	NA	NA
DGWS_M	Spiked Membrane	3	92.4	13.6	95.1	20.9	100.1	6.7	53.5	54.3	NA	NA
DGWS_M	Field sample	9	81.7	13.7	74.8	15.4	99.8	12.0	43.9	28.0	NA	NA
DGWS_RS	Spiked Solvent	6	105.7	6.5	100.1	1.1	102.6	5.1	101.1	1.6	NA	NA
DGWS_RS	Spiked RS	2	64.5	26.1	71.7	14.9	63.6	14.1	68.5	18.7	NA	NA
DGWS_RS	Dermal Blank Exp.	4	61.7	20.2	75.8	20.1	65.9	17.9	68.3	18.3	NA	NA
DGWS_RS	Field sample	45	78.3	24.8	79.5	26.5	71.4	27.3	75.8	28.7	NA	NA
DCRM_Soil	Spiked solvent	6	99.8	3.8	100.3	5.8	124.6	28.4	131.8	27.9	142.3	30.4
DCRM_Soil	Procedural Blank	2	55.8	15.1	76.5	7.3	191.0	2.4	136.9	2.7	96.6	13.7
DCRM_Soil	NIST-1944	6	105.1	5.7	83.5	3.9	168.6	2.8	153.8	4.2	108.3	7.1

DCRM_Soil	BCR-524 Neat	3	100.1	11.3	87.2	2.4	197.6	2.6	160.4	2.2	110.2	7.4
DCRM_Soil	Field sample	21	108.0	13.5	85.7	5.3	205.5	6.8	156.2	4.1	106.9	18.5
DCRM_M	Spiked Solvent	9	105.4	3.6	99.9	1.2	108.6	4.0	94.9	4.4	144.9	5.8
DCRM_M	Dermal Blank Exp.	2	33.6	79.1	65.3	18.2	94.9	2.5	52.5	57.2	109.4	2.3
DCRM_M	Spiked Membrane	1	59.5	NA	80.3	NA	76.9	NA	65.7	NA	84.9	NA
DCRM_M	Field sample	6	81.7	11.5	83.3	2.5	101.4	11.1	72.9	12.6	124.1	17.7
DCRM_RS	Spiked Solvent	6	104.7	5.1	99.5	1.4	99.5	3.4	87.1	4.0	128.8	11.2
DCRM_RS	Spiked RS	1	3.1	NA	4.9	NA	4.9	NA	3.1	NA	7.2	NA
DCRM_RS	Dermal Blank Exp.	1	18.6	NA	23.6	NA	21.1	NA	20.1	NA	26.6	NA
DCRM_RS	Field sample	8	30.8	59.2	31.4	53.7	24.0	31.0	21.7	29.2	26.5	25.4

4.2.4 GC-MS/MS detection limits

HMW PAHs in soils exhibited an LOD range of 0.003 – 0.257 mg/kg and an LOQ of 0.010 – 0.857 mg/kg, while membranes exhibited an LOD range of 0.006 – 0.257 µg/g and an LOQ of 0.038 - 1.71 µg/g (PAH mass per membrane mass). RS had an LOD range between 0.0007 – 0.0312 ng/mL and a LOQ between 0.001 – 0.104 ng/mL (PAH mass per mL of RS) (Table 14).

Table 14. LOD and LOQ for each PAH in each matrix.

PAH	Soil		Membrane		Receptor Solution	
	LOD (mg/kg)	LOQ (mg/kg)	LOD (µg/g)	LOQ (µg/g)	LOD (ng/mL)	LOQ (ng/mL)
Nap	0.003	0.010	0.003	0.020	0.0004	0.001
Acy	0.013	0.044	0.013	0.089	0.002	0.005
Ace	0.009	0.029	0.009	0.057	0.001	0.003
Flu	0.005	0.018	0.005	0.036	0.001	0.002
Phen	0.007	0.024	0.007	0.047	0.001	0.003
An	0.011	0.037	0.011	0.074	0.001	0.004
Fla	0.012	0.042	0.012	0.083	0.002	0.005
Pyr	0.011	0.037	0.011	0.074	0.001	0.004
BcFlu	0.067	0.224	0.067	0.448	0.008	0.027
BaA	0.010	0.032	0.010	0.065	0.001	0.004
Chry	0.018	0.060	0.018	0.120	0.002	0.007
CCP	0.032	0.107	0.032	0.214	0.004	0.013
5-mChry	0.060	0.220	0.060	0.849	0.015	0.051
BbF	0.006	0.019	0.006	0.038	0.001	0.002
BkF	0.018	0.060	0.018	0.120	0.002	0.007
BjF	0.257	0.857	0.257	1.714	0.031	0.104
BeP	0.017	0.058	0.017	0.116	0.002	0.007
BaP	0.019	0.065	0.019	0.129	0.002	0.008
Per	0.025	0.084	0.025	0.168	0.003	0.010
IcdP	0.025	0.084	0.025	0.168	0.003	0.010
DahA	0.021	0.070	0.021	0.139	0.003	0.008
BghiP	0.020	0.066	0.020	0.133	0.002	0.008
DalP	0.027	0.091	0.027	0.182	0.003	0.011
DaeP	0.063	0.210	0.063	0.420	0.008	0.025
DaiP	0.116	0.388	0.116	0.775	0.014	0.047
DahP	0.114	0.381	0.114	0.761	0.014	0.046
Phen-d10	0.003	0.010	0.003	0.021	0.000	0.001
Pyr-d10	0.007	0.023	0.007	0.047	0.001	0.003
BbF-d12	0.009	0.030	0.009	0.061	0.001	0.004
BaP-d12	0.012	0.039	0.012	0.077	0.001	0.005
BghiP-d12	0.031	0.103	0.031	0.205	0.004	0.012

The calculated PAH concentrations for the PAHs BaP, Pyr, BaA and BghiP in samples were subjected to chromatogram verification to ensure the adequacy of the LOQ and LOD in my analytical method. Among the DGWS RS samples, A11 exhibited the lowest soil concentration of BaP (13.5 mg/kg), with only one A11 RS measurement exceeding the LOQ for BaP. The chromatogram of this specific 10-hour RS sample confirmed the accurate measurement of BaP above the LOQ (Figure 19.a), while other A11 RS samples at 1-hour demonstrated BaP concentrations <LOQ (e.g., A11 RS at 1-hour in Figure 19.b). Similarly, one A11 1-hour RS from the triplicates showed a BghiP concentration >LOQ, this result was validated by the corresponding chromatogram (Figure 19.c). All RS measurements for the chosen four HMW PAHs aligned with their respective chromatograms. Additionally, the chromatograms for soil and membrane samples correlated with the calculated detections. As a result, I have high confidence in the sufficiency of the calculated LOD and LOQ for all HMW PAHs.

4.2.5 Blank samples and duplicates

The procedural blanks measured HMW PAHs either below or close to the LOQ. In contrast, LMW PAHs were often above the LOQ and reasoned to originate during the sample preparation procedure, however LMW PAHs were not the focus of my study. Procedural blanks measured Fla at 0.42 mg/kg, in comparison to the average Fla concentration measured in the soil samples 578 mg/kg, this value was negligible (0.07%) and the lowest measured soil Fla concentration was 8.49 mg/kg, (4.9%). Given that this value was ten times greater than the LOQ, I deduced that HMW PAH measurements >LOQ for procedural blanks could be safely subtracted from the soil samples. Thus, making soil concentrations more accurate by removing additional PAHs from sample preparation from the sample's concentration. Additionally, the blank dermal experiment samples measured PAHs in membranes and RS either close to the LOQ or <LOQ (e.g. Fla with 0.085 µg/g compared this to the LOQ 0.083 µg/g). Only the lowest molecular weight HMW PAHs measured concentrations >LOQ in blank samples. Figure 19.d illustrates Pyr measurements in an A11 1-hour RS compared to a blank dermal experiment RS (red filled peak). This comparison revealed the presence of Pyr in the blank dermal experiment RS, which is

assumed to have originated from the sample preparation process due to similar trends observed with the procedural blanks. Following the deduction of the dermal experiments' blank values from the measured A11 RS, the Pyr measurement remained above the LOQ. Consequently, to ensure that the measured HMW PAHs in the DGWS RS and membranes originated solely from the soils and not from other sources of contamination during the experiment or sample preparation, I deducted the mean concentrations of HMW PAHs from the blank dermal experiment matrices (measuring >LOQ) from the respective DGWS RS and membranes.

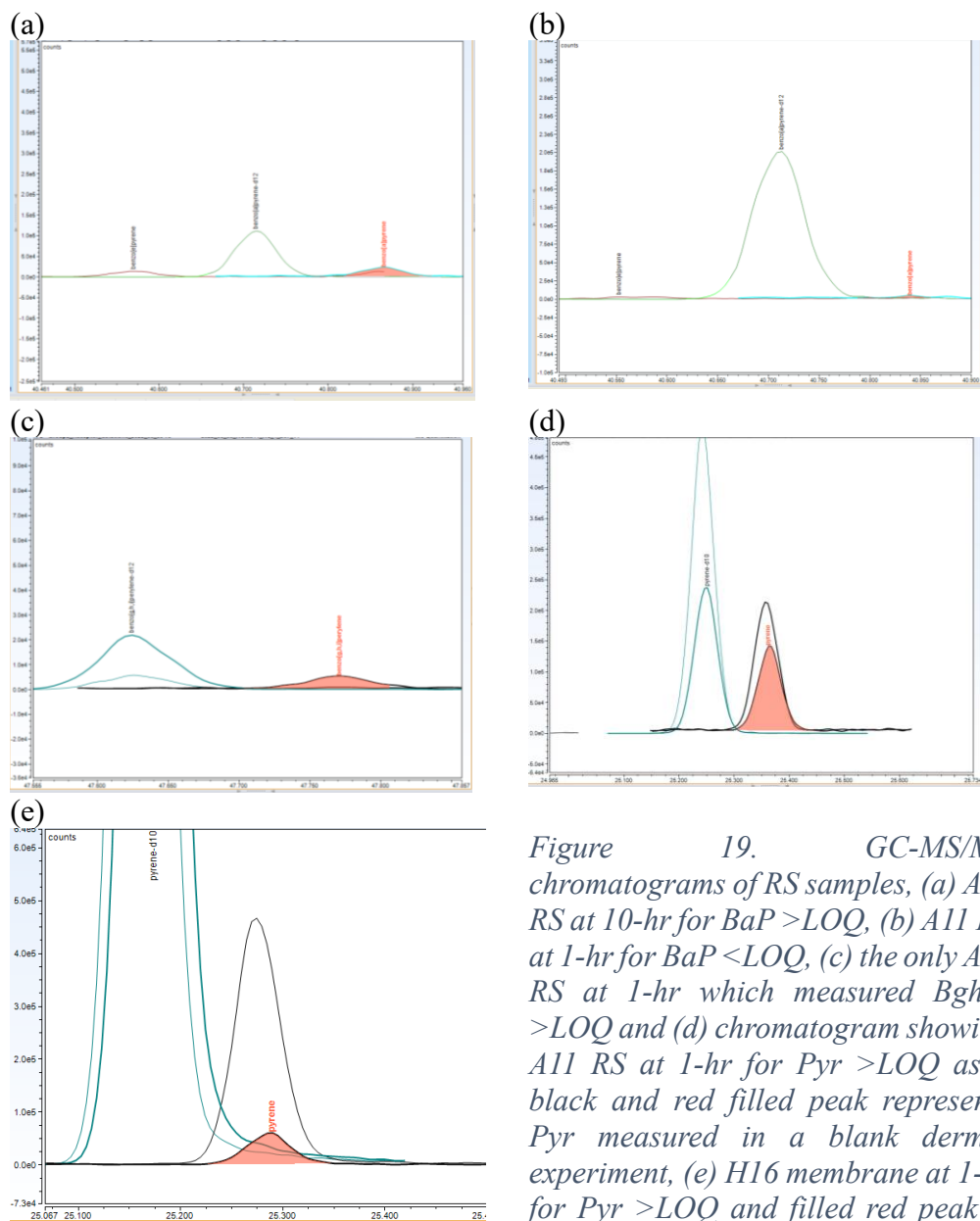


Figure 19. GC-MS/MS chromatograms of RS samples, (a) A11 RS at 10-hr for BaP > LOQ, (b) A11 RS at 1-hr for BaP < LOQ, (c) the only A11 RS at 1-hr which measured BghiP > LOQ and (d) chromatogram showing A11 RS at 1-hr for Pyr > LOQ as a black and red filled peak represents Pyr measured in a blank dermal experiment, (e) H16 membrane at 1-hr for Pyr > LOQ and filled red peak is Pyr measured in a blank dermal experiment.

PAH concentrations for samples run in duplicate aimed for an RPD value of <30% (Udesky et al., 2019). For the DGW three matrices' batches, spiked MX45 solvent duplicates exhibited RPD values ranging from -7.7% to 17.7%, with a mean of 2.4%, indicative of low variability within injections. Similarly, the DGWS NIST-1944 duplicates had an average RPD value of -7.6%, ranging from -18.8% to 4.3%. The BCR-524 duplicates in the DCRM batch demonstrated an average RPD of -1.6%, with a range of -11.1% to 34.1%. These RPD values reinforce the low analytical variability of the instrument for duplicates of the same sample.

4.2.6 Measurements of Certified Reference Materials (CRMs)

The comparison of measured CRMs NIST-1944 and BCR-524 PAH concentrations with the reported certified concentrations demonstrated similar measurements (Figure 20 and Figure 21). For the majority of HMW PAHs, the %Bias was below 30%, indicating the method's accuracy. Only three HMW PAHs, DahA, DaiP, and DahP, with the lowest concentrations in the CRM, fell outside this range. Additionally, most HMW PAHs exhibited a %RSD below 15%, reflecting the precision of my method.

The NIST-1944 certificate's singular alkylated compounds were summed together and compared to my study's concentrations. Confidence in the method's ability to accurately measure a variety of HMW alkyl-PAHs at varying concentrations was strengthened by the satisfactory performance of the HMW alkylated C1-Fla/Pyr, which demonstrated %Bias <30% and %RSD <15%, indicating the similarity of their behaviour to parent HMW PAHs. The CRM BCR-524 also yielded %RSD and %Bias within acceptable ranges for the majority of HMW PAHs. Differences in performance between BCR-524 and NIST-1944 CRMs were attributed to the need for a higher degree of dilution for the BCR-524 samples. Which was required to avoid potential damage to the GC-MS/MS, due to the high Phen concentrations present in BCR-524. NIST-1944 was measured alongside the DCRM batch of soils, yielding measurements similar to the DGWS soils batch, thereby indicating consistent instrument performance throughout the measurements. In summary, the measured PAH concentrations in the CRMs provided confidence in the method's accuracy and precision in measuring a diverse range of HMW PAHs at varying concentrations,

while also highlighting the similarity of behaviour between alkylated HMW PAHs and parent HMW PAHs.

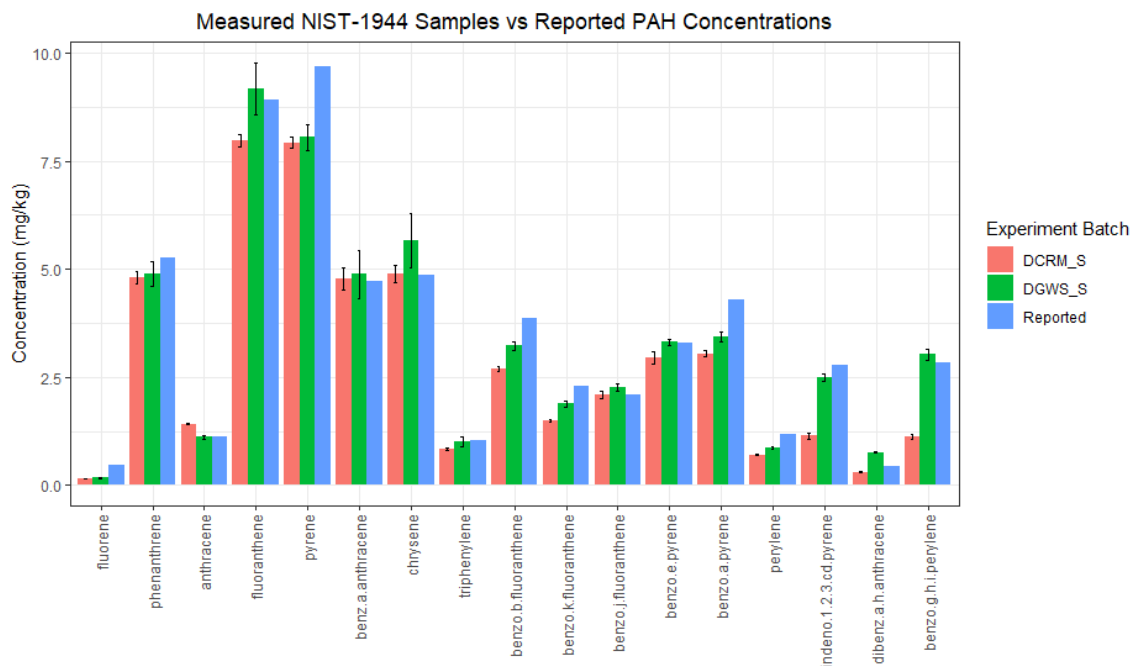


Figure 20. Measured CRM NIST-1944 samples in this study (red – DCRM and green – DGWS batches) compared to certified PAH concentrations (blue), errors bars are 95% CI.

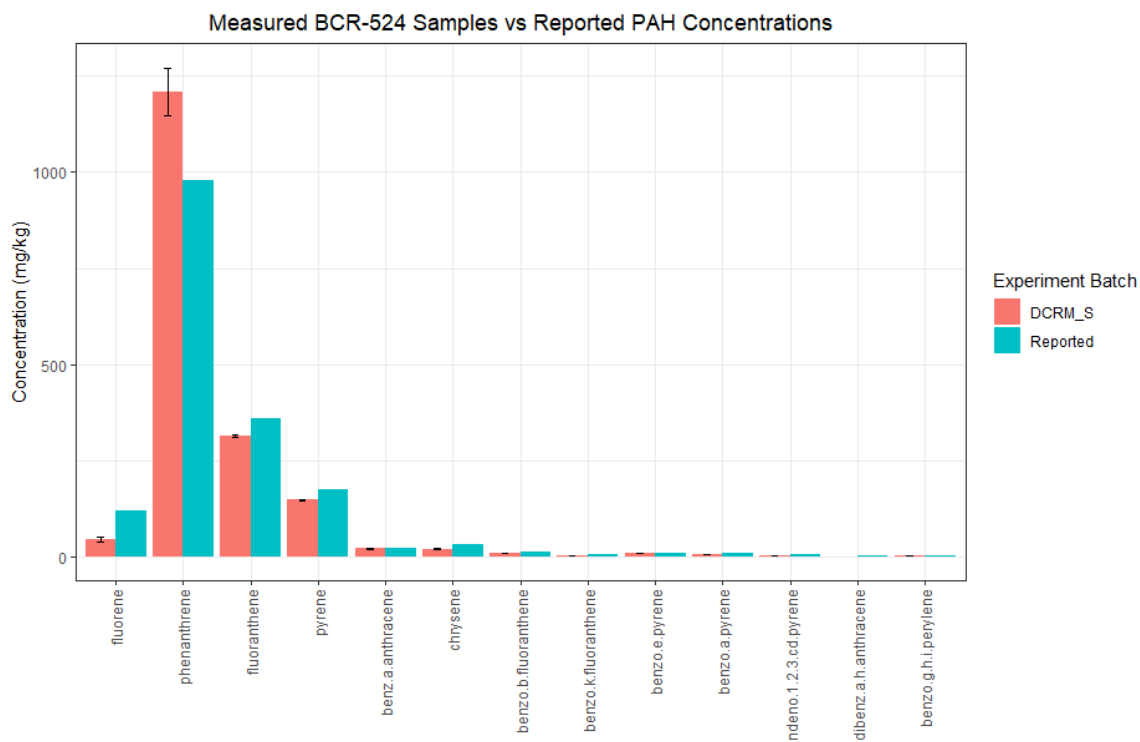


Figure 21. Measured CRM BCR-524 samples in this study (red) compared to certified PAH concentrations (blue), errors bars are 95% CI.

4.3 QC for the *in vitro* dermal experiments

4.3.1 Mass balance

Table 15 presents the mass balance percentages for the dermal experiments with PAH concentrations quantified for all three dermal matrices (soil, membrane and RS). These included sample H16 in the DGWS setup (at 1, 10, and 24-hours) and for the triplicate 24-hour and one 10-hour experiment with BCR-524 in the DCRM experiments. The calculated mass balance percentages ranged between 85-100% for H16 experiments, with a mean of 99%. For the BCR-524 samples in the DCRM experiments, the PAH mass balance ranged between 66-100%, with a mean of 94%. The high mass balance percentages affirm the efficient extraction of PAHs in the dermal experiments, providing a strong indication of the *in vitro* dermal experiment's high performance.

4.3.2 Dermal matrices weight checks

The average weight of the used synthetic membranes was 0.231 g, the change in membrane weight (start and end of experiment) ranged from -0.15 to 0.245 g, with a mean of 2.76×10^{-3} g. The change in membrane weight expressed as a percentage measured a mean of 1.72%, with a range of -38.5% to 110%. The membrane weight demonstrated minimal deviation from the initial weight, confirming the efficacy of the soil removal method, which involved lightly scraping soil and applying deionised water to wash the membrane. Notably, one 24-hour A11 membrane exhibited an additional weight of 0.24 g, indicating tightly bound soil residues that were not completely removed. Moreover, a 1-hour H16 membrane exhibited a reduced weight of -0.15 g, suggesting partial scraping of the membrane during soil removal. In conclusion, the soil removal method proved to be efficient in effectively eliminating soil from the membrane.

Table 15. The mass balance percentages for all H16 experiments and triplicate 24-hour and one 10-hour experiment for BCR-524.

Sample	H16									BCR-524			
	24			10			1			24		10	
Fla	95.1	86.6	84.5	95.3	92.0	96.4	99.2	98.9	98.5	74.4	69.8	66.1	80.1
Pyr	96.3	88.7	86.9	95.5	94.4	96.0	99.4	99.2	98.8	76.7	72.6	67.7	82.1
BaA	99.8	98.5	97.2	99.3	98.7	99.6	99.9	99.8	99.7	98.0	91.2	85.4	95.8
CCP	100.0	100.0	100.0	99.0	100.0	99.1	100.0	100.0	100.0	80.2	100.0	100.0	100.0
TPh	100.0	95.7	94.7	98.6	96.9	98.9	100.0	100.0	100.0	97.8	88.4	85.0	96.1
Chry	99.5	96.2	94.8	98.9	97.3	99.1	99.8	99.7	99.6	93.8	86.8	87.2	95.6
BbF	100.0	98.0	97.0	99.2	98.8	99.2	100.0	99.8	99.7	95.2	96.9	92.9	95.6
BkF	100.0	98.2	97.1	99.5	99.0	99.7	100.0	100.0	100.0	98.9	97.7	95.5	95.7
BjF	100.0	97.9	96.6	100.0	100.0	100.0	100.0	100.0	100.0	100.0	100.0	100.0	100.0
BeP	99.5	96.7	96.0	98.7	97.7	98.7	99.6	99.5	99.3	97.0	95.2	92.8	94.4
BaP	99.8	98.4	97.4	99.4	99.0	99.8	100.0	99.9	99.7	98.8	97.0	92.3	95.8
Per	100.0	98.9	97.9	99.4	99.0	100.0	100.0	100.0	100.0	94.4	94.2	94.2	93.4
IcdP	100.0	98.2	97.6	99.1	98.8	99.2	100.0	100.0	99.5	100.0	99.9	100.0	100.0
DahA	100.0	100.0	98.2	100.0	100.0	100.0	100.0	100.0	100.0	100.0	100.0	100.0	100.0
BghiP	100.0	98.3	97.8	99.0	98.7	99.3	100.0	99.6	99.4	100.0	100.0	92.0	91.5
DalP	100.0	100.0	97.6	100.0	100.0	100.0	100.0	100.0	100.0	NA	NA	NA	NA
DaeP	100.0	100.0	100.0	100.0	100.0	100.0	100.0	100.0	100.0	NA	NA	NA	NA
DaiP	100.0	100.0	100.0	100.0	100.0	100.0	100.0	100.0	100.0	NA	NA	NA	NA
DahP	100.0	100.0	100.0	100.0	100.0	100.0	100.0	100.0	100.0	NA	NA	NA	NA
BcFlu	100.0	95.2	93.7	100.0	96.6	100.0	100.0	100.0	100.0	100.0	99.8	99.9	100.0
C1-Fla/Pyr	98.2	92.9	91.5	97.6	95.5	98.4	100.0	100.0	100.0	87.5	84.7	80.7	89.9
C2-Fla/Pyr	100.0	95.3	94.6	100.0	100.0	100.0	100.0	100.0	100.0	100.0	100.0	100.0	100.0
C3-Fla/Pyr	100.0	100.0	100.0	100.0	100.0	100.0	100.0	100.0	100.0	NA	NA	NA	NA
C1-BaA/Chry/TPh	100.0	100.0	100.0	100.0	100.0	100.0	100.0	100.0	100.0	100.0	99.9	100.0	99.6
C2-BaA/Chry/TPh	100.0	100.0	100.0	100.0	100.0	100.0	100.0	100.0	100.0	100.0	99.9	100.0	100.0
C3-BaA/Chry/TPh	NA	NA	NA	NA									
C4-BaA/Chry/TPh	NA	NA	NA	NA									

The aim was to achieve a -25% difference in soil weight, the -25% difference was to account for the 25% moisture content in soils, actual percentages are shown in Figure 22. The DGWS soils reported a mean difference of -24.6%, while the DC soils reported a difference of -23.9%. Deviations from the targeted -25% may be attributed to factors such as water evaporation, sample loss during soil removal, scrapped membrane within soil or variations in the initially added water weight. Nevertheless, the majority of samples closely approached a -25% difference in soil mass, leading to the acceptance that the experiments were approximately at 25% moisture content.

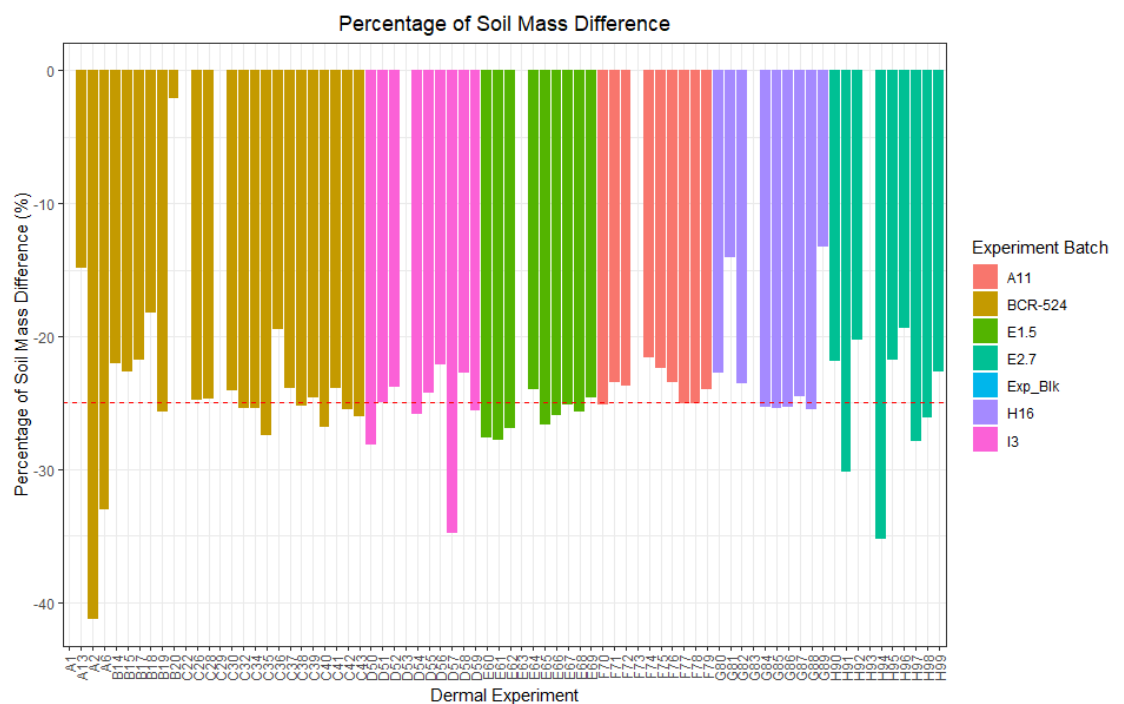


Figure 22. Mass difference percentages between the wet-applied soil on the membrane and the collected dried soil after removal from the membrane post-experiment, a -25% was the target to account for the added moisture to the soil (dashed line on plot). Note experiments with no bar represent dermal blank experiments which did not include applied soil.

4.3.3 Validating dermal results by comparison to other studies

Table 16 presents the RS fluxes, membrane fluxes, and total fluxes (combined RS and membrane flux) from my study and Lort (2022) results. The Wilcoxon signed-rank test demonstrated no statistically significant differences (p-values < 0.05), except for Pyr RS flux, which reported a p-value = 0.049, albeit not considered statistically significant, as it was close to 0.05. These results provide

confidence that the BCR-524 fluxes from both studies are not significantly different, affirming the accurate and repeatable performance of the *in vitro* dermal experiments, consistent with Lort (2022). It should be noted that my BCR-524 RS values had uncertainties associated to the measured RS fluxes due to low surrogate recoveries as described in Section 4.2.3. Therefore, these are used with caution and not reported as results in the Papers 2 and 3, instead are used as approximations. The low recoveries could explain the lower RS fluxes experienced with this study's results, given that the membrane fluxes were considerably close between the two studies.

Table 16. Comparisons of RS, membrane and total fluxes for the sample BCR-524 at 24-hours between my study and Lort (2021).

PAH	Study	No. Exp	RS Flux (ng/cm ² /h)	Membrane Flux (ng/cm ² /h)	Total Flux (ng/cm ² /h)
BaP	Lort (2021)	4	0.021	0.44	0.46
BaP	This study	3	0.0031	0.6397	0.6428
Pyr	Lort (2021)	4	2.6	112.9	115.5
Pyr	This study	3	1.3	111.8	113.1
DahA	Lort (2021)	4	0.0001	0.011	0.011
DahA	This study	3	0	0	0

Furthermore, my measured dermal fluxes aligned within the range of those reported in other research studies, particularly for BaP, which is widely investigated at 24-hours. Table 17 showcases my results for BaP fluxes for comparison with previous studies. For instance, Wester et al. (1990) reported human skin fluxes of BaP at 24-hours at 1.67×10^{-3} ng/cm²/h, 0.23 ng/cm²/h and 0.24 ng/cm²/h for the RS, membrane and total fluxes, respectively. The Wilcoxon signed-rank test revealed no significant evidence ($p > 0.05$) of differences between my RS, membrane, and total fluxes and those reported by Wester et al. (1990) using human skin. Similarly, other studies (Peckham et al., 2017, Roy and Singh, 2001, Moody et al., 2007) presented RS fluxes for BaP at 24-hours from different soil samples, ranging from 0.012 to 4.3 ng/cm²/h. My RS fluxes

were below these studies ranges and presumed to be because of influences of initial soil concentrations, soil composition differences, ageing influences and differences in dermal experimental methods.

Table 17. Summary of the dermal fluxes of 24-hour BaP for my samples results which were compared to other studies to validate this study's findings.

Matrix	Time (hr)	No. soils	Avg. flux (ng/cm²/h)	Min. flux (ng/cm²/h)	Max. flux (ng/cm²/h)	Avg. flux normalised to soil conc. (ng/cm²/h)
RS	24	6	2.36x10 ⁻³	ND	8.91x10 ⁻³	1.50x10 ⁻⁴
Memb.	24	2	2.83	0.64	5.02	0.066
Total	24	2	2.83	0.64	5.02	0.066

ND = not detected.

4.4 QC summary

In summary, the QC assessment encompassed of spiked solvents, sample extraction recoveries, detection limits, blank samples, and measurement of CRM samples. The *in vitro* dermal experiments were evaluated by measuring matrix weight differences, mass balance calculations and comparing fluxes with relevant literature. Through the combined implementation of these methods, I have managed a high level of confidence for a diverse range of HMW PAHs at various PAH concentrations in three matrices. My comprehensive QC measures have validated the accuracy and precision of my analytical method, enabling the reliable quantification of HMW PAHs in various matrices, thus contributing to a robust understanding of dermal bioavailability in my research.

Chapter 5 Characterisation of former Manufactured Gas Plant soils using parent and alkylated Polycyclic Aromatic Hydrocarbons and Rock-Eval(6) Pyrolysis

Alison M. Williams-Clayson^{1,2}, Christopher H. Vane¹, Matthew D. Jones², Russell Thomas³, Alexander W. Kim¹, Christopher Taylor⁴, Darren J. Beriro^{1*}

*corresponding author

¹ British Geological Survey, Keyworth, Nottinghamshire, UK; ² University of Nottingham, Nottingham, UK; ³ WSP UK, Bristol, UK; ⁴ National Grid, Warwick, UK

Accepted for publication: Environmental Pollution, Volume 339, 15 December 2023 (Williams-Clayson et al., 2023)

Statement of Contributions of Joint Authorship

Williams-Clayson, A: (Candidate):

Performed field work for two of the MGP sites. Conducted all laboratory work including sample preparation of soils to GC-MS extracts solution, developed GC-MS/MS method and ran all GC-MS/MS runs for PAH analysis, analysed all the data, and wrote the manuscript. Took the lead role in all writing taking responsibility of drafting and revising manuscript and first author on paper.

Vane C., Beriro, D.; Jones, M.; Thomas, R.: (Supervisors):

Supervised and provided feedback and helped shape the research project and manuscript.

Kim, A.: (BGS Laboratory Technician):

Helped establish laboratory procedures and GC-MS/MS methods.

Taylor, C.: (Industrial Supervisor):

Provided site access for sampling, information regarding sites and feedback on manuscript.

5.1 Abstract

Soils sampled from 10 former manufactured gas plants (MGP) in the UK were investigated using gas chromatography mass spectrometry (GC-MS/MS) and Rock-Eval(6) Pyrolysis (RE). RE is a screening tool used to characterise bulk organic matter in soils *via* the release of carbon compounds during pyrolysis and oxidation. Both the distributions and concentrations of 30 parent and 21 alkylated polycyclic aromatic hydrocarbons (PAHs) and the parameters of RE were analysed to establish relationships between soils and the MGP processes history. Principal component analysis (PCA) using the PAHs distributions and RE parameters can assist with differentiating between MGP processes. MGP processes utilising oil provided the clearest results, from observing petrogenic signatures, with increased low molecular weight PAHs. Processes using lower temperature processes were distinguished by higher proportions of higher molecular weight PAHs. RE parameters alone were unable to distinguish MGP processes but showed potential in estimating the degree of PAH release from soils based on the diversity of different RE parameter results. More generally, our research findings could be useful in understanding and characterising the risks posed to human health from PAHs in soils.

5.2 Introduction

Polycyclic aromatic hydrocarbons (PAHs) are a class of organic compounds and are a concern to human health due to their toxicity, with several PAHs classified as being mutagenic and carcinogenic (International Agency for Research on Cancer, 2010). In the environment, PAHs can be found to be persistent in soil as complex mixtures, comprising of parent PAHs (basic fused aromatic ring structure), alkylated PAHs (additional hydrocarbon chain attached), or heteroatom containing PAHs (containing non carbon/hydrogen elements). The most studied PAH group is the 16 U.S Environmental Protection Agency PAHs (EPA16) which comprise solely of parent PAHs: naphthalene (Nap), acenaphthylene (Acy), acenaphthene (Ace), fluorene (Flu), phenanthrene (Phen), anthracene (An), fluoranthene (Fla), pyrene (Pyr), benzo[a]anthracene (BaA), chrysene (Chry), benzo[b]fluoranthene (BbF), benzo[k]fluoranthene (BkF), benzo[a]pyrene (BaP), indeno[1,2,3-cd]pyrene (IcdP), dibenz[a,h]anthracene (DahA), and benzo[g,h,i]perylene (BghiP). Nap, Acy,

Ace, Flu, Phn and An are categorised as low molecular weight (LMW) PAHs with <4-ring structures, the remaining PAHs are categorised as high molecular weight (HMW) PAHs (≥ 4 -rings) (Meador, 2008). Estimating risks to human health exclusively on the EPA16 creates uncertainty as the suite does not include other potentially more toxic compounds e.g. alkylated PAHs (Andersson and Achten, 2015).

The quantity and type of PAHs present in the environment initially depends on the source and the PAH formation process (Dong et al., 2012, Gao et al., 2016). A petrogenic source (crude oil and petroleum) synthesises PAHs slowly under low temperatures, resulting in a high proportion of LMW PAHs and increased amounts of alkylated PAHs (Andersson and Achten, 2015). However, the petrogenic process of coalification can synthesise HMW PAHs, caused by aromatic ring condensation reactions. Consequently, coals contain large and complex PAH compounds (Ribeiro et al., 2012, Mathews and Chaffee, 2012). Pyrogenic sources (coal carbonisation, vehicle exhaust, wildfires) alternatively form PAHs comparatively quickly by incomplete combustion of organic matter (OM) at high temperatures and result in abundant amounts of thermodynamically stable HMW parent PAHs (Kim et al., 2017, Ribeiro et al., 2012).

Sites where people are exposed to soils with high PAH concentrations e.g. formally contaminated sites under redevelopment, may require human health risk assessments (HHRAs) to evaluate the risks posed by the PAHs to human health and the actions required to address the risks (Gormley et al., 2011, Beriro et al., 2020). HHRAs use exposure models such as the Contaminated Land Exposure Assessment (CLEA) model to generate Generic Assessment Criteria (GAC) based on the exposure pathways, receptors, soil types, land use, and contaminant concentrations (Cole and Jeffries, 2009). Numerous studies have reported that the quantity and type of soil OM is a dominant factor influencing the release and risk arising from PAHs from soil (Yu et al., 2018, Ehlers and Loibner, 2006). It is also known that the contribution of each exposure pathway towards the total exposure to a human will vary depending on the contaminant. LMW PAHs report a higher inhalation contribution percentage compared with HMW PAHs, due to the compound's physicochemical properties (e.g. volatility)

(Nathanail et al., 2015). Thus, knowledge of the expected PAHs present at a site alongside soil properties can help assessors conducting HHRAs. Currently guidance on the BaP GAC for residential land use with plant uptake is 5 mg/kg. Soils above this are considered to pose a potentially unacceptable risk to human health (CL:AIRE, 2014).

Post-industrial sites commonly have soils with PAH concentrations above GAC values and thus pose potential risks. A good example of such sites includes those which previously operated as manufactured gas plants (MGPs), commonly known in the UK as gasworks. MGPs synthesised hydrogen and methane rich gas via the process of pyrolysis of coal or oil. MGPs produced a wide variety of wastes and by-products including scurf, ash, coal tar, coal, benzol, ammoniacal liquor, spent oxide, and fowl lime (Thomas, 2014, Ruby et al., 2016). To improve the manufacturing efficiency, several MGP processes were developed. These include low temperature horizontal retorts (LTHR), high temperature horizontal retorts (HTHR), continuous vertical retorts (CVR), intermittent vertical coke ovens (IVCOs), coke ovens (COs), carburetted water gas (CWG), Tully plants (TP), heavy oil reforming plants (HORP), catalytic oil gas plants (COGP), and processes implemented to convert by-products to profitable goods such as tar distillation plants (TDP) and chemical plants (CP) (Gallacher et al., 2017b, Thomas, 2014).

HHRAs could provide more accurate risk estimations if the MGP process PAH distributions were known and targeted in assessments. Gallacher et al. (2017b), Thomas (2014) and McGregor et al. (2012) provide detailed descriptions of these MGP processes, such as the retort/chamber structures and pyrolysis temperatures used. They classified MGP processes by PAHs from end-member coal tars using two-dimensional gas chromatography (GC×GC) (McGregor et al., 2012, Gallacher et al., 2017b). In contrast our study investigated contaminated gasworks soils (GWS) using gas chromatography-mass spectrometry (GC-MS/MS), selected for its increased selectivity compared to full scan in GC-MS. This study also used a complementary screening technique called Rock-Eval(6) Pyrolysis (RE), initially used for oil exploration and more recently used to investigate different types of OM (Könitzer et al., 2016, Upton et al., 2018) and hydrocarbons in contaminated soils (predominately from oil spills) (Lafargue et

al., 1998). RE characterises the bulk OM by quantifying the release of hydrocarbons (detected by flame ionisation) and the release of CO and CO₂ (monitored by infrared), recorded in response to the increasing temperature versus time throughout the pyrolysis and oxidation stages (Behar et al., 2001b, Lafargue et al., 1998). For our study RE was used to determine whether there were relationships between RE parameters, PAH distributions and MGP processes. To our knowledge only one other paper (Haeseler et al., 1999), measuring fewer samples and using an older technique (Rock-Eval III) has applied RE to GWS.

The research question for this study was whether GWS could be characterised by the MGP processes formally utilised at the site. Techniques to achieve this involved measuring 51 PAHs (30 parent and 21 alkylated) by GC-MS/MS and measuring bulk OM properties by RE. Using a combined approach allows for a comprehensive understanding of GWS organic fractions. RE offers a rapid screening and a broader assessment of the overall organic compositions and GC-MS/MS provides detailed information on the PAH composition. We used the analytical data to explore relationships between RE parameters and PAH concentrations and distributions. In particular, we used the parent and alkylated PAH distributions, PAH diagnostic ratios, and principal component analysis (PCA). In summary, this research provides an understanding on identifying connections between MGP processes and the distributions of PAH contamination and OM fractions. These findings could inform which PAHs to target in risk estimation and management, helping to make HHRAs more accurate.

5.3 Materials and methodology

5.3.1 Sample collection and selection

A total of 93 soil samples were collected between 2016-2021 from 10 UK former MGP sites with periods of site inactivity ranging between 46-99 years, including a gasholder station, and a former tar distillation plant at a chemical works of a large city gasworks site. The locations of the sites are commercially sensitive and are not presented. Site and sample PAH and soil properties are detailed in both Table 18 and Appendix B Chapter 5 Research Papers SI Table S1-2. Sample collection took place while the sites were under investigation or remediation by

National Grid Property Holdings, which influenced where and when sampling could occur. Two background samples (BG) from local parks and a sub-set of 48 GWS (from the 93 collected GWS) were selected for PAH measurement using GC-MS/MS analysis. This sub-set was selected using stratified sampling and k-means clustering (k=5) informed by RE analysis screening data.

5.3.2 Sample preparation

Directly after collection soils were freeze-dried, disaggregated, and sieved through a 250 µm stainless steel mesh. Freeze drying minimises the effect of PAH losses from drying in comparison to other methods (Beriro et al. 2014). ~1 g of the <250 µm fraction was spiked with 25 µg of deuterated PAH standards (surrogates used were phenanthrene-d10, pyrene-d10, benzo[b]fluoranthene-d12, benzo[a]pyrene-d12 and benzo[g,h,i]perylene-d12). PAHs from GWS were extracted by accelerated solvent extraction (ASE, Dionex-300) using DCM/acetone 1:1 v/v at a temperature of 100 °C and a pressure of 1500 psi. ASE extracts were diluted to 50 mL and a 400 µL aliquot was filtered by solid phase extraction (SPE) cartridges (Varian, Bond Elute TPH). The first SPE elution (1.5 mL of pentane) was discarded, the second elution containing PAHs was retained in 6 mL hexane/iso-propanol (96.6:3.4 v/v). Samples were blown down to 1 mL with a gentle stream of nitrogen before being spiked with 200 ng/mL of internal standards: fluorene-d10, fluoranthene-d10, perylene-d12 and indeno(1, 2, 3-cd)pyrene-d12. Further details of the spiking and extraction methods are presented in other papers (Vane et al., 2021, Garcin et al., 2022b).

5.3.3 PAH concentration

A total of 51 PAHs (PAH51) were quantified by GC-MS/MS; 30 parent PAHs (PAH30) and 21 grouped alkylated PAHs (Alkyl21) (Chapter 5 Research Paper SI Appendix B Table S3 and S6). PAH concentrations were determined by Thermo Scientific Trace 1300 GC coupled to a Thermo Scientific TSQ9000 triple quadrupole (GC-MS/MS) using the selected reaction monitoring (SRM) mode, equipped with an Agilent Select PAH column (30 m length x 0.25 mm diameter x 0.15 µm film thickness). A 1 µL aliquot of sample was injected in splitless mode using a split flow of 15 mL/min at 0.7 min with an injection temperature of 70 °C, which was held for 2 minutes, ramping at 10 °C/min to 180 °C and a final ramp of 4 °C/min to 350 °C. Helium was used as the carrier

gas. The GC-MS/MS measurements on the alkylated PAH series were determined following Ghetu et al. (2021) and Sørensen et al. (2016).

Calibrations were performed using six calibration concentrations of PAH reference mixtures (PAH-Mix 9, PAH-Mix 45 and PAH-Mix 183, Dr. Ehrenstorfer), spiked with deuterated surrogates and internal standards. To determine instrument performance and background signals, standards were processed the same as GWS and inter-dispersed every 20 samples within the GC-MS/MS runs. The standards included the calibration samples of 200 pg/ μ L, procedural blanks of toluene and 1g of the certified reference material (CRM) (NIST-1944: New York/New Jersey Waterway). Surrogate recoveries in all samples and standards were quantified to determine method efficiency and used for analyte concentration corrections (Appendix B Chapter 5 Research Papers SI Section S1 and Table S4).

5.3.4 Rock-Eval(6) Pyrolysis

GWS were analysed using a Rock-Eval(6) pyrolyser (Vinci Technologies) to characterise OM (Behar et al., 2001a). Powdered dry samples (~30 mg) underwent the RE technique applied from Upton et al. (2018), the performance of the instrument was tested, by comparison to accepted values of Institute Français du Pétrole standards (IFP 160000, S/N1 5-081840). Eighteen parameters were determined and defined by Cooper et al. (2019), Behar et al. (2001b), Waters et al. (2020) and include:

- S1 (HC mg/g)- quantity of thermo-vaporised free hydrocarbons released during pyrolysis heating up to 200 °C.
- S2 (HC mg/g) - quantity of hydrocarbons released from thermal cracking of mature OM during pyrolysis temperatures up to 650 °C.
- TpkS2 (°C) - true temperature value of the maximum yield of hydrocarbon released for the S2 peak.
- S3, S3', S3CO, and S3'CO (mg CO₂/g or mg CO/g) – measure of CO and CO₂ produced during pyrolysis for organic and/or mineral source.
- TOC(%) – total organic carbon calculated from the sum of the carbon moieties (HC, CO, and CO₂).

- RC(%) – residual carbon composed of thermally resistant OM that remains after pyrolysis and is combusted in the oxidation stage, calculated by $(S4CO_2 \times \frac{12}{440}) + (S4CO \times \frac{12}{280})$.
- PC(%) - pyrolysable carbon yielded during the pyrolysis stage, calculated using $(S1 + S2) \times 0.083 + (S3CO_2 \times \frac{12}{440}) + (S3CO \times \frac{12}{280})$.
- HI (mg HC /g TOC) – hydrogen index measures the extent of hydrogenation and provides indication of bound hydrocarbons released relative to TOC, calculated from $S2 \times 100/TOC$.
- OI (mg O₂/g TOC) – oxygen index corresponds to the released amounts of oxygen from CO and CO₂ relative to TOC, deduced from $S3 \times 100/TOC$.
- PI – production index, gives an indication of maturity of sample using the calculation $S1/(S1 + S2)$.

The thermal stability of OM in the GWS was determined by 1) deconvolution of temperature nodes of 200 - 340 °C (A1), 340 - 400 °C (A2), 400 - 460 °C (A3) and > 460 °C (A4), 2) determination of the immature OM index (I-index) and the refractory OM index (R-index), *I – index* = $Log_{10} ((A1 + A2)/ A3)$, and *R – index* = $((A3 + A4) /100)$ (Brown et al., 2023, Garcin et al., 2022a, Sebag et al., 2016).

5.3.5 Data evaluation and statistical analysis

Data evaluation and statistical analyses included principal component analysis (PCA), Shapiro-Wilk test, Levene’s test, one-way ANOVA, Welch’s ANOVA, and the post-hoc tests – Tukey HSD, Games-Howell and Pairwise Wilcoxon Rank Sum tests, were performed using R Statical Software (R Core Team, 2023) (Appendix B Chapter 5 Research Papers SI: Section S3).

5.4 Results and discussion

5.4.1 Distributions and concentrations of PAHs

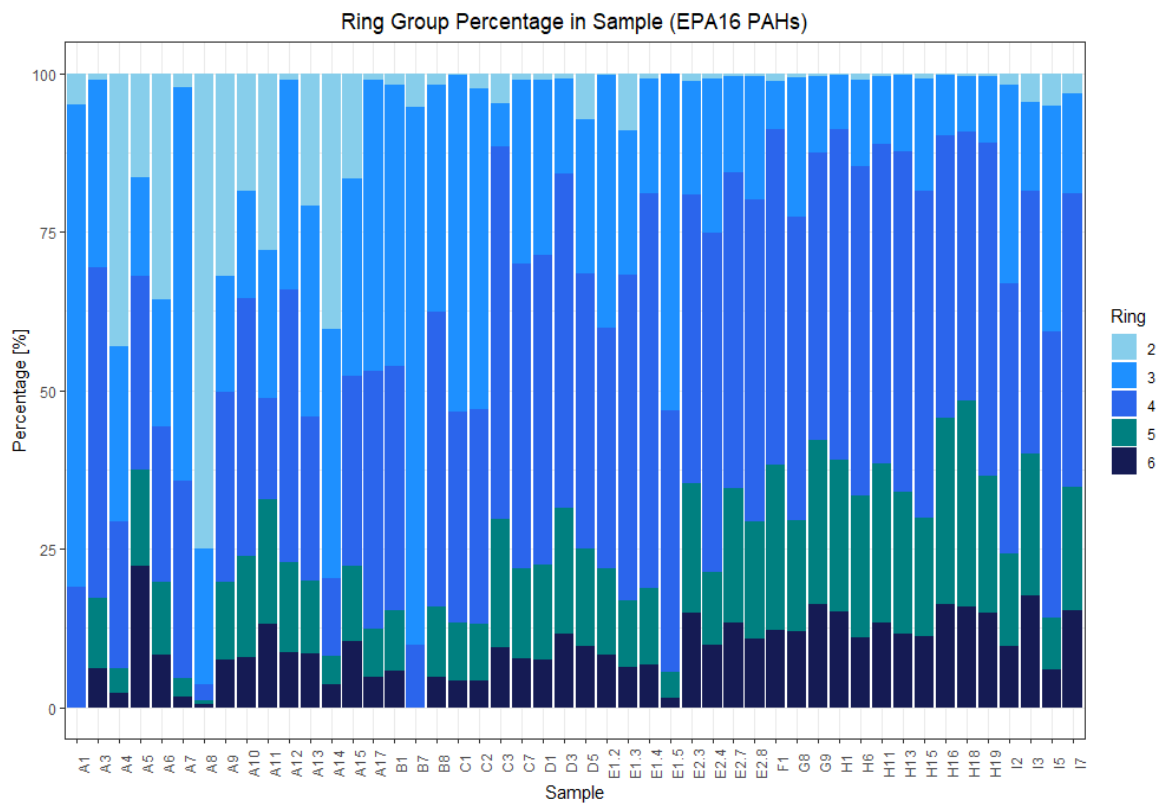
Total PAH concentrations and ring number contributions

A summary of the sites MGP processes and resulting PAH concentrations are shown in Table 18. PAH concentrations for each GWS are shown in Appendix B Chapter 5 Research Papers SI Table S6. Overall, Σ PAH51 concentrations in the GWS range between 23 mg/kg to 29,500 mg/kg (median of 636 mg/kg) and Σ EPA16 range between 15 mg/kg to 23,400 mg/kg (median of 375 mg/kg), these

ranges are similar to previous MGP investigations (Thavamani et al., 2012, Haeseler et al., 1999, Stout and Brey, 2019). In comparison, the BG soils recorded a Σ EPA16 mean concentration of 60 mg/kg, comparable to the London soils Σ EPA16 mean of 56 mg/kg reported by Vane et al. (2014).

Site A had the largest variation in PAH ring number distributions with high amounts of 2- and 3- ring PAHs compared to other sites, see Figure 23. Sites B, C, E1 and I also exhibited higher contributions towards 2- and 3-ring PAHs compared to other sites. 2-ring PAHs showed several statistically significant differences ($p < 0.05$) between sites E2, F, G, and H vs sites A, C, E1, D, and I. In contrast, sites D, E2, F, G and H had the highest proportion of 5- and 6-ring PAHs. No significant differences between sites using one-way ANOVA were found for the 3- to 6-ring PAHs for the Σ EPA16 and Σ Alkyl21 log transformed concentrations (Appendix B Chapter 5 Research Papers SI Section S3). The results indicate that sites associated with multiple processes including processes utilising oil are positively related to higher proportions of LMW PAHs.

(a)



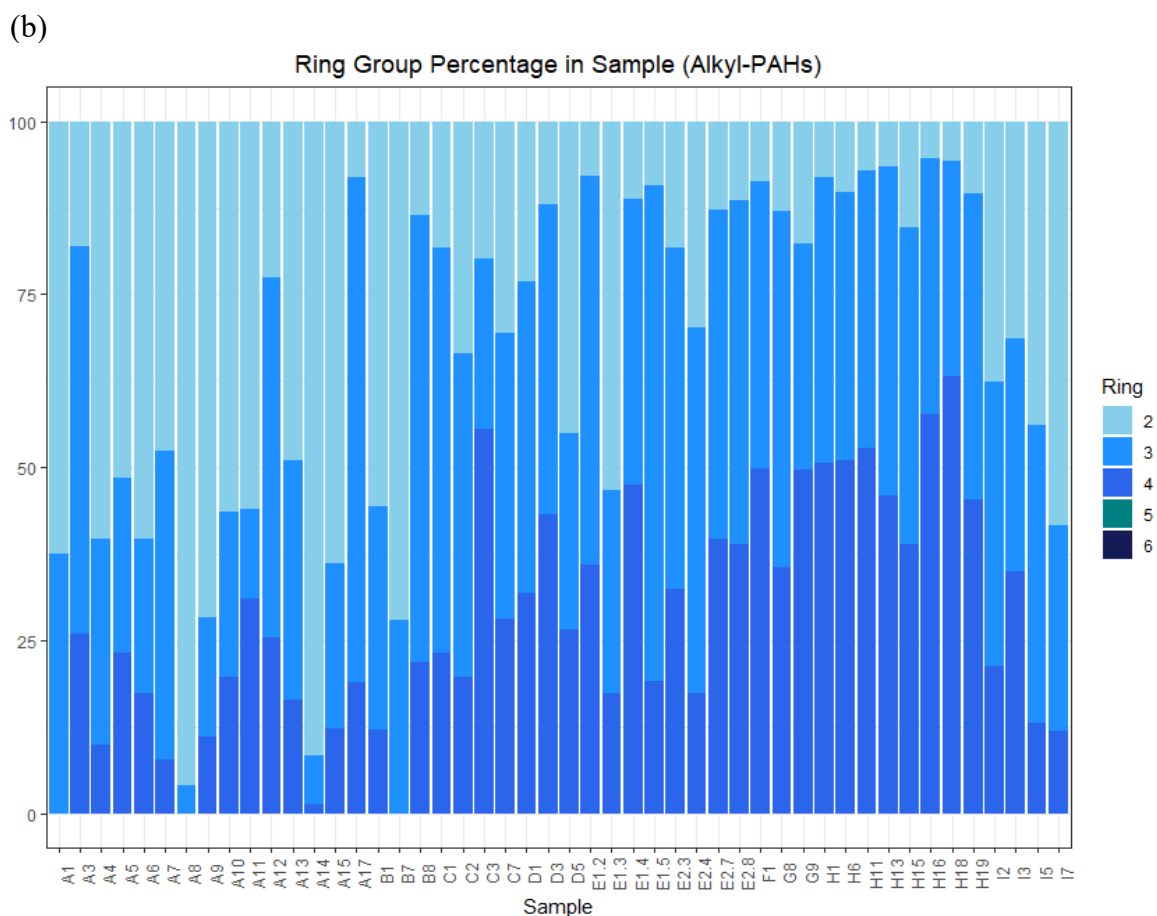


Figure 23. Bar chart showing the percentages of the proportions of the PAHs with different number of rings for (a) EPA16 and (b) Alkyl21.

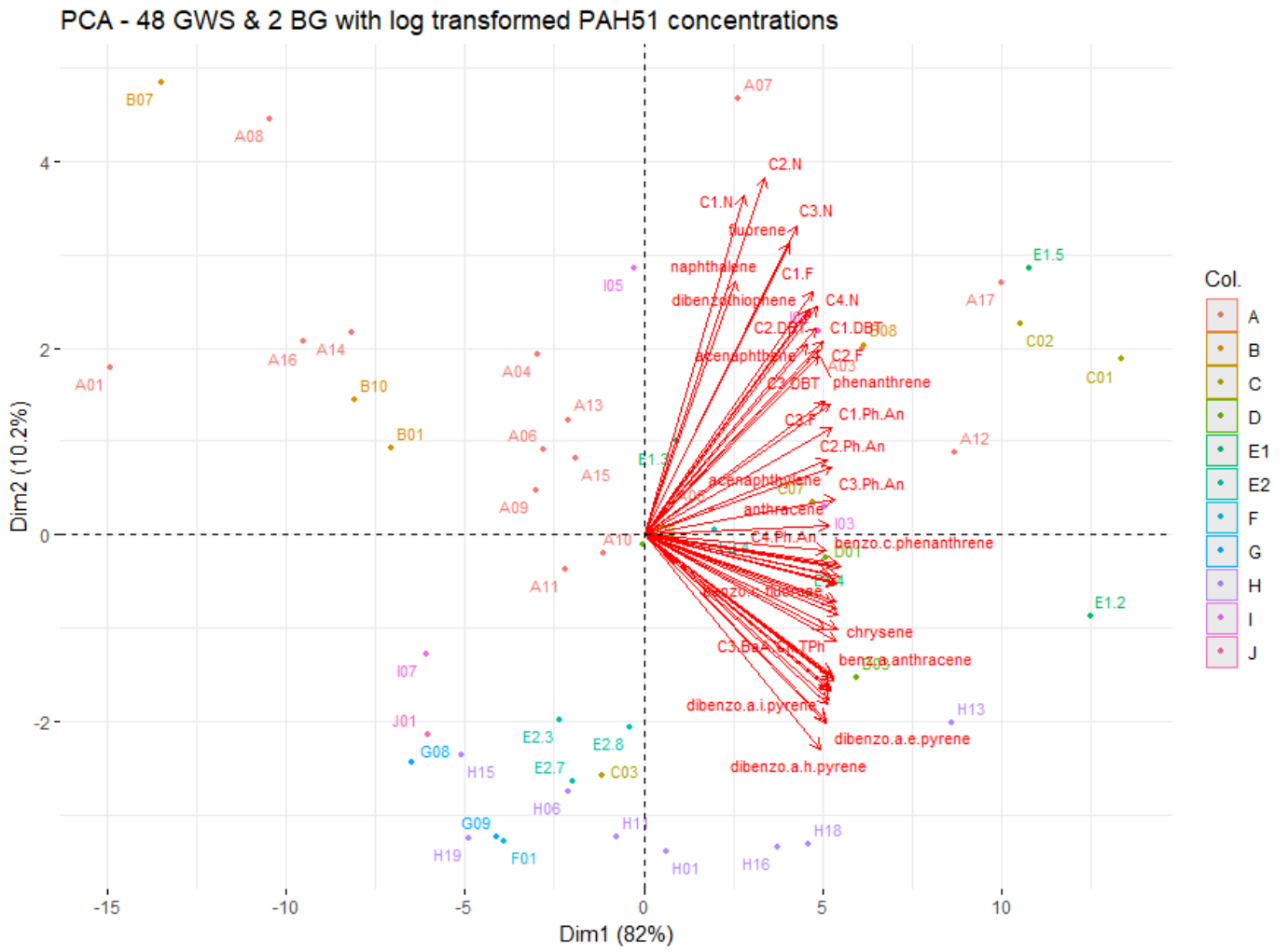
Parent and alkylated PAH distributions

Parent and alkylated PAH ratios (Appendix B Chapter 5 Research Papers SI Table S8) identified sites A, B, and I with the highest proportions of alkylated PAHs (low ratios). Sites C, D, and E1 reported the widest and most varied range of parent/alkylated PAH ratios. Sites C and E1 used multiple processes, which can account for the spread of ratios. The highest PAH concentrations (Appendix B Chapter 5 Research Papers SI Table S6) were for the HMW PAHs Fla, Phen, and Pyr which are generated by high temperature condensations of LMW PAHs (Thavamani et al., 2012). Sites C and E1 gave the highest PAH concentrations with similar PAH distributions (Phen > Fla > Pyr > An > BaA > Flu ~ Chry > BaP ~ BbF > BghiP) and observed higher contributions of anthracene than other sites as well as higher Flu contributions. Site D is documented operating the IVCO process only and recorded the next highest PAH concentrations which yielded similar median PAH distributions to sites E2 and G, (Fla > Pyr > Phen

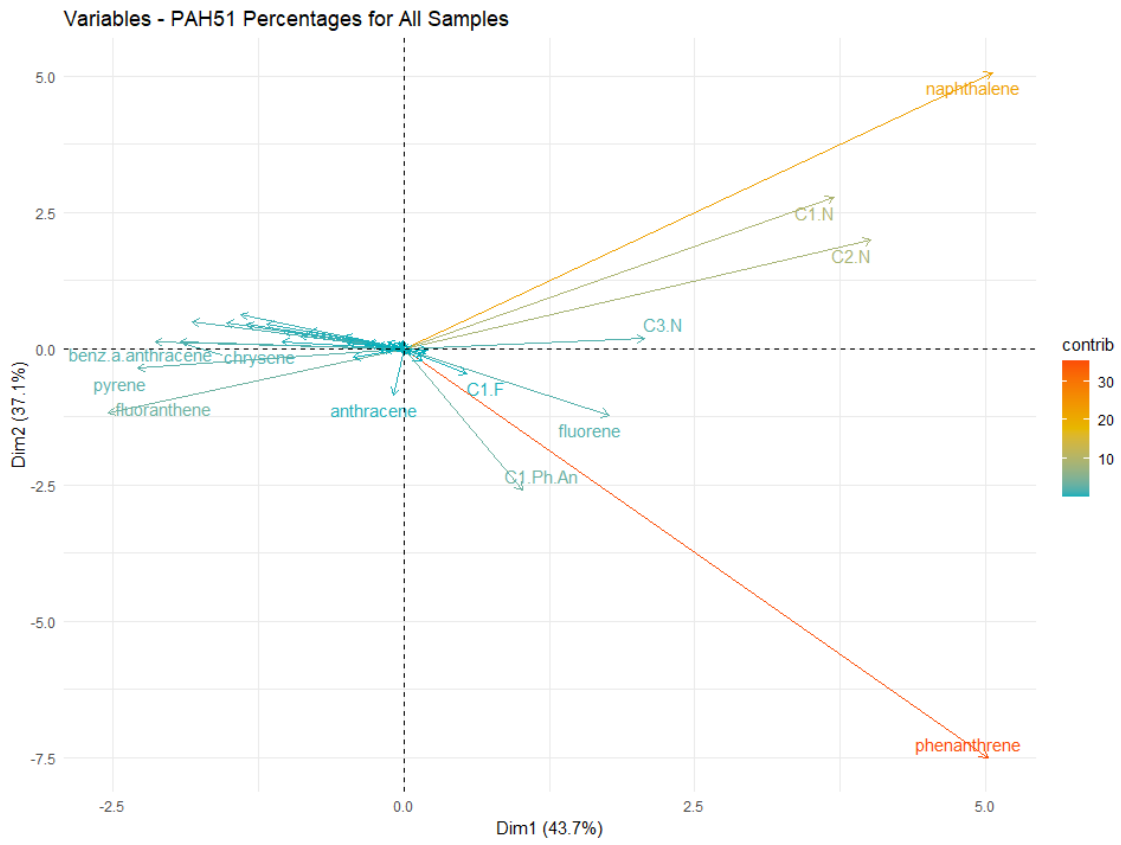
> BaA/Chry), sites E2 and G can both be associated to HTHR. The median PAH distribution order was identical for sites H and F (except for anthracene) with highest contributions from Fla > Pyr > BaA > Chry, which both operated the LTHR process.

PCA was used to investigate whether PAH distributions could characterise MGP processes. PCA was trialled on multiple data sets (Figure 24a-e) the most distinguishable clustering of MGP processes was achieved using the individual PAHs as relative contribution percentages towards the \sum PAH51 and removing GWS with \sum PAH51 concentrations <100 mg/kg. Figure 25 shows an annotated overview of the main observations detected in the multiple PCAs. The predominant observation shows positive associations between parent and alkylated Nap derivatives for site A, site I also had high contributions but not to the same degree. GWS sampled in locations of known CWG contamination (A17 and B8) were found in close proximity, showing strong positive associations from Phen, Flu, and An and their alkylated derivatives, as were GWS reporting the highest PAH concentrations from sites C and E1. Indicating sites with CWG, HTHR and CVR processes are associated to higher contributions from the 3-ring PAH compounds.

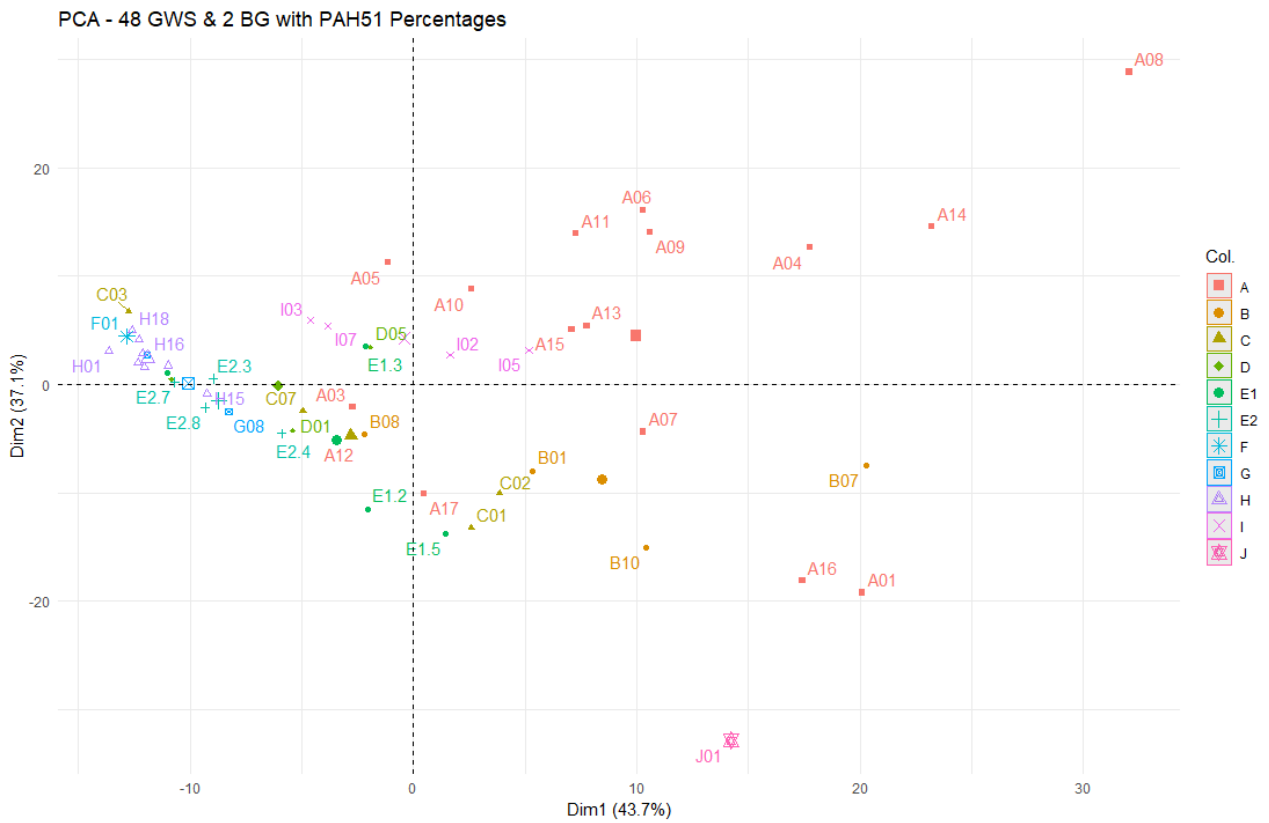
(a)



(b)

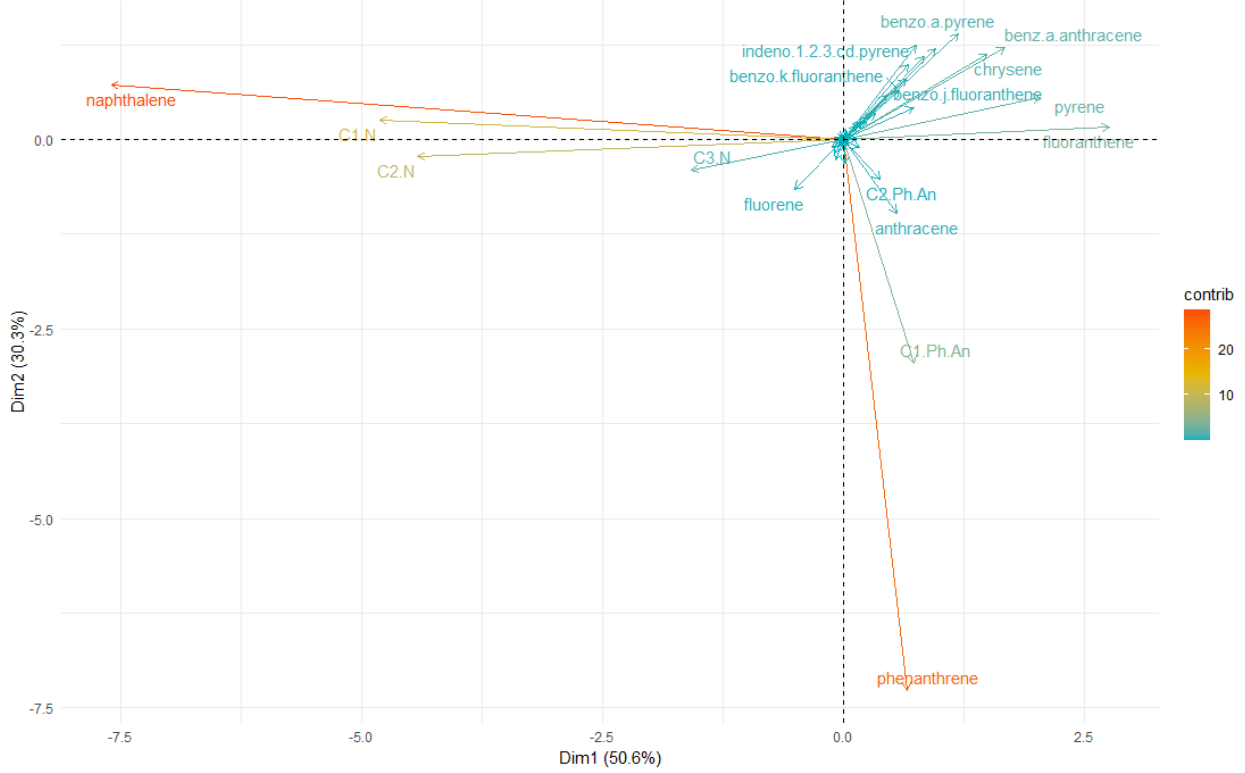


(c)



(d)

Variables - PAH51 Percentages (Removed below 100mg/kg samples)



(e)

PCA - 45 GWS with PAH51 Percentages (removal of samples below 100mg/kg)

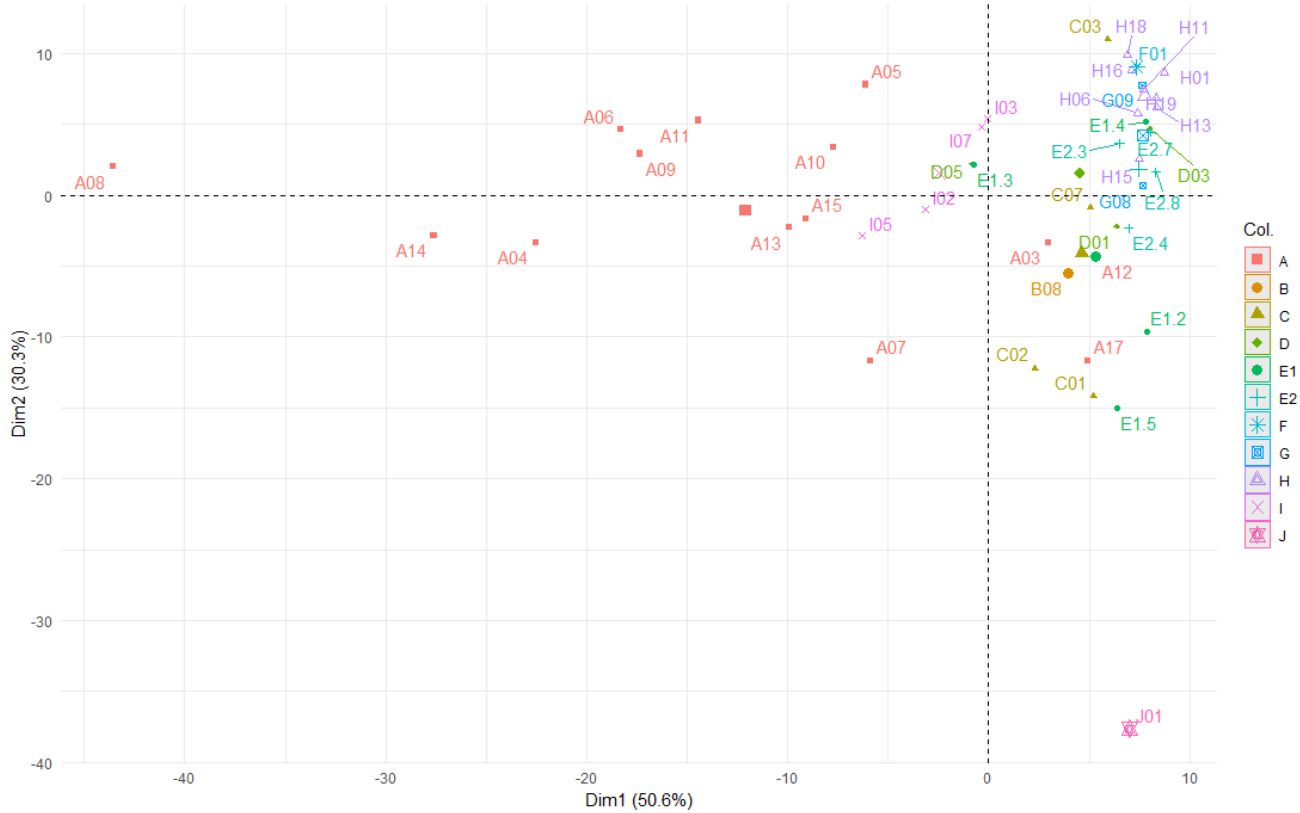


Figure 24. (a) PCA biplot created using the log transformed PAH51 concentrations of all 48 gasworks soils and 2 background park soils. (b) PAH51 individual PAH contributions of all 48 gasworks soils and 2 background park soils towards PCA (c) PAH51 individual PAH PCA biplot of all 48 gasworks soils and 2 background park soils. (d) PAH51 individual PAH contributions of all gasworks soils with a \sum PAH51 concentration >100 mg/kg towards PCA. (e) PAH51 individual PAH PCA biplot of all gasworks soils with a \sum PAH51 concentration >100 mg/kg towards PCA.

GWS from sites associated with the LTHR process (sites F, G and H) showed positive associations towards the HMW PAHs (BaA, Chry, and BaP) and strong negative associations with LMW PAHs (Phen, Nap and Flu). GWS from the chemical works site E2 had slightly higher PC2 eigenvectors (weaker associations to Phen compounds) compared to the sites associated MGP site E1. Site D GWS populated near the origin of both PC1 and PC2, indicating no dominating influence from individual PAHs associated with the IVCO process. Site C and E1 GWS in contrast varied by the PC2 eigenvector caused by differences with Phen compounds and HMW PAHs contributions, these sites have a range of processes including CVR, which would produce a diverse range of PAHs due to the process using a wide temperature gradient.

Table 18. Overview of sites MGP processes and PAH concentrations.

Site	Background	A	B	C	D	E1	E2	F	G	H	I
Type of Site	Background Park	MGP site	MGP site	MGP site	MGP site	MGP site	Chemical works	MGP site	MGP site	MGP site	Gasholder station
HTHR	-	Yes	Yes	Yes	-	Yes	Yes	-	Yes	-	Yes
LTHR	-	-	-	-	-	-	-	Yes	Yes	Yes	-
VR	-	CVR	CVR	CVR	IVCO	CVR	CVR	-	-	-	CVR
CWG	-	Yes	Yes	TP	-	Yes	Yes	-	-	-	Yes
Other Process	-	COGP, PFD, RP, OGR	CP	HORP	-	TDP	TDP	-	-	-	-
Samples collected	2	16	9	7	8	6	9	1	9	20	8
GC-MS/MS sampled	2	16	3	4	3	4	4	1	2	8	4

ΣEPA16 [mg/kg]	52 – 68 (60, 60)	15 – 5,173 (264, 905)	20 – 1,448 (57, 510)	419 - 16,669 (4,988, 6,767)	375 – 2,486 (1,928, 1,596)	564 – 23,370 (5,299, 8,633)	201 – 880 (356, 448)	135	76 – 163 (119, 119)	103 – 4,195 (465, 1,009)	61 – 921 (453, 472)
ΣAlkyl21 [mg/kg]	28 – 29 (28, 28)	8 – 4,207 (183, 732)	30 – 1,327 (33, 463)	99 – 6867 (210, 2,794)	197 – 693 (621, 504)	259 – 5954 (1,315, 2,211)	69 – 263 (101, 133)	53	22 – 31 (26, 26)	33 – 1,411 (143, 342)	32 – 1,295 (638, 651)
ΣPAH51 [mg/kg]	85 – 98 (91, 91)	23. – 10,015 (455, 1,756)	51 – 2,981 (96, 1042)	594 – 2,517 (7,597, 10,239)	636 – 3,638 (2,829, 2,368)	887 – 29,544 (8,899, 12,057)	310 – 1,285 (521, 659)	221	110 – 233 (173, 173)	155 – 6,576 (709, 1,607)	104 – 2,106 (1,338, 1,222)

HTHR = high temperature horizontal retort, LTHR = low temperature horizontal retort, CWG = carburetted water gas, VR = vertical retort, CVR = continuous vertical retort, IVCO = intermittent vertical chamber oven, CP = chemical plant, RP = reforming plant, COGP = catalytic oil gas plant, TP = Tully plant (VR + CWG), TDP = tar distillation plant, OGR = Onia-Geigy reformers, and HORP = heavy oil reforming plant. PAH concentrations in brackets are median and mean.

Gasworks Processes Relation to PAH51 Percentage Contributions with PCA

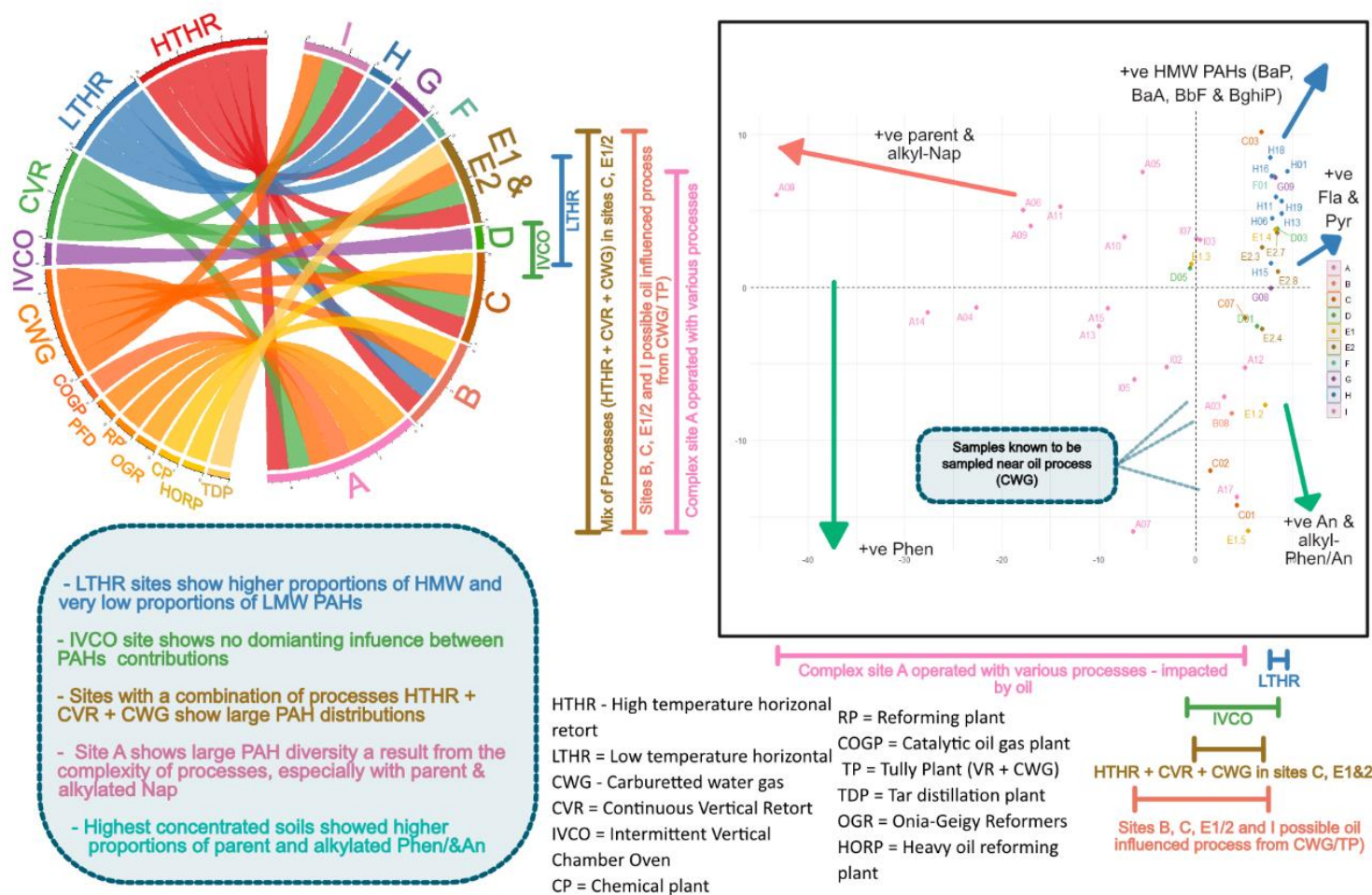


Figure 25. Chord diagram to show the MGP processes related to each site and an annotated PCA biplot of GWS PAH percentage contributions towards Σ PAH51, GWS with Σ PAH51 < 100 mg/kg removed.

- LTHR sites show higher proportions of HMW and very low proportions of LMW PAHs
- IVCO site shows no dominating influence between PAHs contributions
- Sites with a combination of processes HTHR + CVR + CWG show large PAH distributions
- Site A shows large PAH diversity a result from the complexity of processes, especially with parent & alkylated Nap
- Highest concentrated soils showed higher proportions of parent and alkylated Phen/An

HHRAs typically concentrate on the EPA16 (Nathanail et al., 2015), in this study the EPA16 accounted for 32-79% of the total Σ PAH51%. Large proportions of alkylated PAHs were reported in the GWS, with the Σ Alkyl21 contributing between 7-65% to the total Σ PAH51%. This suggests that alkylated PAHs can be present in high proportions at MGP sites but are generally not accounted for in a HHRA, and thus HHRAs could be incorrectly estimating risks posed. The relative contribution of each alkylated series towards the Σ Alkyl21% between sites are in Figure 26. Generally, the alkylated series for alkyl-Flu and alkyl-DBT provide the lowest contributions, and the alkyl-Ph/An and alkyl-Fla/Pyr alkylated series provided the highest contributions. Conversely, sites A, B, and I (associated with CWG) differed to this trend by conferring the highest contribution from the alkyl-Nap series and lower contributions from the HMW alkylated-PAHs, presumed to be a result due to the CWG process typically using Gas Oil (similar to diesel). Sites F, G and H associated with LTHR processes in contrast observed the highest contributions from the HMW alkylated series alkyl-Ph/An > alkyl-Fla/Pyr > alkyl-BaA/Chry/TPh than other sites, with sites E1 and E2 displaying similar series distributions.

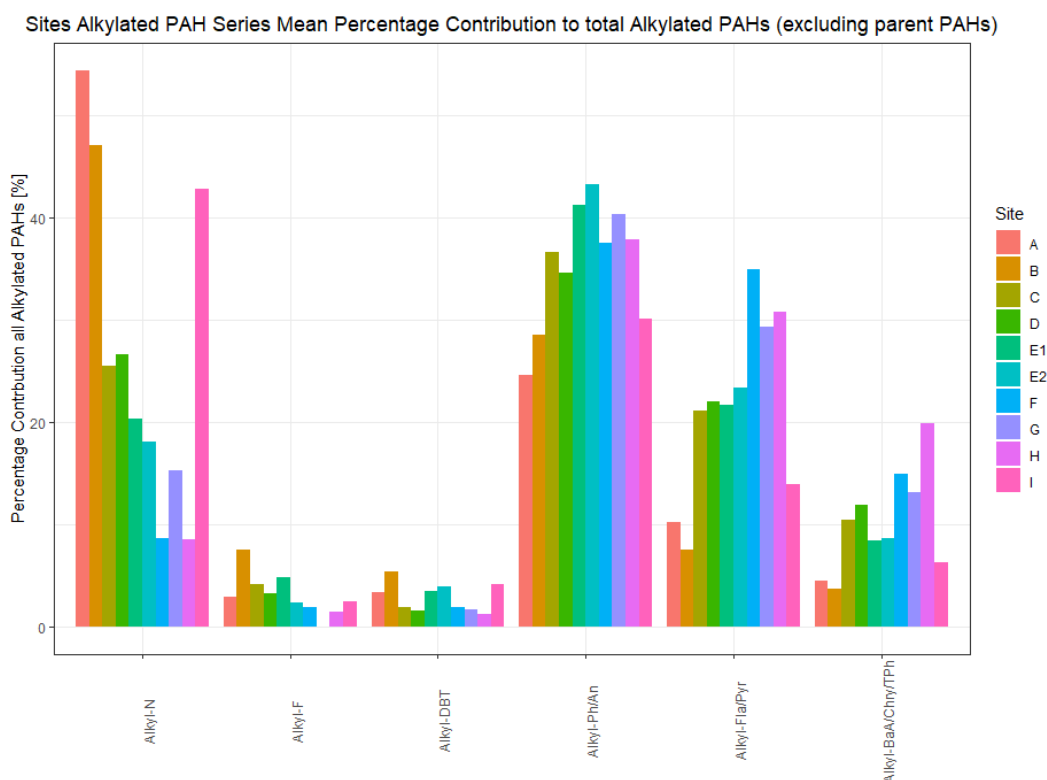
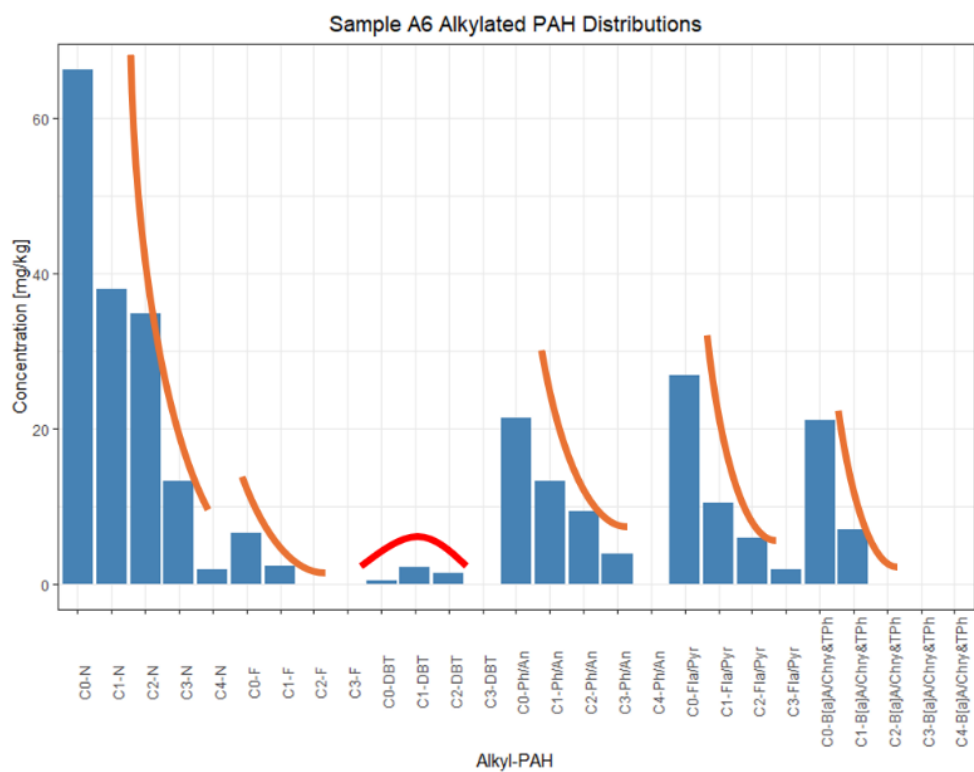


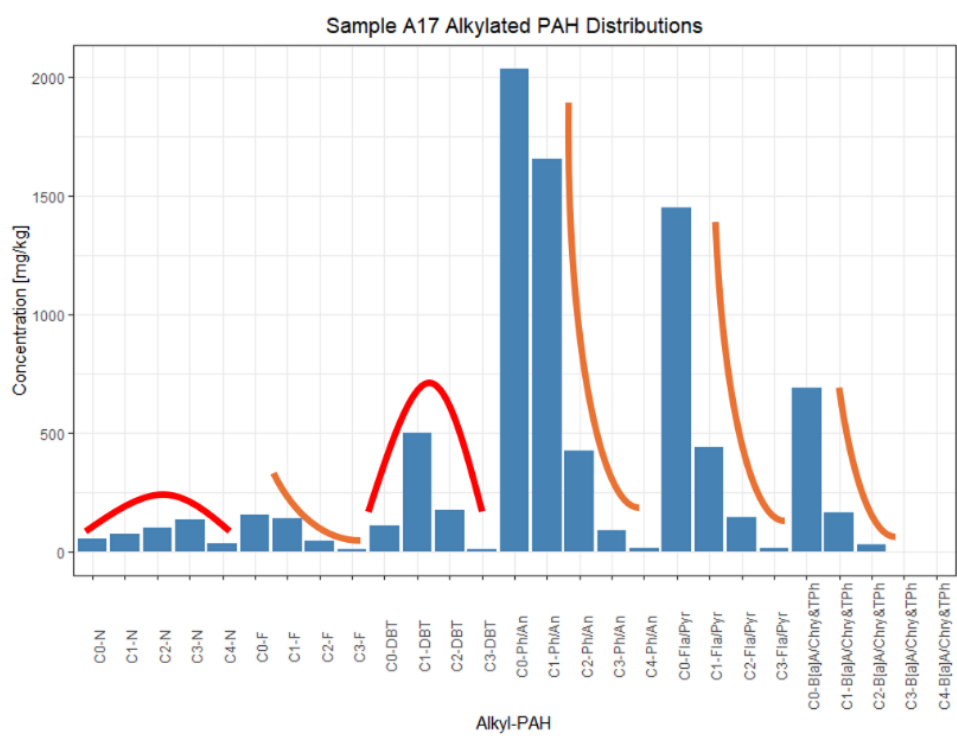
Figure 26. Bar charts of the mean percentage contribution of each alkylated series towards the Σ Alkyl21% for each site.

Alkylated PAH distribution signatures can assist in assigning PAH sources and were investigated for use in characterising MGP processes. An alkylated PAH homologue series with a “bell-shape” distribution signature is characterised as petrogenic, whereas a “slope-shape” following a decrease in concentration with an increase in the degree of alkylation is characterised as a pyrogenic source (Vane et al., 2021, Hindersmann and Achten, 2018). The slope of a pyrogenic alkylation distribution is dependent on the temperature, higher temperatures produce fewer alkylated PAHs creating a substantial decrease in the distribution slope (Stout et al., 2015). Examples of the alkylated PAH distributions for some of the GWS are shown in Figure 27. All GWS observed pyrogenic distributions for the alkylated series alkyl-Fla/Pyr and alkyl-BaA/Chry/TPh, and most GWS displayed pyrogenic distributions for alkyl-Ph/An except for samples A3, A7, and F1 which showed a petrogenic signature. The alkyl-DBT series displayed a petrogenic signature for all samples (except E1.2), a consequence of sulphur compounds associated with different oils (Douglas et al., 1996, McGregor et al., 2012). Distribution signatures were diverse within and between sites for the lower alkylated PAHs series alkyl-Nap and alkyl-Flu, potentially due to LMW PAHs being more susceptible to higher degrees of degradation compared to HMW PAHs, resulting in altered distribution signatures that differ from the original PAH source (Lima et al., 2005).

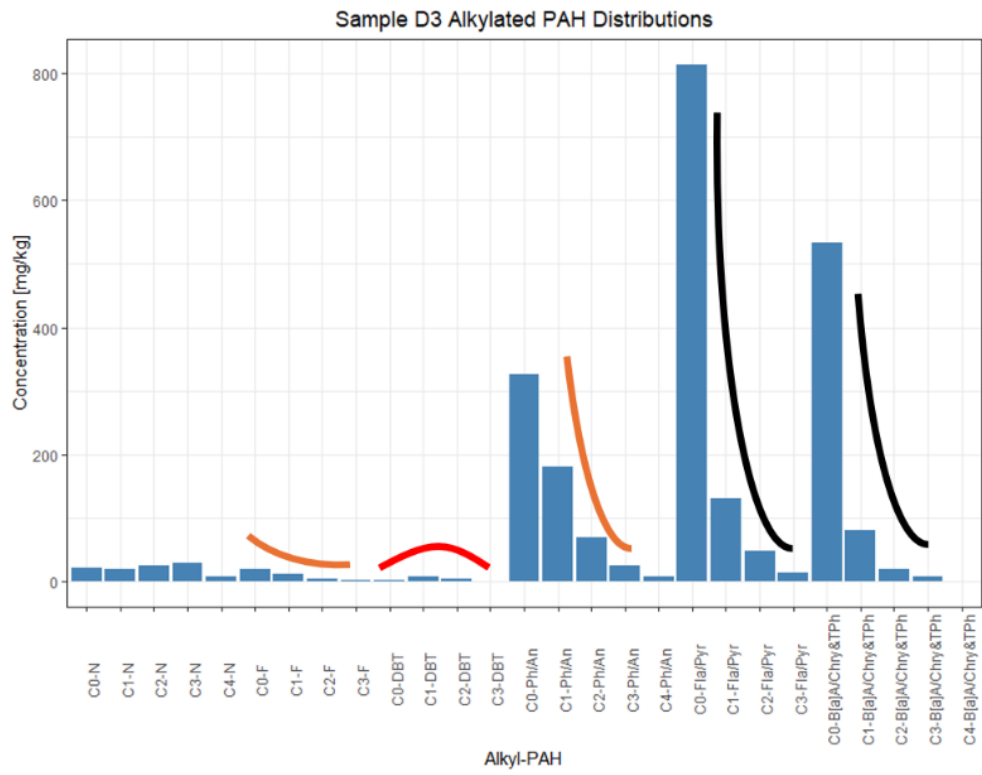
(a)



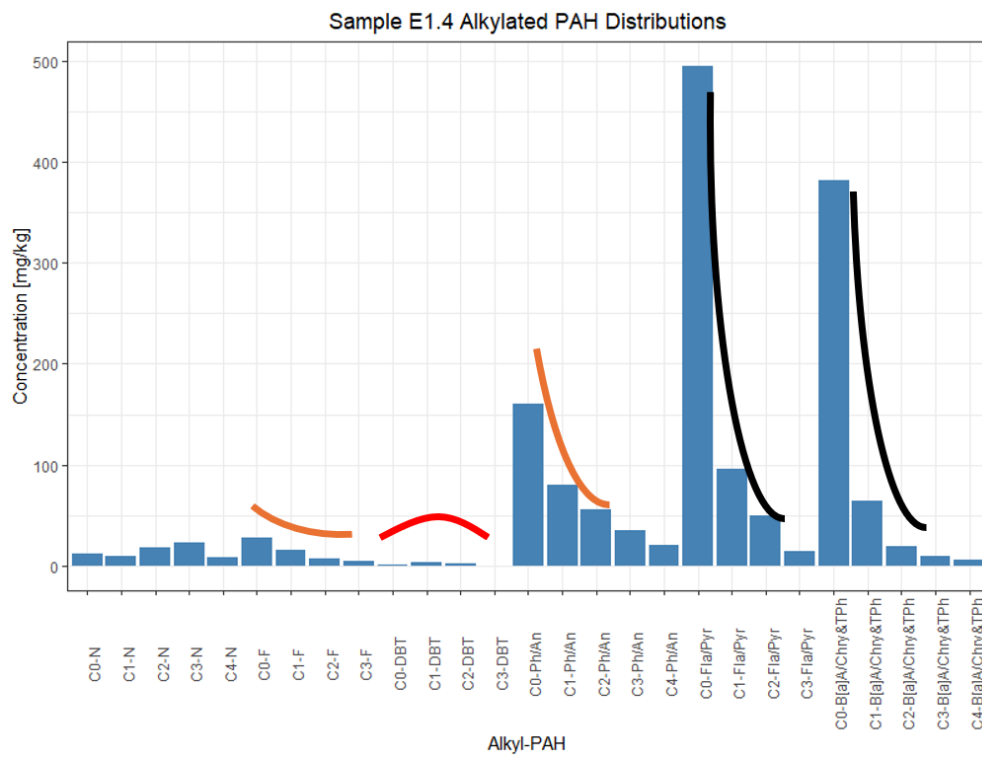
(b)



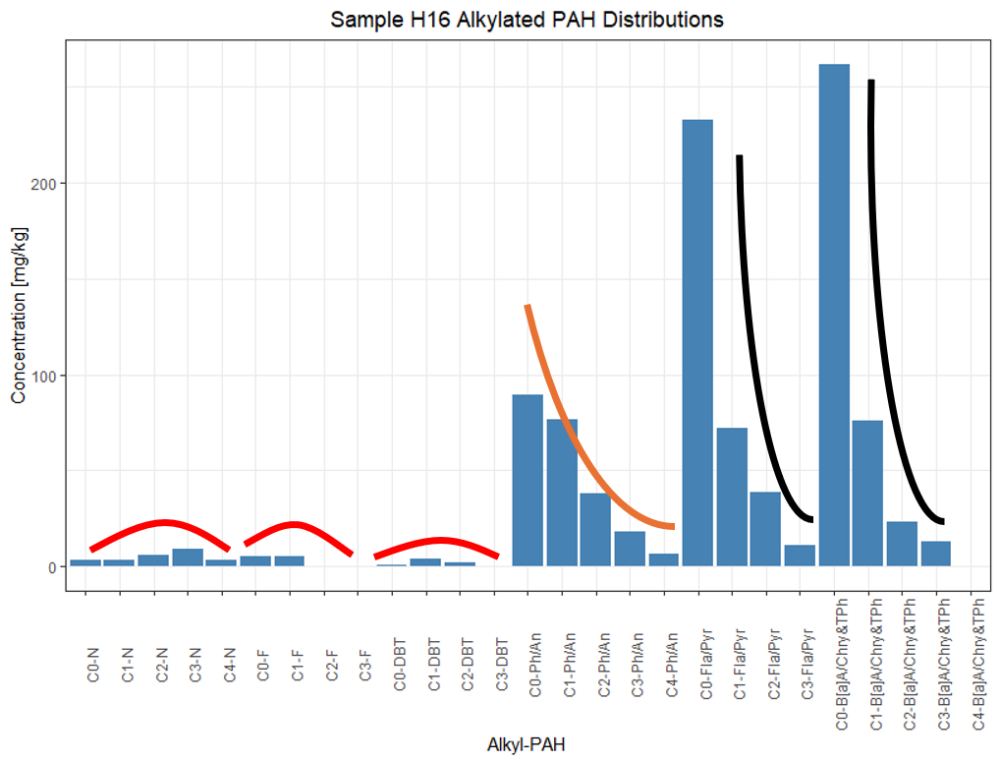
(c)



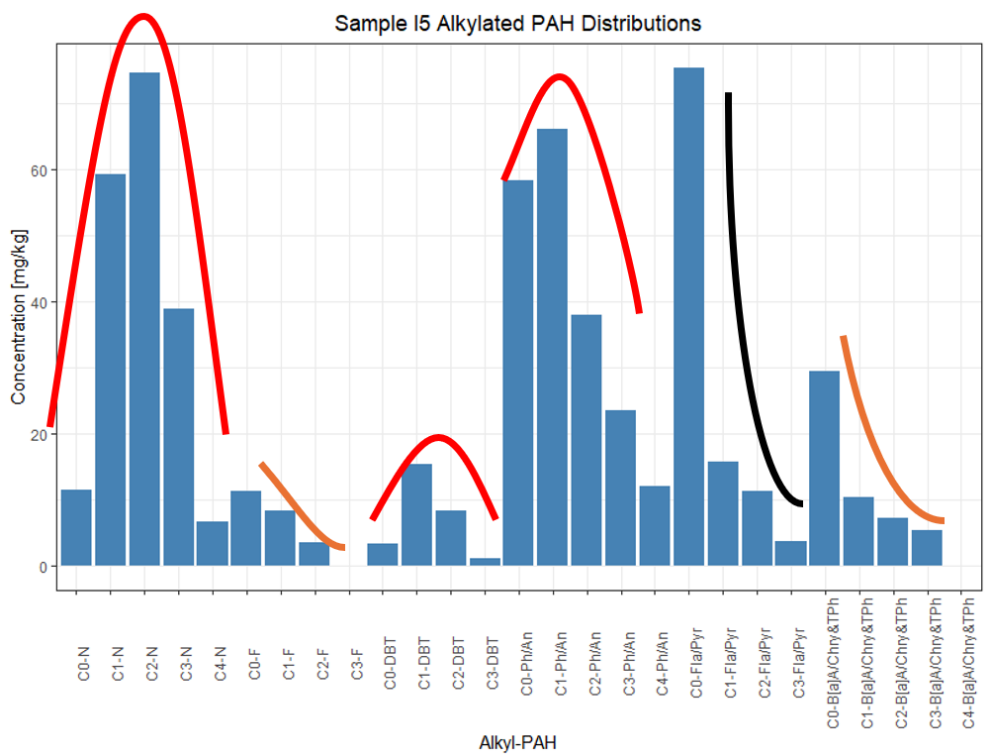
(d)



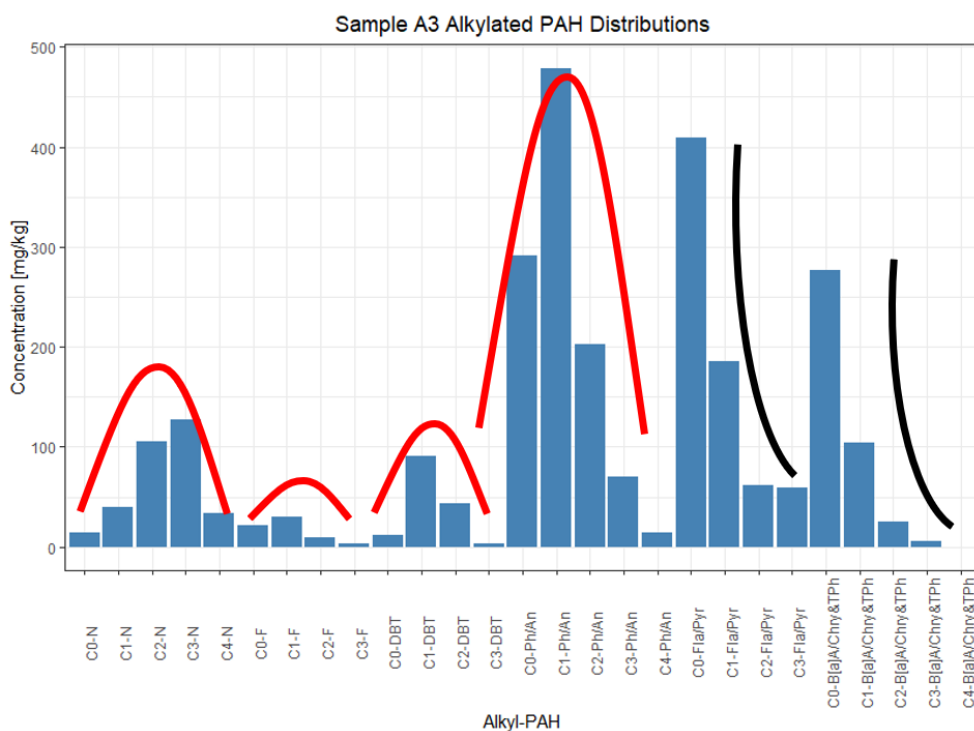
(e)



(f)



(g)



(h)

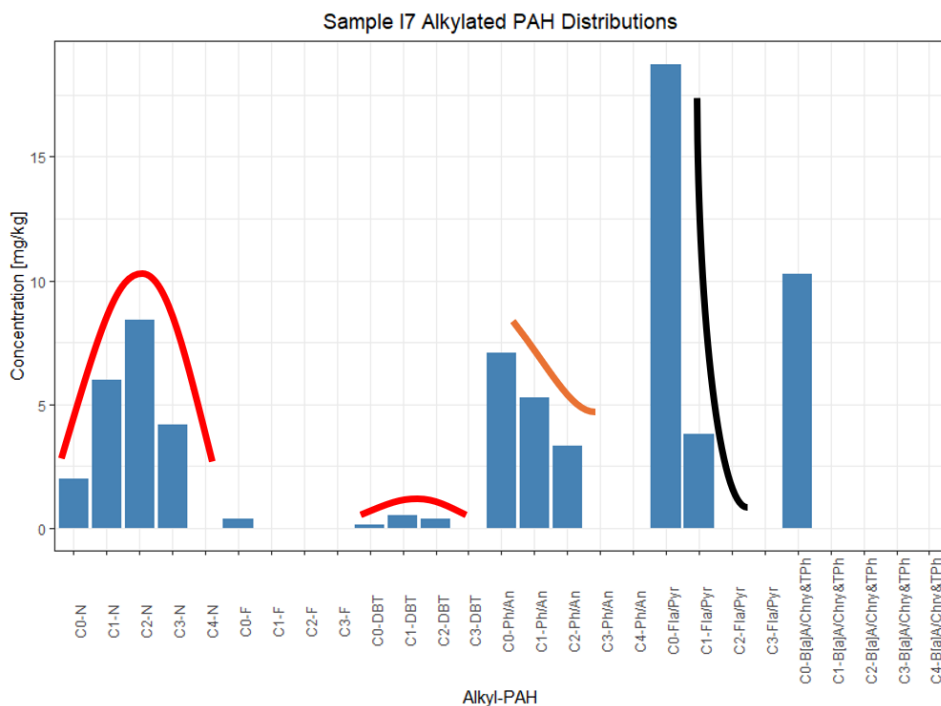


Figure 27. Alkylated PAH distributions for six gasworks soils. (a) sample A5, (b) sample A17, (c) sample D3, (d) sample E1.4, (e) sample H16, (f) sample I5, (g) sample A3 and (h) sample I7. Colour of lines: red=petrogenic, orange=pyrogenic with moderate temperature, black=pyrogenic with higher temperature.

Consequently, the alkylated PAH distributions were unable to confidently characterise all MGP processes. However, they do show that the alkyl-Ph/An and alkyl-Fla/Pyr short chain alkylated compounds were the most predominant compounds from all the Σ Alkyl21 for GWS, apart from GWS highly influenced from oil processes reporting high alkyl-Nap compounds. Higher alkylation increases hydrophobicity and lowers vapour pressure (Achten and Andersson, 2015). This suggests that these heavier alkylated PAHs could potentially pose a greater risk through the human dermal and ingestion exposure pathways, compared to the inhalation which is driven by more volatile compounds. This study reports the widespread presence of alkylated PAHs in GWS, suggesting that a further understanding of their exposure and risk to humans from soil might form a focus in future HHRAs.

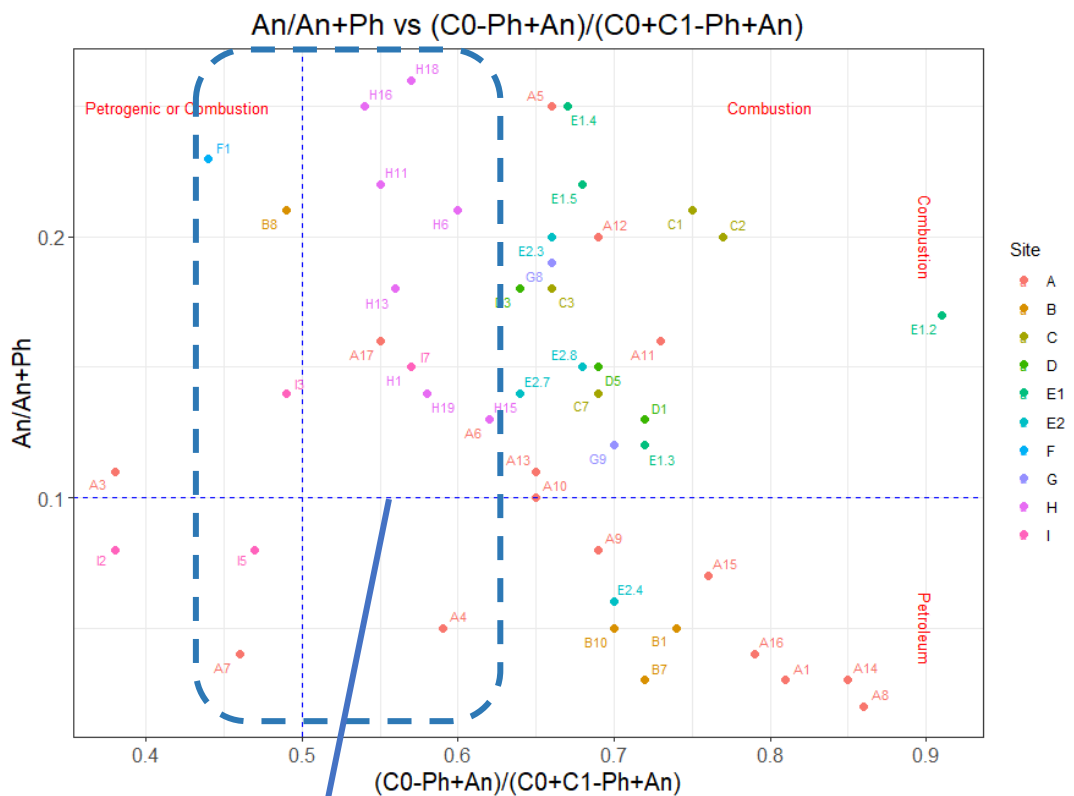
PAH diagnostic ratios

Contamination sources can be approximated by PAH diagnostic ratios which plot paired PAH isomer concentrations. The approach relies on the relative thermodynamic stabilities associated with different PAHs. Increased proportions of the less stable isomers are often found for parent PAHs formed at higher temperatures in combustion sources (Yunker et al., 2002, Vane et al., 2014). Twenty-one diagnostic ratios were explored in this study and several plotted into cross plots (Appendix B Chapter 5 Research Papers SI: Table S8 and Figure S2.a-k). These included thirteen diagnostic ratios which have been used previously by Ghetu et al. (2021) to accurately identify sources of PAHs from CRMs. This study showed that most diagnostic ratios investigated were unable to distinguish GWS into related MGP processes. Generally, the ratios estimated pyrogenic/combustion sources, except for several GWS (from sites A, B, and I) linked to oil processes which often showed petrogenic ratio values.

The PAH diagnostic ratio cross plot which was the most useful at distinguishing processes was $An/An+Phen$ vs $Phen+An/(C0-C1-Ph/An)$ (Figure 28a) previously used by Pies et al. (2008). 32 GWS were in the combustion quadrant, and 16 GWS (from sites A, B, I and F) were in quadrants regarding petroleum influences. Sites H and F GWS (LTHR) displayed lower $Phen+An/(C0-C1-Ph/An)$ ratios (0.44-0.62) than the other sites in the combustion quadrant suggesting lower C1-Phen/An proportions, however, site F is associated to a

large degree of uncertainty due to the measurement on a single low concentrated GWS. Additionally, the cross-plot Fla+Pyr/(Fla+Pyr+C2-C4-Phen/An) vs (C1-C4-Phen/An)/Phen+An (Figure 28b) taken from Pies et al. (2008) showed GWS from site H with lower proportions of alkylated species (higher C1-C4-Phen/An)/Phen+An ratios) than the sites C, D, E1/2 and G. Whereas sites A, B, F and I GWS observed higher (C1-C4-Phen/An)/Phen+An ratios located in petrogenic zones. These cross-plot ratios suggest oil influenced processes can be associated with petrogenic ratio values and ratios involving alkylated species can differentiate LTHR processes from the other processes.

(a)



- GWS from LTHR measure lower Phen+An/(C0-C1-Ph/An)

(b)

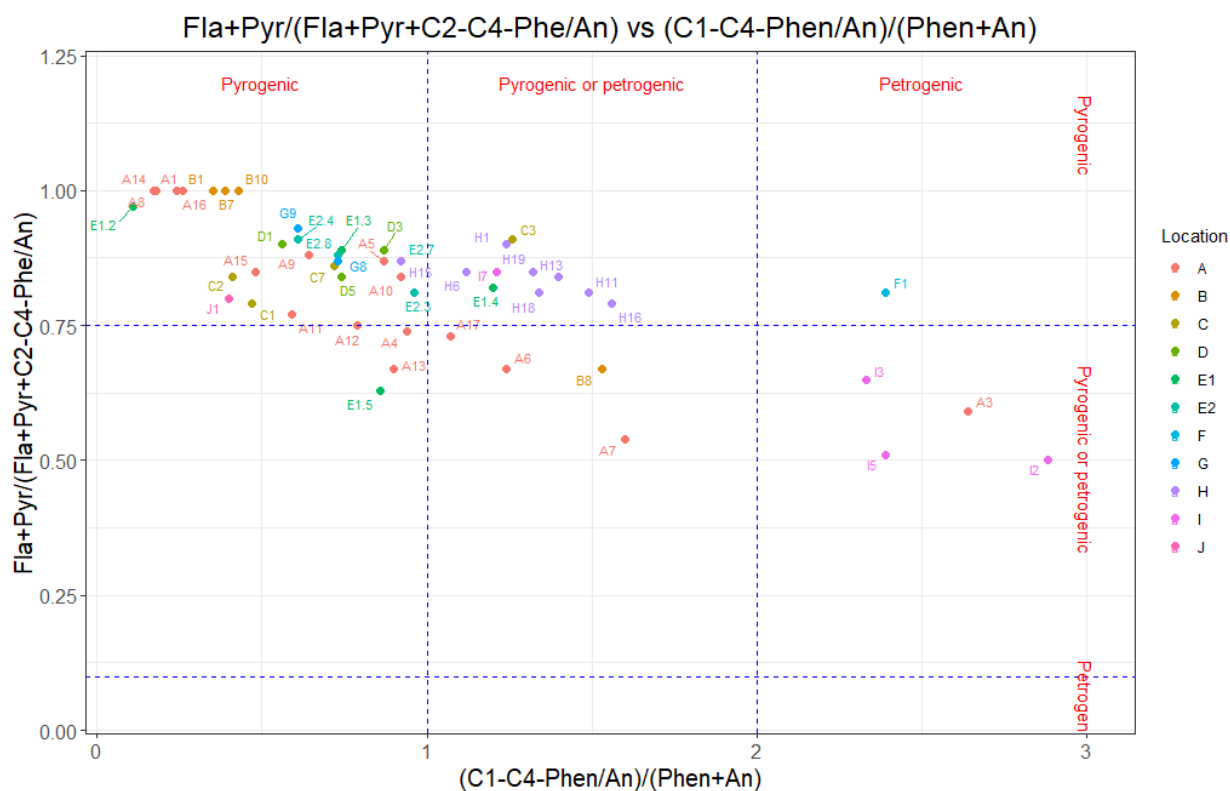


Figure 28. PAH diagnostic ratio cross plots applied to gasworks soils, (a) $An/An+Phen$ vs $(C0-Ph/An)/(C0:C1-Phen/An)$, and (b) $(Fla+Pyr)/(Fla+Pyr+C2-C4-Phen/An)$ vs $(C1-C4-Phen/An)/(Phen/An)$.

5.4.2 Rock-Eval(6) Pyrolysis

S1 and S2

Twenty RE parameters were reported for the GWS (Appendix B Chapter 5 Research Papers SI: Table S9), parameters S1 and S2 represent two hydrocarbon release stages at two temperature ranges during pyrolysis. S1 for the GWS ranged from not detected (ND) – 47.83 mg/g (median of 0.23 mg/g), with 69% of GWS being <1.00 mg/g. This shows that the bulk of GWS do not contain a large quantity of thermo-vaporised free hydrocarbons, S1 values are usually minor in soils as increased humification increases the degree of more complex hydrocarbons that typically require higher cracking temperatures (Disnar et al., 2003). Sites D, E2, F, G and H contained low S1 values. Sites A, B, C, E1 and I reported boarder S1 ranges (ND-47.83 mg/g) with higher S1 max values, this suggests that these sites were exposed to LMW organics, which corresponds to oil processes (Lafargue et al., 1998, Scheeder et al., 2020). GWS S2 values

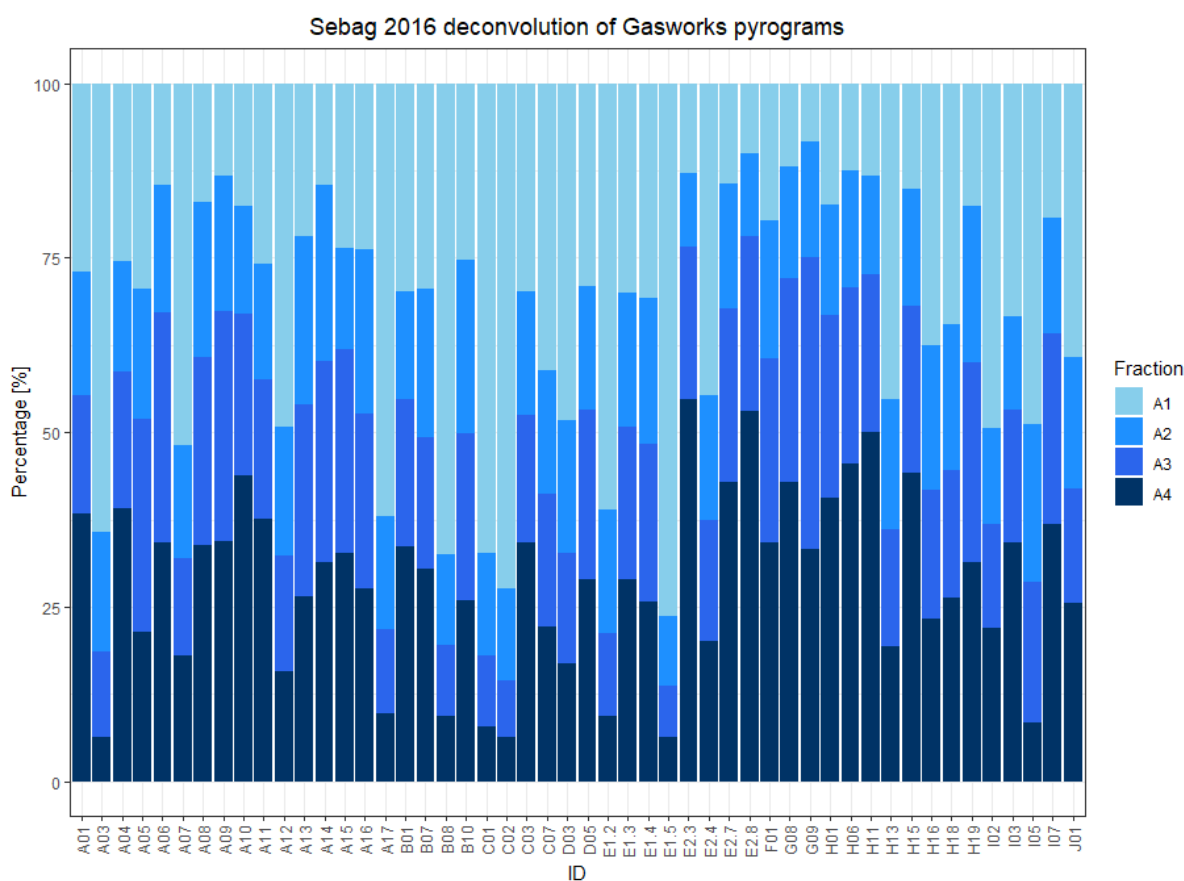
varied from 0.09 to 84.82 mg/g (median 6.02 mg/g), whereas Haeseler et al. (1999) reported GWS with a narrower ranges for both S2 (0.9-23.1 mg/g) and S1 values (0.2-14.2 mg/g), but both within this study's range. Hydrocarbons cracked in S2 are from natural and/or anthropogenic OM, which can have high PAH sorption capabilities depending on their abundance of macromolecular aliphatic chains, aromatic carbon components and quantities of flexible pores (Ukalska-Jaruga et al., 2019, Garcin et al., 2022b). The different S2 values in the GWS could be related to types of OM influencing the release of PAHs from soil.

The thermal stability of OM released in the pyrolysis cracking stages of the RE analysis can be explored using mathematical deconvolution of the S2 peak, either by calculating fractions using the base/tops of peaks or by focusing on peak areas in specified temperature ranges (Newell et al., 2016, Sebag et al., 2016, Ordoñez et al., 2019). Only Haeseler et al. (1999) has applied the deconvolution of S2 to GWS previously, but only into two fractions whereas recent studies use 4-5 temperature fractions. This study explored the selected temperature ranges specified by Sebag et al. (2016), Ordoñez et al. (2019), Malou et al. (2020) and Haeseler et al. (1999) (Appendix B Chapter 5 Research Papers SI Figure S5). A positive correlation ($R^2 = 0.6245$) between the log transformed \sum PAH51 concentrations and the lowest temperature range fraction percentage indicated that hydrocarbons cracked at these lower temperature ranges (A1) (Figure 29b) included PAHs. Haeseler et al. (1999) concluded that the main constituents of the S1 and S2a peaks were aromatic hydrocarbons and resins, supporting this study's observations. Although no MGP processes were distinguished by deconvolution, GWS with the lowest PC2 values from PCA reported the highest A1 fraction percentages, implying that the extent of PAH contamination can be linked to the A1 fraction percentage. Future work exploring the relationship between a soils ability to release PAHs and the S2 deconvolution fractions has the prospect of relating rapid releasing PAH fractions with labile OM (James et al., 2016, Luthy et al., 1997) expressed by lower S2 temperature fractions.

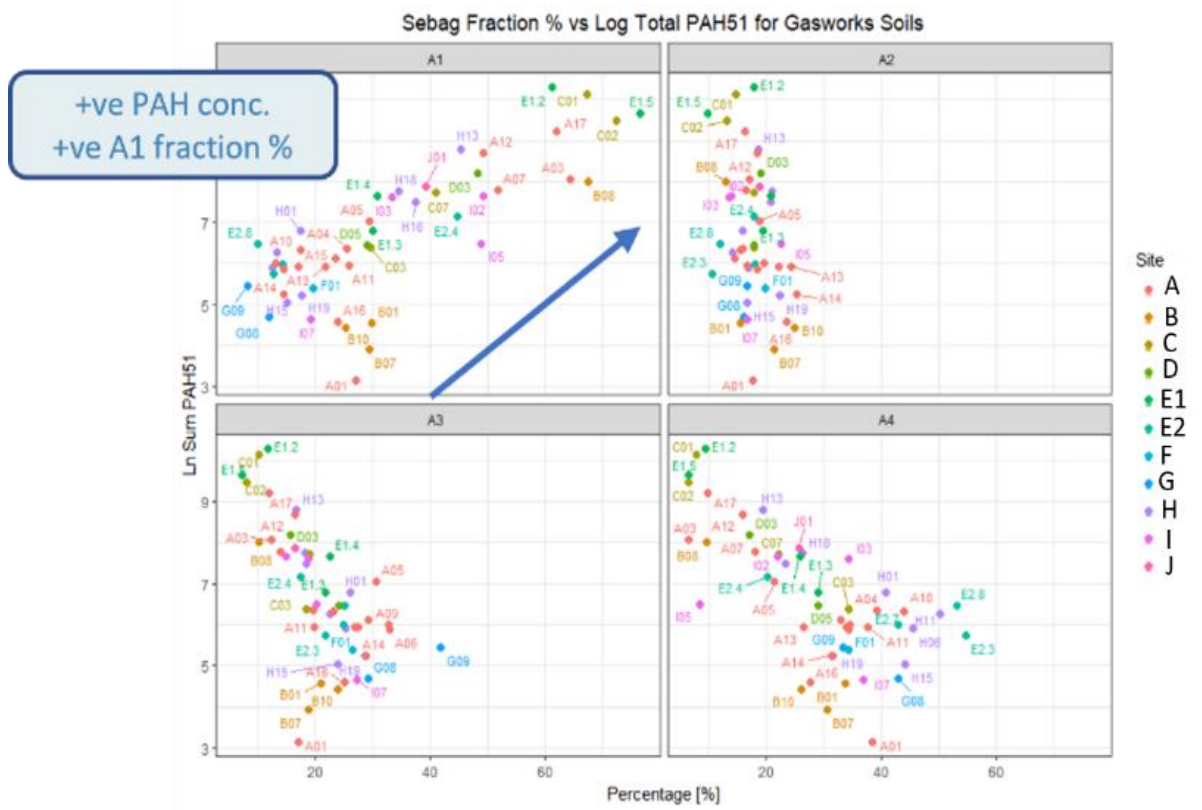
The I-index and R-index calculated by the S2 deconvolution fractions can assess the preservation of thermally labile immature (readily decomposes) OM and the most persistent/refractory OM fractions (Sebag et al., 2016, Brown et al., 2023).

The I/R diagram (Figure 29.d) shows GWS with the highest R-index originated from sites A, E2, G and H, however, the I/R diagram was unable to distinguish GWS by MGP process. The majority of GWS clustered at similar I-index values (-0.32-1.07) while the R-index spanned from 0.14-0.85. GWS with the highest concentrations observed the lowest R-index values and the highest I-index values. This suggests that GWS with higher concentrations contain high abundances of labile OM cracked at lower temperatures (e.g. LMW OM and aliphatics). Several GWS (in sites E2, G and H) had R-index (0.8-1.0) similar to coal reported by Sebag et al. (2016). These GWS can be assumed to have high amounts of immature geopolymers and/or refractory geopolymers, such as black carbon (BC), a source known to inhibit PAH release from soil (Luthy et al., 1997).

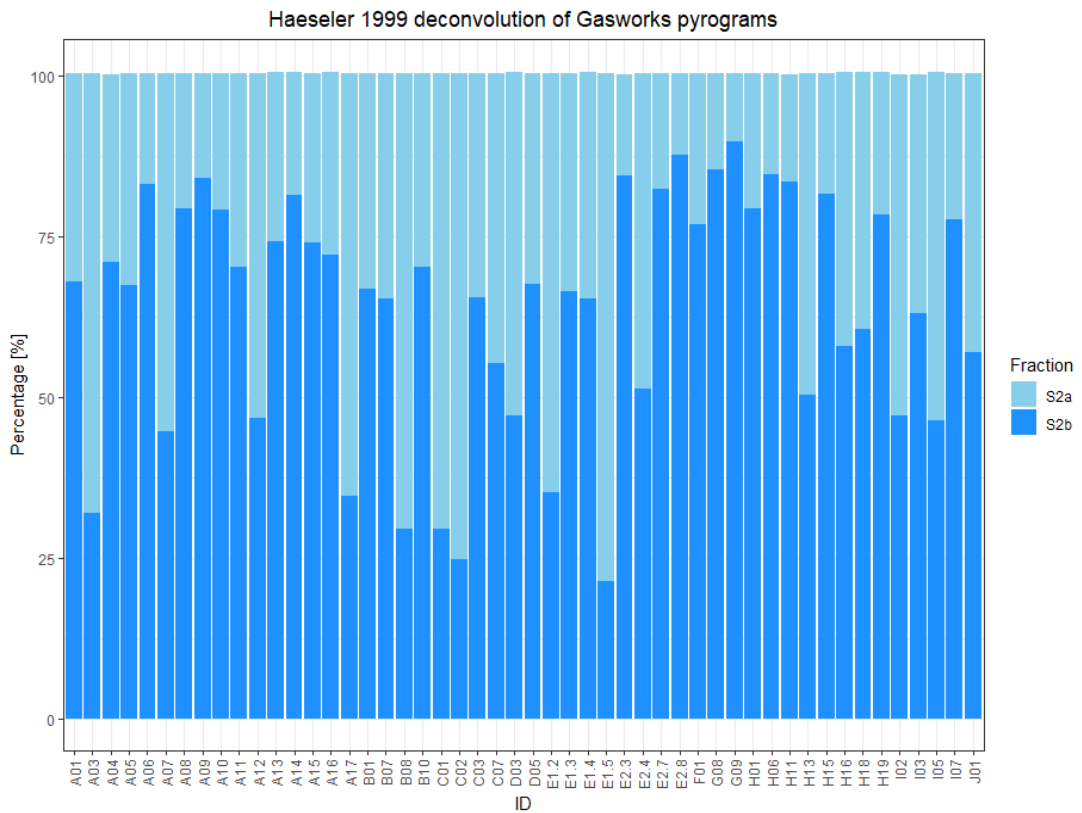
(a)



(b)



(c)



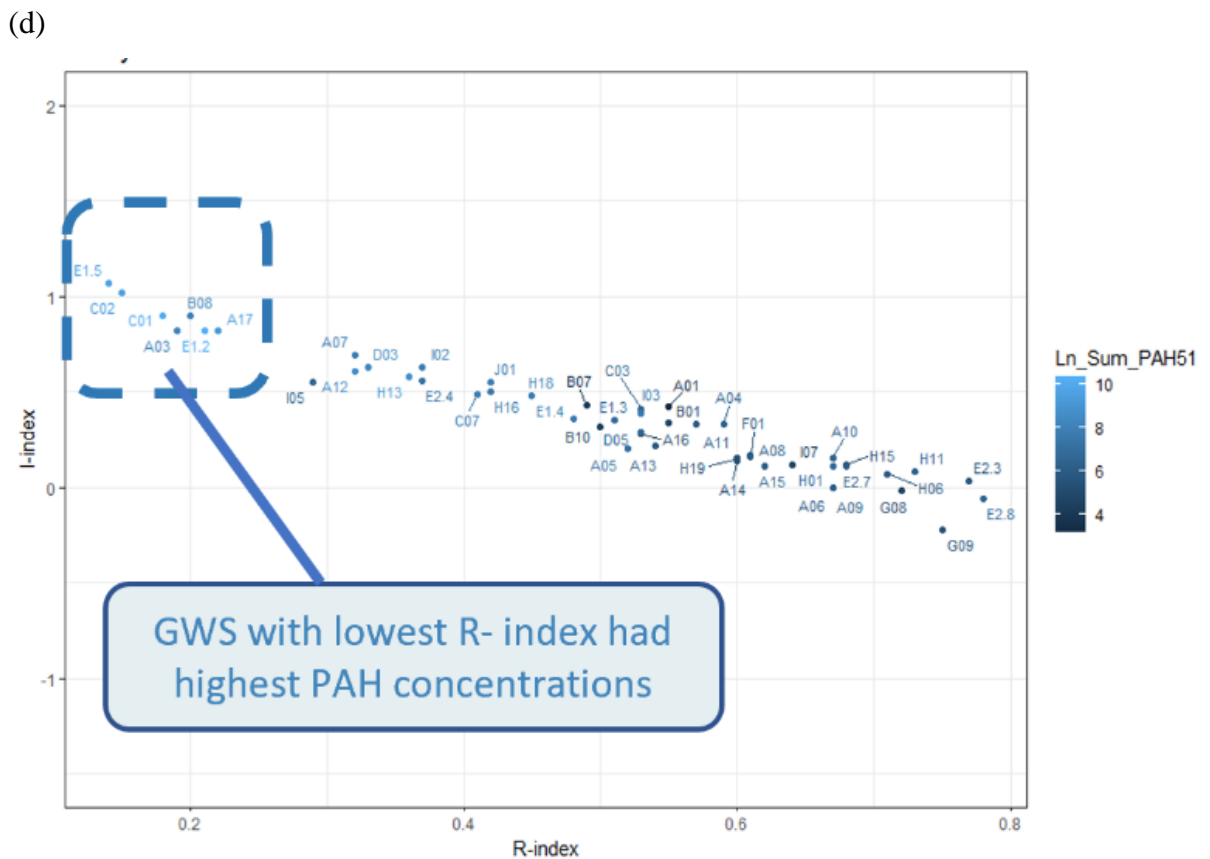


Figure 29. S2 deconvolution fractions applied to GWS, (a) use of Sebag et al. (2016) fractions, (b) log PAH51 plotted against Sebag et al. (2016) fractions percentages, (c) use of Haeseler et al. (1999) fractions, (d) Sebag et al. (2016) I-index vs R-index plot created with 50/94 soils (soils with measured PAH concentrations).

Overall, RE showed the pyrolysed hydrocarbon fractions reporting oil impacted GWS with high S1, whereas S2 is more varied among GWS due to different combinations of OM types. Deconvolution of S2 showed PAHs released at lower temperatures (200 - 340 °C). Higher quantities of labile OM have been related to increased PAH desorption from soils compared to soils with higher proportions of recalcitrant/refractory OM (James et al., 2016, Lueking et al., 2000). Future research to enhance HHRA could investigate using the R-index and S2 deconvolution to understand how likely PAHs may release from soils.

Total Organic Carbon (TOC%), Pyrolysed Carbon (PC%) and Residual Carbon (RC%)

A wider range of TOC% was measured in this study (0.11-25.72%) compared to the study of US gasworks soils by Haeseler et al. (1999) (TOC% 1.82-10.14%). The PC% for this study was between 0.04-10.8% (mean 1.69%) and RC% between 0.07-23.3% (mean 6.6%), which couldn't be compared to Haeseler et al. (1999) as they did not report these parameters. Poot et al. (2014) discovered that approximately 7% of the RE RC% is BC, and that the RC% and BC correlations with PAH concentrations were associated with PAHs becoming trapped within the aromatic structure, hindering PAH release (Poot et al., 2014, Semple et al., 2013). Weak positive correlations were seen for this study's GWS TOC%, PC% and RC% against the log transformed total PAH concentrations. The PC% showed a broadly exponential increase for higher PAH concentrations than RC% and TOC%, an expected result given PAHs contribute towards lower temperature pyrolysed fractions. Haeseler et al. (1999) also concluded that pyrolysed hydrocarbons released ≤ 350 °C corresponded to 35-50% aromatic compounds. The PC%, RC% and TOC% for the background soils (means of 1.49%, 6.31%, and 7.80%) were within the ranges for the GWS, implying that without prior knowledge of the soil PAH concentrations these RE parameters would be unable to make assumptions about the soil's contamination history. However, the variation within these parameters suggests they have potential to be related to the ability of soil to capture/release PAHs.

Production Index (PI), Hydrogen Index (HI), and Oxygen Index (OI)

Soil maturity can be estimated using PI, where $PI < 0.1$ is classed as immature (Waters et al., 2020). GWS PI ranged from ND-0.38 (mean of 0.08), GWS with the highest $\sum PAH_{51}$ concentrations showed the highest PI values (Appendix B Chapter 5 Research Papers SI Table S9). The HI measures the extent of hydrogenation. GWS provided a wide HI range between 8-549 mg/g where the highest HI values generally corresponded with the highest $\sum PAH_{51}$ concentrations (e.g. the tar like materials A12 and E.12). A high HI suggests high contributions from hydrogen rich compounds such as long alkyl chains or alkyl-C and O-alkyl compounds, whereas a low HI indicates dehydrogenated and aromatic structures (BC and humic compounds) (Saenger et al., 2013). OI

indicates the proportion of compounds containing oxygen, most GWS observed similar OI values <100 mg/g (58% GWS), GWS with high OI values appear to have lower total PAH concentrations. Low OI for highly concentrated PAH GWS were expected given the elemental composition of coal tar is 5% oxygen and inorganics, compared to 86% carbon (Thomas, 2014).

Van Krevelen diagram plots HI against OI and are widely used in oil exploration to classify the type of OM origin (Waters et al., 2020). The van Krevelen diagram (Figure 30.a) shows that GWS with lower OI have higher PAH concentrations. Specifically, a divide can be seen for GWS with HI > 200 mg/g reporting the highest Σ PAH51 concentrations, although some samples in this range do not report high concentrations but have high HI values from natural OM, (e.g. one BG sample reported HI of 272 mg/g). Therefore, the van Krevelen diagram can help distinguish oil influenced processes (high HI) or non-oil influenced (low HI) when the PAH concentrations are known. GWS with HI >200 mg/g were the same GWS reporting the strongest negative associations to PC2 in PCA and the highest A1 fraction percentages and were assumed to originate from a CWG petrogenic source. This contradicts the PAH ratios which suggested combustion origin for sites B, C and E1, indicating that the PAH ratios were unable to distinguish certain petrogenic identities found by the van Krevelen diagram.

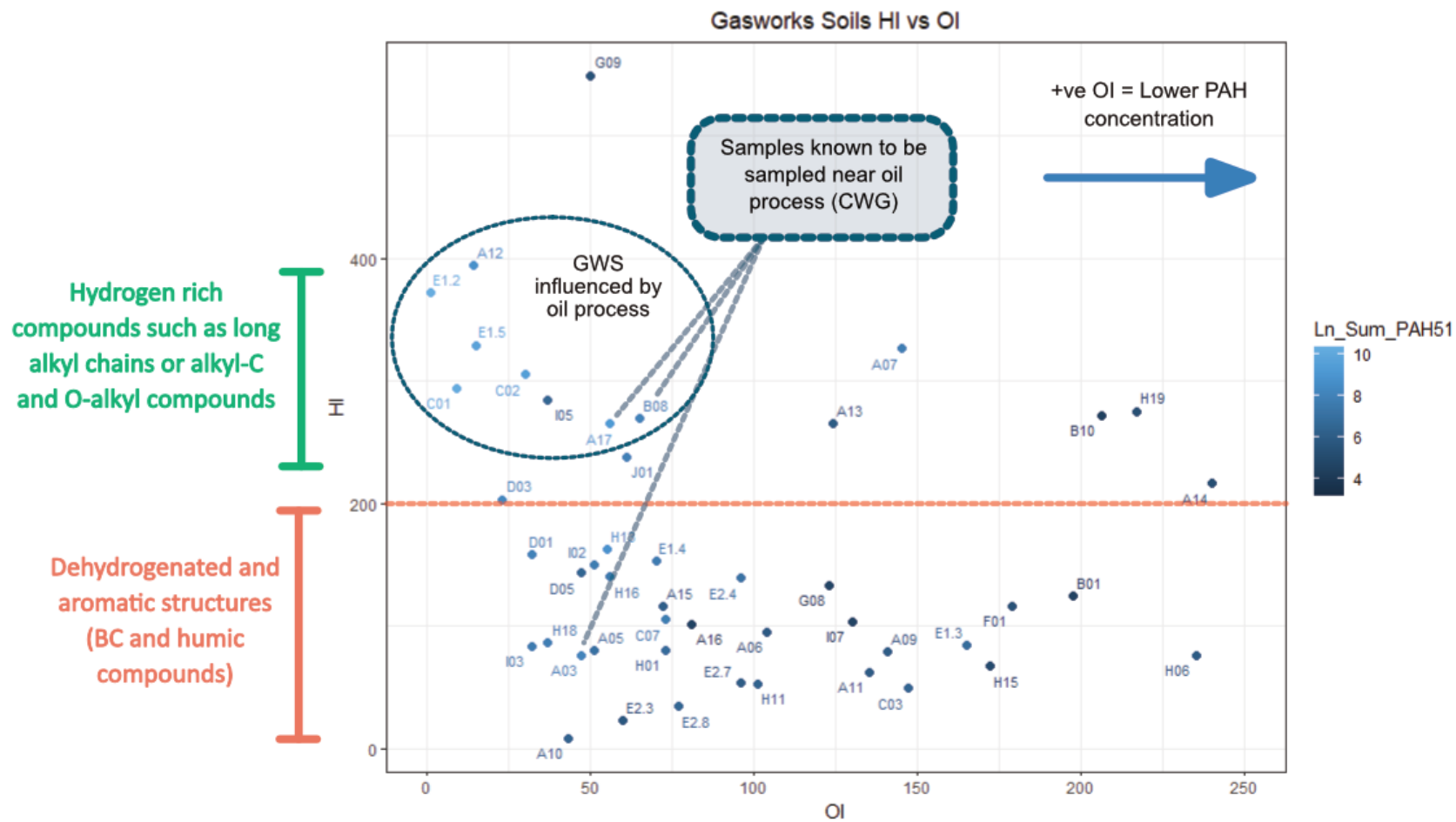
TpkS2

The temperature at which the maximum amount of hydrocarbons released in S2 is described as the TpkS2. Higher TpkS2 temperatures indicate higher proportions of larger/stronger bound OM compounds in soils, GWS TpkS2 temperatures ranged from 241-480 °C. Different TpkS2 temperature range clusters were identified and plotted against the log transformed PAH concentrations and the HI shown in Figure 30.b. 35% of GWS had low TpkS2 temperatures between 241-327 °C, these GWS observed high log transformed PAH concentrations and high HI values. GWS with the lowest TpkS2 temperatures (≤ 254 °C) were obtained from sites (A, B, C, E1 and I) associated with oil, and observed the highest amounts of Σ Alkyl21 concentrations. This implies that GWS with lower TpkS2 temperatures compromise of large proportions of long chains/aliphatic hydrocarbon compounds that are thermally cracked at lower temperatures. Gallacher et al. (2017a) reported CWG tars with

the highest relative concentrations of the n-alkanes, agreeing with this study that CWG/oil GWS will be dominated by aliphatic compounds compared to PAHs.

GWS from sites D, E2 and H (not associated to oil processes) also reported low TpkS2 temperatures between 283-327 °C. However, these GWS had lower HI ≤ 203 mg/g, implying either lower amounts of aliphatics or the presence of higher amounts of PAHs compared to aliphatics. 56% of the GWS had a TpkS2 temperature between 434-469 °C and observed lower log transformed PAH concentrations and lower HI values than the GWS with lower TpkS2. This suggests that GWS with higher TpkS2 temperatures contain OM with a lower degree of hydrogenation and instead yield higher amounts of aromatic compounds such as PAHs, BC and natural macromolecular compounds that require higher cracking temperatures due to the quantity and strength of bonds. Although the lower PAH concentrations associated to the higher TpkS2 suggests influence from natural OM (Sebag et al., 2006). A low TpkS2 temperature therefore has the potential to relate to high PAH contamination from petrogenic sources containing higher amounts of aliphatic hydrocarbons (labile OM), potentially the TpkS2 could be used to predict PAH release from different soil OM fractions.

(a)



(b)

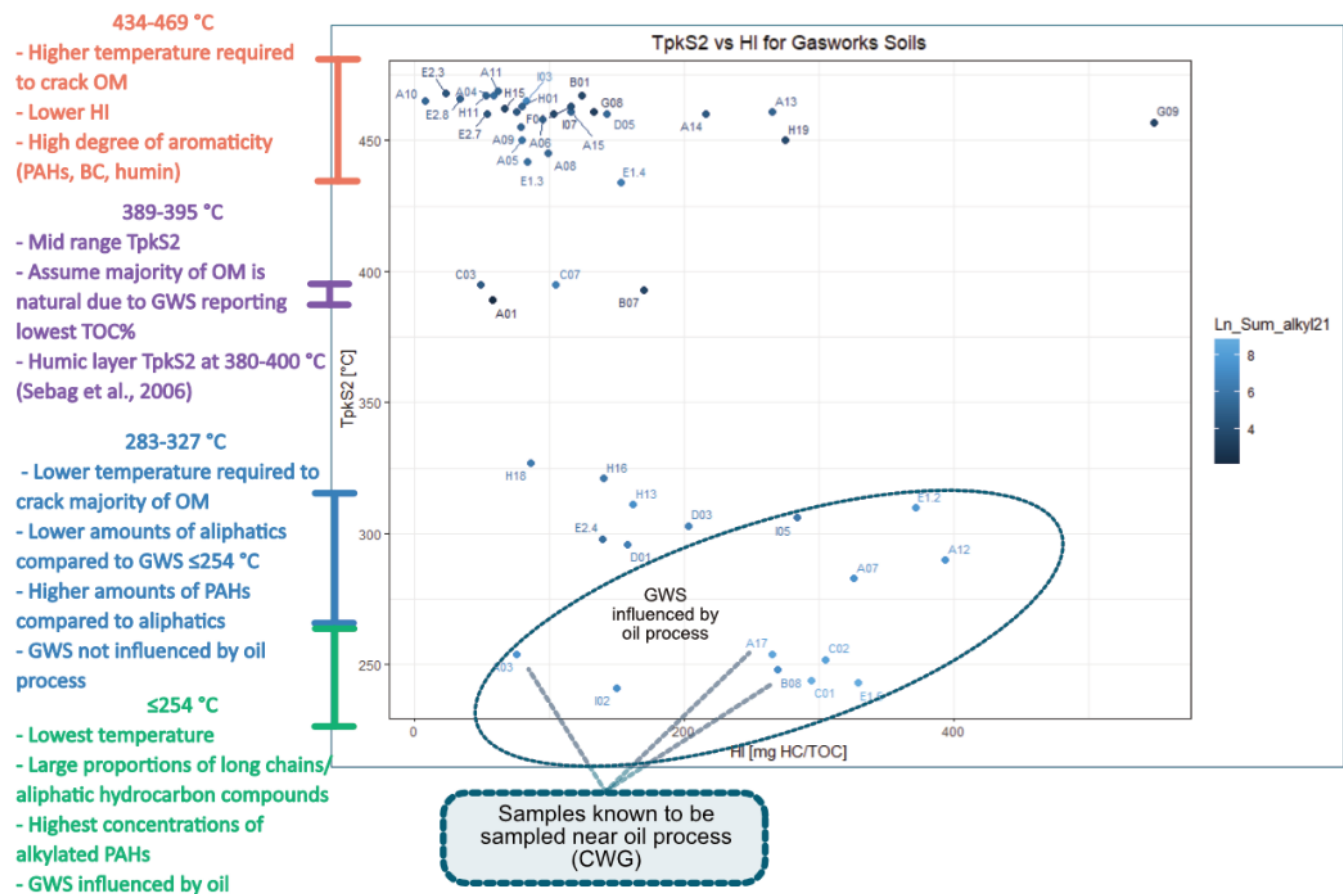


Figure 30. (a) annotated van Krevelen diagram (OI values above 250 have been removed), and (b) annotated TpkS2 vs HI plot.

5.4.3 Characteristics of gasworks processes

Several methods were able to identify oil influenced and LTHR processes, whereas other processes were difficult to segregate from each other. The detailed results of these different analyses are described in Appendix B Chapter 5 Research Papers SI Sections S4-8. Petrogenic characteristics were repeatedly reported for GWS from sites A, B, C, E1, E2 and I. These include high abundances of aliphatics, LMW PAHs, alkylated PAHs, and sulphur containing heterocycles (DBT compounds) compared to other processes (Gallacher et al., 2017b, McGregor et al., 2012). RE parameters showed high S1, low R-index values (≤ 0.22), and low TpkS2 temperatures linked to high HI values. Sites containing petrogenic origin PAHs can be related to the CWG and Tully plant processes, which operated at relatively low temperatures (650-700 °C) and sprayed oil to enrich the generated gas (Gallacher et al., 2017b, Thomas, 2014).

GWS associated with LTHR processes had higher distributions of HMW PAHs and lower proportions of LMW PAHs compared to other sites. Previous studies have reported higher levels of HMW PAHs associated with higher pyrolysis temperatures (Dong et al., 2012) and lower temperatures associated to LMW PAHs (Gao et al., 2016), due to the cracking of coal being the dominant reaction to PAHs formation. Potential reasons for our contrasting results include the potential that these sites had experienced greater degrees of weathering, particularly sites F and G which showed low PAH concentrations. Alternatively, both the low pyrolysis temperature and the coal type could influence the higher proportions of HMW PAHs (Dong et al., 2012, Yan et al., 2015, Gao et al., 2016). Pyrolysis of a high rank coal consisting of ≥ 4 -ring PAHs (Yan et al., 2015), would generate HMW PAHs during pyrolysis. Han et al. (2020) reported higher emissions of HMW PAHs from lower temperatures in coal combustion, caused by the pyrolysis of the coal structure. However, Han et al. (2020) focused on combustion rather than pyrolysis.

This study did not investigate a site which solely operated with the HTHR or CVR process, which means making assumptions on these MGP processes is problematic. GWS associated with the HTHR and CVR tended to cluster together with pyrogenic characteristics. However, these GWS showed a great degree of variability for PAH distributions, which is expected due to the CVR

temperature gradient generating products resembling characteristics of both low and high temperature processes (Gallacher et al., 2017b). Only site D operated solely under the IVCO process, IVCO used narrow, deep, and static chamber ovens to pyrolyse coal. The resulting IVCO products were very degraded, as seen in the PCA where no PAH species dominated the relative contributions. Additionally, differences between site E1 MGP and its associated chemical works plant site E2 were investigated and found that distillation released/decomposed LMW PAHs hence their lower abundance at Site E2.

5.4.4 Evaluation of applied methods

Previous studies (McGregor et al., 2012, Gallacher et al., 2017b) have succeeded in characterising tars to a specific MGP process. Instead, this study investigated soils and was not able to separate all MGP processes to the same degree. Reasons for this include not incorporating all compounds (e.g. alkanes) studied in the previous studies, potential weathering of samples affecting PAH distributions, impact of collection and site's inactivity time spans, sites operating with multiple processes, and several soils being retrieved from mixed contamination sources. In addition, this study did not have access to end members to compare the soils to and at some sites there were only a small number of samples available. However, these challenges can be expected in real-world risk assessments where MGP sites might present several unknowns due to missing information about the site's history or sampling challenges. Despite the limitations identified this research provides novel insights into characteristics of different GWS from MGPs expected in real life scenarios using a carefully designed range analytical methods associated data evaluation tools.

This research observed several distinctive GWS characteristics linked to petrogenic oil processes and LHTR processes. Similar to McGregor et al. (2012), this study found PCA to be one of the best techniques to separate GWS based on MGP process, particularly between CWG and LTHR processes which observed contrasting distributions between LMW and HMW PAHs. The PAHs with the strongest influence in the PCA were Nap and Phen derivatives, Fla, Pyr and BaA, with Phen proportions influencing the MGP processes without oil application. RE parameters were able to strengthen the attribution for petrogenic

contamination. However, the applied methods struggled to distinguish the IVCO, CVR and HTHR processes, for the reasons described.

PAH ratios using alkyl-Phen/An were able to characterise MGP processes influenced by oil and LTHR but were unable to characterise other processes, in contrast to McGregor et al. (2012) who were unable to distinguish processes using PAH diagnostic ratios on tars. The ratios used for this study were able to separate site H (LTHR) from the predominant pyrogenic cluster, however, sites F and G were dissimilar to site H ratios (Figure 28). These differences may have been caused by the small number of samples from site F and G which were unable to fully represent the LTHR, use of different coals, different weathering patterns, or other processes impacting GWS signatures. Although alkylated PAH distributions have been shown to be more reliable with source identification than PAH ratios (Hindersmann and Achten, 2018), GWS alkylated PAH distributions generally had similar results between MGP processes. LTHR sites were shown to have a higher degree of alkylated and parent HMW PAHs, although it is uncertain if weathering of LMW PAHs impacted this result.

RE parameters were unable to characterise MGP processes, however the RE parameters S1, TpkS2, HI, OI and the R-index used in conjunction with PAH concentrations and percentages provided insight into relationships between PAH contamination. This was particularly seen for processes with oil applications. GWS showed a large diversity in different RE parameters (e.g., S2, R-index), which showed potential for future work to relate these RE parameters with estimating the release of PAHs from soil OM fractions and the subsequent risk from PAHs. Other future work characterising GWS by MGP processes should include end members (specifically single process sites), investigate the impact of the time span of sample collection on PAH distributions and analyse greater numbers of GWS.

5.5 Conclusions

This research explores the characterisation of GWS by their retrospective MGP processes by: i) detailed evaluation of PAHs concentrations and their distributions of 30 parent and 21 alkylated PAHs quantified by GC-MS/MS; ii) characterisation of bulk organic matter properties using the relatively rapid

evaluation method of RE. These methods facilitated the differentiation of GWS associated with oil contamination for CWG processes based on their distinctive PAH distributions (petrogenic origin) and reduced RE parameters (HI and TpkS2). While classifying other MGP processes proved more challenging due to mixed contamination or limited samples, GWS associated to the LTHR process exhibited specific PAH profiles compared to other MGP processes.

PCA was able to characterise oil-contaminated and LTHR-associated GWS, aided by RE indices S1, TpkS2, HI, OI and the R-index. LMW PAHs predominated in oil related GWS, indicating an elevated inhalation exposure risk, while HMW PAHs were prominent in LTHR GWS, intensifying dermal and ingestion exposure concerns. Integration of PAH and bulk organic matter data suggests the potential for identifying GWS with labile organic matter fractions prone to higher PAH release and human health risks. This study supports risk assessment by informing the selection of critical PAHs linked to specific MGP processes. Importantly, alkylated PAHs emerged as process-dependent contributors to GWS, bearing heightened persistence and risk compared to parent PAHs. This research enhances understanding of PAH distributions and bulk organic matter fractions in former MGPs soils, facilitating accurate risk evaluation. By merging analytical techniques and data tools, it advances insights into PAH presence, distribution, and process-related risks.

5.6 Acknowledgements

The authors gratefully acknowledge the funding and support from the NERC Envision DTP [NE/S007423/1], BGS [BUFI studentship S431], the University of Nottingham, and National Grid Property Holdings. We also acknowledge the support provided by WSP and LQM. National Grid Property Holdings provided access to sites for sampling and information regarding the site history. CHV, AWK and DB publish with the permission of the Director of the British Geological Survey. We thank Vicky Moss-Hayes for conducting the Rock-Eval(6) Pyrolysis measurements and the BGS Sample Preparation team for freeze drying and sieving soils prior laboratory procedures.

Chapter 6 Dermal absorption of high molecular weight parent and alkylated Polycyclic Aromatic Hydrocarbons from Manufactured Gas Plant soils using *in vitro* assessment

Alison M. Williams-Clayson^{1,2}, Christopher H. Vane¹, Matthew D. Jones², Russell Thomas³, Christopher Taylor⁴, Darren J. Beriro^{1*}

*corresponding author

¹ British Geological Survey, Keyworth, Nottinghamshire, UK; ² University of Nottingham, Nottingham, UK; ³ WSP UK, Bristol, UK; ⁴ National Grid, Warwick, UK

Submitted for publication to Journal of Hazardous Materials

Statement of Contributions of Joint Authorship

Williams-Clayson, A: (Candidate):

Performed all *in vitro* experiments, performed all sample preparations, performed the measurements, analysed the data, and wrote the manuscript. Took the lead role in all writing taking responsibility of drafting and revising manuscript and first author on paper.

Vane C., Beriro, D.; Jones, M.; Thomas, R.: (Supervisors):

Supervised and provided feedback and helped shape the research project and manuscript.

Taylor, C.: (Industrial Supervisor):

Provided site access for sampling, information regarding sites and feedback on manuscript.

6.1 Abstract

An enhanced *in vitro* human dermal bioavailability method was developed to measure the release of 20 parent and 7 alkylated high molecular weight (HMW) polycyclic aromatic hydrocarbons (PAHs) from contaminated soils collected from five former manufactured Gas Plants (MGP) in England. GC-MS/MS was used to quantify HMW PAHs in soil, Strat-M artificial membrane representing skin, and synthetic receptor solution (RS) representing systemic circulation at 1-h, 10-h, and 24-h timesteps. Fluoranthene and pyrene exhibited the highest fluxes from soils to membrane (ranging from 9.5 - 281 ng/cm²/h) and soil to RS (<LOQ to 16.9 ng/cm²/h). Chrysene, benzo[*a*]anthracene, benzo[*b*]fluoranthene and the alkylated C1-fluoranthene/pyrene homologue series demonstrated fluxes higher than other HMW PAHs. The dermal fluxes were generally lower than those reported in previous investigations and suggest that dermal absorption varies between both HMW parent and alkylated PAHs and individual PAHs. The utilisation of real-world contaminated soils allowed for a more realistic representation; this is significant because current risk assessment guidance uses artificially spiked soils. This research is important because it suggests that the different dermal fluxes are likely to impact on the mass of PAH absorbed from soil after dermal exposure and therefore the potential risk contaminated soil pose to human health.

6.2 Introduction

Polycyclic aromatic hydrocarbons (PAHs) are a group of thousands of individual organic compounds that are widespread in the environment, originating from both natural and anthropogenic sources (Stout et al., 2015). Certain PAHs are known or suspected carcinogens and mutagens to humans, with benzo[*a*]pyrene (BaP) being a well-studied example of a confirmed carcinogen (International Agency for Research on Cancer, 1965-2023). The 16 PAHs listed by the U.S. Environmental Protection Agency (EPA16) are commonly investigated during site investigation and risk assessment of contaminated post-industrial land (Keith, 2015). However, the environmental presence of numerous other PAHs in complex mixtures with varying toxicities is notable, with non-EPA16 PAHs accounting for 69.3-95.1% of the overall toxic equivalents (TEQ) from 24 PAHs (Richter-Brockmann and Achten, 2018). TEQ are calculated using individual

PAH concentrations and their corresponding toxic potential relative to BaP, referred to as the toxic equivalent factor (TEF) (Richter-Brockmann and Achten, 2018, Public Health England, 2017). Evaluation by the TEF method is one approach to estimate human health risks from chronic exposure to hazardous chemicals. Another is the surrogate marker, which assumes that the cancer risk from a PAH mixture is proportional to the concentration of a surrogate marker PAH, typically BaP (Public Health England, 2017). However, these methods become problematic as assume either that all PAHs have a linear dose-response relationship sharing similar mechanisms, or that all PAHs exhibit similar concentrations and behaviours to BaP and is not applicable for PAH profiles diverging from study (Nathanail et al., 2015). For example, earlier work by the authors shows the distribution of PAHs in real-world soils vary (Williams-Clayson et al., 2023).

Alkylated PAHs (alkyl-PAHs) are characterised structurally by the presence of aliphatic hydrocarbon chains of various lengths attached to the fused aromatic rings (e.g. C1-fluoranthene) and are widely present in mixtures (Williams-Clayson et al., 2023). Alkyl-PAHs have received limited attention in human health risk assessments (HHRAs) despite expectations that they are equally or more toxic than their parent compounds (Meador, 2008, Richter-Brockmann and Achten, 2018). For instance, 5-Methylchrysene possesses a TEF of 1 (BaP = 1), while its parent PAH chrysene (Chry) exhibits a TEF of 0.01 (Richter-Brockmann and Achten, 2018). Additionally, 1-methylpyrene has demonstrated mutagenic and chromosome-damaging activities in mammalian cells (Jiang et al., 2015), while alkylation has been shown to enhance the toxicity of Chry and benzo[*a*]anthracene (BaA) (Lin et al., 2015, Richter-Brockmann and Achten, 2018). The limited research on alkyl-PAHs can be attributed to challenges associated with gas chromatography mass spectroscopy (GC/MS) and/or liquid chromatography mass spectrometry (LC/MS), including stronger fragmentation of the alkylated chain and overlapping peaks (Andersson and Achten, 2015). Understanding the behaviour of both parent and alkylated PAHs in soils is crucial for accurately assessing human exposure and managing associated risks with contaminated soils. Particularly because increasing the alkylation of PAHs increases the hydrophobicity and lowers the vapour pressure of the compound

(Achten and Andersson, 2015). These properties mean that alkyl-PAHs could be more persistent in soil than parent PAHs, potentially creating a higher contribution towards oral and dermal human exposure pathways than parent PAHs (Wassenaar and Verbruggen, 2021).

Brownfield land form an important part of the sustainable growth of urban areas, as their reuse helps to avoid developing greenfield sites (Rankl, 2023). An example of brownfield land investigated in this research are former manufactured gas plant (MGP) sites, which often exhibit extensive contamination by PAH mixtures due to the historical production, storage and distribution of coal tar and other hydrocarbon-rich solid and gaseous sources on these sites (Thomas, 2014). Williams-Clayson et al. (2023) measured 30 parent PAHs and 21 alkylated PAHs in 48 MGP soils, finding that alkyl-PAHs accounted for 7-65% of the total concentration of the 51 parent and alkylated PAHs. Over 80% of the 48 MGP soils in our previous study measured BaP concentrations above the current Generic Assessment Criteria (GAC) for residential use with plant uptake (>5 mg/kg) (CL:AIRE, 2014). These findings imply that MGP soils are likely to be at a level of unacceptable risks to human health, requiring remediation prior to change in land use. Prior to any proposed remediation, risk assessments are conducted to determine whether soils pose unacceptable risks to human health and the environment. These assessments consider three main exposure pathways: oral, inhalation, and dermal. However, limited research has been conducted to investigate the human dermal exposure risk from PAHs in soils (Beriro et al., 2016, Ruby et al., 2016, Spalt et al., 2009).

High molecular weight (HMW) PAHs, containing ≥ 4 aromatic rings provide a higher dermal contribution when compared to oral and inhalation routes than low molecular weight (LMW) PAHs (Nathanail et al. 2015). This feature is driven mainly by their lower vapour pressures. HMW PAHs are also generally more persistent in soils due to their low water solubility and high lipophilicity (Nathanail et al., 2015, Beriro et al., 2016). Improving our understanding of the dermal exposure to HMW PAHs is prioritised in this research. Current risk assessment software makes assumptions about the proportion of the total concentration of PAH in soil that following intake are available for uptake into body tissues and circulation (Environment Agency, 2009a, Nathanail et al.,

2015). This proportion is referred to as a bioavailable fraction (BAF) and assumes that the toxicity posed is primarily through its systemic (lymphatic and circulatory system) circulation rather than localised effects. For the dermal pathway localised effect such as the development of skin tumours are largely ignored (Nathanail et al. 2015). To account for both potential systemic and localised effects, we define dermal bioavailability as the proportion of compound/pollutant absorbed into human skin (our artificial membrane), where it may remain or be further released to systemic circulation (our synthetic receptor solution) (Beriro et al., 2016). Dermal diffusion from a chemical containing matrix is typically quantified as flux (Fiserova-Bergerova et al., 1990), representing the rate (time) of transfer per unit area (cm^2), facilitating cross-study comparisons of dermal absorption results (Beriro et al., 2016, Peckham et al., 2017, EFSA et al., 2017).

HHRAs assumption of the dermal bioavailability of PAHs from soil are largely based on one of the first studies investigating PAH dermal bioavailability by Wester et al. (1990). Wester et al. (1990) used a *in vivo* method to quantify the absorption of BaP from soil into monkeys. Their study examines only one PAH in one type of soil, neglecting the potential effects of other soil properties and physicochemical characteristics of PAHs on dermal bioavailability. Subsequent research on the dermal bioavailability of PAHs from soils has been limited (Beriro et al., 2016, Ruby et al., 2016, Spalt et al., 2009).

Several dermal studies reported the PAH dermal absorption as a fraction or percentage of the applied dose (e.g. percentage absorbed of the dose applied (PADA)) (Moody et al., 2007, Wester et al., 1990). However, comparisons between studies using PADA are problematic, due to PADA being dependent on the loading rate and experimental time (Spalt et al., 2009, Moody et al., 2011). Dermal studies tend to primarily focus on a small number of parent PAHs (typically BaP) which are spiked into artificial soils (Roy et al., 1998, Yang et al., 1989, Wester et al., 1990, Moody et al., 1995, Abdel-Rahman et al., 2002, Moody et al., 2007, Moody et al., 2011, Peckham et al., 2017). Studies using spiked soil neglect to account for the influence of different PAH mixtures and the environmental impacts (such as weathering, biodegradation, and aging) on the desorption of PAHs from soils (Barnier et al., 2014, White et al., 1997,

Hatzinger and Alexander, 1995). Whereas dermal studies using real-world contaminated soils exposed to the impacts of weathering, interactions with natural organic matter and containing a diversity of PAH compounds can help establish dermal absorption results that are more representative of real-world dermal exposure scenarios (Lort, 2022).

To address these gaps in the dermal literature, our study presents an *in vitro* human dermal bioavailability method to measure the dermal absorption of 27 HMW PAHs from MGP soils. One of the novelties of our research is measuring the dermal bioavailability of the alkyl-PAHs, as well as parent PAHs in historically contaminated MGP soils. Our study aims to provide a more comprehensive understanding of the dermal absorption dynamics in PAH mixtures in soils that are more representative of real-world conditions. Our method builds on method development research in the same laboratory by Lort (2022), Our study enhances this method by measuring the *in vitro* dermal bioavailability of 20 parent PAHs and 7 alkyl-PAH groups using five MGP soils for comparison, in addition to control reference soil study with the certified reference material (CRM) BCR-524. The research objectives of our study are as follows: 1) develop an *in vitro* method to measure the dermal bioavailability of both parent and alkylated PAHs in former MGP soils; and 2) compare and contrast the dermal PAH fluxes from soil to the membrane and receptor solution with similar studies. The findings of this research are important as they have practical implications for risk assessments and provide broader scientific understanding of dermal absorption processes.

6.3 Materials and methods

6.3.1 Sample selection

Detailed information regarding soil sampling, soil properties, sample preparation, and associated sample selection can be found in Chapter 5 and in the Appendix B Chapter 5 Research Papers SI Table S1 and S2. In summary, five freeze dried sieved (<250 μm) soils were selected for this study from a larger sample set of MGP soils from England. K-means clustering ($k=5$) was employed to define distinct clusters within the wider 94 sample set. Dependent parameters were bulk organic matter (OM) properties obtained using Rock-Eval(6)

Pyrolysis (RE). One soil sample was chosen from each cluster, and a filter applied to exclude soils with BaP concentration <5 mg/kg (BaP GAC).

6.3.2 *In vitro* dermal absorption experiments

Figure 31 provides an overview of the *in vitro* dermal absorption experiment design. Full details of the dermal *in vitro* methodology can be found in Section 3.9 *In vitro* dermal experiments.

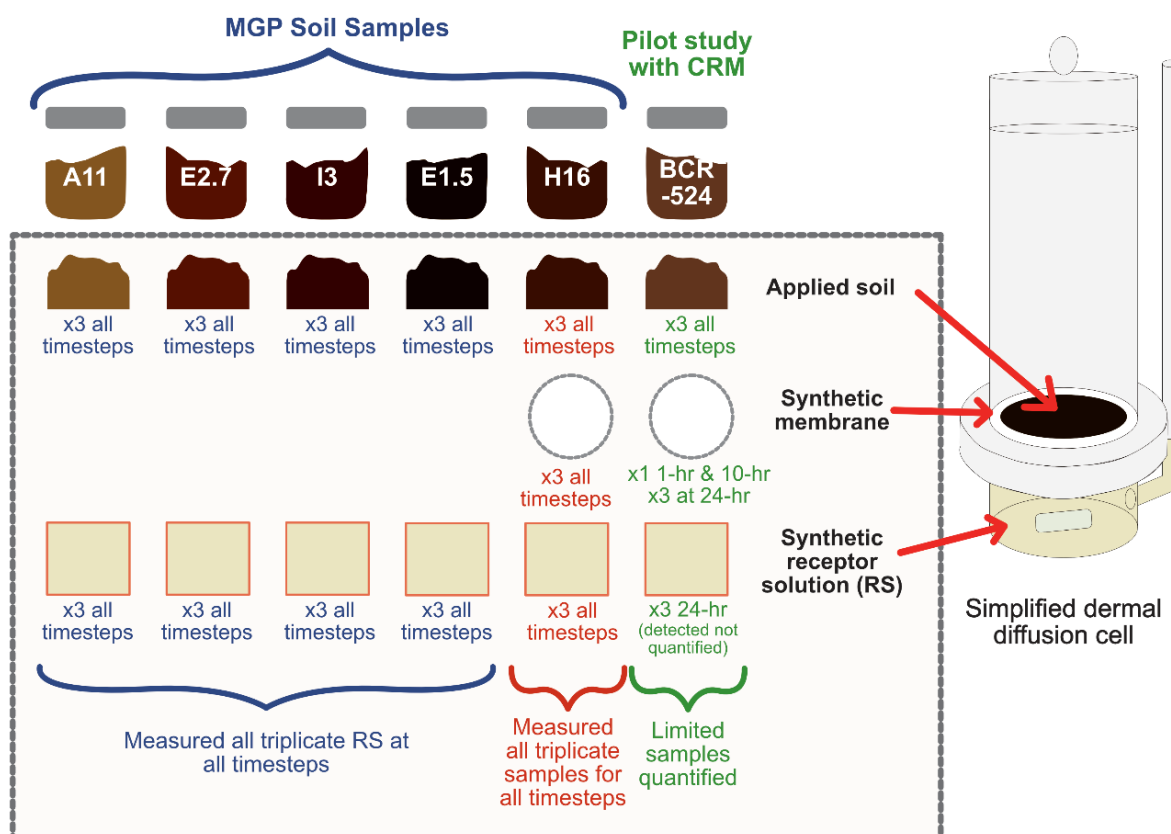


Figure 31. Diagram illustrating the dermal experiments conducted in the control reference soil study and the five MGP samples, including which dermal matrices were measured for each sample at each timestep.

Figure 31 shows the dermal matrices measured in the control reference soil study utilising the CRM BCR-524, which has previously been employed to investigate BaP desorption (Posada-Baquero et al., 2022) and enabled comparison with Lort (2022). The uncertainties associated with the dermal absorption results of BCR-524 RS samples are fully described in Section 4.2.3, providing details on issues with surrogate recoveries due to prolonged RS storage (>3 months).

6.3.3 Sample analysis

HMW parent and alkylated PAHs in all three dermal matrices (soils, membranes, and RS) were measured using gas chromatography-tandem mass spectrometry (GC-MS/MS) (Thermo Scientific Trace 1300 GC coupled to a Thermo Scientific TSQ9000 triple quadrupole. The 20 parent PAHs measured included fluoranthene (Fla), pyrene (Pyr), benz[*a*]anthracene (BaA), cyclopenta[*c,d*]pyrene (CCP), triphenylene (TPh), chrysene (Chry), benzo[*b*]fluoranthene (BbF), benzo[*k*]fluoranthene (BkF), benzo[*j*]fluoranthene (BjF), benzo[*e*]pyrene (BeP), benzo[*a*]pyrene (BaP), perylene (Per), indeno[1,2,3-*cd*]pyrene (IcdP), dibenz[*a,h*]anthracene (DahA), benzo[*g,h,i*]perylene (BghiP), dibenzo[*a,l*]pyrene (DalP), dibenzo[*a,e*]pyrene (DaeP), dibenzo[*a,i*]pyrene (DaiP), dibenzo[*a,h*]pyrene (DahP) and benzo[*c*]fluorene (BcFlu). The 7 alkyl-PAHs measured included C1-fluoranthene/pyrene (C1-Fla/Pyr), C2-Fla/Pyr, C3-Fla/Pyr, C1-benzo[*a*]anthracene/chrysene/triphenylene (C1-BaA/Chry/TPh), C2-BaA/Chry/TPh, C3-BaA/Chry/TPh and C4-BaA/Chry/TPh. Detailed information regarding the soil sample preparation and the instrument method can be found in Chapter 5.

Membrane samples underwent identical sample preparation techniques as soils, using accelerated solvent extraction (ASE) and solid-phase extraction (SPE). However, the spiking concentrations, dilutions, and aliquots were adjusted to ensure appropriate detection levels of PAHs (Section 3.7 Sample preparation and PAH extraction). RS samples were prepared using a different SPE procedure than membranes/soils, utilising Strata-PAH SPE cartridges (Phenomenex, UK). The RS samples were concentrated into 250 μ L GC-MS vial inserts to enable sufficient concentration of PAH for detection (see 3.7.2 Membrane and receptor solution sample preparation for details).

6.3.4 Dermal flux

The membrane flux represents the absorption rate of PAHs from the soil to the membrane per unit area, while the RS flux equated to the penetration rate of PAHs diffusing through the membrane into the RS. The total flux was calculated by summing the RS and membrane fluxes. Dermal fluxes (J) expressed as $\text{ng}/\text{cm}^2/\text{h}$ were calculated using Equation 8, , where Q is the measured PAH mass

(ng) in the dermal matrix, A is the surface area of the membrane (8.55 cm²) and T is the timestep of the exposure (h).

$$J = \frac{Q}{A \times T}$$

Equation 8. Calculation of dermal fluxes in dermal experiments for membrane and RS.

6.3.5 Data analysis

The R statistical software (R Core Team, 2023) was used to perform statistical analysis. The Kruskal-Wallis test and Dunn's tests were employed to assess differences between PAH fluxes within the same sample and timestep. T-tests and Wilcoxon signed-rank tests were performed to compare BCR-524 fluxes in this study with those reported by Lort (2022).

6.3.6 Quality control

Comprehensive details of the quality control for the *in vitro* dermal absorption experiments and the analytical measurements are presented in Chapter 4 Quality Control Assessment. Methods assessing the quality control (QC) of the dermal experiments involved mass balance, conducting weighed matrix balance checks, and measuring PAH levels in dermal matrices from blank dermal experiments (without soil application). T-tests and Wilcoxon signed-rank tests were performed to compare BCR-524 fluxes in this study with those reported by Lort (2022) and MGP sample fluxes were compared to other dermal studies. The performance of sample extraction and analysis was assessed through spiked solvent measurements, surrogate extraction efficiencies and by the measurement of two CRMs (BCR-524 and NIST-1944) whose measured PAH concentrations were compared to certified concentrations. Calculated detection limits (limit of quantification (LOQ) and limit of detection (LOD)) were compared to chromatogram peaks to ensure that membrane and RS peaks corresponded to analytes and not background noise.

6.4 Results

6.4.1 PAH concentrations in soils

The initial concentrations of PAHs in the real-world field soils are presented in Figure 32 and can be found in Appendix C Chapter 6 Research Paper SI Table

S10. The mean soil concentration for BaP was in a range of 6.53 – 160.5 mg/kg. All soil samples exceeded the GAC for BaP (5 mg/kg), indicating potential risks associated with dermal chronic absorption by humans for residential land use with plant uptake (CL:AIRE, 2014).

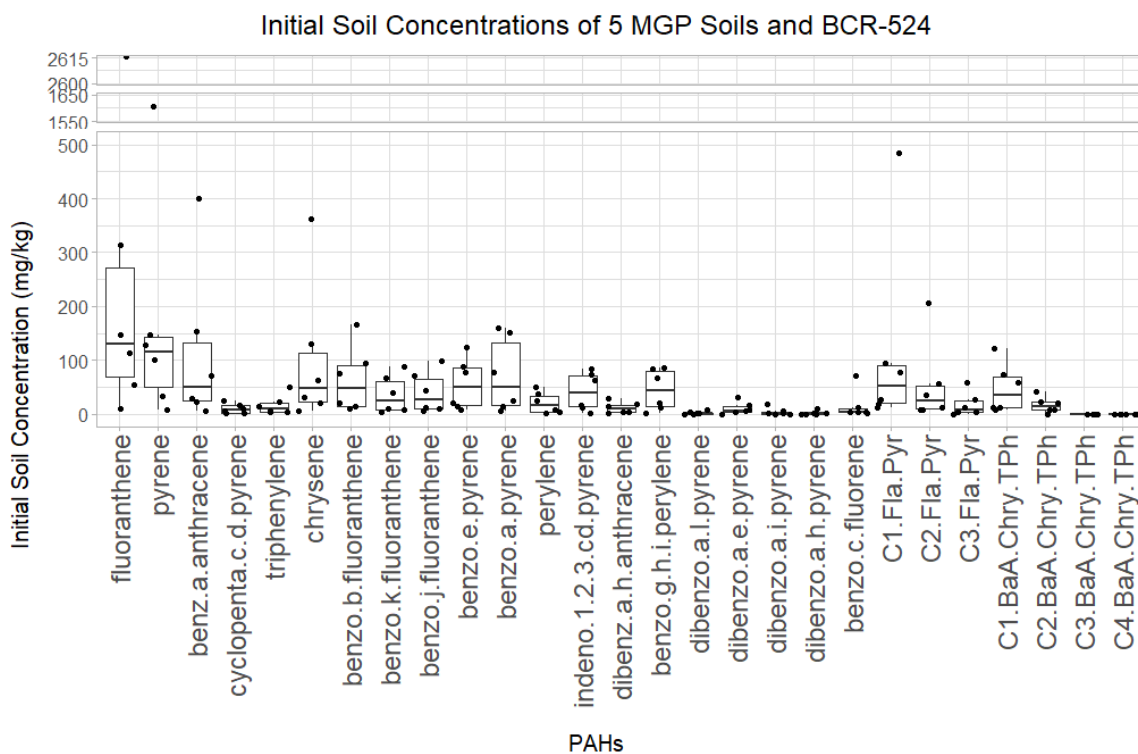
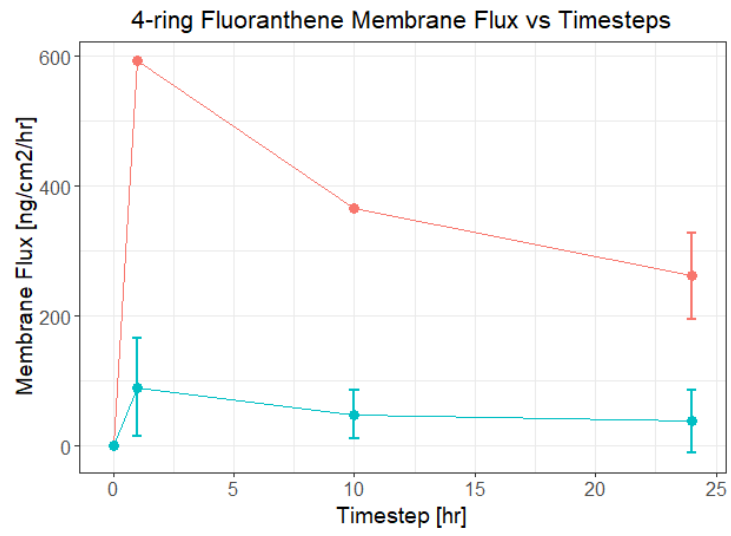


Figure 32. Boxplot of the initial soil concentrations of the 27 HMW PAHs in the 5 MGP soils and BCR-524. Note y-axis breaks and change in scale for the extreme PAH concentrations for E1.5.

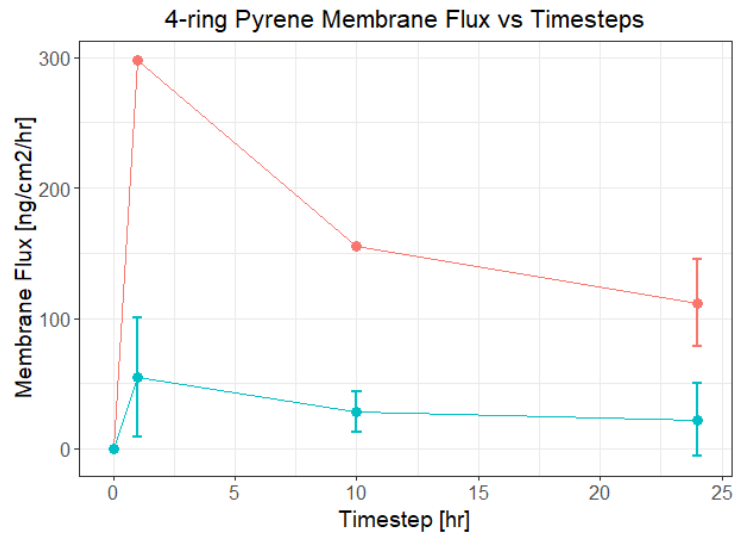
6.4.2 Membrane flux

H16 membranes were measured for all timesteps in triplicate and the BCR-524 sample 24-h membranes were measured in triplicate and one membrane from the 1-h and 10-h experiments (Figure 31). Figure 33 illustrates the initial rapid intake of PAHs (higher fluxes) into the membranes at shorter timesteps. The membrane fluxes were higher than the RS fluxes, for example, BaP flux means were 5.02 ng/cm²/h for membranes and 0.0018 ng/cm²/h for RS for the H16 sample at 24-h. Figure 34 shows all HMW PAHs membrane fluxes at each timestep for each soil.

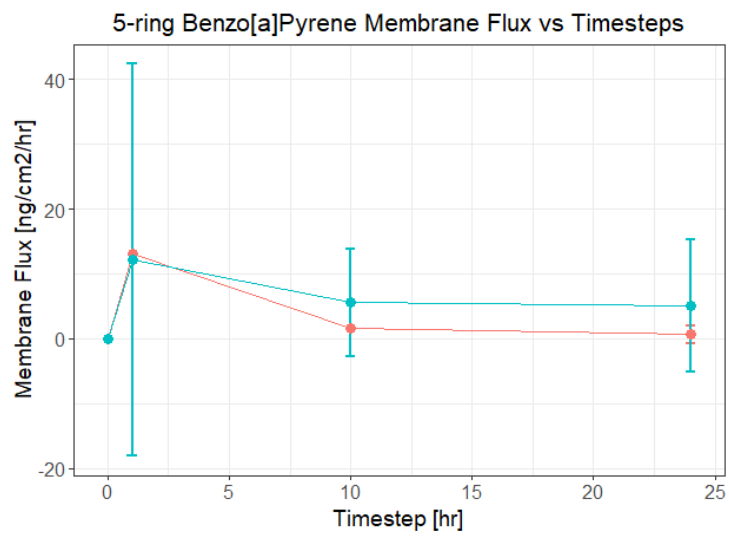
(a)



(b)



(c)



(d)

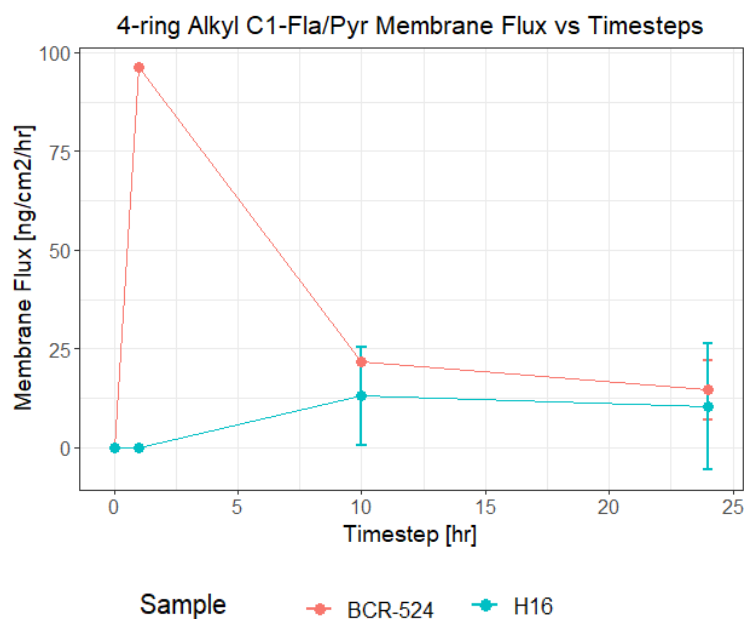


Figure 33. Mean membrane fluxes for the four HMW PAHs (a) Fla, (b) Pyr, (c) BaP and (d) C1-Fla/Pyr over the timesteps 1-h, 10-h and 24-h. Data points represent mean membrane fluxes and error bars are the 95% CI. The H16 sample uses triplicate experiment results for each timestep, whereas the BCR-524 uses triplicate membranes for 24-h and one membrane measured at 1-h and 10-h. Note different y-axis scales in all plots and lines representing different samples.

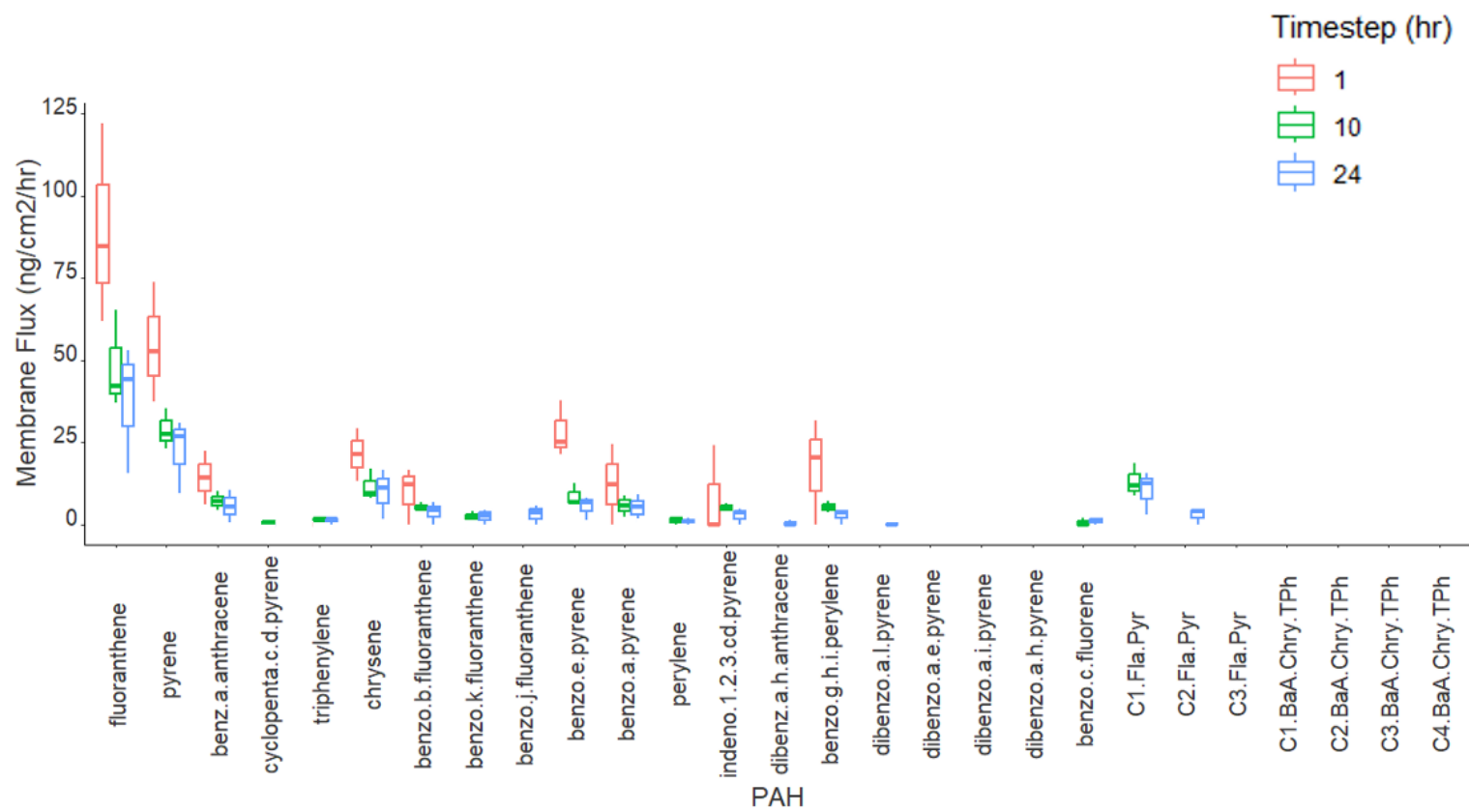
The number of HMW PAHs compounds detected in the membranes increased with longer timesteps, H16 detected 9, 15, 18 HMW PAHs respectively for the timesteps 1-h 10-h and 24-h. In comparison H16 RS detected 2, 8, 10 HMW PAHs species with increasing timesteps, indicating a delayed diffusion of PAHs from membrane into RS. The membrane flux for each PAH was consistently highest at the 1-h timestep the PAH (for >LOQ) (Figure 33). For example, BaP mean membrane flux for H16 decreased from 12.1 ng/cm²/h to 5.54 ng/cm²/h and then 5.02 ng/cm²/h respectively. The HMW PAH membrane fluxes at each timestep for the H16 sample followed order of:

- H16 at 1-h: Fla > Pyr > BeP > Chry > BghiP > BaA > BaP > BbF > IcdP
- H16 at 10-h: Fla > Pyr > C1-Fla/Pyr > Chry > BeP > BaA > BaP > BbF > BghiP > IcdP > BkF > TPh > Per > BcFlu > CCP
- H16 at 24-h: Fla > Pyr > C1-Fla/Pyr > Chry > BaA > BeP > BaP > BbF > BbF > C2-Fla/Pyr > IcdP > BghiP > BkF > TPh > BcFlu > Per > DahA > DalP

Fla and Pyr showed the highest membrane fluxes for H16. C1-Fla/Pyr measured the third highest membrane fluxes at the longer timesteps 10-h and 24-h but was not detected at 1-h. No other alkyl-PAHs from either the alkylated Fla/Pyr or alkylated BaA/Chry/TPh homologue series were detected in the H16 membranes at the other timesteps except for C2-Fla/Pyr which showed breakthrough into the membrane at 24-h. The BCR-524 24-h membranes detected the presence of C1-Fla/Pyr only, however the BCR-524 RS samples detected C2-Fla/Pyr, C3-Fla/Pyr, C1-BaA/Chry/TPh and C2-BaA/Chry/TPh compounds at the 24-h timestep suggesting that potentially alkyl-PAHs had passed through the membrane by 24-h into the RS.

Interestingly the subsequent highest membrane fluxes for H16 after Fla and Pyr at 1-h was the 5-ring BeP > 4-ring Chry > 6-ring BghiP (mean membrane fluxes of 28.0 ng/cm²/h > 21.3 ng/cm²/h > 17.2 ng/cm²/h). This suggests that the ring number might not be a dominant factor for desorption rate of HMW PAHs from soils into membranes at shorter timesteps. Longer timesteps measured 4-ring PAHs with higher membrane fluxes compared to the 5-ring and 6-ring PAHs. The HMW parent PAHs that were not detected in any of the H16 membranes within 24-h included the 6-ring PAHs CCP, DaeP, DaiP, and DahP. The Kruskal-Wallis test was conducted on membrane fluxes, and it revealed statistically significant results ($p < 0.05$) for the H16 membranes at each time step. However, the Dunn's test did not identify any statistically significant differences in membrane fluxes among HMW PAHs.

(a)



(b)

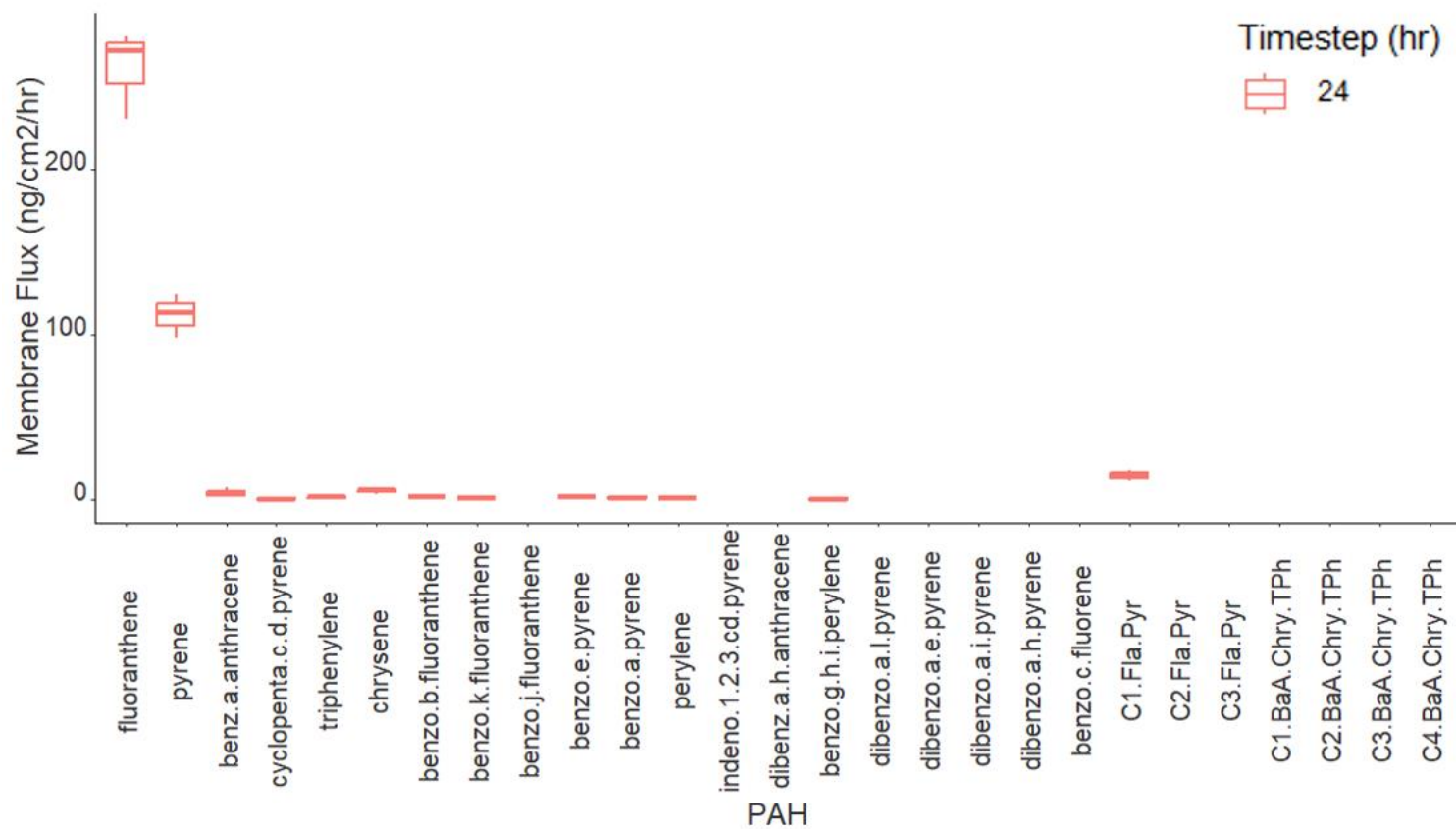
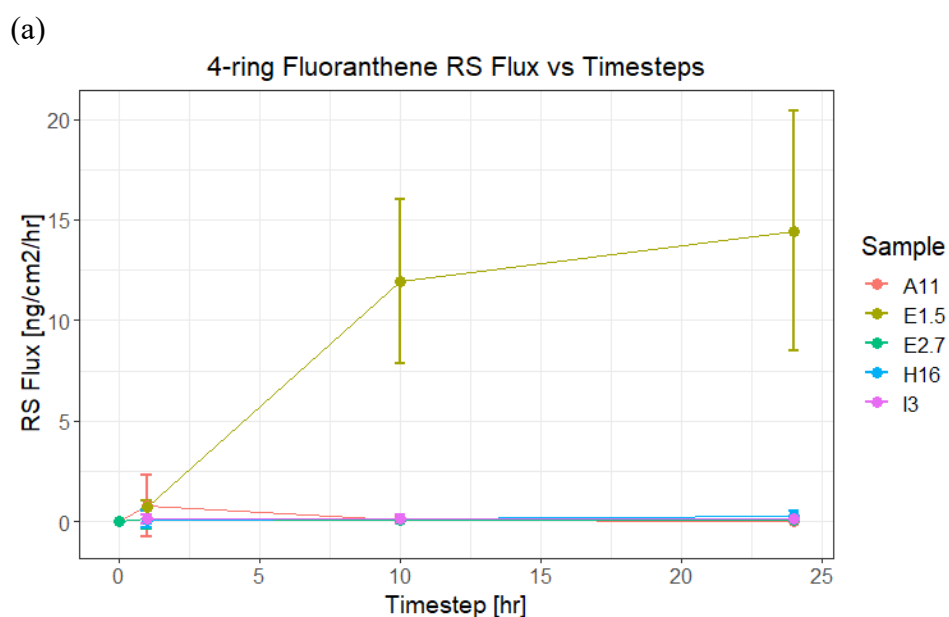


Figure 34. Boxplots of the membrane fluxes for (a) H16 triplicate experiments at each timestep and (b) BCR-524 triplicates experiments for 24-h). Absence of boxplot indicates PAHs are <LOQ in membrane.

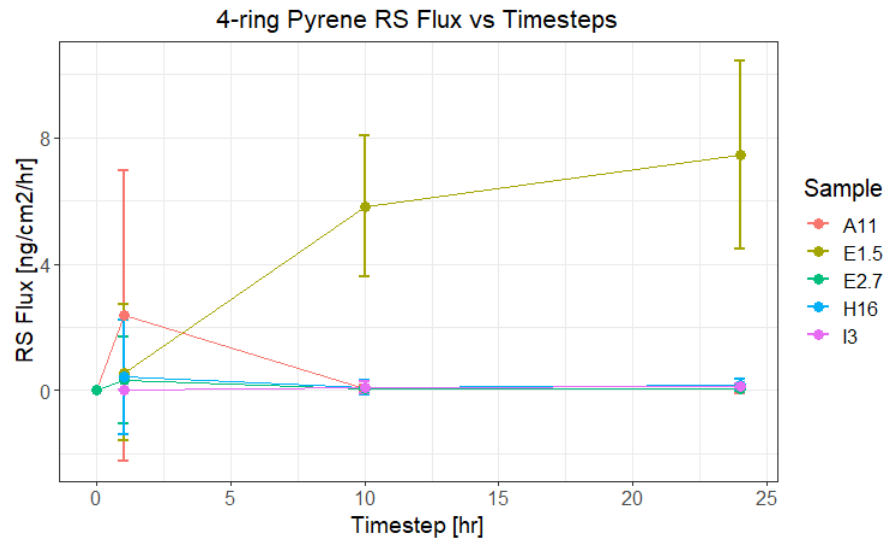
6.4.3 Receptor solution flux

All five MGP samples RS at each timestep fluxes were quantified in triplicate, whereas the RS samples from the 24-h timestep for BCR-524 were stated as detected or non-detected (not quantified) (Figure 31). BCR-524 RS samples were not quantified due to issues with surrogate recoveries due to prolonged RS storage (>3 months) during method development and discussed in Section 4.2.3. The fluxes from soil to RS (RS flux) varied between HMW PAH compounds, samples and timesteps. The dermal flux measurements are provided in the Appendix C Chapter 6 Research Paper SI Table S10. Higher RS fluxes were generally measured for PAHs with lower ring number, longer timesteps and samples with higher initial soil PAH concentrations.

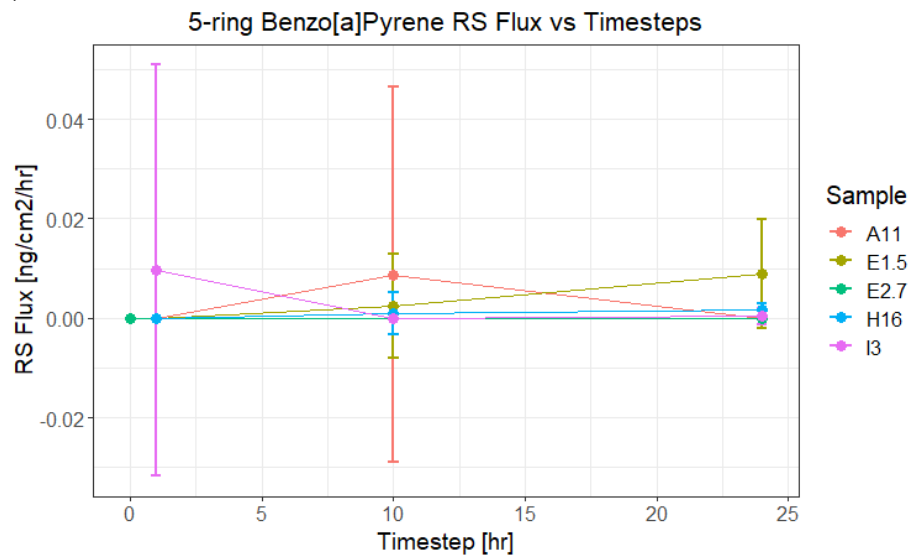
Figure 35 shows that the mean RS fluxes of the 4-ring PAHs (Fla and Pyr) increased rapidly with longer timesteps, while 5-ring BaP showed increased RS flux with increasing timesteps but at lower flux rates. Samples with the highest initial soil concentrations (E1.5, H16 and I3 Fla & Pyr ranged between 100 – 2,616 mg/kg) showed higher RS fluxes at longer timesteps. This is in contrast to samples with lower initial soil concentrations (A11 and E2.7 Fla & Pyr ranged between 8.1 – 54 mg/kg) which measured higher RS fluxes at shorter timesteps. Samples A11 and E2.7 showed higher variability for the RS flux for each PAH compared to the higher concentrated samples.



(b)



(c)



(d)

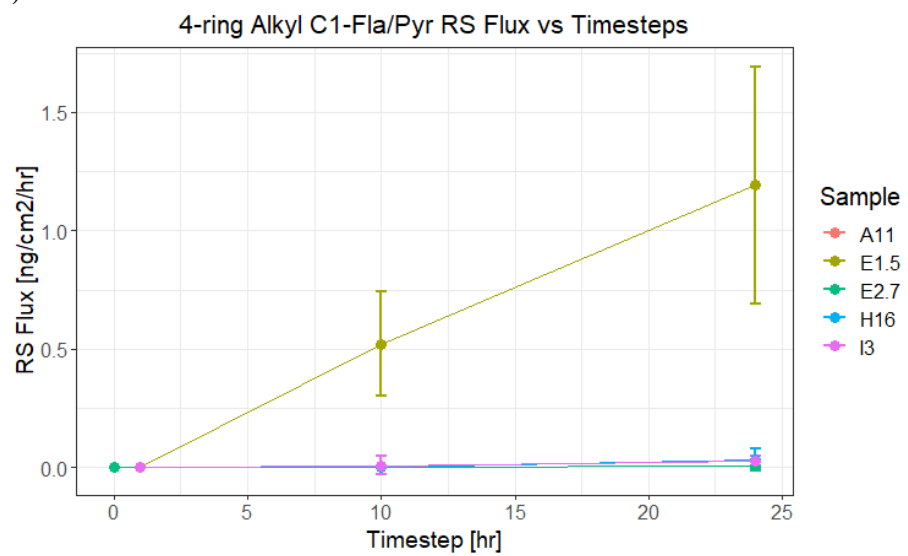


Figure 35. Mean RS fluxes for the four HMW PAHs (a) Fla, (b) Pyr, (c) BaP and (d) C1-Fla/Pyr over the timesteps 1-h, 10-h and 24-h. Data points represent mean fluxes of the triplicate experiments performed for each timestep for each MGP sample, and error bars are the 95% CI. Note different y-axis scales in all plots and lines representing different samples.

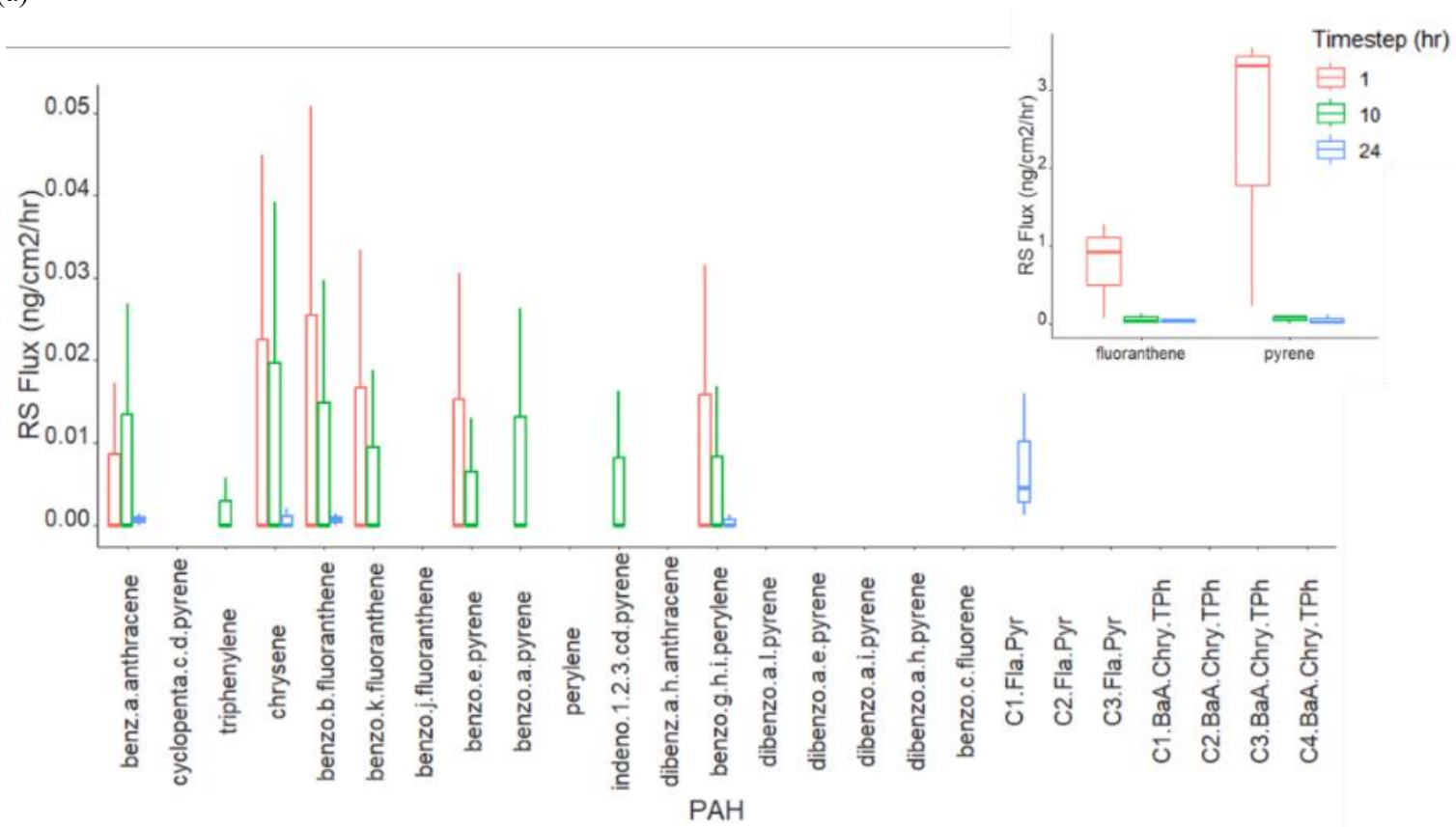
Boxplots presented in Figure 36a-e illustrate the differences in RS fluxes between the 27 HMW parent and alkylated PAHs in each MGP sample. Fewer HMW PAHs were detected in RS at 1-h compared to longer timesteps, indicating lower soil to RS flux for the heavier PAHs with a larger ring number. The differences in RS flux values between short and long timesteps and HMW PAH indicated changes in PAH availability for dermal absorption over time. The HMW PAH RS fluxes at 1-h for each sample showed the following in the descending order:

- E1.5: Fla > Pyr > Chry > BaA > BbF > BghiP > BeP
- H16: Pyr > Fla
- I3: Fla > Chry > BaA > BbF > BghiP > BeP > IcdP > BaP > BkF
- E2.7: Pyr > Fla > BaA
- A11: Pyr > Fla > BbF > Chry > BkF > BghiP > BeP > BaA

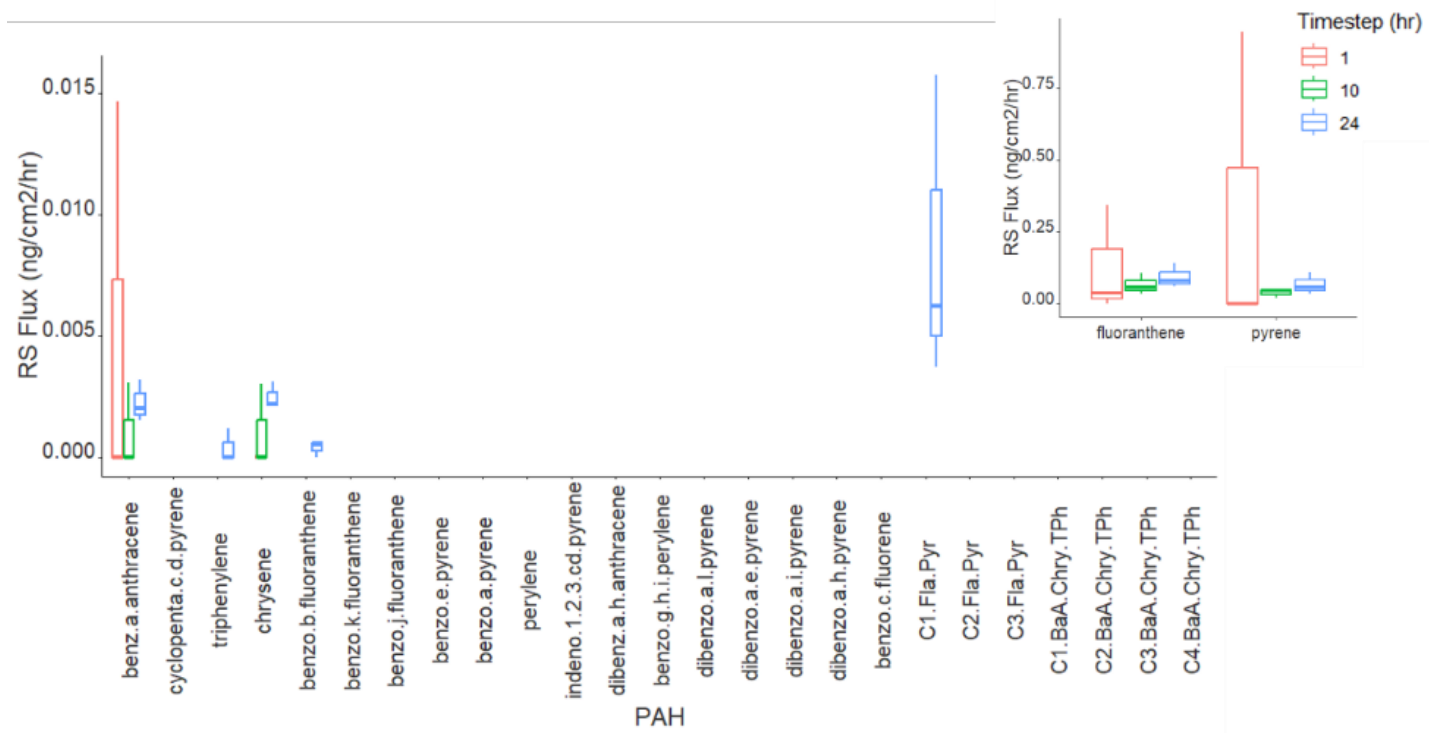
Compared to the HMW PAH RS fluxes at 24-h for each sample showed the following descending order:

- E1.5: Fla > Pyr > C1-Fla/Pyr > BcFlu > C2-Fla/Pyr > BaA > Chry > TPh > BbF > BaP > BeP > BkF > CCP > BghiP > IcdP
- H16: Fla > Pyr > C1-Fla/Pyr > BaA > Chry > BbF > BaP > BcFlu > TPh > BeP
- I3: Fla > Pyr > C1-Fla/Pyr > Chry > BaA > BeP > BaP > TPh > BbF
- E2.7: Fla > Pyr > C1-Fla/Pyr > Chry > BaA > TPh > BbF
- A11: Pyr > Fla > C1-Fla/Pyr > Chry > BbF > BaA > BghiP

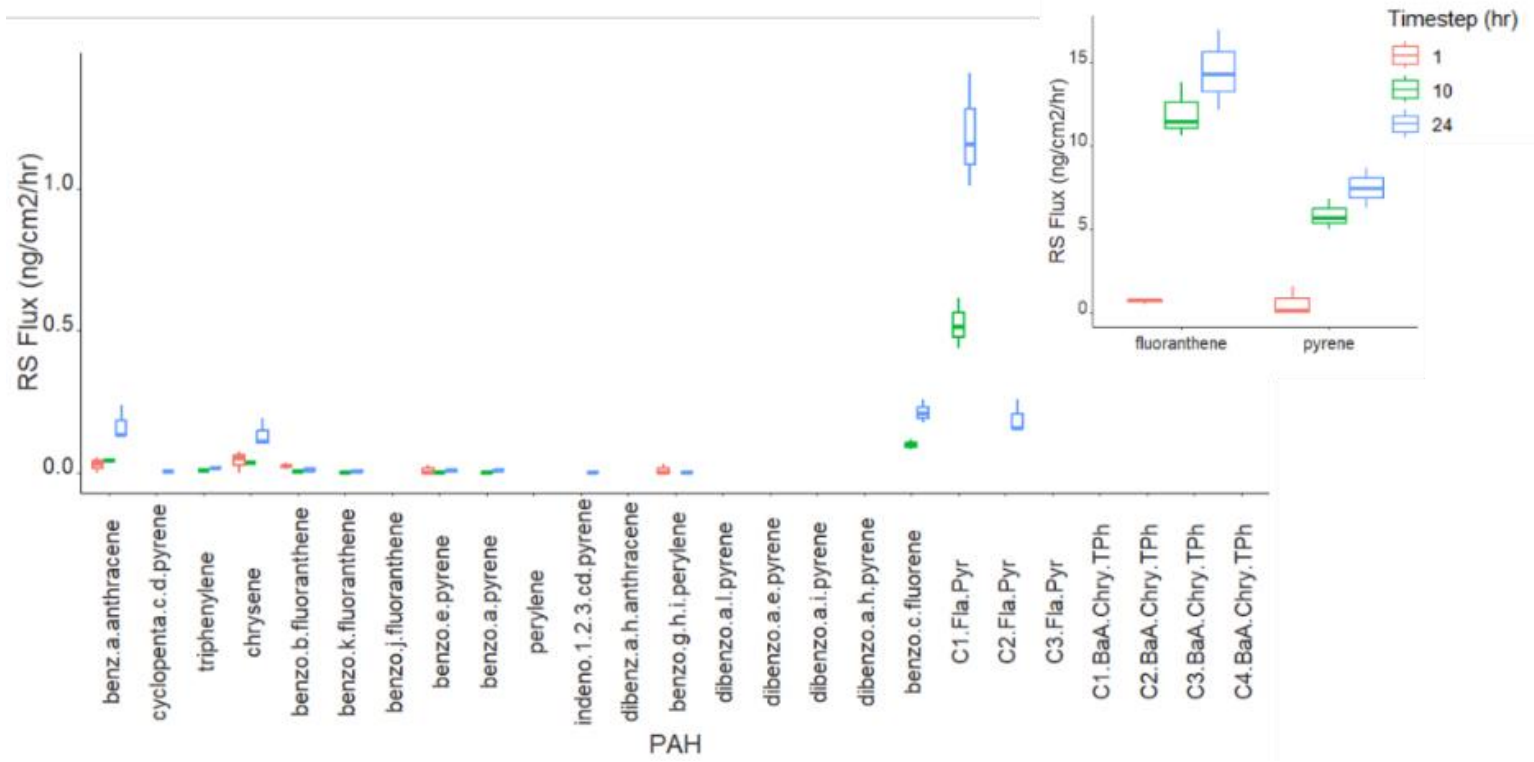
(a)



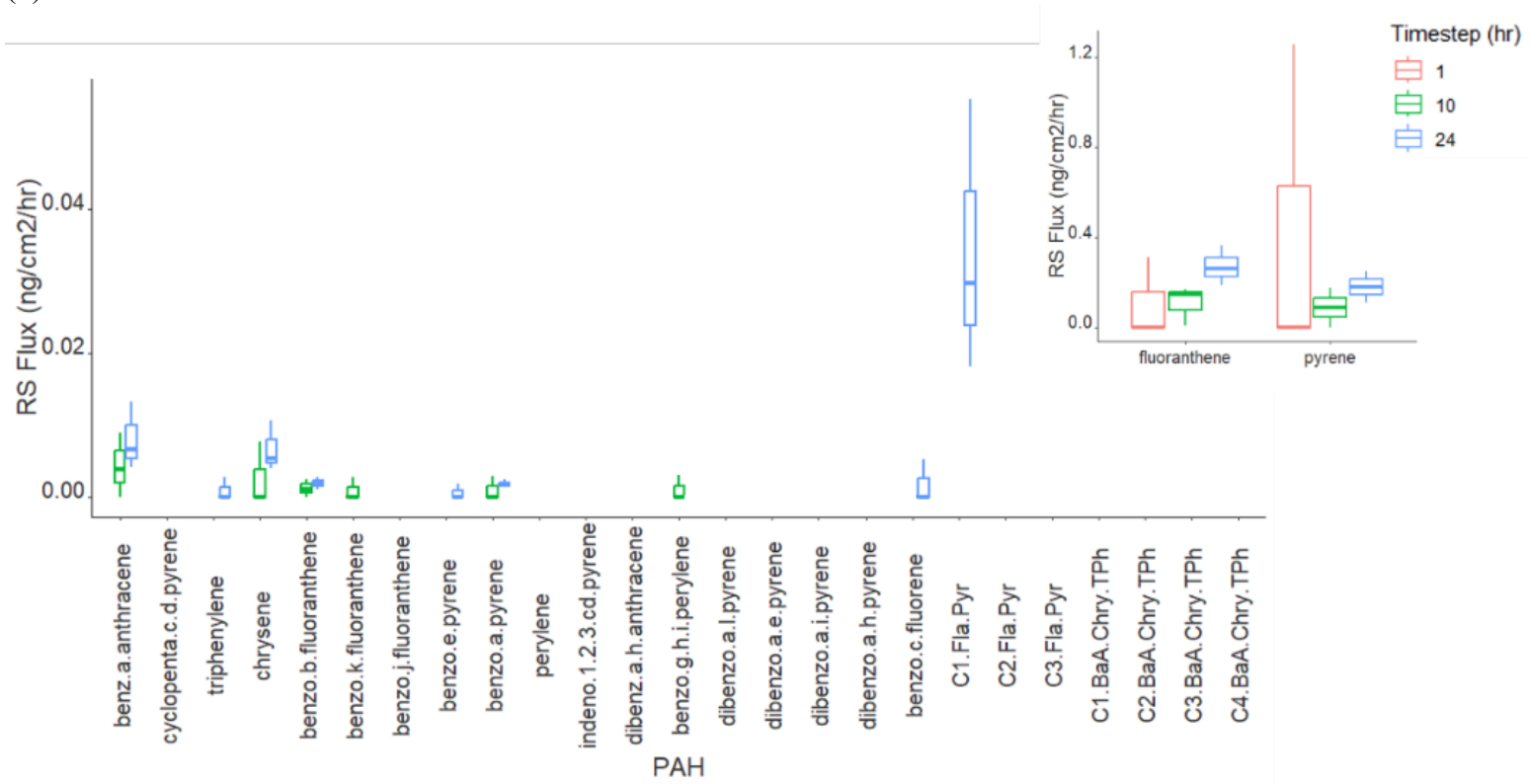
(b)



(c)



(d)



(e)

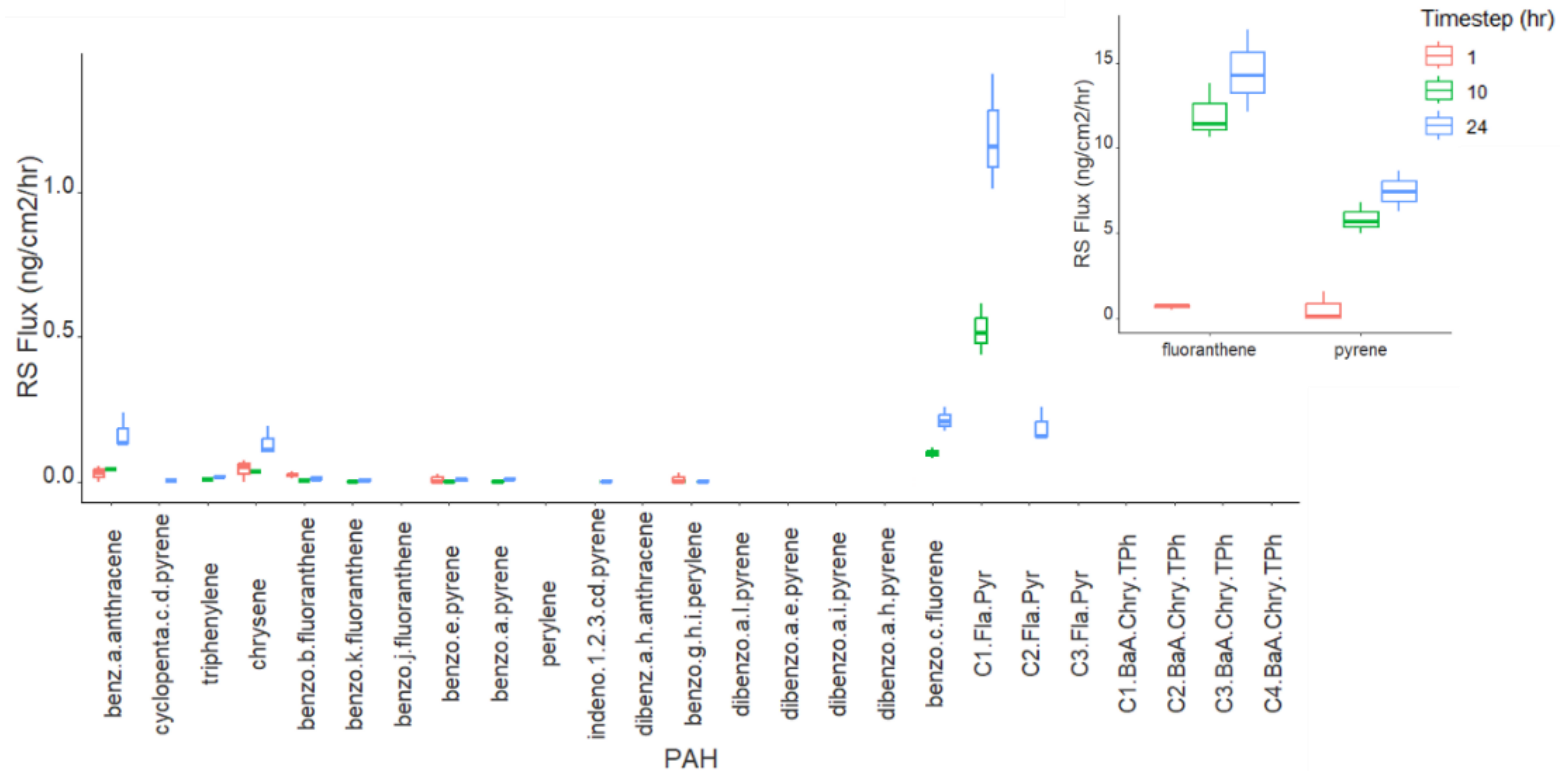


Figure 36. RS flux for individual PAHs at each timestep, data based on three experiments per timestep, (a) A11, (b) E2.7 (c) I3, (d) H16 and (e) E1.5 reported as boxplots. Samples ordered by ascending soil PAH concentration, Fla and Pyr removed from larger boxplot to allow the scale of fluxes for other PAHs to be represented. Absence of boxplot indicates PAHs are <LOQ in RS.

Comparing the fluxes between different HMW PAHs within each sample and time step revealed that Fla and Pyr consistently yielded the highest RS fluxes across all samples and timesteps, followed by C1-Fla/Pyr homologue series at longer time steps. Fla and Pyr were only statistically significant (p -value <0.05) from the other HMW PAHs fluxes for the samples I3 and E2.7 at 10-h when tested by the Dunn's test. Although the Kruskal-Wallis test indicated statistically significant results (p -value <0.05) for A11, I3 and E1.5 at the 1-h timestep, I3, E2.7, E1.5, and H16 at 10-h, and all samples at the 24-h.

C1-Fla/Pyr was detected in all RS samples at 24-h, with RS fluxes ranging between 0.007 to 1.19 ng/cm²/h (mean: 0.25 ng/cm²/h in comparison to BaP mean 0.002 ng/cm²/h). However, the C1-Fla/Pyr was not detected in the RS for any sample at 1-h and only in two samples at 10-h, indicating a slower absorption than their parent derivatives. None of the other alkylated PAHs from either Fla/Pyr and BaA/Chry/TPh homologue series were detected in RS for the MGP samples at any timestep, except for C2-Fla/Pyr detected in E1.5 RS at 24-h (mean: 0.19 ng/cm²/h). Although the control reference soil study with BCR-524 measured breakthrough of alkyl-PAHs with increased alkylated chain lengths (C2-Fla/Pyr, C3-Fla/Pyr, C1-BaA/Chry/TPh and C2-BaA/Chry/TPh) at longer timesteps. BCR-524 samples were collected from former wood treatment activities involving creosote oil.

In addition to Fla and Pyr, other HMW PAHs with elevated fluxes included BaA, Chry, BcFlu, and BbF. These PAHs measured mean RS fluxes of 0.035, 0.029, 0.043 and 0.003 ng/cm²/h, respectively for the MGP samples. HMW PAHs not detected in the RS for either of the three-timesteps included one 5-ring PAH BjF, and the 6-ring PAHs DahA, DalP, DaiP, DahP, and DaeP.

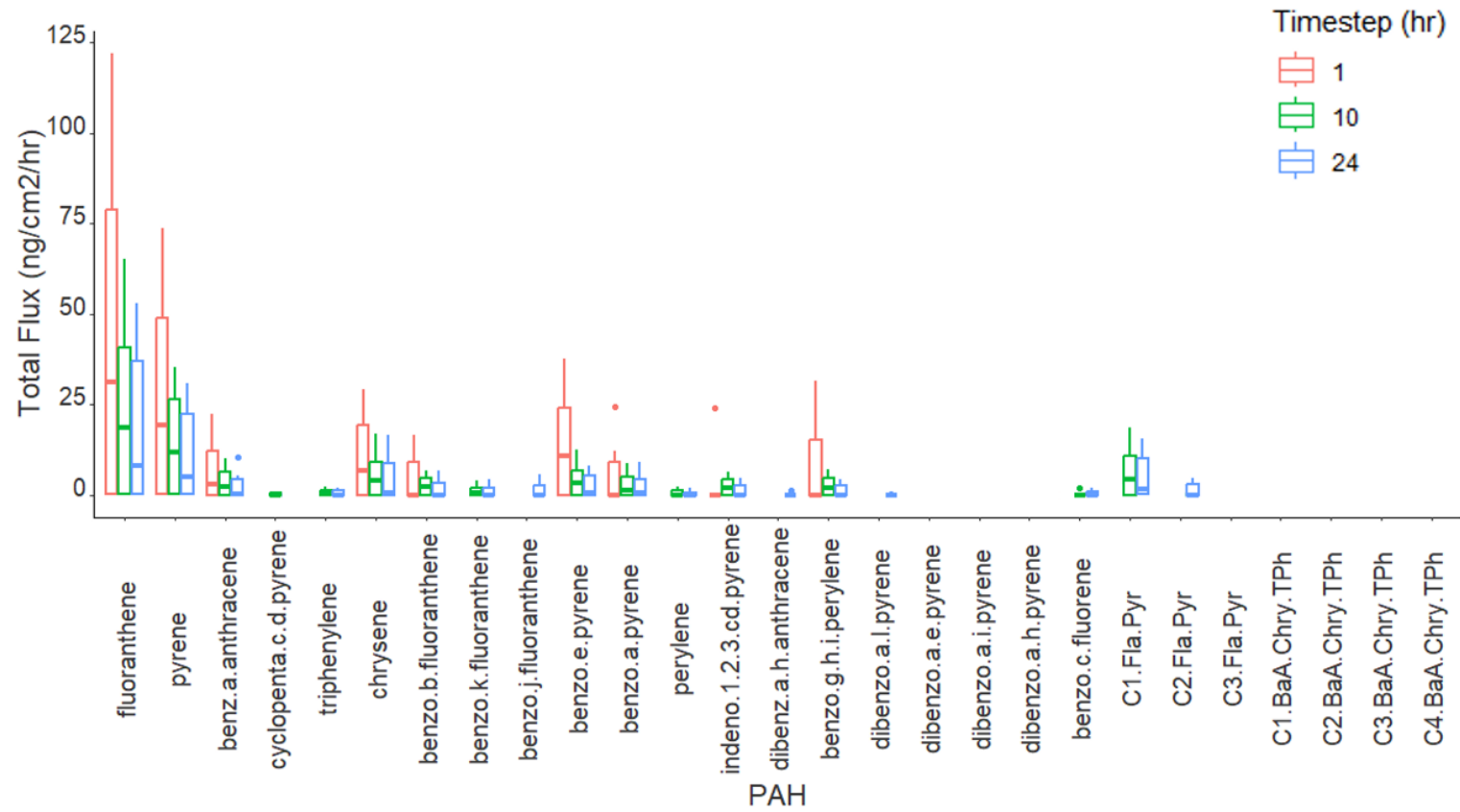
6.4.4 Combined receptor solution and membrane flux

Combined membrane and RS fluxes (total flux) were calculated for samples H16 and BCR-524 (Figure 37a-b) by adding the two flux values together. H16 total fluxes ranged from LOQ to 122.5 ng/cm²/h (mean: 6.38 ng/cm²/h) for all timesteps and HMW PAHs. Membrane flux consistently provided the highest contribution to total flux, therefore total flux trends within samples were similar to membrane. For example, the H16 sample membrane flux contributions to the total flux for each timestep was 100.00%, 99.98% and 99.91% for 1-h, 10-h and 24-h for BaP, in comparison Fla 99.92%, 99.79% and 99.18% for 1-h, 10-h and 24-h.

6.4.5 PAH Physicochemical Properties and Initial Soil Concentration Influences

The relationship between PAH physicochemical properties and RS fluxes was examined. Results for sample H16 are shown in Figure 38, results for other samples are presented in Appendix C Chapter 6 Research Paper SI Figure S11. The plots show that RS flux rapidly decreased with increased Log K_{OW} and MW. Figure 39 showed that several PAHs with high initial soil concentrations had higher dermal fluxes, however there were many PAH with no correlation between initial soil concentrations and the dermal flux.

(a)



(b)

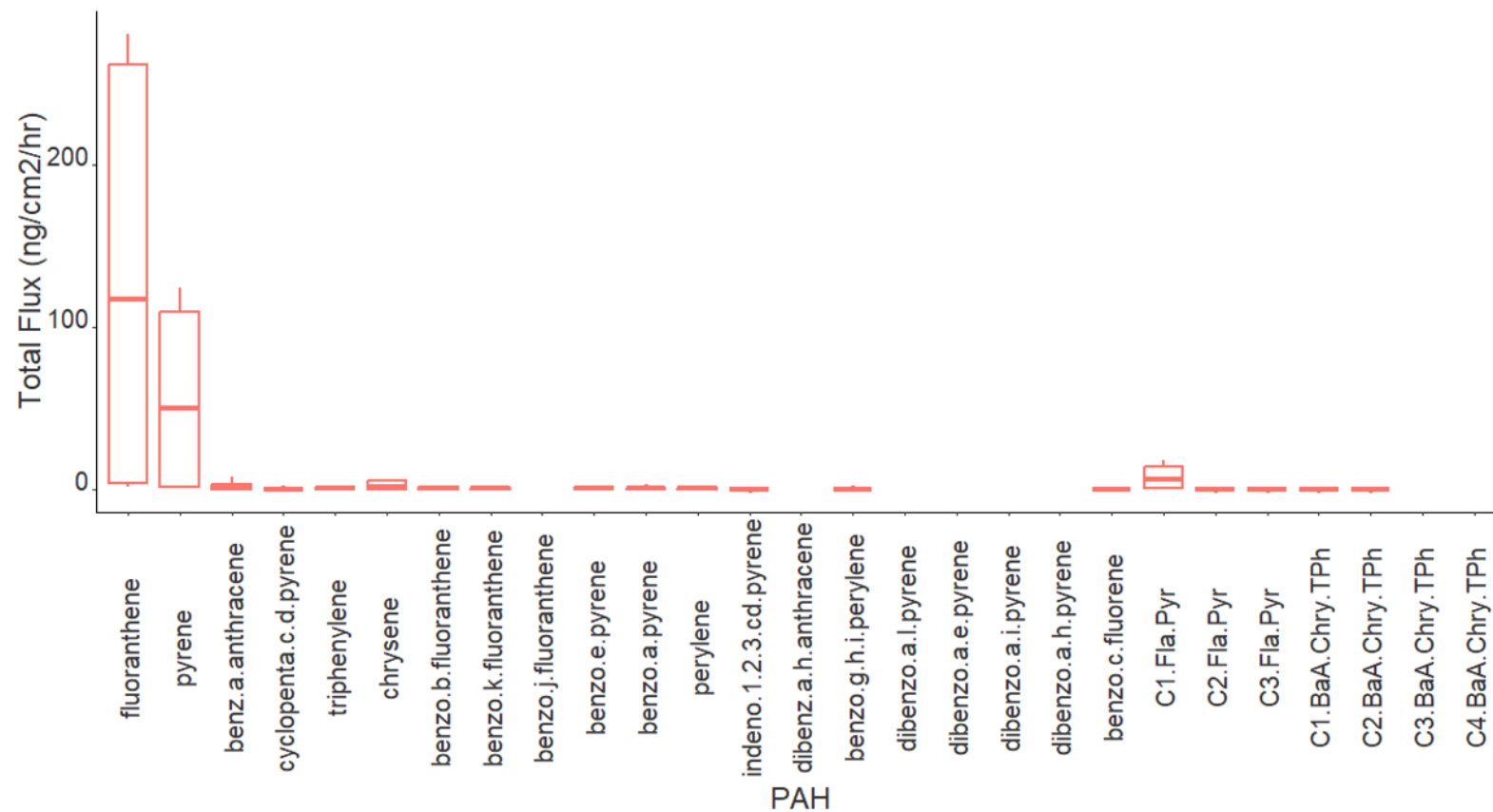


Figure 37. Boxplots of the total fluxes for (a) H16 triplicate experiments at each time step and (b) BCR-524 triplicates experiments for 24-h). Absence of boxplot indicates PAHs <LOQ.

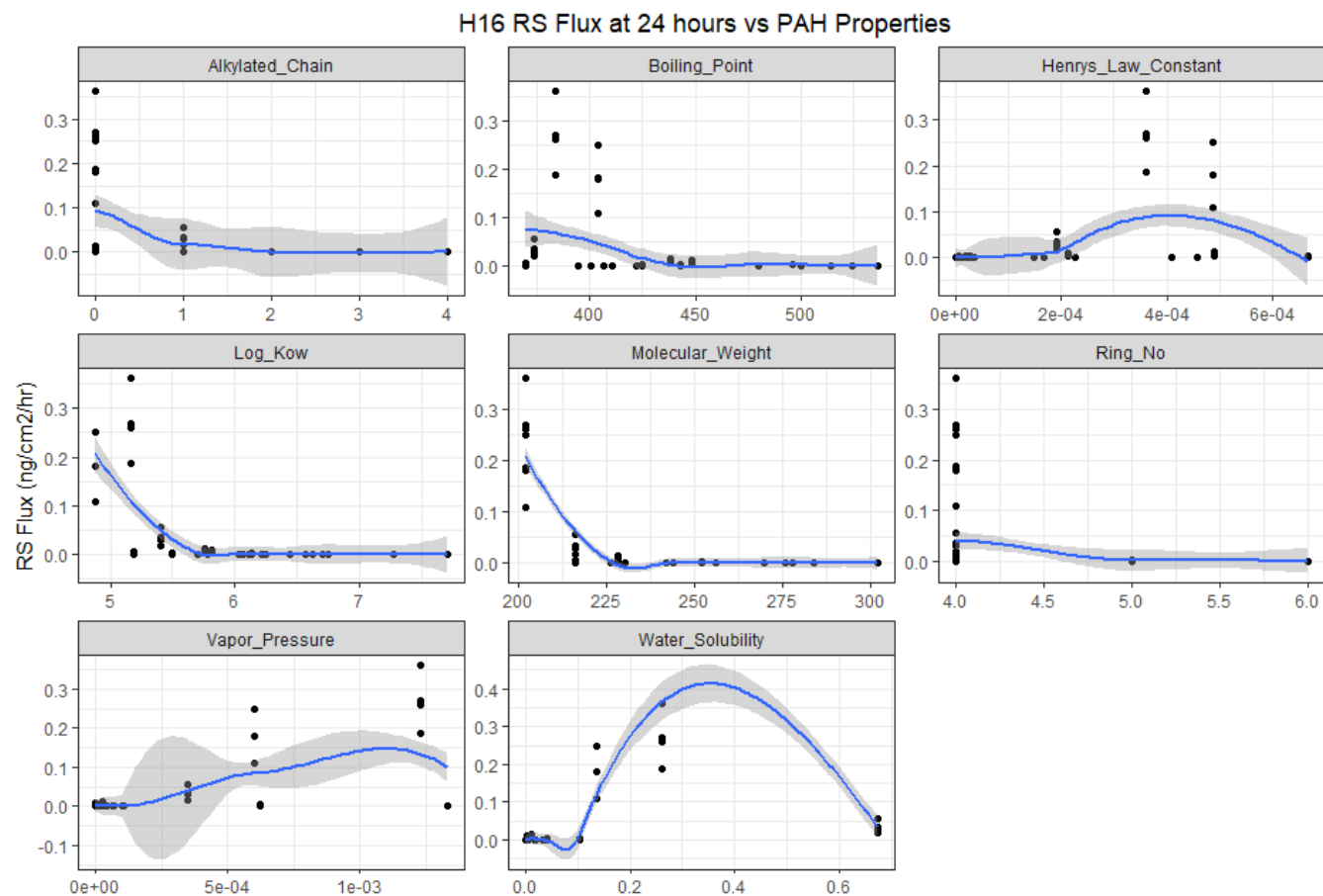
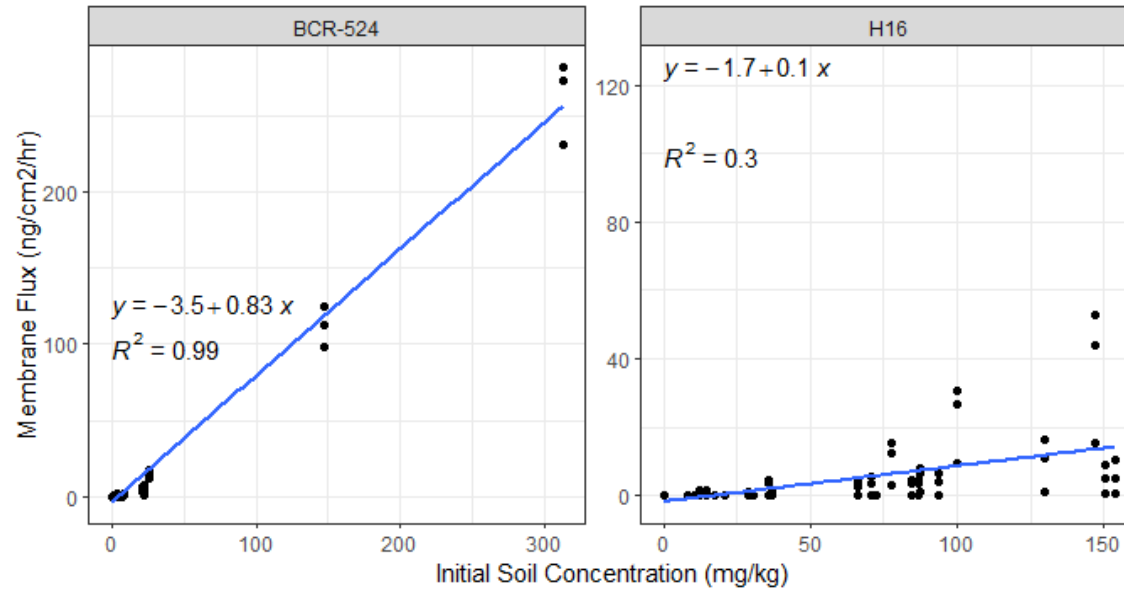


Figure 38. Multiple plots of the sample H16 RS flux relationship with PAH physicochemical properties. The y-axis plots the H16 RS fluxes at 24-h for triplicate experiments and the x-axis plots the PAH physicochemical properties: alkylated chain length, boiling point (°C), Henry's Law Constant, Log Kow, Molecular weight (Da), number of rings in structure, vapour pressure (Pa) and water solubility (mg/L). Physicochemical property values taken from Achten and Andersson (2015) whereby the mean physicochemical property values of individual alkyl-PAHs were used to represent the alkylated homologue series. Line of best fit calculated with locally estimated scatterplot smoothing (LOESS).

(a)



(b)

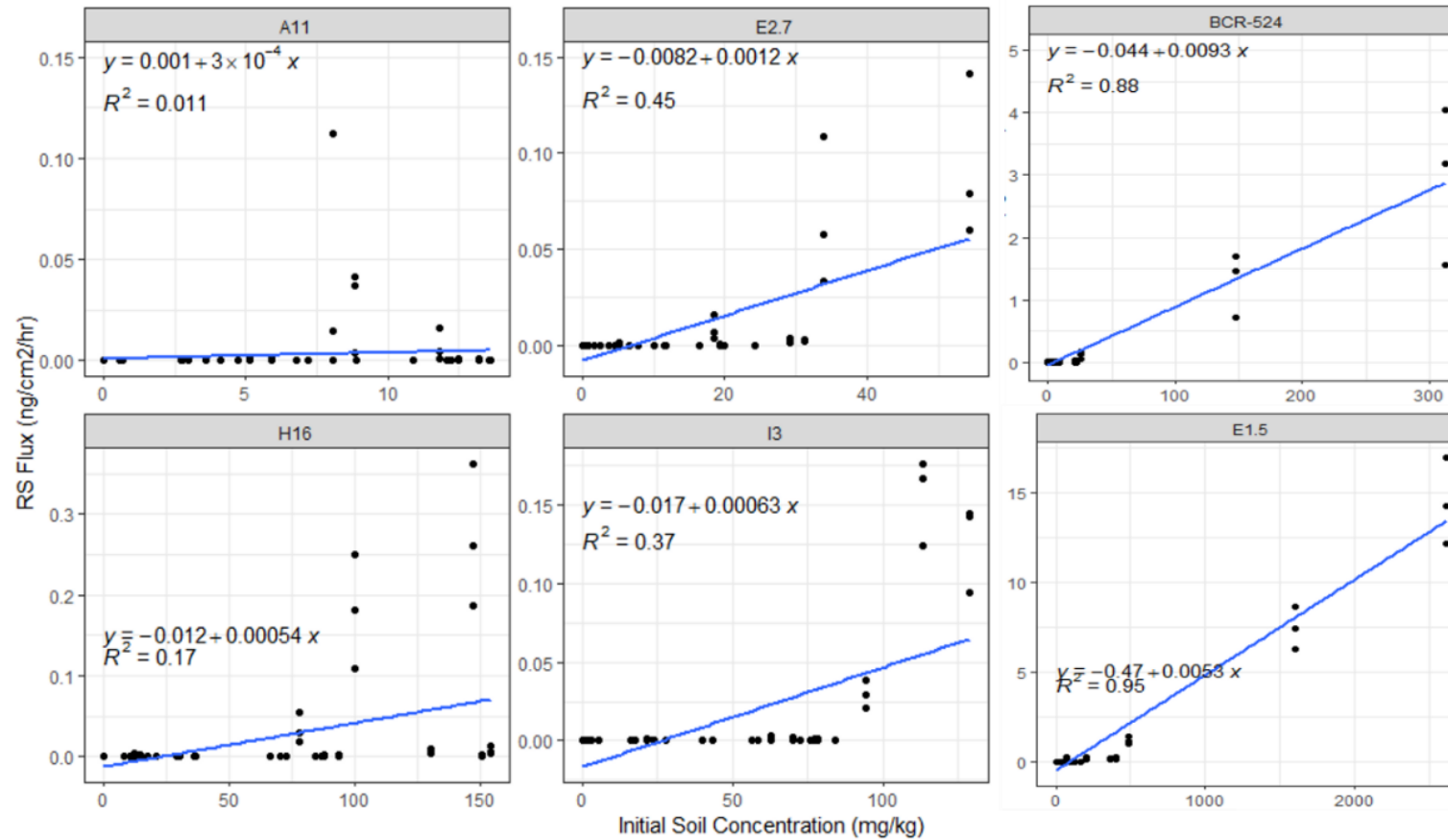


Figure 39. The initial soil PAH concentration (mg/kg) of the 27 HMW PAHs plotted against (a) 24-h membrane fluxes for H16 and BCR-524 and (b) 24-h RS fluxes for all samples, line produced from linear regression.

6.4.6 Quality control

The full details of the performance of the *in vitro* method, sample extraction and analysis are presented in Chapter 4 Quality Control Assessment. The QC regime results are presented in Table 19. In summary the results from the QC procedures provided confidence that the *in vitro* method was executed correctly and that the sample preparation and analysis were appropriate to quantify the range of HMW PAHs.

Table 19. QC regime procedures and results for study.

QC Procedure	QC Result
Spiked solvent measurements	%Bias ¹ <30% and relative standard deviation (%RSD) <15% as per Environment Agency (2018).
Surrogate extraction efficiencies	Satisfactory mean recoveries: 81% for soils, 75% for membranes and 76% for RS. BCR-524 RS fluxes were not quantified due to unacceptable surrogate recoveries. These were caused by prolonged storage of RS samples during method development which impacted the RS extraction from SPE, instead of concentrations the detection of the presence of PAHs is reported for BCR-524 RS samples (see 4.2.3 Extraction efficiencies – Sample recoveries for details).
Calculated detection limits subjected to chromatogram verification	Verifications all aligned with their respective chromatograms for four PAHs, ensuring sample peaks were analytes and not background noise.
Measurement of two CRMs (NIST-1944 and BCR-524)	The majority of HMW PAHs exhibited %Bias <30% and a %RSD <15% (including C1-Fla/Pyr), hence further supporting the method's accuracy and precision in measuring a diverse range of HMW PAHs at varying concentrations.
Dermal experiments mass balance	Mean values of 98.3% and 92.1% for H16 and BCR-524.
Weighed matrix balance checks	Low membrane weight differences (mean of 1.72%) and collected dried soils close to targeted weight.

PAH concentration measurements from blank dermal experiments	RS and membranes indicated no additional HMW PAH contamination to samples, e.g. Fla in blank RS measured 0.085 µg/g compared the limit of quantification (LOQ) 0.083 µg/g.
Dermal study comparisons	The measured fluxes in the control reference soil study with BCR-524 did not significantly differ from the fluxes reported by Lort (2022). Furthermore, the fluxes obtained in this study fell within the range of fluxes reported in other studies, further reinforcing the standardisation of this study.

¹Bias determines the accuracy of measurement evaluating the difference between the true CRM value and our measured value.

²RSD provides an indication of precision of method by interpreting the distribution of repeated measurements.

6.5 Discussion

6.5.1 HMW parent PAH dermal flux

This study shows that the majority of HMW PAHs enter the membrane within the 24-h timestep (19/27 PAHs were detected in the H16 membranes), but delays in diffusion through the membrane into the RS occurred for PAHs with a higher ring number. The dermal flux values demonstrate significant variation between HMW PAHs across different soil samples and exposure times, with membrane fluxes consistently higher than RS fluxes. For example, Fla membrane fluxes were two orders of magnitude higher than the RS fluxes, whereas PAHs with a higher ring number were not detected in the RS at shorter timesteps or had higher orders of magnitude differences between matrices (e.g. membrane flux for BaP at 24-h was three orders of magnitude higher than the RS flux). The membrane flux was higher than the RS flux most likely due to HMW PAHs favouring partitioning into lipid medias such as skin/membranes (Swartjes, 2011).

The total flux was predominately contributed by the membrane flux, this shows that the membrane is likely to be acting primarily as a sink but also a slow-release source for dermally absorbed HMW PAHs in soils. This suggests that to obtain a comprehensive assessment of the dermal risk from HMW PAHs in soils, the

membrane and RS should be assessed to address for the potential future PAH release from the membrane when acting as a source for the RS. PAHs with the highest membrane fluxes at 1-h after Fla and Pyr did not follow the trend of increasing flux with increasing ring number. This suggests that the ring number might not be a dominant factor for desorption rate of HMW PAHs from soils into membranes at shorter timesteps. However, the 5-ring and 6-ring PAHs penetration rates decrease with increased timesteps compared to the 4-ring PAHs.

4-ring Fla and Pyr consistently showed the highest fluxes in both the membrane and RS, regardless of the sample or exposure time or concentration. This result is similar to previous dermal studies which reported higher desorption of lower molecular weight (MW) PAHs in the EPA16 PAHs from soils (Hu and Aitken, 2012). Alalaiwe et al. (2020) found Pyr to have the greatest flux across pig skin in an *in vitro* skin permeation experiment, further supporting its high dermal absorption potential. However, the relative fluxes of Fla and Pyr differed between our study and Alalaiwe et al. (2020) who used an aqueous vehicle instead of soil. This difference is most likely due to the soil matrix effect, which decreases fluxes compared to aqueous media (Wester et al., 1990).

The higher fluxes for Fla and Pyr are concomitant with their physicochemical properties, including their 4-ring structure (smallest among HMW PAHs), low MW, lower boiling points, higher vapor pressures, higher water solubilities, higher Henry's Law constants, and lower Log K_{ow} values. In summary, smaller, lighter more volatile HMW PAHs appear to promote rapid dermal absorption from soil into both the membrane and RS. Other 4-ring PAHs (BaA, Chry and BcFlu) also showed faster dermal absorption compared to higher ring number PAHs.

5-ring PAHs BbF, BaP, and BeP showed lower RS fluxes compared to the 4-ring PAHs, and their membrane fluxes decreased with increased exposure time. This suggests that the larger ring structure hinders their initial diffusion through the membrane into the RS but potentially results in increased flux to RS over time. BeP exhibited the highest membrane fluxes compared to BaP and BbF, which may be attributed to its lower vapor pressure, water solubility, and Henry's Law

constant. On the other hand, HMW PAHs with opposing physicochemical properties to the 4-ring PAHs, such as CCP, DahA, DaIP, DaiP, DahP, and DaeP, exhibited the lowest fluxes or were <LOQ in either the membrane or RS. These findings suggest a strong influence of PAH physio-chemical properties on dermal absorption.

6.5.2 HMW alkylated PAH dermal flux

The MGP samples showed similar alkyl-PAH behaviour where increases in the alkyl chain size decreases dermal absorption. A cut-off point was observed between one and two alkyl groups for Fla/Pyr compounds, where alkyl-PAHs with >1 alkyl chain were not detected in RS or membranes. Notably, C1-Fla/Pyr exhibited some of the highest RS and membrane fluxes among all PAHs, surpassing most parent PAHs except for Fla and Pyr. Addition of an alkyl chain on BaA/Chry/TPh seemed to inhibit dermal absorption. This is shown by measuring flux for the 5-ring parent compounds (BaA, Chry, and TPh) while their corresponding alkylated derivatives were not detected in H16 membranes or any of the RS samples. This suggests that increasing the alkylated chain for alkyl-PAHs decreases the PAH ability to desorb from the soil into the membrane and will only reach the membrane at longer timesteps.

The control reference soil study utilising the CRM BCR-524 has previously been employed to investigate BaP desorption (Posada-Baquero et al., 2022) and enabled comparison with Lort (2022). BCR-524 flux measurements show additional alkyl-PAHs compounds other than C1-Fla/Pyr were detected in the RS compared to the MGP samples. BCR-524 contains lower PAH concentrations than MGP soils despite the observation that concentration seems to relate to higher flux values in real-world soils. Possible reasons for this include a different contamination source than MGP soils and/or factors such as soil properties and the presence of other PAHs influencing the dermal absorption of alkyl-PAHs from soils (Madrid et al., 2022, White and Pignatello, 1999). Creosote is known to have a large number of alkylated compounds (Gallacher et al., 2017c) which can effect solubility through co-solvency, which would support the increased presence of alkyl-PAHs within the dermal experiments with BCR-524. The differences in detecting other alkyl-PAHs in BCR-524 compared to the MGP soils suggests different contamination sources or matrix effects have different

dermal absorption behaviours for alkyl-PAHs. These results suggest that soils contaminated by sources with numerous alkyl-PAH species might increase the dermal absorption of alkyl-PAHs.

6.5.3 PAH physicochemical properties and initial soil concentration influences

RS flux decreased with increasing Log K_{OW} and PAH MW, this direction of relationship between MW and flux is in agreement with other research (Humel et al., 2017, Wang et al., 2021). PAHs with lower vapor pressures generally showed lower fluxes, however several PAHs with similar Log K_{OW} and PAH MW values exhibited varying RS fluxes, prompting an investigation into the initial soil concentration as a confounding variable affecting flux. Initial PAH concentrations in soils presented in Figure 32 appear to play a role in PAH diffusion by creating a concentration gradient at the membrane surface for only a few PAHs (predominately Fla and Pyr), shown in **Error! Reference source not found.** Figure 39 Considering Fick's Second Law of diffusion in Equation 9.

$$J = -D \frac{\delta C}{\delta x}$$

Equation 9. Fick's Second Law of diffusion.

Whereby δC is the concentration gradient, J is the flux, δx is the travelled distance and D is the diffusion coefficient (Crank, 1979). The results in Figure 39 suggest that higher soil concentrations provide a larger driving force for PAH diffusion, leading to increased fluxes for several PAHs (Yu et al., 2018, Barnier et al., 2014). However, the majority of HMW PAHs did not show a trend, this suggests that other factors such as PAH physicochemical properties, PAH sources and soil properties are likely influences. 1-h RS fluxes were the highest among the other exposure times for the soil A11 with the lowest PAH concentrations. The causations of the different RS fluxes at different timesteps between soils with high and low initial PAH concentrations is difficult to interpret without further experimentation. One possible explanation is that soils with a lower concentration have lower absolute PAH to soil mass ratio. Previous studies have reported strong influences of PAH concentrations increasing the

dermal absorption or flux (Forsberg et al., 2021, Stroo et al., 2005). In addition, supersaturated soils containing free PAHs are unable to help research determine the impact of soils properties on PAH release from soils, as these freely available PAHs as are not impacted by soil (Roberts and Walters, 2007). However, Xia et al. (2016) reported that PAH dermal fluxes could not be explained by the PAH concentration differences in soils, but they did determine a strong positive correlation to freely dissolved PAH concentrations in soils. Our study shows that the relationship between RS fluxes and initial soil concentration varied among the MGP samples. This suggests that, like Xia et al. (2016), other factors, such as PAH properties, PAH mixtures and soil properties, influence dermal absorption more strongly than concentration.

6.5.4 Comparison to other studies

We compared our BaP flux data with a range of other dermal studies including: Moody et al. (2007), Peckham et al. (2017), Roy and Singh (2001), Lort (2022), Wester et al. (1990). Overall, our BaP fluxes fell within the lower reported ranges. Membrane fluxes showed no statistically significant differences (p -values >0.05) using the Wilcoxon signed rank test between our study and Lort (2022) using a similar dermal *in vitro* method in the same laboratory. Lort (2022) investigated three parent HMW PAHs (BaP, Pyr and DahA) with eight timesteps in two MGP soils and BCR-524. Lort (2022) concluded that his method provided results in agreement with other published work, establishing its appropriate use for comparisons for PAH absorption in *in vitro* human dermal experiments and hence the method was improved and applied in this research. Differences in soil properties, soil moisture content (SMC%) (Hu and Aitken, 2012, Kottler et al., 2001), and analytical methodologies can account for the variations in fluxes observed between studies. Our study demonstrated lower dermal fluxes for real-world MGP soils compared to studies using spiked soils (Wester et al., 1990), indicating the impact of soil properties and sources of PAHs, such as bulk organic matter properties on fluxes.

Risk assessment guidance on the dermal exposure of PAHs from soils (Environment Agency, 2009b) is currently based on Wester et al. (1990), which showed that 13% of the BaP dose applied is bioavailable using an *in vivo monkey* model. Spalt et al. (2009) calculated the average uptake flux using Wester et al.,

data to be 2.2 ng/cm²/h for 24-h. However, Wester et al. (1990) collected urine for a total of 7 days, producing a lower flux (0.31 ng/cm²/h) closer to the RS fluxes for BaP measured in our study (which mimic PAH uptake into the systemic circulation within 24-h). The higher membrane fluxes in our study suggest the membrane may be acting as a sink and then a source. Other studies have shown that BaP in the membrane have the potential to diffuse slowly into RS over time (Stroo et al., 2005, Barnier et al., 2014). PAHs remaining in the skin after soil removal pose potential risks to human health, due to potentially absorption into the systemic circulation later or causing localised health problems to skin (skin tumours). Previous studies (Kennaway, 1955, Cavalieri and Rogan, 2014, Siddens et al., 2012) have identified PAHs as skin carcinogens, hence the presence of PAHs remaining in the membrane is a potential health risk. This is supported by Forsberg et al. (2021), who showed continued absorption and diffusion of BaP from skin after soil removal suggesting the possible risks from PAHs remaining in skin.

Forsberg et al. (2021) also showed influence of weathering, biodegradation, and aging on PAH desorption from soils. Roy et al. (1998) determined that soil hinders the dermal flux rates by a factor of 160-900 compared to dermal experiments with PAHs from soil extracted solutions. This supports our findings of low fluxes with field-contaminated soil. Roy et al. (1998) measured higher BaP fluxes in their *in vitro* study than our study. This is assumed to be because Roy et al. (1998) calculated fluxes factoring the recovery of the spiked ³H-BaP in each matrix rather than individual PAH released from real-world contaminated soils. The use of spiked PAHs in studies can overestimate dermal fluxes as compared to real-world soils, as PAHs undergo various transformations in natural environments (Barnier et al., 2014, Umeh et al., 2019b, Stroo et al., 2005). Studies investigating the role of PAH sources (Xia et al., 2016) in dermal fluxes and soil properties in bioavailability studies (Cipullo et al., 2018) have indicated their significant impact on PAH release from soils. Soot, char, and other black carbon sources present in MGP soils can sequester PAHs and decrease their release, thereby affecting dermal absorption (Ruby et al., 2016, Umeh et al., 2019b). Our study shows lower 24-h RS fluxes than other dermal

studies measured, with differences between samples, potentially highlighting the influence of soil properties and PAH sources on fluxes.

6.5.5 Future work and implications

There are several limitations in this study that could be addressed in future research.

The study measured dermal absorption of PAHs from a limited number of MGP samples (n=5). It is recommended that future work uses a larger sample set including end member materials such as coal tar, Chapter 5 highlighted the diversity of PAHs measured between different MGP sites with varying contamination histories and extend the different sources.

This study was able to fully analyse one MGP sample membrane fluxes at three timesteps, with results suggesting that the membrane accounts for the majority of PAH dermally absorbed from soil. A larger dataset on dermal flux from soil to membrane could be created as part of a wide range of *in vitro* experiments.

Three timesteps were investigated in this study to demonstrate the proof-of-concept of the enhanced *in vitro* dermal absorption experiment. Further research might increase the number of timesteps incorporated for both early stages and extension of the longest timestep.

BCR-524 was considered a useful proxy reference material in the absence of a formal dermal CRM. The use of BCR-524 showed that a larger number alkyl-PAHs were present in the RS than the MGP samples. This suggests that the contamination source may impact the release of PAHs, and therefore future work investigating soils contaminated by other anthropogenic sources would help identify the impact of contamination sources on dermal absorption.

Extending the research to account for the uncertainties in this study would help build a more comprehensive understanding of the PAH diffusion rates from soil to membrane and then RS for a range of parent and alkylated PAHs. The physicochemical properties of PAHs and the initial soil concentrations appear to influence the RS fluxes to some extent, but other factors, including PAH mixtures, source materials, and soil properties, also impact dermal absorption.

Notwithstanding these limitations the experiments presented here highlighted a variety of novel findings, including the high fluxes associated to C1-Fla/Pyr at longer timesteps. C1-Fla/Pyr is potentially a unidentified health risk, since alkyl-PAHs are expected to be as toxic or of greater toxicity than their respective parent compounds (Meador, 2008, Richter-Brockmann and Achten, 2018, Fallahtafi et al., 2012). The specific individual alkylated compounds present in the calculated C1-Fla/Pyr flux remain unknown, as this study analysed the total concentrations of alkylated compounds in a homologue series. Additionally, more exotic parent PAHs dermal bioavailability were explored, including BcFlu, which has a TEF of 20. This indicates a carcinogenic potential about 20 times that of BaP (Richter-Brockmann and Achten, 2018) and therefore the higher fluxes experienced in E1.5 and H16 samples from BcFlu could be a significant risk, as BcFlu was dermally absorbed into both the membrane and RS.

6.6 Conclusion

This study utilised an *in vitro* method to examine the dermal fluxes of HMW parent PAHs and, for the first time, HMW alkylated PAHs extracted from five real-world MGP soils. The results revealed that the PAHs with lower molecular weights exhibited higher dermal flux, particularly in the case of Fla and Pyr, including the alkylated C1-Fla/Pyr. Alkylated PAHs are suspected to be equally or more toxic than their parent compound counterparts which poses a potential risk to human health due to their high dermal fluxes compared to heavier PAHs. Membrane fluxes were found to be higher than the RS fluxes, indicating that the membrane acted as a sink and then a source for PAHs released from soils, driving delayed diffusion of HMW PAHs from the membrane into the RS. Consequently, HMW PAHs that diffused more slowly through the membrane had the potential to reach the RS (a proxy for human systemic circulation) at later timesteps, potentially greater than those measured in this study. A comprehensive assessment of dermal risk from PAHs in soils should consider the PAH content in both the membrane and the RS to assess the prolonged release from skin into systemic circulation.

Our study highlights the variations in PAH absorption between PAH mixtures in real-world contaminated soils, with the initial soil concentration and the

physicochemical properties of PAHs potentially influencing HMW PAHs dermal fluxes. This research demonstrated that real-world contaminated soils exhibited lower fluxes than studies using spiked soils. These findings have important implications for decision-making processes in the fields of environmental remediation, land management, consultancy, and regulation, as they contribute to key uncertainties in the human health risk assessment associated with chronic exposure to carcinogenic chemicals in soils found in contaminated brownfield sites. We recommend further study of the membrane as a sink and source of PAHs, investigating larger soil subsets with a wider range of properties and their influences on both RS and membrane PAH fluxes.

Chapter 7 Effect of bulk organic matter from Rock-Eval(6) Pyrolysis and particle size on dermal absorption of high molecular weight parent and alkylated polycyclic aromatic hydrocarbons in Manufactured Gas Plant soils

Alison M. Williams-Clayson^{1,2}, Christopher H. Vane¹, Matthew D. Jones², Russell Thomas³, Christopher Taylor⁴, Darren J. Beriro^{1*}

*corresponding author

¹ British Geological Survey, Keyworth, Nottinghamshire, UK; ² University of Nottingham, Nottingham, UK; ³ WSP UK, Bristol, UK; ⁴ National Grid, Warwick, UK

Research yet to be submitted for publication.

Statement of Contributions of Joint Authorship

Williams-Clayson, A: (Candidate):

Undertook the experimental analysis as previously stated in the above papers. Conducted the statistical linear regression analysis and wrote the manuscript. Took the lead role in all writing taking responsibility of drafting and revising manuscript and first author on paper.

Vane C., Beriro, D.; Jones, M.; Thomas, R.: (Supervisors):

Supervised and provided feedback and helped shape the research project and manuscript.

Taylor, C.: (Industrial Supervisor):

Provided site access for sampling, information regarding sites and feedback on manuscript.

7.1 Abstract

This study investigates the relationships between bulk organic matter (OM) characterised by Rock-Eval(6) Pyrolysis (RE) and particle size analysis (PSA) upon the dermal bioavailability of high molecular weight (HMW) PAHs from contaminated manufactured gas plant (MGP) soils. Linear regression between the soil properties and the dermal fluxes of both parent and alkylated HMW PAHs from soil into receptor solution (RS) (measured using *in vitro* dermal experiments) were examined. The resultant relationships showed that HMW PAHs with the highest fluxes displayed strong associations with specific RE parameters, S1, S2, PC%, HI, I-index, R-index, and the silt size fraction percentage.

Nevertheless, it becomes evident that these relationships are primarily driven by a solitary sample characterised by notably elevated PAH concentrations and bulk OM values. However, the application of RE as a technique to characterise contaminated soil holds promise as a screening tool to facilitate estimating dermal exposure risks from soils. MGP soils had high RC% values demonstrating high proportions of soil thermally refractory OM. The R-index values in MGP soils were particularly extensive and demonstrated significant negative relationships with RS fluxes for an array of HMW PAHs. However, further MGP soils dermal flux relationships with the R-index are needed to strengthen this estimate. The research provides future recommendations for further advancements in the understanding of soil-mediated impacts on the dermal bioavailability of PAHs, thus contributing to the overarching body of knowledge in this domain.

7.2 Introduction

Polycyclic aromatic hydrocarbons (PAHs) are a class of persistent harmful organic pollutants primarily formed by incomplete combustion processes such as fossil fuel combustion, natural wildfires and industrial activities. Former manufactured gas plant (MGP) sites have historically generated various waste by-products, including crude tar, oil tar, coal, char, soot and pitch, which serve as sources of various quantities and types of PAHs (Thomas, 2014). By-products from MGPs with limited markets were sometimes disposed of on-site (Thomas, 2014), resulting in elevated concentration of PAHs at MGPs, encompassing of

both parent and alkylated PAHs. High molecular weight (HMW) PAHs known for their prolonged persistence in soils due to low vapor pressures and limited water solubilities, manifest in varying concentrations at these sites (Nathanail et al., 2015, Beriro et al., 2016).

The repurposing of brownfield sites, like former MGP sites, for alternative use offers environmental and societal benefits (Rankl, 2023, Thomas, 2023). However, the potential risks to human health from PAHs in soils necessitate rigorous assessment and suitable remediation strategies. Human exposure to PAHs can occur through inhalation, ingestion and dermal contact. Dermal exposure has received relatively limited research attention compared to other routes (Beriro et al., 2016, Ruby et al., 2016, Spalt et al., 2009). With regards to the total contributions of the three exposure pathways, the dermal pathway is the second highest contributor HMW PAHs owing to their physicochemical properties (Nathanail et al., 2015)(Chapter 6). Dermal bioavailability refers to the fraction of PAHs in soil that are released and penetrate the skin, potentially entering systemic and lymphatic circulation (Riding et al., 2013). This definition of bioavailability addresses localised skin health effects and can account for PAHs that persist within the skin, gradually diffusing to the systemic and lymphatic circulation, aspects that have often been overlooked in prior studies (Beriro et al., 2016, Ruby et al., 2016).

The factors governing dermal bioavailability are complex and multifaceted, encompassing effects from physicochemical attributes of PAHs (James et al., 2011), competition effects within PAH mixtures (Ruby et al., 2016), as well as, different PAH contamination sources (Xia et al., 2016, Yu et al., 2018, Duan et al., 2014). Previous investigations into soil-property influences on bioavailability have predominantly employed spiked soils, which have been reported to overestimate PAH release from soil compared to real-world contaminated soils, due to the absence of weathering, biodegradation and aging processes (Barnier et al., 2014, Duan et al., 2015, Chung and Alexander, 1998). Despite extensive research on soil properties' influence on the oral pathway (James et al., 2016, Duan et al., 2014, Cave et al., 2015); investigations into soil properties influences on the dermal bioavailability remain relatively sparse (Ruby et al., 2016, Beriro et al., 2016). The few studies exploring soil properties'

impact on dermal absorption have considered factors such as soil vs. solvent, PAH sources, and the presence of specific organic, carbonaceous and mineral fractions (Wester et al., 1990, Xia et al., 2016, Kadry et al., 1995, Turkall et al., 2010, Stroo et al., 2005, Peckham et al., 2017).

A majority of studies have proposed that the organic fraction of soil plays a dominant role in governing PAH sorption and release (Yu et al., 2018, Ehlers and Loibner, 2006, Chen et al., 2007). Some studies have even proposed overlooking mineral content in soils if organic matter (OM) content exceeds 0.1% (Pan et al., 2006). The continuum of soil OM (SOM) spans from biomass to charred biomass, charcoal, and soot; with the quantity and quality of OM significantly influencing the desorption behaviour of PAHs (Poot et al., 2014, Oen et al., 2006). A dual-mode sorption model has been proposed, categorising SOM into "hard" and "soft" OM fractions, each possessing distinct adsorption potentials (Xing and Pignatello, 1997, Poot et al., 2014, Crampon et al., 2014). Within this framework, rigid carbonaceous "hard" organic carbon (OC) with aromatic enrichment is correlated with robust adsorption and slower non-linear PAH desorption. Examples include black carbon (BC), coke, and kerogen. In contrast, labile gel-like "soft" OC with aliphatic dominance facilitates rapid and linear desorption, examples include amino acids, lipids and oils (Pehkonen et al., 2010, James et al., 2016, Luthy et al., 1997). This model has been exemplified by the heightened bioavailability of PAHs from semi-solid coal tar pitch compared to carbonaceous particles such as coal and charcoal (e.g. coal, coke and charcoal) (Ghosh et al., 2003); likewise, PAH loss diminishes in PAH source materials in the order of solvent > fuel oil > soot > skeet (Xia et al., 2016).

Recently, Rock-Eval(6) Pyrolysis (RE) has emerged as a screening tool for characterising diverse forms of OM, encompassing both natural and anthropogenic carbon sources (Könitzer et al., 2016, Upton et al., 2018, Poot et al., 2014, Lafargue et al., 1998, Garcin et al., 2022b) RE quantifies hydrocarbons, CO and CO₂ emissions in response to the increasing temperature versus time throughout pyrolysis and oxidation stages (Behar et al., 2001b, Lafargue et al., 1998). This simple, relatively quick technique offers valuable insights into bulk OM composition by providing a variety of multiple RE parameters in a single measurement. Thus, RE has potential implications for

determining OM relationships with the dermal bioavailability of PAHs from soils. To our knowledge only one other paper (Haeseler et al., 1999) and my research has applied RE to MGP soils, but this former study did not explore the relationship between RE parameters and PAH dermal bioavailability. Poot et al. (2014) recommended that the RE parameter measuring residual carbon (RC) is relevant for characterising PAH release from sediments using Tenax extractions. The complex relationships between RE parameters characterising bulk OM and the parameters prospective influence on dermal flux of HMW PAHs determined from previous literature are summarised in Table 20.

Table 20. RE parameters relation to bulk OM in soils and the potential influence these variables can have on the release and dermal bioavailability of HMW PAHs in soils based on previous studies.

RE Variable	RE variable in relation to soil	Estimated Implication on HMW PAH Dermal Flux
S1 (HC mg/g)	S1 quantifies the amount of free hydrocarbons released at lower pyrolysis temperatures < 200 °C. It includes the release of small low molecular weight (LMW) volatile hydrocarbon compounds (Carrie et al., 2012, Disnar et al., 2003). S1 is usually minor in soils given humification increases the amounts of natural OM macromolecules, such as humin which requires higher cracking temperatures (Disnar et al., 2003). High S1 values indicate contamination from sources releasing smaller hydrocarbon compounds (e.g. PAHs) and weaker single C bonds compounds (e.g. alkanes) (Haeseler et al., 1999), Chapter 5 reported that MGP processes utilising oils reported the highest S1 values.	It is estimated that high S1 values will indicate a high level of PAH contamination from the MGP soils, therefore creating a steeper dermal PAH diffusion gradient causing increased dermal fluxes.
S2 (HC mg/g)	S2 quantifies the amount of bound (heavy and non-volatile) hydrocarbons released in a wider temperature range of 200-650 °C. Multiple peaks or a primary peak with a shoulder are generated in pyrograms of S2, due to the response of different biopolymers with different intra and inter polymer bond strengths requiring different temperatures to break aromatic C-C bonds (Newell et al., 2016). High S2 values can result from natural OM compounds (e.g. cellulose, xylans, lignin, kerogen and geopolymers like humic acids (Kemp et al., 2017) and/or anthropogenic OC (e.g. BC).	The correlation between S2 and dermal fluxes is complex, as high S2 values may indicate large concentrations of complex natural geopolymers and/or anthropogenic macromolecules capable of PAH entrapment. Or high S2 values may indicate large proportions of non-PAH-bound OC resulting with no correlation.

TpkS2 (°C)	The TpkS2 temperature provides insight into the type of OM that is predominant in the soil. Higher temperatures indicate larger macromolecules or compounds with increased thermally stable bonds (Newell et al., 2016). For natural soils, higher TpkS2 temperatures are reported for the lower soil horizons compared to upper soil layers due to the breakdown of immature humic substances (Disnar et al., 2003). MGP soils are expected to have varying TpkS2 temperatures dependant on the amounts of different anthropogenic materials present. Whereby high TpkS2 temperatures are associated to BC and coal, and low TpkS2 temperatures are associated to oil spill contamination.	Lower dermal fluxes are estimated for higher TpkS2 temperatures due to high proportions of OC (“hard”) capable of PAH entrapment structures which subsequently decrease PAH release from soil.
TOC% (%)	The total organic carbon (TOC%) represents carbon moieties (HC, CO, and CO ₂) from both natural and anthropogenic sources. Higher TOC% in soils indicate high amounts of OC, but does not distinguish the type of OC.	The dermal flux relationship with TOC% has the potential to vary depending on the type of OC. High TOC% may indicate high proportions of OC with the ability to entrap PAHs reducing dermal flux or OC with low/no affinity toward PAHs resulting with no correlation to dermal fluxes.
PC% (%)	The PC% value indicates the pyrolysable carbon yielded during the pyrolysis stage, including both natural and anthropogenic sources. Haeseler et al. (1999) concluded that pyrolysed hydrocarbons released ≤ 350 °C corresponded to 35-50% aromatic compounds including PAHs in MGP soils.	Higher PC% in contaminated soils could estimate the PAH contamination level and potentially lead to increased PAH desorption and flux.
RC% (%)	The RC% is residual carbon composed of thermally resistant OC that remains after pyrolysis and is combusted in the oxidation stage. Increased RC% means increased amounts of carbonaceous materials which PAHs can reside in, causing PAH release to become slow (Poot et al., 2014).	Increasing the RC% is estimated to decrease freely available PAHs desorbed from the soils, resulting in lower dermal fluxes (Poot et al., 2014).

HI (mgHCg⁻¹ TOC)	The hydrogen index (HI) measures the extent of hydrogenation, with high HI values indicating increased amounts of hydrogen-rich compounds (e.g. polysaccharides or <i>n</i> -alkanes from oils) and low HI values suggesting dehydrogenated and aromatic structures (BC and humic compounds) (Saenger et al., 2013, Brown et al., 2023).	Lower HI values are expected to correlate with lower dermal fluxes due to high amounts of compounds with high degrees of carbonisation, capable of entrapping PAHs. Or low HI also suggest higher PAH concentrations in soils creating a steeper diffusion gradient and higher flux.
OI (mgO₂g⁻¹ TOC)	The oxygen index (OI) corresponds to the released amounts of oxygen from CO and CO ₂ relative to TOC. Lower OI values indicate lower amounts of oxygen species and increased amounts of hydrocarbon compounds. MGP soils are estimated to have low OI values, as coal tar is 5% oxygen and inorganics, compared to 86% carbon (Thomas, 2014).	Lower OI values are predicted to have increased amounts of hydrocarbon compounds with high degrees of carbonisation (Luo and Agraniotis, 2017) capable of entrapping PAHs and decreasing fluxes.
I-index	The immature OM index (I-index) is calculated using the lower temperature fractions from S2 and represent the more thermally labile OM (Brown et al., 2023, Garcin et al., 2022b, Girkin et al., 2019).	Higher I-index values are expected to correlate with higher dermal fluxes as the soil will have larger proportions of labile OM containing available PAHs.
R-index	The refractory OM index (R-index) is calculated using the higher temperature fractions from S2, representing more thermally refractory OM (Brown et al., 2023, Garcin et al., 2022b, Girkin et al., 2019).	Higher R-index values are expected to correlate with lower dermal fluxes, as refractory OM may have complex structures that can entrap PAHs and hinder their release (Xing and Pignatello, 1997).
S3 (mg CO₂/g)	Variable measures the CO ₂ produced during pyrolysis for organic and/or mineral source.	No significant relationship between flux and these variables has been estimated.

In this study, we investigated the influence of specific soil properties on the dermal bioavailability of parent and alkylated HMW PAHs in soil samples, including five MGP soils and the certified reference material (CRM), BCR-524. The methodology integrates Rock-Eval(6) Pyrolysis (RE) for bulk OM characterisation, particle size analysis (PSA) on particles with sizes <250 µm, and gas chromatography-tandem mass spectrometry (GC-MS/MS) for HMW PAH quantification (previously reported in Chapter 5). Dermal absorption measurements taken from Chapter 6, included the dermal fluxes of membrane and predominately receptor solutions (RS) which served as an indicator of realistic systemic and lymphatic circulation exposure. This study encompasses exposure timesteps of 1-hour, 10-hours, and 24-hours, mirroring maximum human exposure times for real-world scenarios and allowed for results to be compared to other dermal studies (often 24-hours). Employing real-world contaminated soils facilitates the replication of authentic scenarios, thereby mitigating the potential overestimations observed in spiked soil studies (Lort, 2022).

The objective of this study was to identify the key soil properties influencing the dermal bioavailability of both parent and alkylated HMW PAH using the RS flux. Attainment of this objective, aims to advance the understanding of PAH dermal exposure pathways from contaminated soils, consequently improving risk assessment methodologies, and guide evidence-based decision-making for managing PAH-contaminated sites. The combination of bulk OM screening through RE and *in vitro* dermal absorption methods is expected to contribute valuable insights into the intricate relationships between soil properties and HMW PAH dermal bioavailability, ultimately contributing to the knowledge base for protection of human health and the environment.

7.3 Methodology

7.3.1 Sample collection and *in vitro* dermal experiments

Soil samples selected for this study were previously described in detail in our preceding publications (Chapter 5 and 6). Gas chromatography-tandem mass spectrometry (GC-MS/MS) was utilised to measure HMW parent and alkylated PAHs concentrations within the dermal matrices (soils, membranes, and receptor

solution (RS)). The GC-MS/MS analytical method is reported in Chapter 5 and Appendix B Chapter 5 Research Papers SI.

Chapter 6 provides a comprehensive account of the *in vitro* experiments (method developed from Lort (2022)), extraction and analytical techniques. In summary, 1.0 g of moistened soils (soil moisture content 25% wt:wt%) was applied to synthetic membranes (Strat-M) with a surface area of 8.55 cm². Membrane-soil assemblies were subsequently placed into Franz glass diffusion cells containing ~33 mL of RS. The formulation of RS employed Hank's Balanced Salt Solution (HBSS) (ThermoFisher Scientific), Bovine Serum Albumin (BSA) (Merck Life Science UK Ltd.) and the buffering agent HEPES (ThermoFisher Scientific). The diffusion cells were maintained in water baths set at 32 °C for specified timesteps (1-hour, 10-hours, or 24-hours). Following exposure, PAHs in the dermal matrices were extracted and quantified (refer to Chapter 6). The quantification of dermal fluxes (J) (expressed as ng/cm²/h) was accomplished through Equation 8.

7.3.2 Soil properties – Rock-Eval(6) Pyrolysis and Particle Size Analysis

Organic matter soil properties were measured using Rock-Eval(6) Pyrolysis (RE) (Vinci Technologies). Detailed information on the RE operating conditions and parameters measured in this study can be found in Chapter 5. For particle size analysis (PSA), the previously sieved soils (<250 µm) underwent digestion with 30% w/v hydrogen peroxide (H₂O₂) to eliminate OM, until excessive bubbling had diminished (Mikutta et al., 2005). Digested soils were washed with milli-Q water and Calgon solution (comprising 35g of Sodium hexametaphosphate and 7g of sodium hydrogen carbonate in 1 liter of water) added to hinder aggregation (Kaur and Fanourakis, 2018). Particle size analysis (PSA) was measured using a Beckman Coulter LS 13 320 Particle Size Analyser. PSA was not measured on the BCR-524 CRM PSA because as the sample was received pre-ground to < 125 µm.

7.3.3 Statistical analysis

R Statistical Software (R Core Team, 2023) was utilised for data evaluation, statistical analyses, and simple linear regression. Simple linear regression was

used to evaluate the relationships between the soil properties and HMW PAH fluxes at the distinct timesteps.

7.4 Results

7.4.1 Rock-Eval(6) Pyrolysis and Particle Size Analysis

The collective results for the RE parameters for the five MGP soils and BCR-524 are depicted in Figure 40. Each soil appears in a separate cluster when 94 MGP soils underwent k-means clustering using ten RE parameters undertaken in Chapter 3.6 shown in Figure 16. Among the MGP soils, soil E1.5, had the highest PAH concentrations and exhibited elevated quantities of OC released during the pyrolysis stages. As indicated by high S1, S2, and PC% values. Conversely, soil I3 displayed the highest TOC% derived from large RC%. Soils A11 and E2.7 shared similar measurements, characterised by lower OC measurements as indicated by S1, S2, TOC, PC%, and RC%, but measured the highest R-index values. However, A11 and E2.7 differed in their OI values, with E2.7 exhibiting the highest OI compared to all other samples. Four of the samples gave TpkS2 temperatures ≥ 460 °C, except for soils H16 and E1.5, which exhibited lower TpkS2 temperatures, implying a higher proportion of OC in these samples undergoing cracking at lower temperatures compared to other soils.

Inspection of the S2 pyrograms showed variation in the type of hydrocarbons released from soils < 650 °C, visually shown in Figure 41. Parameters S1, S2, PC%, the I-index, and R-index are graphically represented within the S2 pyrogram, whereby the R-index and I-index are calculated using the proportions of hydrocarbons released at different temperatures (Girkin et al., 2019). For example, the R-index is calculated from hydrocarbon fractions release between 400-460 °C and > 460 °C. All MGP soils exhibited a characteristic peak between 460-469 °C, representing the TpkS2 temperature for A11, E2.7 and I3. This peak indicates the presence of mature thermally refractory OC, from either natural or anthropogenic origins (Malou et al., 2020, Sebag et al., 2006). Examples of this type of OC include highly humified natural macromolecules (Brown et al., 2023, Saenger et al., 2013, Garcin et al., 2022b), HMW kerogen (Wu et al., 2012), residues of fires (Sebag et al., 2006) or anthropogenic pollutants of BC (e.g. soot, charcoal etc...) (Sebag et al., 2006, Disnar et al., 2003).

Rock-Eval(6) Pyrolysis Variables for Samples

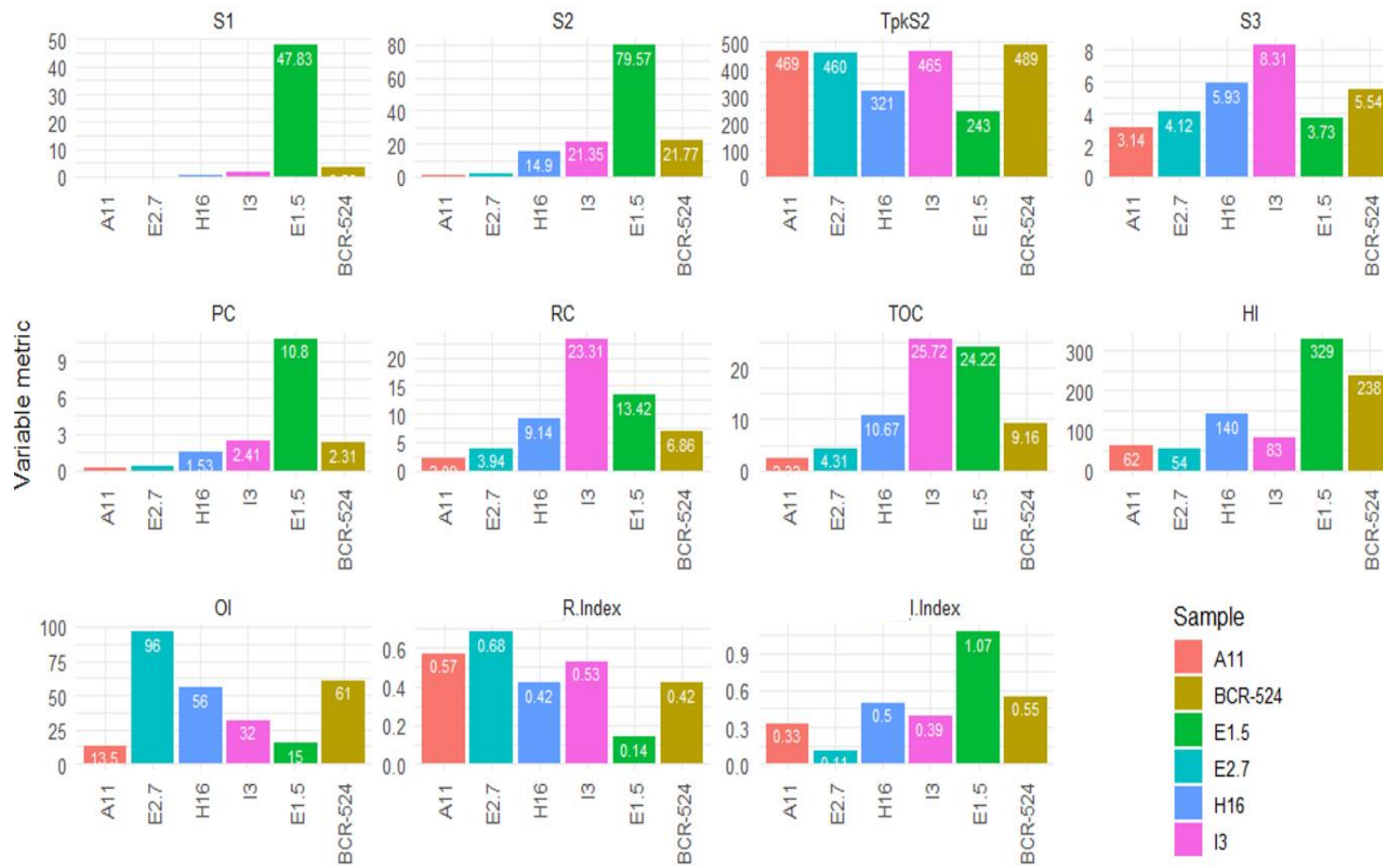


Figure 40. RE parameters for the five MGP soils and BCR-524. Units for each RE parameter displayed on the y-axis are: S1 (HC mg/g), S2 (HC mg/g), TpkS2 (°C), S3 (CO2 mg/g), PC (%), RC (%), TOC (%), HI (mgHCg⁻¹ TOC), OI (mgO2g⁻¹ TOC), and Sebag et al. (2016) R-index and I-index are unitless.

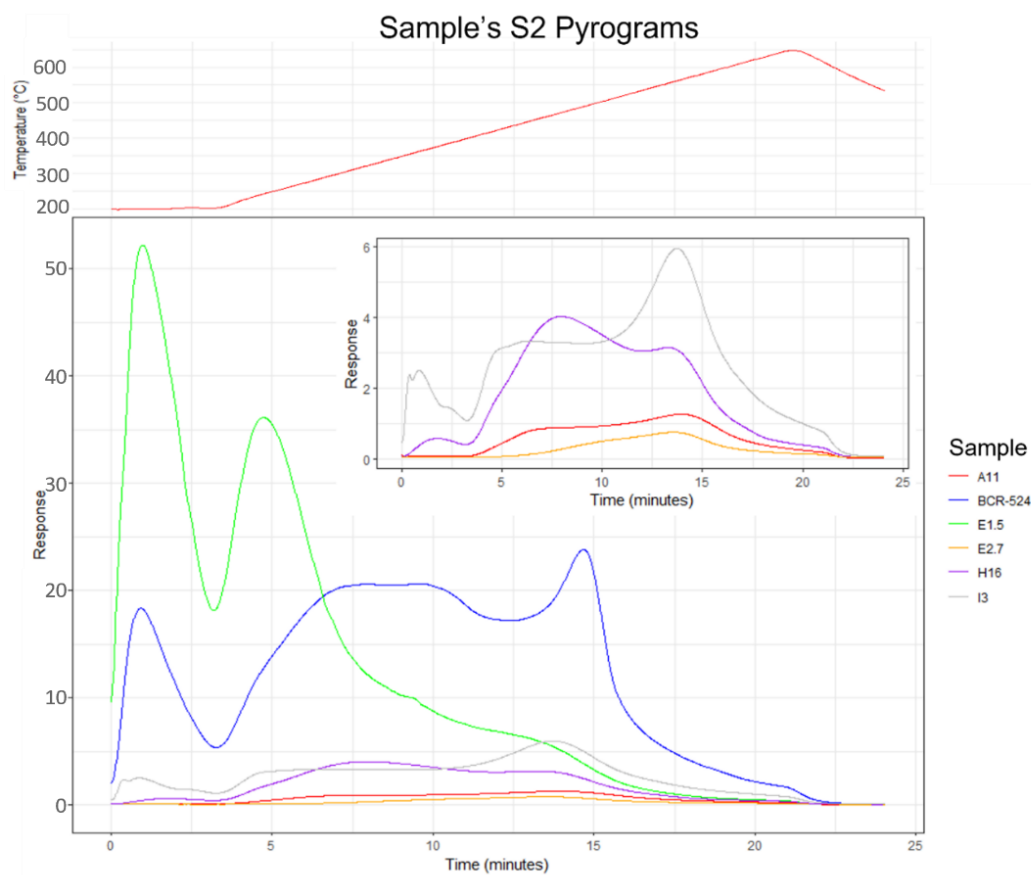


Figure 41. S2 pyrogram of the five MGP soils and BCR-524 sample, the temperature ramping of RE is illustrated in the upper plot corresponding to the plot displaying all samples. Samples with lower responses zoomed in for the inside plot.

Although soil H16 yielded a peak at 460-469 °C, this was not the dominant TpkS2 peak, instead a larger proportion of OC was released at a lower temperature (TpkS2 of 321 °C). This indicated H16 with higher proportions of highly labile carbon than A11, E2.7 and I3 (Malou et al., 2020, Garcin et al., 2022b). Examples of OC within this fraction could either be another form of natural OC (fresh plant material and soil litter) or an anthropogenic OC requiring lower temperatures for cracking (Sebag et al., 2006, Hetényi et al., 2005, Disnar et al., 2003). The CRM also measured a relatively high peak at 321 °C, however, BCR-524 yielded the highest TpkS2 temperature (489 °C) surpassing all the MGP soils TpkS2. This suggests that the BCR-524 sample comprises a substantial proportion of condensed polymers not observed in the five MGP

soils. In contrast, soil E1.5 exhibited prominent peaks at lower temperature ranges, with an especially elevated S1 peak and a TpkS2 peak at 243 °C. While other soils also exhibited hydrocarbon release around 243 °C, their quantities were considerably lower, following the order E1.5 >> BCR-524 >> I3 > H16 > A11; E2.7, however, did not exhibit a distinct peak in this fraction.

Although the employment of H₂O₂ for soil digestion was intended to eliminate OM, studies have indicated the potential for residual OC in the samples to persist after digestion (Mikutta et al., 2005, Harada and Inoko, 1977). MGP soils are likely to have particles of coal, coke soot, scurf or tar which preventing the degrading of the material at the centre of tar particles. Hence, non-inorganic materials may contribute to the particle size of inorganic fractions. Nevertheless, the method provided insights into the particle size distributions present in MGP soils below <250 µm, this size fraction was selected due to being the typical “upper” end size fraction prone to adhere to the skin (Beriro et al., 2016, Forsberg et al., 2021). Particle size fractions (<250 µm) of the MGP soils are illustrated in the particle size distribution triangle in Figure 42. These soils displayed high proportions of particles in the larger size range, with sand and silt fractions accounting for 85-92% of the <250 µm particles. Brownfield soils are typically man made by demolition of pre-existing structures (crushed brick), sand and other anthropogenic materials engineered for buildings and not for plant growth (Jorat et al., 2020). MGP soils are therefore atypical to typical soils, containing narrow PSA distributions and high PAH concentrations. Interestingly the MGP soils particle size fractions were similar to the fractions measured for two background (BG) samples sourced from park location in close proximity to two of the MGP sites (BG mean fractions of clay 13%, silt 41% and sand 46%). The BG soils are suspected to have high proportions of natural macromolecules potentially persistent to soil digestion.

Particle Size Distribution for Soil Fractions <250µm

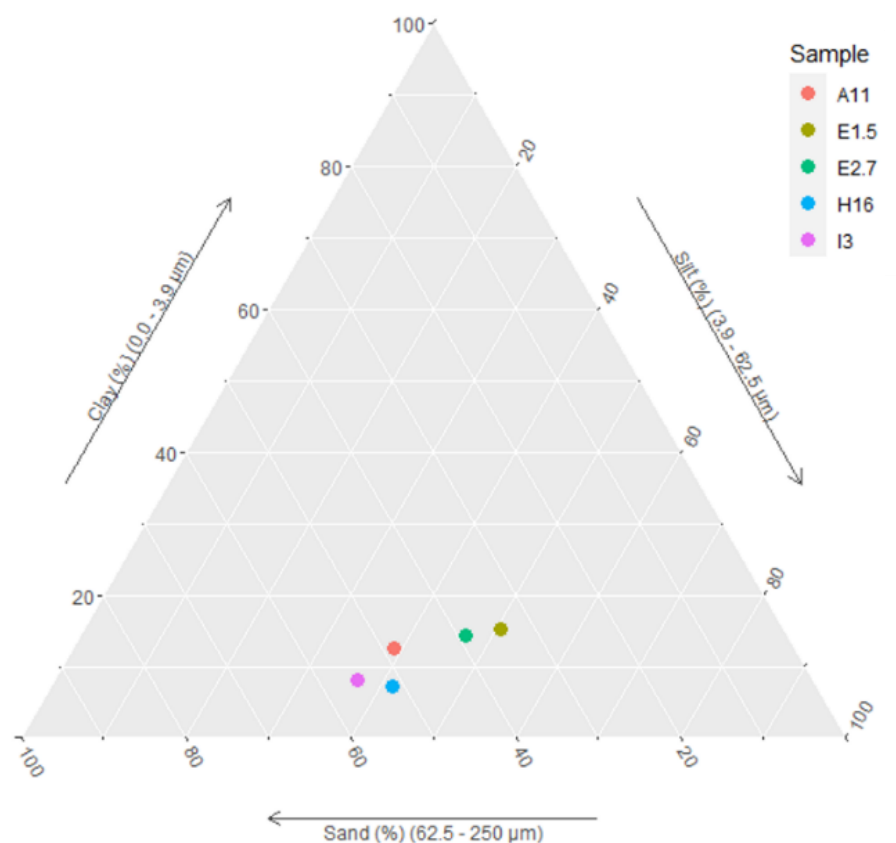


Figure 42. Particle size distribution triangle of the MGP soils, showing percentages of fractions determined with particles <250 µm.

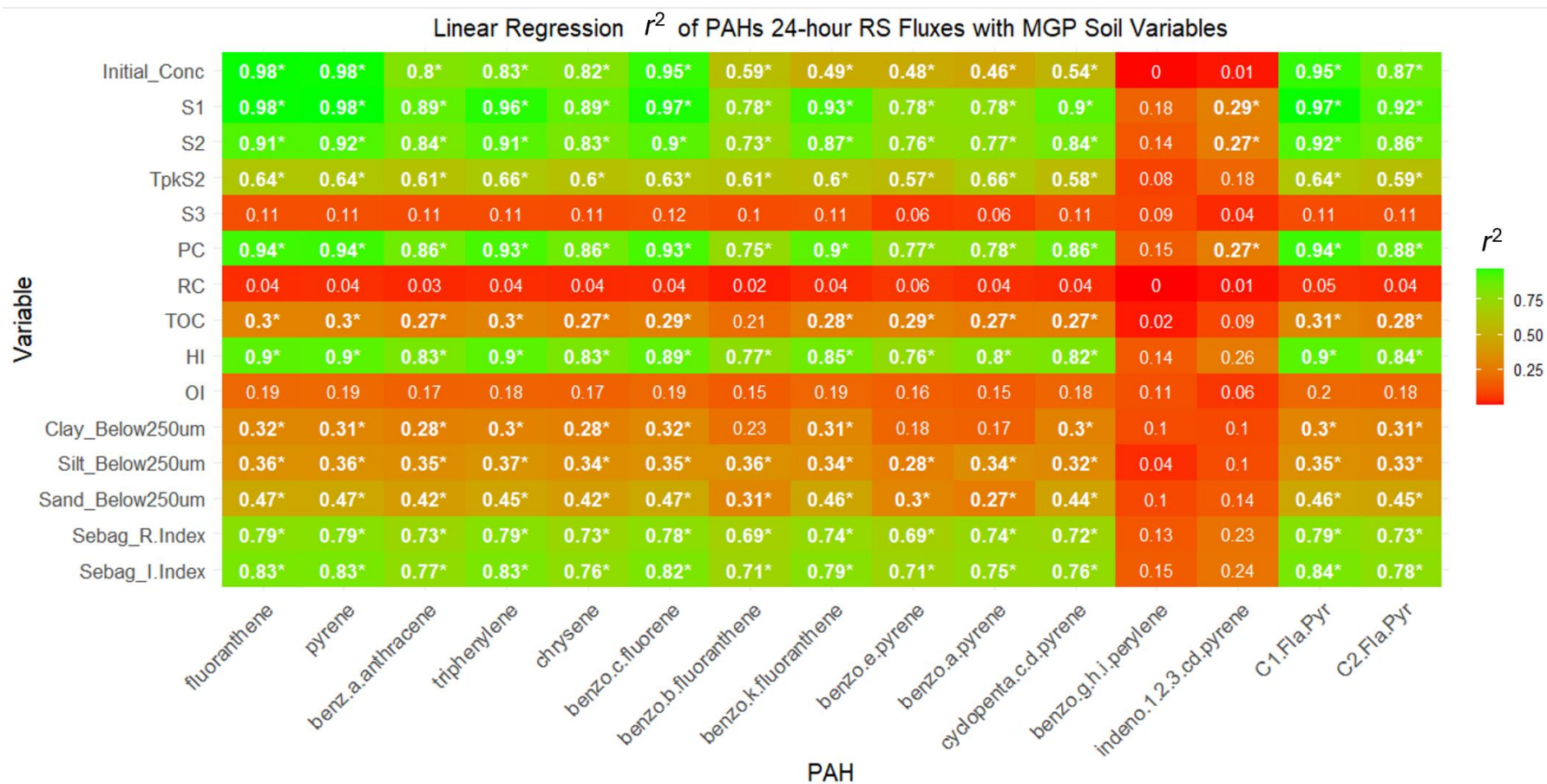
7.4.2 Linear regression between PAH RS fluxes and soil properties

Linear regression analysis between was used to test if the major soil properties for the five MGP soils influenced the HMW PAHs RS fluxes. The r^2 values for all HMW PAHs at the 24-hour timestep are depicted in Figure 43.a and line plots for fluoranthene (Fla) in Figure 43.b. Other regression line plots for alternate timesteps are presented in Appendix D Chapter 7 Research Paper SI Figure S14-S16). Generally, the HMW PAHs with the lowest molecular weight exhibited higher values of r^2 results. For example, S1 accounted for 98% of the variability in the RS flux for Fla at 24 hours, compared to 78% for benzo[a]pyrene (BaP) respectively (Figure 43.a).

The regression analysis showed most of the soil properties regression coefficients observing statistically significant p-values (p-values <0.05) for the majority of the HMW PAHs RS fluxes at 24 hours. Fourteen HMW

demonstrated significant positive relationships between the RS flux and the RE parameters S1, S2 and PC%. These three RE parameters provided the highest r^2 values for all PAHs compared to the other RE parameters, ranges of $r^2 = 0.98-0.73$, $p < 0.05$ for the 14 PAHs excluding indeno[1,2,3-c,d]pyrene (IcdP) which had a low r^2 value. These fourteen PAHs included Fla, pyrene (Pyr), benzo[a]anthracene (BaA), triphenylene (TPh), chrysene (Chry), benzo[c]fluorene (BcFlu), benzo[b]fluoranthene (BbF), benzo[k]fluoranthene (BkF), benzo[e]pyrene (BeP), BaP, cyclopenta[c,d]pyrene (CCP), IcdP, C1-Fla/Pyr, and C2-Fla/Pyr. Additionally, thirteen of these fourteen PAHs (exclude IcdP) had significant positive relationships with the initial PAH concentration, HI, I-index and the silt fraction ($< 250 \mu\text{m}$), and significant negative relationships with TpkS2, HI, R-index, and the sand fraction ($< 250 \mu\text{m}$). Other soil properties displaying significant r^2 values included TOC (positive relationship) for twelve PAHs and the clay fraction ($< 250 \mu\text{m}$) for ten PAHs (positive relationship). No significant r^2 values were observed between any HMW PAHs and the RE parameters RC%, S3 and OI.

(a)



(b)

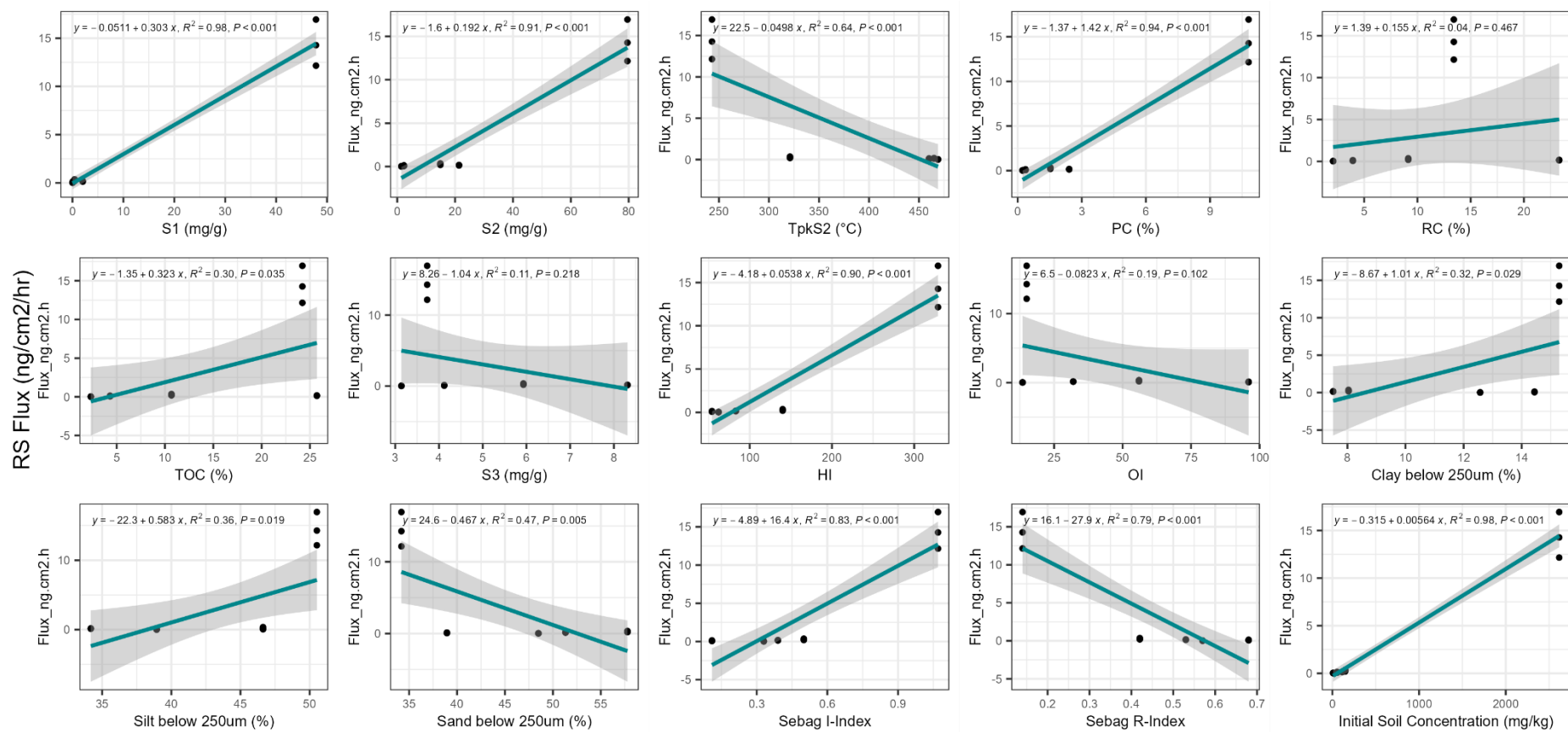


Figure 43. (a) Linear regression r^2 values between each HMW PAH RS flux at the 24-hour timestep with the soil properties and initial soil concentration for the MGP samples only (BCR-524 not included). Linear regression created using results for each of the three dermal experiment conducted for one MGP soil (e.g. 3 dermal experiments \times 5 soils = 15 points). Brighter green tiles signify linear regression models with performing the best by fitting better to the data (high r^2 values), brighter red colours are associated to linear regression models not fitting with the data. * Indicates a p -value < 0.05 for the tested linear regression, this indicates that the soil property has a meaningful addition to the model. (b) Simple linear regression plots for Fla RS flux at 24-hours and the soil properties. Points represent the observation from one of the three dermal experiments undertaken for each MGP soil - triplicate dermal experiments occurred for each MGP soil (e.g. three experiments undertaken with the MGP soil H16 and each experiments observation is a point).

7.4.3 Soil properties potential influence on PAH membrane flux

Membranes from two dermal experiment samples, H16 and the CRM BCR-524, were evaluated at the 24-hour timestep. Regression analysis with membranes were exclusively established from this subset. Significant positive relationships ($r^2 = 0.95 - 0.97$, $p < 0.005$) were observed only for Fla and Pyr, RS fluxes and between S1, S2, TpkS2, PC%, HI and OI. Conversely, negative relationships were observed with S3, RC%, and TOC%. The R-index exhibited identical values for both samples, rendering the regression analysis indeterminable. H16 experimental membranes did not detect larger alkyl-PAHs, precluding the calculation of regression analysis for such compounds. Potential reasons for limited HMW PAHs exhibiting significant relationships include that higher membrane fluxes occur at shorter timesteps (Chapter 6), however only the 24-hour membranes were measured for BCR-524 hence statistical interpretation at shorter timesteps were not possible.

7.5 Discussion

7.5.1 RS fluxes relationships with bulk OM

The regression analysis revealed that seven of the RE parameters (S1, S2, TpkS2, PC%, HI, R-index and I-index) provided significant relationships with the RS fluxes. The largest proportions of variability explained by these RE parameters within the regression analysis occurred for the 4-ring PAHs (predominantly Fla and Pyr, $r^2 = 0.79 - 0.98$, $p < 0.005$). In contrast, these significant relationships were not observed for the 6-ring PAHs (BghiP and IcdP). PAHs with a lower ring number exhibited higher fluxes, attributed to their relatively smaller size facilitating easier diffusion through soil and membrane pores compared to bulkier HMW PAHs (Chapter 6). Conversely, heavier PAHs tend to adsorb to OM and expandable clay minerals, rendering them less bioavailable (Crampon et al., 2014). This observation aligned with previous reports suggesting that lighter PAHs, such as 4-ring PAHs, demonstrate higher bioavailability (Oen et al., 2006, Poot et al., 2014), thus corroborating the findings of the current study. Increasing the timestep resulted in more HMW PAHs displaying significant relationships between RS fluxes and soil properties. Particularly for the heavier PAHs that were not detected in the RS at the shorter timesteps. The rapid desorption fraction has been associated to multiple timesteps in previous studies including 6, 15, 24, and 30-hours (Poot et al., 2014, Barnier et al., 2014, Oen et al., 2006), and varied depending on the type of PAH. Highly hydrophobic HMW PAHs, which exhibited strong binding affinity to OC, demonstrated improved predictive capabilities with longer timesteps (Poot et al., 2014). Agreeing with our results, that the timesteps for the rapid desorption fractions of different HMW PAHs will vary depending on the PAH attributes.

Common trends occurred among 10-14 HMW PAHs, revealing significant relationships between RS flux and soil properties associated to pyrolysable carbon cracked at lower temperatures (S1, S2, PC%, I-index and the R-index. These relationships imply that soils rich in amorphous labile OC, containing highly hydrogenated compounds (e.g., *n*-alkanes in fuel oil), would exhibit increased PAH desorption. The presence of such compounds, which weakly absorb PAHs, leads to their rapid desorption and higher flux measurements (Ruby et al., 2016, Xia et al., 2016). The soil E1.5, gave the highest PAH

concentrations and highest OC content in S1, S2, PC% and I-index, consequently this sample was identified as a key driver for generating these significant relationships between RE parameters and RS flux.

The initial soil PAH concentration exhibited significant relationships with the RS fluxes of thirteen PAHs, however lower r^2 values were reported for 5-ring PAHs. Removal of the soil with the highest PAH concentration, E1.5 (see Figure 44), led to the loss of significant relationships between RS flux and the initial soil concentration for nine HMW PAHs. However, relationships remained for Fla, Pyr, BaA, Chry, BaP and C1-Fla/Pyr. This alteration also resulted in the loss of statistically significant relationships from regression analysis between various soil properties and RS flux for various PAHs. Fla, Pyr, C1-Fla/Pyr and BaP retained the majority of their significant relationships including S2, TpkS2, PC%, HI, R-index and I-index. This suggests that the relationships between the bulk OM descriptors (in particular S1 which lost significance for all PAHs) and RS flux were highly associated with the extent of contamination. This is expected as it is acknowledged that the hydrocarbons found in S1 include PAH contamination (Chapter 5.4.2). Competitive effects between PAHs and other organic contaminants for adsorption sites were postulated in soils with higher concentrations of PAHs, enhancing PAH release (Ruby et al., 2016). Whereas lower soil concentrations may be influenced by OC, such as black carbon (BC), resulting with decreased PAH release (Ruby et al., 2016).

However, this may imply that the PAH contamination source present in soil E1.5, is capable of readily releasing PAHs comparative to the other MGP soils. PAH sources are known to influence PAH release from soil, with slower releases reported for soot contamination than fuel oil sources (Xia et al., 2016). E1.5 showed high S1, HI and I-index values and low R-index and TpkS2 values, that have been previously been associated with PAHs of a petrogenic origin (Lafargue et al., 1998)(Chapter 5), such as MGP processes utilising oil as shown in Chapter 5. In Figure 16, E1.5 is found in the cluster (yellow coloured cluster) with the most diverse RE parameters compared to other MGP soils, with only two other MGP samples present in the cluster. One assumption is that the samples in this cluster are contamination sources or have high amounts of

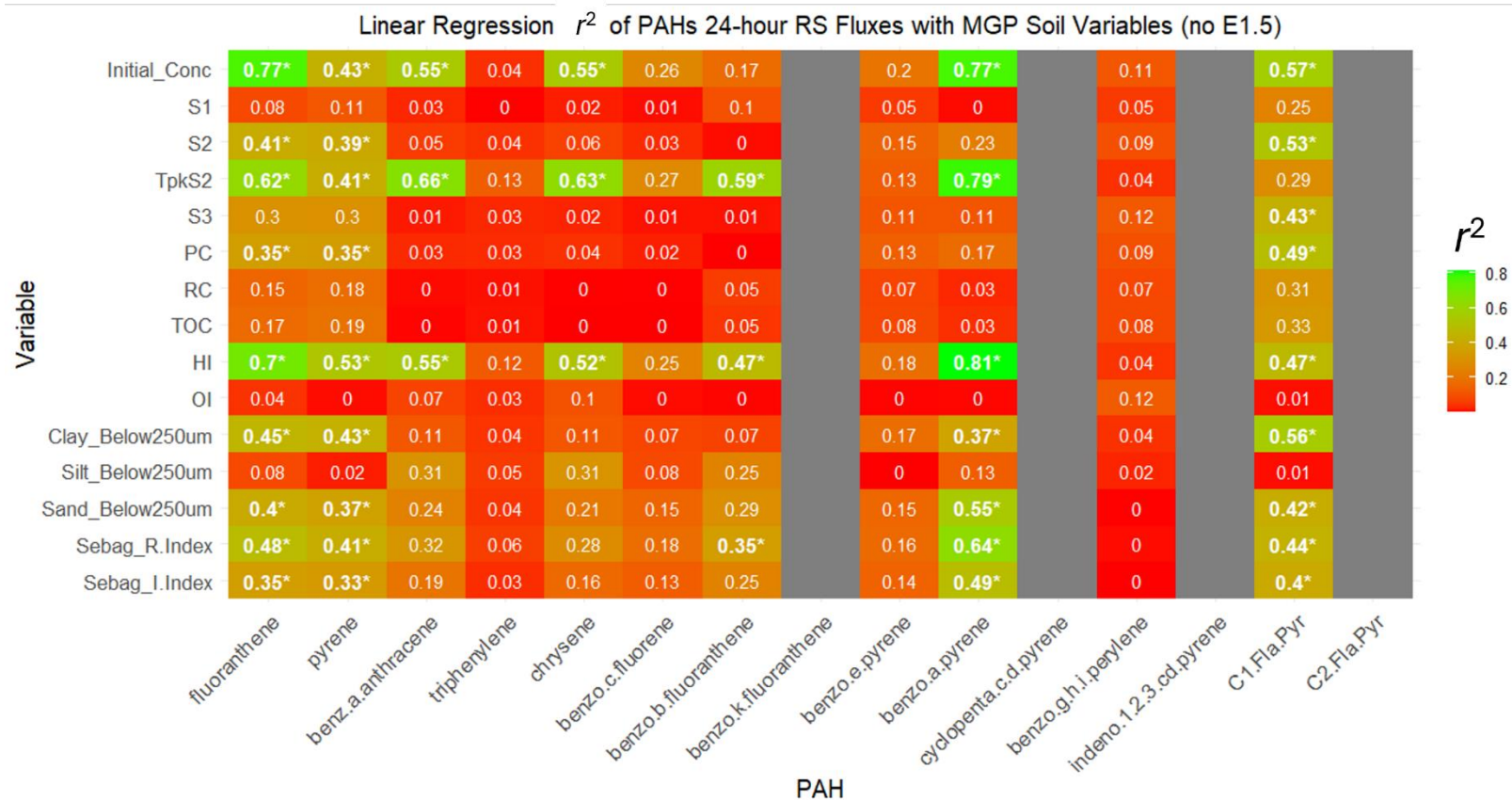


Figure 44. Linear regression r^2 values between RS flux (triplicate dermal experiment results) vs soil properties of MGP samples with the removal of sample E1.5 at the 24-hour timestep for each HMW PAH. Brighter green tiles signify higher r^2 values (higher percentage of variation explained by soil property), while brighter red tiles are associated to lower r^2 values. * Indicates significant regression with a p -value < 0.05 .

sources present. The contamination source and the subsequent initial PAH concentration could potentially have a combined effect on PAH release from soil, resulting with E1.5 acting as a strong driver for the relationships between soil properties and RS flux.

As initially predicted, a negative relationship between the RS flux and the R-index and a positive relationship to the I-index were reported. Implying that thermally refractory condensed OC has a higher sorption affinity to PAHs and resulted with lowering the release of PAHs compared to soils with soft liable OC (Semple et al., 2013, Lueking et al., 2000, Luo et al., 2012, Umeh et al., 2018, Xing and Pignatello, 1997). In particular, the lower R and higher I-indices for E1.5 and H16 related to increased RS fluxes comparative to the other MGP soils. This implies that both E1.5 and H16 RS flux could have been impacted by either 1) increasing the amount of labile material capable of releasing PAHs or 2) by the high initial soil PAH concentrations or 3) a combination of both effects. Soil E1.5 exhibited dominating peaks at lower temperature ranges, indicating high amounts of anthropogenic distillable hydrocarbons, which Haeseler et al. (1999) determined to be mostly aromatic hydrocarbons and resins for soils contaminated by coal tars. E1.5 was assumed to have less soil material and higher quantities of contamination source (coal tar) than other soils. Due to the extremely high PAH concentration and the lower quantities of hydrocarbons released at higher temperatures compared to other soils. Given that, MGP soils have higher amounts of non-extractable OM (cracked at higher temperatures) compared to extracted coal tars without soil (Haeseler et al., 1999). The S2 curves OC compositions illustrate how the I-index (the lower temperature fractions) and the R-index (higher temperature fractions) can help in distinguishing the PAH contamination sources and show potential to relate to dermal flux.

We initially hypothesised a negative relationship between the RC% and RS flux, given that Poot *et al.*, (2014) reported this correlation for the rapid desorbing PAH fraction in sediments. In contrast, our results showed no statistically significant relationships between the HMW PAHs RS fluxes and RC%. No relationships occurred due to the E1.5 reporting a lower RC% than I3. Removing soil I3, characterised by the highest RC% value, led to thirteen HMW PAHs

regaining significant relationships between RS fluxes and RC% ($r^2 = 0.59-0.68$, $p < 0.005$). The high RC% value for I3 indicates that the sample contains higher proportions of BC and other highly condensed thermally refractory OC than the other soils. BC is known for its strong PAH sorption capacity (Semple et al., 2013, Ukalska-Jaruga et al., 2019, Ruby et al., 2016, Vane et al., 2022) due to its structure capable of entrapping PAHs, hence lowering the release of PAHs (Poot et al., 2014). I3 notably measured a high RC% value relative to its TOC% (23.31% for RC% and 25.72% for TOC%), highlighting its predominantly RC composition, capable of restricting larger proportions of PAH release comparative to the other MGP soils. include the quantity and types of RC within the samples. Our MGP soils measured higher RC% ranging from 2.09 – 23.31 % (mean 10.39%), compared to Poot et al. (2014) which sediments measured RC% 0.01- 4.89% (mean 1.08%). Furthermore, it was observed that our MGP soils TOC% consisted predominately of the RC% compared to the PC%. This suggests that the MGP soils OC composition is predominantly RC consisting of either anthropogenic material or large humin material. Although, it is suspected that the larger proportion will be contributed by anthropogenic origin because the soils are highly contaminated.

It is proposed that the higher proportions of RC contamination exhibited at the MGP soils will impact the PAH release mechanisms (Ruby et al., 2016, Poot et al., 2014). One assumption for why the RC% did not show any relationships with RS fluxes in this study is that these MGP soils have high amounts of labile hydrocarbons, which have become the dominant influence in PAH release from soils. Other studies have proposed that different mechanisms of binding and releasing PAHs have caused differences in PAH release between different biochars (Godlewska and Oleszczuk, 2021) and RC% fractions (Poot et al., 2014).

Our study has shown improved relationships between RS flux and the R-index and I-index compared to the RC%. Explanations for this include the RC% correlating more effectively to slower desorption fractions or the RC% overshadowed by other factors such as PAH concentrations (Poot et al., 2014, Oen et al., 2006), or that the R-index provides greater insights into specific OC fractions relating to PAH release. Other studies have reported no correlation with

PAH release rates and “hard” and “soft” OC (Hawthorne et al., 2002) or soot content (Kukkonen et al., 2003), indicating that PAH release is not easily predicted using sample matrix compositions (Hawthorne et al., 2002). Our study focused on the desorption fraction most likely to occur for human exposure (within 24-hours). Field-contaminated soils vary considerably with variations in OC compositions, PAH sources and degrees of weathering, leading to highly variable dermal measurements for field-contaminated soils compared to spiked samples (Oen et al., 2006). Therefore, our study has contributed to the understanding of bulk OM properties relationship to parent and alkylated PAH dermal bioavailability in a more realistic scenario with atypical MGP soils.

7.5.2 PSA influence on RS flux

Particle size fractions relationships with RS flux did not perform as well as the RE parameters (smaller r^2 values and less statistically significant results among the PAHs). Variations in the relationships between PAH release and soil particle size have been observed in different studies, showing negative correlations (Crampon et al., 2014, Duan et al., 2014, Brändli et al., 2008), positive correlations (Oen et al., 2006), and no correlation (James et al., 2016). The complexity arises from the influence of other soil properties on these relationships. This study purposes that the OC fractions in the samples have a more dominant role than the particle size fractions. Additionally, this study has considered that considerable amounts of OM may remain after H₂O₂ digestion (Harada and Inoko, 1977), therefore the percentages may not exclusively include mineral fractions, making assumptions based on inorganic fractions behaviours with PAHs less reliable.

7.5.3 Comparison with other MGP soils

The five MGP soils analysed in this study were a subset of 94 MGP soils previously measured by RE, as reported in Chapter 5. Ten of the RE parameters were used for k-means clustering with k=5, to group soils based on similar RE parameters (see Figure 16). 90% of MGP soils clustered into two distinct groups (clusters 1 and 5), reflecting shared bulk OM properties among these samples. A11 and E2.7 were in these two clusters; and exhibited low RS fluxes relative at 24-hours and 10-hours compared to the other three soils (Chapter 5). However, A11 gave some of the highest RS fluxes for the 4-ring PAHs at 1-hour. It would

be assumed that the majority of MGP soils would behave similarly to A11 and E2.7 and subsequently measure low RS fluxes due to the majority of MGP soils exhibiting similar RE measurements. The I-index and R-index are valuable parameters because they summarise proportions of different thermally released hydrocarbons. In this study they provided statistically significant relationships with thirteen PAHs and were one of the RE parameters that remained significant for many PAHs with the removal of the E1.5 soil. In Chapter 5, 94 MGP soils measured I-index values in a range of -0.32-1.07, and a R-index range of 0.14-0.85, which resulted with dispersing the MGP soils on I/R diagram (Chapter 5 Figure 29.d). The dispersed index measurements for MGP soils suggest that the indices can provide valuable insights into the PAHs release from MGP soils. Particularly in relation to membrane fluxes which are in direct contact with the soil, hence soil properties are presumed to have a greater significant relationship with the amount of PAH entering the membrane than RS. Chapter 6 also showed that the total flux (sum of RS and membrane fluxes) was predominately contributed by the membrane fluxes, emphasising the membranes importance in capturing available PAHs for dermal absorption.

7.5.4 Implications and future research

Further research should include a larger dataset MGP soils RS and membrane fluxes, to strengthen the results of the R-index and I-index relationships shown in this study. It is predicted that stronger relationships with the OM bulk properties would occur with the membrane flux compared to the RS flux, due to the membrane being in direct contact with the soil and containing the majority of released PAHs. Hence, future dermal bioavailability studies would benefit in investigating the membrane flux influence from bulk OM expressed by RE parameters.

To address for the undetected heavier PAHs in RS and membranes, extended exposure timesteps and spiked weathered soils could unveil their behaviour. Since differing PAH release mechanisms may exist for various PAH types and concentrations. This would help determine whether this was a consequence of PAH properties or because of the lower concentrations for the heavier PAHs not being at an adequate level for detection. Although previous studies (Crampon et al., 2014, Oen et al., 2006, Poot et al., 2014) reported lower PAH desorption with

increasing ring numbers, which suggests that our study was correct in not detecting these higher HMW PAHs within the RS within 24-hours. This study discovered that the soil with the highest PAH concentration was the main driver for many of the bulk OM relationships. This should be investigated further by using a range of different PAH concentrations for different PAH species, to determine whether the results were contributed by the abundance of available PAHs or impacted by the type of PAH source material as reported by Xia et al. (2016).

7.6 Conclusion

In this investigation, we explored the influence of bulk OM, characterised using Rock-Eval(6) Pyrolysis variables, and particle size fractions (<250 μm), on the *in vitro* dermal fluxes of HMW PAHs from soils into receptor solutions. The evaluation revealed significant relationships between certain RE parameters including S1, S2, TpkS2, PC%, HI, I-index and R-index and hydrocarbon contamination. However, it is important to acknowledge that these relationships were primarily driven by one sample exhibiting exceptionally high PAH concentrations. Nevertheless, even after removing this highly contaminated sample, significant relationships between RS fluxes remained for Fla, Pyr, and C1-Fla/Pyr. Our findings showed that the R-index and I-index representation of the diverse hydrocarbon fractions related with a large number of HMW PAHs RS fluxes, thus providing a more comprehensive understanding of the types of OC impacting PAH release. Considering the variability of MGP soils in terms of the R-index, its application may prove valuable for risk assessors in evaluating the risks associated with HMW PAHs in MGP soils.

This study has highlighted the complexities inherent in bulk OC characterised by Rock-Eval(6) Pyrolysis, which can yield divergent results for MGP soils. Such variations could potentially lead to misinterpretations, especially when highly contaminated samples are measured. The relationship between RC% and RS fluxes differed from those reported in previous studies, suggesting that OC compounds measured as RC% are highly variable in MGP soils. Predicting the PAH release based on sample matrix compositions may not be straightforward, due to the diversity of pollutants generated at MGP processes (Hawthorne et al., 2002). To advance this research, future investigations should encompass a larger

and more diverse array of MGP soils, with measurements conducted for both membrane and RS PAH fluxes, and to trial multiple linear regression with multiple RE parameters. The current study's constraints, attributed to the limited number of membrane measurements in dermal absorption experiments, thus uncertainties remain on the prospective significance of membrane fluxes in relation to bulk OM. This data contributes to the knowledge base available to risk assessors in determining the potential health risks associated with former MGP sites. By exposing the complex interactions between soil properties and dermal bioavailability of PAHs, such research endeavours can support the development of effective strategies for managing and remediating contaminated sites.

CHAPTER 8

GENERAL DISCUSSIONS

8.1 Introduction

This chapter integrates the pivotal discoveries from Chapters 5, 6 and 7, elucidating their implications and describing opportunities for further investigations.

8.2 Discussion of results

8.2.1 Review of research focus

If brownfield land is to be used for redevelopment, e.g. for solving challenges around housing demand, the remediation of such land needs to be cost effective. Costs could be lowered if uptake of contaminants into the human body from contaminated soils was shown not to be a risk to human health. This would be either no, or very low, contaminant uptake into the body such that it does not result in health problems, and therefore where there is no requirement for soil remediation practices. This thesis has focused on targeting the chronic dermal exposure route component of HHRAs, by investigating uncertainties associated with the dermal bioavailability of PAHs from soils.

Eight research objectives were followed (Section 1.2.3) to help this research achieve its aim (Section 1.2.1) of investigating the distributions of parent and alkylated PAHs with characterised bulk OM in former MGP soils, and to determine whether bulk OM variables contribute to differences in both PAH distributions at sites/industrial processes and in human *in vitro* dermal bioavailability.

8.2.2 Research key findings

The key findings from Chapters 5, 6 and 7 are listed below.

Chapter 5 (Research paper 1) addressing Research Question 1 (Williams-Clayson et al., 2023)

- Characterising soils by their MGP processes using PAH distributions in PCA was clearest for processes utilising oil (CWG) and lower temperature processes (LTHR). Classifying other MGP processes proved more challenging due to mixed contamination or limited samples or environmental impacts. Findings address research objective 4.
- The majority of MGP sites had high proportions of HMW PAHs that can be associated with higher contributions to dermal exposure pathways than LMW PAHs. Σ Alkyl21 proportions were diverse between soils, but HMW alkyl-PAHs had the highest contribution to Σ Alkyl21, yet alkyl-PAHs are currently unaccounted for in HHRAs. Findings address research objectives 4 and 5.
- The RE parameter values characterising the bulk OM of soils was highly variable amongst the MGP soils, particularly with the I-index and R-index. This suggests that RE applied as a screening tool could help estimate soil fractions governing PAH binding and influences on dermal bioavailability for PAHs. Findings address research objectives 3 and 4.

Chapter 6 (Research paper 2) addressing Research Question 2 (Williams-Clayson et al. submitted)

- Artificial skin membranes act as PAH sinks in dermal *in vitro* experiments. HMW PAH dermal fluxes decreased with increases in the ring number or alkylation, notably the only alkyl-PAH detected for all samples was C1-Fla/Pyr and was not detected at shorter timesteps showing that alkyl-PAHs behaved differently to parent PAHs. Findings address research objectives 5, 6 and 7.
- Dermal fluxes notably fall below previous dermal bioavailability investigations and the current HHRAs standards set for BaP. This is attributed to measuring real-world contaminated soils rather than spiked soils. Findings address research objectives 5 and 7.

- The initial soil concentration and the physicochemical properties of PAHs influenced the dermal bioavailability of a small fraction of HMW PAHs, generally the PAHs with lower ring numbers exhibited the higher fluxes.

Chapter 7 (Research paper 3) addressing Research Question 3

- Common trends in regression analysis between the RS fluxes and RE parameters occurred among 14-10 HMW PAHs. However, relationships were primarily driven by a single sample (E1.5) characterised by notably elevated PAH concentrations and OM bulk values. This created uncertainties around the potential reasons for the flux and RE parameters relationships. Findings address research objective 8.
- Nevertheless, persistence of significant regression analysis after the removal of E1.5 from the dataset occurred for HMW PAHs with the highest fluxes (Fla, Pyr, and C1-Fla/Pyr). Finding addresses research objective 8.
- Findings suggest the implications of RE parameters, especially the S1, S2, TpkS2, HI, I-index and R-index, can help in shaping predictive models for dermal bioavailability of HMW PAHs, although validation through comprehensive soil investigations is required. Findings address research objective 8.

8.2.3 Research discussion

MGP soils characterising processes

The research questions (Section 1.2.2) and research objectives (Section 1.2.3) were derived for this research from examining the gaps in the literature (Section 2.6) (Research Objective 1). Gaps identified in the literature included previous studies investigating low numbers of real-world contaminated soils (particularly MGP soils) and limited types of PAH compounds were investigated in studies (Section 2.6).

This research addressed these gaps by answering Research Objectives 2, 3 and 6 in Chapter 5, by analysing 48 real-world contaminated MGP soils for their PAH distributions and soil bulk OM properties. This was the first study to investigate how soils characteristics (opposed to previous research on coal tars) can be linked back to their corresponding MGP process. Section 5.4.3 separated soils linked to MGP processes involving oil application (CWG) or lower

temperatures (LTHR) from the broader spectrum of MGP soils using data on both PAH distributions and RE parameters.

However, the allocation of other MGP processes (Figure 25) remained elusive, possibly attributed to the intricate challenges associated with real-world contaminated soils. These findings addressed Research Question 1, highlighting the complexities in using environmentally impacted soils in characterising MGP processes. The findings showed that the majority of MGP soils had similar PAH distributions (except for oil associated processes), the majority of MGP soils had HMW PAHs as their greatest contributor to the $\sum\text{PAH}_{51}$. This provides useful knowledge for risk assessors, by having prior knowledge on the expected types of PAHs most likely to be present at MGP sites, risk assessors can focus their assessments to these PAH types which could potentially lower investigation costs. HMW PAHs contribute more to the dermal exposure pathway than LMW PAHs (Nathanail et al., 2015) (Section 2.2.1), therefore knowledge into the dermal bioavailability of HMW PAHs at MGPs is of great importance due to the persistence in MGP soils and investigated in Chapter 6.

PAH distribution in MGP soils

Another novelty of this research is the investigation of the concentration, distribution, and the dermal bioavailability of alkyl-PAHs in MGP soils. The proportion of alkyl-PAHs contributing to the total $\sum\text{PAH}_{51}$ was highly variable among soils (7-65%), in comparison to the proportion of EPA16 in the $\sum\text{PAH}_{51}$ (32-79%). Alkyl-PAHs currently lie beyond the scope of most HHRA investigations, yet my research has spotlighted that alkyl-PAHs can contribute substantial concentrations across a range of different MGP soils. This has important implications for HHRAs as these compounds are not routinely considered, thus potentially underestimating human and environmental health risks from contamination at MGP sites (Section 2.3.3).

Skin as a sink and source of PAH

Chapter 6 presented several findings from the *in vitro* dermal experiments conducted in this research and addressed the Research Objectives 5, 6 and 7. One of the key findings was that the lipophilic nature of the membrane encouraged the preference of PAHs to partition into or/and remain in the skin

(Haq et al., 2018, James et al., 2011, Nathanail et al., 2015). This occurred for all HMW PAHs that were >LOQ for the MGP soil H16. These membrane-related insights are in accordance with prior investigations studies including Lort (2022), Wester et al. (1990), Moody et al. (1995), Abdel-Rahman et al. (2002), Moody et al. (2007), Peckham et al. (2017). This implies the importance of considering both the dermal barrier (skin/membrane) and external media (soil type) when assessing human exposure risks (Section 2.4.3). Suggesting toxicity/carcinogenic effects from PAHs to skin itself should be investigated with the HMW PAHs with the highest dermal fluxes (Nathanail et al., 2015).

Parent PAH

The *in vitro* dermal experiments result in Section 6.5.1 also highlighted that PAHs with a lower ring number (4-ring PAHs), such as Fla and Pyr, exhibited the highest dermal fluxes across all soil samples and matrices. These two PAHs are classified as IARC Group 3 compounds (not classifiable as to their carcinogenicity to humans, because of limited or inadequate experimental evidence) (International Agency for Research on Cancer, 1965-2023). This indicates that the human health risks associated to the two HMW PAHs is unknown, thus there is an unknown potential risk with these two HMW PAHs entering the body through the dermal pathway. Currently, HHRAs use a BaP study to make assumptions about all PAHs (Section 6.2), all HMW PAHs dermal fluxes were lower than the single BaP study (Wester et al., 1990). Therefore, current HHRAs might be overestimating potential risks of PAHs.

Chapter 6 dermal results unveiled differences in fluxes between PAH isomers. Both BkF and BbF were detected in the RS for several MGP samples at 1-hour, in contrast to BjF, which was only detected in the H16 membranes at 24-hours, even though these isomers had similar initial soil concentrations (Figure 32). These findings suggest that isomers have different dermal absorption properties, emphasising the potential influence of PAH properties such steric hindrances, boiling points, LogKow, vapor pressure and water solubility. Similarly, dermal flux trends between BaP and BeP were different, with BeP showcasing heightened membrane fluxes, particularly at 1-hour intervals and even in cases where BaP had higher initial soil concentrations. The Length-to-Breath ratio (L/B) parameter, as introduced by Sander and Wise (1997), elucidated that BeP

possesses a compact molecular structure conducive to enhanced diffusion through soil and membrane, thereby accentuating its dermal absorption. These observations support the hypothesis that dermal bioavailability will vary between different HMW PAHs, due to PAH physicochemical properties (Section 6.5.3) and structure, which helps address Research Objective 7.

Other HMW PAHs focused upon in the study included the 4-ring PAHs BaA, Chry and BcFlu, which exhibited the next highest RS fluxes after Fla and Pyr. Notably, BaA and Chry belong to IRAC Group 2B (possibly carcinogenic to humans) compounds (International Agency for Research on Cancer, 1965-2023). While BcFlu has been categorised as Group 3 due to limited experimental evidence, Richter-Brockmann and Achten (2018) reported a TEF of 20 for BcFlu (Section 2.3.3), indicating a carcinogenic potential approximately 20 times that of BaP. The combined evidence of heightened dermal fluxes for these HMW PAHs, coupled with their potential health implications, suggests that they warrant consideration in dermal bioavailability assessments. This is particularly appropriate, given that current HHRA are predominantly reliant on BaP assumptions, which if used as a surrogate, would underestimate the dermal exposure risks for these HMW PAHs given their higher fluxes than BaP. This finding signifies a need for reconsidering risk assessment methodologies for the PAHs with highest dermal flux in this study (Haney et al., 2020).

The heaviest PAHs, B_jF, DahA, DalP, DaiP, DahP, and DacP were undetected in all RS samples, suggesting that using BaP as a surrogate marker for these HMW PAHs would overestimate the risk posed by these PAHs. DahA was also measured by Forsberg et al. (2021), who also was unable to detect DahA in any RS or skin samples. These findings are important, as assuming all HMW PAHs have the same dermal bioavailability of BaP can either overestimate or underestimate risk estimations for different PAHs. This study answers this by reporting that 4-ring PAHs have the higher dermal fluxes than BaP, and that increasing the molecular weight of PAHs decreases the flux, therefore these heavier PAHs dermal bioavailability would be overestimated when using BaP as a surrogate marker (Section 6.5.1 and 6.5.3).

Alkyl-PAH

Previous dermal studies had only investigated a maximum of 14 PAHs (Section 2.4.4), in this thesis I expanded this to include 27 HMW PAHs, including for the first-time alkyl-PAHs. A key finding in this thesis is that alkyl-PAHs had lower dermal fluxes than their associated parent PAHs (Section 6.5.2). Interestingly, the C1-Fla/Pyr measured the third highest RS fluxes at the longer timestep of 24-hours (Section 6.5.2). 1-methylpyrene has demonstrated mutagenic and chromosome-damaging activities in mammalian cells (Jiang et al., 2015). The high dermal fluxes experienced by C1-Fla/Pyr raises concerns for potential health risks due to the compounds suspected mutagenic activities. Section 5.4.1 showed that the shorter alkylated Fla/Pyr PAHs had one of the greatest contributions to the \sum Alkyl21. Therefore, C1-Fla/Pyr PAHs are present at varying concentrations in MGP soils.

C1-Fla/Pyr, demonstrated a slower dermal flux from soil to membrane or RS compared to its parent derivatives. Therefore, suggesting that alkyl-PAHs have an increased retention in the soil matrix and that increasing alkylation of PAHs decreases the compounds dermal absorption. It is suspected that the alkyl-PAHs experience greater steric hindrance or that their increased hydrophobicity increases their sorption to soil components, hence causing slower desorption of the PAH through the soil before entering the skin. Therefore, Chapter 6 unveiled the significance of exposure time in determining the risk associated with different PAHs, with alkyl-PAHs or heavier larger PAHs posing a concern to humans *via* the dermal pathway if soil remains on skin for long exposure times. The potential dermal risks posed by alkyl-PAHs were previously not explored, and other HMW PAHs offer novel insights into the broader types of PAH dermal bioavailability. These findings suggest that humans in direct contact with contaminated soils for shorter periods of time present a lower risk from the alkyl-PAHs and/or heavier HMW PAHs by dermal exposure. Studies investigating the risks from oral exposure of these PAHs may differ, however, if similar to this study, these PAHs might be considered for exclusion from HHRAs, making investigations potentially quicker and cheaper by targeting only the PAHs of concern.

Other alkyl-PAHs were not being detected (<LOQ) in dermal matrices for MGP soils. A possible explanation is that the additional chain or increased chain length caused steric hinderance, preventing the alkyl-PAHs movement and release from soil. It was acknowledged that the initial PAH concentration was not the cause of the other undetected alkyl-PAHs, given that several HMW parent PAHs with lower concentrations were detected (Figure 32). Therefore, this finding suggests that alkylated BaA/Chry/TPh compounds are not a risk to dermal absorption under 24-h exposure period. Potentially alkylated BaA/Chry/TPh compounds may be less likely to present a risk over a 24-hour exposure period, however this may not be the case for longer exposure times not tested in this study. These findings answer Research Question two (Section 1.2.2), showing that there are differences between alkylated PAHs and parent PAHs dermal bioavailability.

Use of soil reference material

Although the BCR-524 RS fluxes were not quantified due to uncertainties associated to the surrogate recoveries, breakthrough into the RS was observed for both C1- and C2-BaA/Chry/TPh at 10-hours and 24-hours (Section 6.5.2). However, no detection of these compounds was noted in the 24-hour BCR-524 membrane measurements. A plausible reason for this observation is that the available alkyl-PAHs have traversed the membrane. A comparison between the 24-hour BCR-524 membrane measurements and MGP sample H16 membrane measurements revealed increased fluxes for Fla, Pyr and C1-Fla/Pyr for BCR-524, whereas other HMW PAH fluxes were more pronounced for H16. This outcome aligns with expectations, considering that the H16 sample exhibited higher concentrations of heavier PAHs than BCR-524, akin to other MGP soils. This disparity in HMW PAH concentrations for BCR-524 is attributed to the historical creosote oil contamination inherent in BCR-524. The former wood treatment sources in BCR-524 led to elevated concentrations of smaller PAHs in contrast to MGP soils. Previous studies have agreed that the source of contamination can impact the dermal absorption (Xia et al., 2016). My findings suggest that soils contaminated by different scenarios will have different dermal bioavailability capabilities due to the differences in contamination.

Posada-Baquero et al. (2022) also explored the bioavailability of PAHs using BCR-524, employing Tenax or hydroxypropyl- β -Cyclodextrin extractions. Their

study demonstrated a bioavailable concentration of 1.84 mg/kg for BaP using the Tenax extraction method for a 20-hour duration. The 24-hour membrane bioavailable concentration in my research measured 0.18 mg/kg (with a mean BaP measurement of 131.26 ng in a membrane from an application of 0.75 g of BCR-524 soil). It is evident that the measured bioavailable concentrations in my study were generally lower than those of the Tenax study. Disparities between the two studies might be attributed to variations in extraction methods, experimental setups, and analytical techniques. Notably, my *in vitro* dermal experiment involved a passive 24-hour contact between soils and membranes, whereas Posada-Baquero et al. (2022) experiments involved an active 20-hour shaking and a higher surface area to volume ratio for the Tenax extractions, which could have influenced the release dynamics of PAHs. Despite these distinctions, both studies concurred on the order of PAHs with the highest bioavailable fractions in BCR-524 as: Pyr > BaA > BbF > BaP > IcdP. Indicating a congruence in the general release behaviour of PAHs using *in vitro* bioavailability experiments.

Comparisons to other dermal studies

Comparisons between the dermal fluxes in this current research with the PhD thesis of Lort (2022) showed consistency. The comparison demonstrates that RS and membrane measurements between the studies were not significantly different ($p < 0.05$) (Section 4.3.3 and Section 6.5.4). Although uncertainties were associated with BCR-524 RS measurements in my study, the resemblance in membrane fluxes between studies was similar. For instance, the mean 24-hour membrane flux for Pyr in my study was 112 ng/cm²/h compared to 113 ng/cm²/h in Lort (2022), which highlights the reliability of the *in vitro* dermal experiment methodology between studies.

This study's RS fluxes were lower Lort (2022) results, potential reasons for this may stem from variations in soil properties, SMC, or analytical methodologies (Hu and Aitken, 2012, Kottler et al., 2001). The employment of GC-MS/MS for quantification in my research, was used to increase selectivity and reduce background noise could of led to quantification differences, compared to the use of GC-MS selected ion mode or full scan mode by Lort (2022) (Niessen, 2017). However, both my study and Lort (2022) measured lower dermal RS fluxes than

other dermal studies RS fluxes. This emphasises that “real-world” contaminated soils observe lower dermal bioavailability than spiked soils. This finding is significant because current HHRA dermal bioavailability are based on studies with spiked soils which could be overestimating the dermal bioavailability of PAHs and leading to a greater number of soils classified as a risk and potentially requiring expensive remediation.

The observed temporal dynamics of fluxes in my study contrasted to Lort (2022) findings. While Lort (2022) identified a maximum flux within the first hour, I found only the lowest concentrated soil A11 to measure the highest fluxes at 1-hour, whereas other sample’s RS fluxes increased with time. Explanations for the differences between studies again might include different soil properties delaying the release of PAHs or differences with SMC. Added moisture to soil can increase the relative extractability of PAHs compared to air dried soils (Kottler et al., 2001) whereas wetting and drying cycles during ageing of soils can reduce PAH extraction (White et al., 1997). Moisture changes the pore sizes (swelling) and the wettability of soil OM and has been shown to decrease sorption of compounds (White et al., 1997). These features are expected to increase the amount of available PAH capable of release, explaining the trends seen between these studies.

Roy et al. (1998) RS fluxes of MGP soils were generally higher than those reported in this thesis, except for their lowest concentration MGP soil (Section 6.5.4). A plausible explanation for this is that Roy et al. (1998) MGP soils had significantly higher PAH concentrations (20.9 – 86,400 mg/kg) compared to my study (6.5 – 160.5 mg/kg), which would result with them experiencing higher fluxes. Moody et al. (2011) used a novel “by difference” approach (measurement of the soil PAH reduction) and reported the total BaP flux to be 5 ng/cm²/h for a coal-tar contaminated site. This value closely aligns with my findings, with two of the triplicate H16 experiments reporting a total BaP 24-hour flux of 5.02 ng/cm²/h and 5.54 ng/cm²/h. Finally, the BaP dermal fluxes from the oil MGP soils measured by Stroo et al. (2005) were higher than my values. This difference can be attributed to the notably higher PAH soil concentrations in the other study or by the potential oil contamination, as also observed with my results for sample E1.5. Oil-gas MGP sites used oil as a feedstock thus based on the findings of

Section 5.4.3, the soil contamination will have petrogenic characteristics associated with enhanced amount of labile OC linked to heightened PAH releases (Bartolomé et al., 2018, Barnier et al., 2014). The differences in fluxes between my study and other studies is suggested to be caused by differences in soil PAH concentrations and types of contamination, therefore a standard method to compare dermal studies is required.

One approach to account for and normalise the effect of the different initial PAH concentrations between the real-world soils is to use an equation to make flux relative to the initial soil concentration (Xia et al., 2016, Roy et al., 1998). Normalising the flux to the initial soil concentration lowered the flux values for the MGP soils (e.g. E1.5 Fla changed from 14.5 ng/cm²/h to 0.006 ng/cm²/h), and changed the order of which soils had the highest flux. For example, the following PAHs order of increasing flux at 24-h changed when normalised from:

- Fla: A11 < E2.7 < I3 < H16 < E1.5 to I3 < E2.7 < H16 < A11 < E1.5
- Pyr: A11 < E2.7 < I3 < H16 < E1.5 to I3 < H16 < E2.7 < E1.5 < A11
- C1-Fla/Pyr: A11 < E2.7 < I3 < H16 < E1.5 to I3 < H16 < E2.7 < A11 < E1.5

The order of PAHs for normalised flux differed slightly from the order when using flux for each soil. However, the PAHs with the highest fluxes remained the highest with normalised flux. For example, the mean values H16 at 24-h changed from:

- Fla > Pyr > C1-Fla/Pyr > BaA > Chry > BbF > BaP > BcFlu > TPh > BeP to
- Fla > Pyr > C1-Fla/Pyr > BcFlu > TPh > BaA > Chry > BbF > BaP > BeP.

The PAHs which tended to increase in value using normalised flux were TPh, BcFlu (4-ring PAHs), whereas BaP and BeP (5-ring PAHs) decreased, which suggests that PAH properties influences are important (Section 6.5.3).

The A11 and E2.7 soil (generally the soils with the lowest initial concentrations) flux were increased when normalised to the initial concentration compared to other soils. This finding was evaluated further to determine whether this change in flux order from the soils would influence the relationships with the bulk OM variables characterised by RE and the normalised flux. The linear regression results between the normalised flux and RE parameters for the PAHs showed either a decreased correlation, the same correlation or a minor increase in the

correlation (several examples of PAHs normalised flux relationships with RE parameters in Appendix A Figure S3). The results show that the normalised flux for E1.5 is still the main driver for PAHs showing significant relationships. As a result, the flux values were reported in Chapter 7 instead of the normalised flux values, this was to avoid any potential loss in information by the normalisation element, as it can be seen that the amount of PAHs in soils directly impacts the bulk OM variables relating to the lower pyrolysis temperatures (S1, I-index etc.). These are interesting results as one MGP soil (E1.5) had different results to the others, understanding why this soil has a higher dermal bioavailability can help determine the main factors influencing the dermal bioavailability and should be further investigated.

The MGP soils in my study were selected to have BaP concentrations above the GAC value of 5 mg/kg (Section 3.6). Soils with BaP concentrations at the lower end were of particular interest in this study, as these soils may realistically be left and not remediated and be subjected to human exposure, while grossly contaminated soil would require remediation. In the context of the UK, the current dermal absorption fraction (ABS_d) for BaP is established at 0.13 (13% of BaP assume available from dermal exposure) (Environment Agency, 2009b) and is used to calculate the chemical uptake rate for dermal contact with soil (Section 2.4.4). The ABS_d value in HHRA is based on Wester et al. (1990) data, both Forsberg et al. (2021) and Lort (2022) employed dermal fluxes to calculate ABS_d values. While my study was confined to a limited number of timesteps rendering determination of the peak flux and steady state flux uncertain, I consistently observed higher RS fluxes at longer timesteps (except A11).

To facilitate comparisons between studies, ABS_d values for the 24-hour and 10-hour H16 experiments were calculated and compared against Lort (2022) and Wester et al. (1990), as detailed in Table 21. These ABS_d values were derived using the methodology proposed by Forsberg et al. (2021) using Equation 10 and Equation 11. Where ABS_{exp} is the experimental PAH dose absorbed (ng), F_{RF} is the flux of the PAH through the skin into the RS (RS flux) ($ng/cm^2/h$), ET is the experimental time (hr), ABS_s is the dose of PAH remaining in the membrane at the end of the experiment (ng/cm^2), $ESLR$ is the soil loading (ng/cm^2), C is the initial soil concentration of the soil (ng/mg) (Forsberg et al., 2021, Lort, 2022).

$$ABS_{exp} = (F_{RF} \times ET) + ABS_S$$

Equation 10. Calculation of ABS_{exp} .

$$ABS_d = \frac{ABS_{exp}}{C \times ESLR}$$

Equation 11. Calculation of ABS_d .

Table 21. Parameters applied to calculate the dermal absorption fraction (ABS_d) for BaP as applied by Forsberg et al. (2021).

	F_{rf} (ng/cm ² /h)	ET (h)	ABS_s (ng/cm ²)	ABS_{exp}	C (ng/mg)	ESLR (mg/cm ²)	ABS_d
H16	0.002	24	120.5	129.3	150.5	93.6	0.0086
H16	0.001	10	55.4	55.4	150.5	93.6	0.0039
Lort (2022) Site A	0.01	24	175	175.2	179	81.5	0.0120
Lort (2022) Site A	0.96	1	21.3	22.3	179	81.5	0.0015
Lort (2022) Site B	0.26	24	34.5	40.7	104	81.5	0.0048
Lort (2022) Site B	12.5	1	15.3	27.8	104	81.5	0.0033
Wester et al. (1990) <i>in vitro</i>	0.002	24	0.23	0.3	10	40	0.0007
Wester et al. (1990) <i>in vivo</i>	2.2	24	NA*	52.8	10	40	0.132

**In vivo* study did not provide details on the BaP concentration in the skin.

My results are broadly consistent with Lort (2022) results in revealing lower ABS_d values for BaP compared to the current 0.13 based on Wester et al. (1990). ABS_d values for H16 BaP at the 24-hour timestep fell within the range of ABS_d values for Site A and B in Lort (2022). However, the 1-hour ABS_d value could not be calculated due to the non-detection of BaP in H16 RS. Additionally, the results identified that the 1-hour ABS_d values in Lort (2022) were lower than both Lort (2022) 24-hour results and sample H16 24-hour and 10-hour results. Extending the H16 ABS_d values to HMW PAHs with the highest fluxes, showed higher 24-hour ABS_d values for lighter PAHs such as Fla, C1-Fla/Pyr, BaA and BcFlu (0.066, 0.034, 0.0092 and 0.021 respectively). Furthermore, highlighting the variability in dermal bioavailability for individual PAHs, confirming field-

contaminated soils measuring lower ABS_d values falling below 0.13. This concordance with Lort (2022) undercovers the need for reevaluating ABS_d values, as existing spiked soil estimations can considerably overstate the dermal exposure risks of HMW PAHs from contaminated soils.

Although ABS_d is the preferred value for HHRAs, problems using percentages/fractions such as ABS_d include the fraction absorption being dependent on the soil load applied to skin (Section 6.2). The fraction absorbed decreases as the soil load increases (Peckham et al., 2017). My study used a higher soil loading compared to Wester et al. (1990) (93.6 ng/cm^2 vs 40 ng/cm^2), this ensured that my experiments had an infinite dose and allow for a higher chance of detection of PAHs in the RS samples. Additionally, an infinite dose ensured that the flux was not limited by PAH concentration and that the whole surface area was covered by soil to allow for PAH diffusion (given that a monolayer is difficult to achieve) (Spalt et al., 2009). Therefore, the low ABS_d values observed in my findings are influenced by a combination of high soil loadings and for the samples being real-world soils. This factor highlights the uncertainty with comparing studies with ABS_d values. Potentially comparisons between flux values could resolve issues with ABS_d values sensitivity to loadings (Kissel, 2011), as flux is based on penetration rates. My research focused on determining flux values using infinite dose conditions, future work should determine whether flux changes proportionally with soil loadings and whether flux could be used in HHRAs (Kissel, 2011). My dermal flux values were lower than other dermal studies flux values, which suggest the impact of using real-world soils. This thesis has provided 27 HMW PAHs dermal fluxes, these results can be used to narrow the PAH compounds analysed for dermal investigations by targeting PAHs with the highest fluxes with highest toxicity/carcinogenic group.

Rock-Eval(6) Parameters relationships with Flux

PAH dermal flux varied between the MGP soils (Section 7.4.2) where relationships between RE parameters and the dermal flux were primarily driven by one soil sample (E1.5). This sample exhibited exceptionally high PAH concentrations and extreme RE measurements. This does suggest that MGP soils exhibiting RE measurements similar to the E1.5 sample are likely to comprise

contamination sources with the capacity to generate higher PAH dermal fluxes. The evidence for this is supported by other studies which hypothesised that labile fraction or petrogenic sources positively influence the availability of HMW PAHs (Ukalska-Jaruga and Smreczak, 2020, Bartolomé et al., 2018). In contrast, studies investigating natural OM have seen nonlinear sorption isotherms increasing with aromaticity (Xing, 2001, Xing, 1997), resulting with soils measuring increased aromaticity OM fractions resulting with decreased PAH bioavailability (Ahangar et al., 2008). Which in terms of RE parameters include decreased HI and I-index and increased R-index.

Upon the removal of the E1.5 sample, significant relationships persisted between RS fluxes and the majority of RE parameters for Fla, Pyr, and C1-Fla/Pyr. Conversely, other PAHs exhibited complete loss or significant reduction in regression relationships with RE parameters, this divergence presupposes that relationships with RE apply for the HMW PAHs with the most dominant flux values. It is well-documented that heavier PAHs characterised by high K_{oc} and $\log K_{ow}$ values, exhibit increased hydrophobicity compared to lighter PAHs. For that reason, PAHs with a low ring number exhibit enhanced mobility within soil matrices, as opposed to their heavier counterparts that tend to favour sequestration processes (Wang et al., 2013, Yang et al., 2010). This trend was identified in sections 6.4.5 and 6.5.3, whereby a rapid decrease of RS flux was measured with increasing $\log K_{ow}$ up to a $\log K_{ow} \sim 5.5-6$ and the correlation plateaued for heavier HMW PAHs. The plateauing effect suggests a saturation point where the influence of RS flux on HMW PAHs with the highest $\log K_{ow}$ values becomes negligible.

Interestingly, the influence of RC% on RS fluxes yielded unexpected outcomes, were the results did not show negative correlations between RC% and dermal flux, as presented by prior studies (Poot et al., 2014) (Section 7.5.1). One point of view is that an influence of the different contamination sources and heightened PAH contamination in this study caused conflicting result to other studies. RC% associated with BC was inferred to play a role in preventing PAH release in soils, however the BC and RC in these MGP soils originated from diverse by-products contamination sources that have been subjected to environmental impacts in the soils for decades (Section 7.5.1). As a result, introducing complexity to

understanding RC or BC, with limited research on the types of BC and the behaviour of BC over long timescales (Semple et al., 2013). The physicochemical attributes of BC fluctuate based on its origin, combustion, weathering conditions and mode of formation (Semple et al., 2013). These considerations explore the idea that BC present within the RC% fraction in MGP soils differ with their ability to sequester PAHs, thus adding uncertainty into estimating bioavailability of PAHs using RC% values. Other studies (Bartolomé et al., 2018, Barnier et al., 2014) have also measured no apparent correlations with soil properties on the PAH behaviour in soils. The outcomes emphasise the complexity of soil properties and the variability in results within and between studies. Section 7.51 presents possible bulk OM parameters that have the potential to be indicators of the extent of PAH bioavailability, uncertainties persist as to the causation of these relationships. Whether the relationships stem from the extent of contamination, contamination source or soil properties remains difficult to determine.

8.3 Implications and future directions

8.3.1 Implications

The findings in this research have presented numerous insights into providing a greater understanding of both the distributions of parent and alkyl-PAHs in MGP soils and the dermal bioavailability of a wider set of PAHs in contaminated soils. Implications of the findings in these chapters have been presented in Sections 5.4.4, 6.5.5 and 7.5.4. This research builds on earlier research conducted by Lort (2022). It also relates to a wider programme of work on dermal bioavailability being conducted by the British Geological Survey with WSP, National Grid and the University of Nottingham (Beriro et al., 2016, Beriro et al., 2020)(Williams-Clayson et al., *in review*). The previous work determined that both soil type and selected HMW-PAH properties affected the amount of HMW PAH released from soil into sebum (Beriro et al., 2020) and membrane (Lort, 2022) (Section 2.4.4). As a result, this study investigated a greater number of PAHs and explored soil properties (bulk OM) influence on the dermal bioavailability.

Both my study and Lort (2022) measured native *in vitro* PAH dermal bioavailability from real-world contaminated soils from former MGP sites. Both studies found the dermal flux and ABS_d values were lower than the current 13%

value used in the CLEA HHRA software (Environment Agency, 2009a). My findings suggest that real-world soils impacted by environmental conditions hinder the release of PAHs from soil, therefore current HHRAs are potentially overestimating the risks of HMW PAHs by dermal exposure (Section 6.5.5). This overestimation might lead to further soils needing remediation, when in fact they are not a risk. As a result, landowners of brownfield land might be currently required to undertake unnecessary remediation work incurring high costs, such work and costs might forestall brownfield land from being re-developed into useful urban developments, meaning cheaper alternatives like greenfield land might be developed (Section 2.2.2).

The findings in this thesis can help improve understanding of the risks MGP contaminated soils pose *via* the dermal exposure pathway. Chapter 5 showed that classifying soils by their MGP processes to be difficult but could identify two MGP processes. I have provided a data set of the PAH distributions (parent and alkylated PAHs) in MGP soils, the results reported in this thesis could be used by risk assessors to understand the typical PAHs present in contaminated soils from UK MGP sites, especially that alkyl-PAHs are present at potentially high concentrations. Knowledge of the distribution and abundance of PAHs at MGP soils provide new insights and focus points for HHRAs, that can be related to exposure pathways. For example, LMW PAHs would be suspected as not being a priority at sites with no association to oil in MGP process and the investigation to focus on HMW PAHs, which have higher contributions to the dermal and oral exposure pathways compared to inhalation. The key finding from this thesis is the reported dermal bioavailability of 27 HMW PAHs, the highest number of HMW PAHs found in the literature (Section 2.4.4). The PAH studied uniquely include alkyl-PAHs, which as shown in Section 5.4.1 are present at varying proportions at MGP sites. Therefore, my work has helped provide knowledge on both the expected PAHs at MGP and their potential dermal uptake into the human body, eluding that different PAHs have different dermal uptakes. This is important because current guidance using the surrogate marker approach, particularly when assessing risks using BaP, as it may lead to both underestimation and overestimation of risks associated with other PAHs.

My research has provided a large dataset that can be used by stakeholders, policy makers, consultants, remediation contractors etc.. To inform an understanding of the distributions and abundance of PAH and dermal bioavailability in MGP soils. In addition, my work has indicated the feasibility of measuring and integrating RE parameters into future models for dermal bioavailability estimation. RE is a relatively quick and low-cost screening tool, which provides a high number of parameters describing bulk OM properties from a single measurement with limited sample preparation and low sample mass requirements. These factors could potentially mean high numbers of samples analysed relatively quickly before sending large sample sets to be analysed by other more expensive methods (such as GC-MS). Overall, this research has the potential to help more brownfield land be redeveloped into beneficial urban developments, as this thesis findings suggest that the dermal bioavailability of 27 HMW PAHs are lower than current HHRA guidance values and the RE method can potentially screen large batches of soils quickly. This research helps contribute to the work on making better informed HHRAs which have the potential to increase the development on brownfield land can help prevent new building developments on greenfield land and help with sustainability goals.

8.3.2 Research Constraints

Although this thesis reported several significant findings to further understand the contamination of PAHs in MGP soils and their dermal bioavailability, the research had several constraints which influenced the direction of the scope of this PhD. Sections 5.4.4, Section 6.5.5 and Section 8.5.2 provide examples of several of the constraints experienced in this research.

The main constraint in my research was that limited samples were measured for dermal bioavailability due to the time constraints imposed by the pandemic – related to the lockdown and laboratory access limitations. The unforeseen delay also impacted the work of Lort (2022) who was developing the *in vitro* experiment method to be used in this research, thus further delaying this research because my research required the method being developed. The GC-MS instrument was available for a limited timeframe, resulting with samples needing to be prepared for specific periods and fewer samples investigated than initially planned. If more time was available, this PhD would have measured more MGP

soils for dermal bioavailability and more membrane samples. PAH quantification of RS samples was prioritised over membrane measurements. A limited number of membranes were run at the end of this research as a precaution, as one of the concerns in this research was that the membrane samples could damage the GC-MS instrument. Membranes contain a number of different lipid compounds which have the potential to damage the GC-MS/MS instrument and column.

Derivatisation is usually performed on lipids before GC analysis to convert less volatile and thermally labile compounds into compounds that are able to be analysed in a gaseous state (Řezanka et al., 2016). As a result, derivatisation prevents lipids damaging the instrument and reduces analyte adsorption in the GC system, thus improving detector response and peak shapes (Orata, 2012). In this PhD, a quick examination in the laboratory found that a new clean membrane extracted by ASE, cleaned by SPE and blown down by a gentle stream of nitrogen, resulted with the remains of a gel-like substance that would not evaporate further. This suggests that the Strat-M membrane lipids were extracted and present in GC-MS/MS analysis undertaken in this research. Derivatisations of the lipids were not undertaken in my research because the exact lipids present in the membranes were unknown and there was not enough time to investigate. Lort (2022) discovered that isopropyl myristate appeared as a large peak at m/z 166 when analysing Strat-M membranes, however reported that no PAHs were detected at the same retention time. Therefore, the Strat-M matrix did not affect the detection of PAHs from membranes and could be used. However, Lort (2022) stated that isopropyl myristate could reduce the GC column lifespan and have adverse effects on the GC-MS operation, he suggested that the presence of the isopropyl myristate should be minimised. Future work should incorporate a derivatisation method on the Strat-M membrane in order for the membranes to be able to run on the GC-MS/MS instrument without potential damage.

8.3.3 Future directions

This thesis has presented a range of findings intended to aid with the development of future research and guidance associated to factors influencing the dermal bioavailability of PAHs from contaminated soils. Each of the research

papers have proposed several future work ideas based, presented in Sections 5.4.4, 6.5.5 and 7.5.4. This section highlights some of the key suggestions for future research with a more detailed description and makes further suggestions.

Investigating a greater number of MGP soils and sources to determine the key drivers impacting PAH release from soil

Future research can use this study's dermal *in vitro* experiment method to investigate the key factors influencing the dermal bioavailability of PAHs by experimenting with greater number of MGP soils (Section 7.5.4). A comprehensive site investigation and source characterisation should be conducted to obtain a sub selection of soils with a wide range of initial PAH concentrations, PAH distributions, RE parameters and be composed of different sources. Investigating a boarder range of soils would determine whether the extreme PAH concentrations from soil E1.5 was the main driver for the RS flux or whether it was a combination of factors. Particularly, whether the RE parameters stated in Section 7.5.1 have a relationship with the PAHs with the highest fluxes. The findings of this future work would enhance our understanding of the key properties influencing the dermal bioavailability of PAHs from real-world soils. This knowledge can be used to create a predictive model that factors in PAH physicochemical attributes, exposure duration, and soil properties (such as RE parameters) to yield more accurate dermal bioavailability estimations. Such estimations can help make HHRA assess contaminated land with greater accuracy, help create new improved guidance for the development on brownfield land and potentially decrease contamination remediation costs.

Determine how representative the dermal in vitro method is

Future work should determine how representative the dermal *in vitro* method is. Although Lort (2022) validated the method by comparing the dermal fluxes generated from spiked solutions with published data (Section 3.9.1), for an *in vitro* method to be both regulatory and scientific accepted, the *in vitro* method should be correlated to a *in vivo* method (Section 2.4.3) (Wragg et al., 2011, Juhasz et al., 2014). Future work should validate the method against a *in vivo* study so that the findings using this method can be used in guidance.

Exploring impacts of exposure time for different PAHs

The number and duration of the exposure timesteps using the dermal method should be extended. My work found that a large number of PAHs were not detected in the membrane or RS within 24-hours (Section 6.5.1 and Section 6.5.2), particularly heavier PAHs and alkyl-PAHs were not detected. One exploration, perhaps involving spiking experiments (to ensure PAH concentration is not the limiting factor) or extended exposure timesteps experiments, would shed light on the dynamics and potential risks associated with these compounds. Although other studies (Forsberg et al., 2021) have agreed with my findings that the heaviest PAHs were not present in the RS. Although future work could confirm whether these PAHs are released from soil eventually, this would also be interesting for the alkylated BaA/Chry/TPh compounds which were not detected. Initial concentrations of these PAHs were low in the MGP soils in my research (Section 6.4.2); thus, it is assumed from this research that these HMW PAHs are not a high risk to human dermal exposure. Future investigations expanding the number of timesteps would also help determine whether all PAHs detected in the membrane ultimately migrate to the RS or if other factors, such as concretion gradients, influence the behaviour of PAHs within the membrane. Drawing parallels to Forsberg et al. (2021) could offer insights into the post-contact behaviour of HMW PAHs in the skin. Additionally, investigating an extended range of timesteps would enable evaluation of the timesteps yielding the highest fluxes (peak flux) and determine when steady state flux occurs. These findings could be added to the created predictive models suggested previously.

Investigate other factors that could potentially impact the dermal bioavailability

My PhD focused on RE and PSA parameters influences on the release of PAHs from soil, however there are other factors that could be investigated in future work. Section 2.5 in the literature review described several other soil properties that other studies have suggested influence the release of PAHs from soil including other OM descriptors (Section 2.5.4), inorganic components (Section 2.5.7), pore sizes (2.5.8), soil moisture (2.5.9), combined soil property effects (Section 2.5.10) and sources (Section 2.3.2).

Xia et al. (2016) has stated that sources are an important factor in controlling PAH release from soil. My study found different dermal bioavailability results between BCR-524 and the MGP soils. However, exploration into the influence of different types of contamination on the dermal bioavailability were not explored due to time constraints in this research. Future work could explore the dermal bioavailability of different contamination types by repeating the dermal experiment with BCR-524 alongside other end members and other soils contaminated by other sources should be incorporated. My research also found that soils rich in amorphous labile OC had increased PAH desorption (Section 7.5.1), potentially this could mean soils contaminated by *n*-alkanes (oils) have greater amounts of PAHs released. Future work could characterise additional organic compounds, such as alkanes, to determine whether these compounds assist with the release of PAHs from soils (Section 7.5.1). Additionally, extending the PCA to encompass a wider range of organic contaminants could refine the characterisation of MGP processes as previously determined for tars (McGregor et al., 2012) (Section 5.4.4).

8.4 Summary

Overall, this general discussion section has evaluated the key findings and how the findings in my PhD link to the research aim, questions and objectives determined from the gaps in the literature (Sections 8.2.1, 8.2.2 and 8.2.3). Section 8.2.3 discusses the research by interlinking the three chapter 5, 6 and 7 findings to answering this PhD research focus, highlighting sections in this thesis and expanding further on discussions not explored in the three chapters. Section 8.3.1 presents what the implications are from these findings and their importance to brownfield land development. This thesis has reported many findings which has subsequently led to new questions and future research worth exploring (Section 8.3.3), implementing the recommended research would allow a comprehensive understanding of the PAH factors impacting PAH release from soils.

CHAPTER 9

CONCLUSION

This research studied the PAHs and bulk OM in former MGP soils. Its aims were:

- to determine whether distributions of parent and alkylated PAHs, alongside the bulk OM, could be used to characterise the MGP processes that contaminated the soils;
- to understand how different types of HMW PAHs, particularly parent versus alkylated PAHs, impact human *in vitro* dermal bioavailability;
- and to investigate potential relationships between bulk OM (characterised by RE) and the dermal bioavailability of HMW PAHs.

To achieve these aims I developed an enhanced *in vitro* bioavailability method for a large number of parent and alkylated PAHs in MGP soils using GC-MS/MS. This section will summarise the progress made towards these aims. The research showed that two MGP processes can be distinguished from the bulk cluster of MGP soils using PCA with 51 PAHs, and that bulk OM can help characterise soils with higher PAH contamination (Section 5.4.3). This research is novel by investigating the greatest number of PAHs for dermal bioavailability (27 HMW PAHs compared to previous studies maximum of 14 PAHs), including for the first-time alkyl-PAHs. This research has shown the differences between the dermal bioavailability of parent and alkylated HMW PAHs and individual PAHs in a range of MGP soils and a CRM BCR-524 (Section 6.5.1 and Section 6.5.2). The results show that higher fluxes occurred for soil to membranes (membrane flux), for PAHs with a lower ring number and that parent PAHs had higher fluxes compared to their alkylated counterpart. Importantly I found that all 27 HMW PAHs investigated in this research had lower dermal bioavailability values than other dermal studies, including the study that the HHRA guidance is based on, which was suggested to be a result of using real-world soils opposed to artificially spiked soils (Section 6.5.4 and Section 8.2.3).

The relationship between the bulk OM and the PAH dermal bioavailability initially showed significant relationships determined by linear regression,

primarily driven by a soil characterised by notably elevated PAH concentrations and OM bulk values (Sections 7.5.1 and 7.5.2). These are interesting findings as one soil is different to the others; this has raised further questions about the main factors influencing the release of PAHs from soil. To obtain a better understanding of the implications of the results found in this research, several recommendations of future research are presented (Section 8.3.3).

Reflecting on the methods applied in this research, the human dermal *in vitro* method has been shown to be a valuable method in understanding the dermal bioavailability of HMW PAHs in soils with varying initial soil concentrations. The results generated by the method show the variability of dermal fluxes among the 27 HMW PAHs and highlighted HMW PAHs with the highest dermal fluxes that could potentially pose a risk to human health through the dermal pathway. BaP concentrations in the MGP soils investigated ranged from 13.54 to 160.49 mg/kg, these concentrations are above the generic assessment criteria (GAC) for residential land use (5 mg/kg). These findings imply that even soils with high concentrations experience lower than expected human dermal bioavailability for HMW PAHs. A possible outcome of this research would be to develop it further and validate the method using an *in vitro in vivo* correlation approach, as these initial findings suggest that the dermal risks from both parent and alkylated HMW PAHs are lower than current guidance. A higher GAC value could possibly result with more brownfield sites being developed into urban sites because an increased number of brownfield sites would not require excessive and expensive remediation.

In summary, the dataset and findings of this thesis presented in Chapters 5, 6 and 7 help advance knowledge on the dermal bioavailability of HMW PAHs. The findings in this PhD help address several knowledge gaps identified in the literature (Section 2.6). The findings provide an understanding of the behaviour of real-world contaminated soils from MGP sites, the dermal bioavailability of both parent and alkylated PAHs and a further understanding of the relationship of bulk OM with the dermal bioavailability. The findings provide an indication of the use of RE as a screening tool to help make predictions of the dermal bioavailability of HMW PAHs in contaminated soils. It is anticipated that the contributions of this thesis will stimulate further inquiry, trigger innovative

methodologies, and ultimately contribute to advancing the HHRA's used in contamination site assessments. This work contributes to the refinement of HHRA's and policies addressing soil contamination and its impact on human health, thereby safeguarding the well-being of communities. This research is important for decision making by landowners, remediation companies, consultants, and regulators as it can help reduce the uncertainties in the HHRA for chronic exposure to carcinogenic chemicals in soils at contaminated brownfield sites.

CHAPTER 10

REFERENCES

- ABDEL-RAHMAN, M. S., SKOWRONSKI, G. A. & TURKALL, R. M. 2002. Assessment of the Dermal Bioavailability of Soil-Aged Benzo(a)pyrene. *Human and Ecological Risk Assessment: An International Journal*, 8, 429-441.
- ABDEL-SHAIFY, H. I. & MANSOUR, M. S. M. 2016. A review on polycyclic aromatic hydrocarbons: Source, environmental impact, effect on human health and remediation. *Egyptian Journal of Petroleum*, 25, 107-123.
- ACHTEN, C. & ANDERSSON, J. T. 2015. Overview of Polycyclic Aromatic Compounds (PAC). *Polycyclic Aromatic Compounds*, 35, 177-186.
- AHANGAR, A. G., SMERNIK, R. J., KOOKANA, R. S. & CHITTLEBOROUGH, D. J. 2008. Separating the effects of organic matter–mineral interactions and organic matter chemistry on the sorption of diuron and phenanthrene. *Chemosphere*, 72, 886-890.
- AHMAD, N., ZHU, Y., IBRAHIM, M., WAQAS, M. & WAHEED, A. 2018. Development of a Standard Brownfield Definition, Guidelines, and Evaluation Index System for Brownfield Redevelopment in Developing Countries: The Case of Pakistan. *Sustainability*, 10, 4347.
- ALALAIWE, A., LIN, Y.-K., LIN, C.-H., WANG, P.-W., LIN, J.-Y. & FANG, J.-Y. 2020. The absorption of polycyclic aromatic hydrocarbons into the skin to elicit cutaneous inflammation: The establishment of structure–permeation and in silico–in vitro–in vivo relationships. *Chemosphere*, 255, 126955.
- ALAWI, M. A. & AZEEZ, A. L. 2016. Study of polycyclic aromatic hydrocarbons (PAHs) in soil samples from Al-Ahdab oil field in Wasit Region, Iraq. *Toxin Reviews*, 35, 69-76.
- AMELLAL, N., PORTAL, J. M. & BERTHELIN, J. 2001. Effect of soil structure on the bioavailability of polycyclic aromatic hydrocarbons within aggregates of a contaminated soil. *Applied Geochemistry*, 16, 1611-1619.
- ANDERSSON, J. T. & ACHTEN, C. 2015. Time to Say Goodbye to the 16 EPA PAHs? Toward an Up-to-Date Use of PACs for Environmental Purposes. *Polycyclic Aromatic Compounds*, 35, 330-354.
- ANDREAE, M. O. 1995. Chapter 10 - Climatic effects of changing atmospheric aerosol levels. In: HENDERSON-SELLERS, A. (ed.) *World Survey of Climatology*. Elsevier.
- BALTRONS, O., LÓPEZ-MESAS, M., PALET, C., LE DERF, F. & PORTET-KOLTALO, F. 2013. Molecularly imprinted polymer-liquid

chromatography/fluorescence for the selective clean-up of hydroxylated polycyclic aromatic hydrocarbons in soils. *Analytical Methods*, 5, 6297-6305.

BARNIER, C., OUVRARD, S., ROBIN, C. & MOREL, J. L. 2014. Desorption kinetics of PAHs from aged industrial soils for availability assessment. *Science of the Total Environment*, 470-471, 639-645.

BARTOLOMÉ, N., HILBER, I., SOSA, D., SCHULIN, R., MAYER, P. & BUCHELI, T. D. 2018. Applying no-depletion equilibrium sampling and full-depletion bioaccessibility extraction to 35 historically polycyclic aromatic hydrocarbon contaminated soils. *Chemosphere*, 199, 409-416.

BEHAR, F., BEAUMONT, V. & PENTEADO, D. B. 2001a. Rock Eval 6 Technology: Performance and Development. *Oil and Gas Science and Technology*, 56, 111-134.

BEHAR, F., BEAUMONT, V. & PENTEADO, H. D. B. 2001b. Rock-Eval 6 technology: performances and developments. *Oil & Gas Science and Technology*, 56, 111-134.

BERIRO, D. J., CAVE, M., KIM, A., CRAGGS, J., WRAGG, J., THOMAS, R., TAYLOR, C., NATHANAIL, C. P. & VANE, C. 2020. Soil-sebum partition coefficients for high molecular weight polycyclic aromatic hydrocarbons (HMW-PAH). *Journal of Hazardous Materials*, 122633.

BERIRO, D. J., CAVE, M. R., WRAGG, J., THOMAS, R., WILLS, G. & EVANS, F. 2016. A review of the current state of the art of physiologically-based tests for measuring human dermal in vitro bioavailability of polycyclic aromatic hydrocarbons (PAH) in soil. *Journal of Hazardous Materials*, 305, 240-259.

BERIRO, D. J., VANE, C. H., CAVE, M. R. & NATHANAIL, C. P. 2014. Effects of drying and comminution type on the quantification of Polycyclic Aromatic Hydrocarbons (PAH) in a homogenised gasworks soil and the implications for human health risk assessment. *Chemosphere*, 111, 396-404.

BOGAN, B. W. & SULLIVAN, W. R. 2003. Physicochemical soil parameters affecting sequestration and mycobacterial biodegradation of polycyclic aromatic hydrocarbons in soil. *Chemosphere*, 52, 1717-1726.

BONIN, J. L. & SIMPSON, M. J. 2007. Variation in Phenanthrene Sorption Coefficients with Soil Organic Matter Fractionation: The Result of Structure or Conformation? *Environmental Science & Technology*, 41, 153-159.

BOONCHAN, S., BRITZ, M. L. & STANLEY, G. A. 2000. Degradation and mineralization of high-molecular-weight polycyclic aromatic hydrocarbons by defined fungal-bacterial cocultures. *Applied and Environmental Microbiology*, 66, 1007-1019.

BRADY, N. C., WEIL, R. R. & WEIL, R. R. 2008. *The nature and properties of soils*, Prentice Hall Upper Saddle River, NJ.

- BRÄNDLI, R. C., HARTNIK, T., HENRIKSEN, T. & CORNELISSEN, G. 2008. Sorption of native polyaromatic hydrocarbons (PAH) to black carbon and amended activated carbon in soil. *Chemosphere*, 73, 1805-1810.
- BROWN, C., BOYD, D. S., SJÖGERSTEN, S. & VANE, C. H. 2023. Detecting tropical peatland degradation: Combining remote sensing and organic geochemistry. *PLOS ONE*, 18, e0280187.
- BUCKS, D. A. W., MCMASTER, J. R., MAIBACH, H. I. & GUY, R. H. 1988. Bioavailability of Topically Administered Steroids: A “Mass Balance” Technique. *Journal of Investigative Dermatology*, 91, 29-33.
- CACHADA, A., ROCHA-SANTOS, T. & DUARTE, A. C. 2018. Chapter 1 - Soil and Pollution: An Introduction to the Main Issues. In: DUARTE, A. C., CACHADA, A. & ROCHA-SANTOS, T. (eds.) *Soil Pollution*. Academic Press.
- CARMICHAEL, L. M., CHRISTMAN, R. F. & PFAENDER, F. K. 1997. Desorption and Mineralization Kinetics of Phenanthrene and Chrysene in Contaminated Soils. *Environmental Science & Technology*, 31, 126-132.
- CARRIE, J., SANEI, H. & STERN, G. 2012. Standardisation of Rock–Eval pyrolysis for the analysis of recent sediments and soils. *Organic Geochemistry*, 46, 38-53.
- CAVALIERI, E. & ROGAN, E. 2014. The molecular etiology and prevention of estrogen-initiated cancers: Ockham's Razor: Pluralitas non est ponenda sine necessitate. Plurality should not be posited without necessity. *Mol Aspects Med*, 36, 1-55.
- CAVE, M. R., VANE, C. H., KIM, A., MOSS-HAYES, V. L., WRAGG, J., RICHARDSON, C. L., HARRISON, H., NATHANAIL, C. P., THOMAS, R. & WILLS, G. 2015. Measurement and modelling of the ingestion bioaccessibility of polyaromatic hydrocarbons in soils. *Environmental Technology & Innovation*, 3, 35-45.
- CHEN, D., XING, B. & XIE, W. 2007. Sorption of phenanthrene, naphthalene and o-xylene by soil organic matter fractions. *Geoderma*, 139, 329-335.
- CHUNG, N. & ALEXANDER, M. 1998. Differences in Sequestration and Bioavailability of Organic Compounds Aged in Dissimilar Soils. *Environmental Science & Technology*, 32, 855-860.
- CHUNG, N. & ALEXANDER, M. 2002. Effect of soil properties on bioavailability and extractability of phenanthrene and atrazine sequestered in soil. *Chemosphere*, 48, 109-115.
- CIPULLO, S., PRPICH, G., CAMPO, P. & COULON, F. 2018. Assessing bioavailability of complex chemical mixtures in contaminated soils: Progress made and research needs. *Science of The Total Environment*, 615, 708-723.
- CL:AIRE 2014. SP1010 – Development of Category 4 Screening Levels for Assessment of Land Affected by Contamination. Department for Environment

Food and Rural Affairs: Contaminated Land: Applications in Real Environments.

CL:AIRE 2015. Soil and Groundwater Remediation Technologies for Former Gasworks and Gasholder Sites. CL:AIRE.

COLE, S. & JEFFRIES, J. 2009. Using Soil Guideline Values. Bristol.

COOPER, H. V., VANE, C. H., EVERS, S., APLIN, P., GIRKIN, N. T. & SJÖGERSTEN, S. 2019. From peat swamp forest to oil palm plantations: The stability of tropical peatland carbon. *Geoderma*, 342, 109-117.

COULING, N. R., TOWELL, M. G. & SEMPLE, K. T. 2010. Biodegradation of PAHs in soil: Influence of chemical structure, concentration and multiple amendment. *Environmental Pollution*, 158, 3411-3420.

CPRE (THE COUNTRYSIDE CHARITY) 2019. State of Brownfield 2019: An updated analysis on the potential of brownfield land for housing.

CRAMPON, M., BUREAU, F., AKPA-VINCESLAS, M., BODILIS, J., MACHOUR, N., LE DERF, F. & PORTET-KOLTALO, F. 2014. Correlations between PAH bioavailability, degrading bacteria, and soil characteristics during PAH biodegradation in five diffusely contaminated dissimilar soils. *Environmental Science and Pollution Research*, 21, 8133-8145.

CRANK, J. 1979. *The mathematics of diffusion*, Oxford university press.

DE JONGE, L. W., MOLDRUP, P., DE JONGE, H. & CELIS, R. 2008. Sorption and leaching of short-term-aged PAHs in eight European soils: Link to physicochemical properties and leaching of dissolved organic carbon. *Soil Science*, 173, 13-24.

DE MELO, B. A. G., MOTTA, F. L. & SANTANA, M. H. A. 2016. Humic acids: Structural properties and multiple functionalities for novel technological developments. *Materials Science and Engineering: C*, 62, 967-974.

DEFRA 2012. Environmental Protection Act 1990: Part 2A. Contaminated land. London, UK: Department for Environment Food & Rural Affairs.

DEFRA & EA 2002. Contaminants in soil: collation of toxicological data and intake values for humans. Environment Agency.

DENYS, S., CABOCHE, J., TACK, K., RYCHEN, G., WRAGG, J., CAVE, M., JONDREVILLE, C. & FEIDT, C. 2012. In vivo validation of the unified BARGE method to assess the bioaccessibility of arsenic, antimony, cadmium, and lead in soils. *Environmental Science & Technology*, 46, 6252-6260.

DISNAR, J. R., GUILLET, B., KERAVIS, D., DI-GIOVANNI, C. & SEBAG, D. 2003. Soil organic matter (SOM) characterization by Rock-Eval pyrolysis: scope and limitations. *Organic Geochemistry*, 34, 327-343.

DOICK, K. J., BURAUDEL, P., JONES, K. C. & SEMPLE, K. T. 2005. Distribution of Aged ¹⁴C-PCB and ¹⁴C-PAH Residues in Particle-Size and

Humic Fractions of an Agricultural Soil. *Environmental Science & Technology*, 39, 6575-6583.

DONG, J., LI, F. & XIE, K. 2012. Study on the source of polycyclic aromatic hydrocarbons (PAHs) during coal pyrolysis by PY–GC–MS. *Journal of Hazardous Materials*, 243, 80-85.

DOUGLAS, G. S., BENCE, A. E., PRINCE, R. C., MCMILLEN, S. J. & BUTLER, E. L. 1996. Environmental Stability of Selected Petroleum Hydrocarbon Source and Weathering Ratios. *Environmental Science & Technology*, 30, 2332-2339.

DUAN, L. & NAIDU, R. 2013. Effect of ionic strength and index cation on the sorption of phenanthrene. *Water, Air, & Soil Pollution*, 224, 1700.

DUAN, L., NAIDU, R., LIU, Y., PALANISAMI, T., DONG, Z., MALLAVARAPU, M. & SEMPLE, K. T. 2015. Effect of ageing on benzo[a]pyrene extractability in contrasting soils. *Journal of Hazardous Materials*, 296, 175-184.

DUAN, L., PALANISAMI, T., LIU, Y., DONG, Z., MALLAVARAPU, M., KUCHEL, T., SEMPLE, K. T. & NAIDU, R. 2014. Effects of ageing and soil properties on the oral bioavailability of benzo [a] pyrene using a swine model. *Environment international*, 70, 192-202.

EFSA, BUIST, H., CRAIG, P., DEWHURST, I., HOUGAARD BENNEKOU, S., KNEUER, C., MACHERA, K., PIEPER, C., COURT MARQUES, D., GUILLOT, G., RUFFO, F. & CHIUSOLO, A. 2017. Guidance on dermal absorption. *EFSA Journal*, 15, e04873.

EHLERS, G. A. C. & LOIBNER, A. P. 2006. Linking organic pollutant (bio)availability with geosorbent properties and biomimetic methodology: A review of geosorbent characterisation and (bio)availability prediction. *Environmental Pollution*, 141, 494-512.

ENELL, A., REICHENBERG, F., EWALD, G. & WARFVINGE, P. 2005. Desorption kinetics studies on PAH-contaminated soil under varying temperatures. *Chemosphere*, 61, 1529-1538.

ENVIRONMENT AGENCY 2009a. CLEA Software (Version 1.05) Handbook.

ENVIRONMENT AGENCY 2009b. *Updated technical background to the CLEA model*, Environment Agency.

ENVIRONMENT AGENCY 2018. Performance Standard for Laboratories Undertaking Chemical Testing of Soil. 5 ed.

EUROPEAN CENTRE FOR ECOTOXICOLOGY AND TOXICOLOGY OF CHEMICALS 2002. Scientific Principles of Soil hazard Assessment of Substances. Brussels, Belgium.

FALLAHTAFTI, S., RANTANEN, T., BROWN, R. S., SNIECKUS, V. & HODSON, P. V. 2012. Toxicity of hydroxylated alkyl-phenanthrenes to the early

life stages of Japanese medaka (*Oryzias latipes*). *Aquatic Toxicology*, 106-107, 56-64.

FISEROVA-BERGEROVA, V., PIERCE, J. T. & DROZ, P. O. 1990. Dermal absorption potential of industrial chemicals: Criteria for skin notation. *American Journal of Industrial Medicine*, 17, 617-635.

FORSBERG, N. D., HANEY, J. T., HOEGER, G. C., MEYER, A. K. & MAGEE, B. H. 2021. Oral and Dermal Bioavailability Studies of Polycyclic Aromatic Hydrocarbons from Soils Containing Weathered Fragments of Clay Shooting Targets. *Environmental Science & Technology*.

FRASCH, H. F., DOTSON, G. S., BUNGE, A. L., CHEN, C.-P., CHERRIE, J. W., KASTING, G. B., KISSEL, J. C., SAHMEL, J., SEMPLE, S. & WILKINSON, S. 2014. Analysis of finite dose dermal absorption data: Implications for dermal exposure assessment. *Journal of Exposure Science & Environmental Epidemiology*, 24, 65-73.

GALLACHER, C., THOMAS, R., LORD, R., KALIN, R. M. & TAYLOR, C. 2017a. Comprehensive database of Manufactured Gas Plant tars—Part B Aliphatic and aromatic compounds. *Rapid Communications in Mass Spectrometry*, 31, 1239-1249.

GALLACHER, C., THOMAS, R., LORD, R., KALIN, R. M. & TAYLOR, C. 2017b. Comprehensive database of Manufactured Gas Plant tars. Part A. Database. *Rapid Communications in Mass Spectrometry*, 31, 1231-1238.

GALLACHER, C., THOMAS, R., TAYLOR, C., LORD, R. & KALIN, R. M. 2017c. Comprehensive composition of Creosote using comprehensive two-dimensional gas chromatography time-of-flight mass spectrometry (GCxGC-TOFMS). *Chemosphere*, 178, 34-41.

GAO, M., WANG, Y., DONG, J., LI, F. & XIE, K. 2016. Release behavior and formation mechanism of polycyclic aromatic hydrocarbons during coal pyrolysis. *Chemosphere*, 158, 1-8.

GARCIN, Y., SCHEFUß, E., DARGIE, G. C., HAWTHORNE, D., LAWSON, I. T., SEBAG, D., BIDDULPH, G. E., CREZEE, B., BOCKO, Y. E., IFO, S. A., MAMPOUYA WENINA, Y. E., MBEMBA, M., EWANGO, C. E. N., EMBA, O., BOLA, P., KANYAMA TABU, J., TYRRELL, G., YOUNG, D. M., GASSIER, G., GIRKIN, N. T., VANE, C. H., ADATTE, T., BAIRD, A. J., BOOM, A., GULLIVER, P., MORRIS, P. J., PAGE, S. E., SJÖGERSTEN, S. & LEWIS, S. L. 2022a. Hydroclimatic vulnerability of peat carbon in the central Congo Basin. *Nature*.

GARCIN, Y., SCHEFUß, E., DARGIE, G. C., HAWTHORNE, D., LAWSON, I. T., SEBAG, D., BIDDULPH, G. E., CREZEE, B., BOCKO, Y. E., IFO, S. A., MAMPOUYA WENINA, Y. E., MBEMBA, M., EWANGO, C. E. N., EMBA, O., BOLA, P., KANYAMA TABU, J., TYRRELL, G., YOUNG, D. M., GASSIER, G., GIRKIN, N. T., VANE, C. H., ADATTE, T., BAIRD, A. J., BOOM, A., GULLIVER, P., MORRIS, P. J., PAGE, S. E., SJÖGERSTEN, S. &

- LEWIS, S. L. 2022b. Hydroclimatic vulnerability of peat carbon in the central Congo Basin. *Nature*, 612, 277-282.
- GEIER, M. C., CHLEBOWSKI, A. C., TRUONG, L., MASSEY SIMONICH, S. L., ANDERSON, K. A. & TANGUAY, R. L. 2018. Comparative developmental toxicity of a comprehensive suite of polycyclic aromatic hydrocarbons. *Archives of Toxicology*, 92, 571-586.
- GERKE, J. 2019. Black (pyrogenic) carbon in soils and waters: a fragile data basis extensively interpreted. *Chemical and Biological Technologies in Agriculture*, 6, 13.
- GHETU, C. C., SCOTT, R. P., WILSON, G., LIU-MAY, R. & ANDERSON, K. A. 2021. Improvements in identification and quantitation of alkylated PAHs and forensic ratio sourcing. *Analytical and Bioanalytical Chemistry*.
- GHOSH, U., ZIMMERMAN, J. R. & LUTHY, R. G. 2003. PCB and PAH speciation among particle types in contaminated harbor sediments and effects on PAH bioavailability. *Environmental science & technology*, 37, 2209-2217.
- GIRKIN, N. T., VANE, C. H., COOPER, H. V., MOSS-HAYES, V., CRAIGON, J., TURNER, B. L., OSTLE, N. & SJÖGERSTEN, S. 2019. Spatial variability of organic matter properties determines methane fluxes in a tropical forested peatland. *Biogeochemistry*, 142, 231-245.
- GODLEWSKA, P. & OLESZCZUK, P. 2021. EFFECT OF BIOMASS ADDITION BEFORE SEWAGE SLUDGE PYROLYSIS ON THE PERSISTENCE AND BIOAVAILABILITY OF POLYCYCLIC AROMATIC HYDROCARBONS IN BIOCHAR-AMENDED SOIL. *Chemical Engineering Journal*, 132143.
- GORMLEY, A., POLLARD, S. & ROCKS, S. 2011. *Guidelines for environmental risk assessment and management: Green Leaves III*, Cranfield University, Department for Environmental Food and Rural Affairs.
- HAESELER, F., BLANCHET, D., DRUELLE, V., WERNER, P. & VANDECASTEELE, J.-P. 1999. Analytical Characterization of Contaminated Soils from Former Manufactured Gas Plants. *Environmental Science & Technology*, 33, 825-830.
- HALE, S. E., LEHMANN, J., RUTHERFORD, D., ZIMMERMAN, A. R., BACHMANN, R. T., SHITUMBANUMA, V., O'TOOLE, A., SUNDQVIST, K. L., ARP, H. P. H. & CORNELISSEN, G. 2012. Quantifying the Total and Bioavailable Polycyclic Aromatic Hydrocarbons and Dioxins in Biochars. *Environmental Science & Technology*, 46, 2830-2838.
- HAN, Y., CHEN, Y., FENG, Y., SONG, W., CAO, F., ZHANG, Y., LI, Q., YANG, X. & CHEN, J. 2020. Different formation mechanisms of PAH during wood and coal combustion under different temperatures. *Atmospheric Environment*, 222, 117084.

HANEY, J. T., FORSBERG, N. D., HOEGER, G. C., MAGEE, B. H. & MEYER, A. K. 2020. Risk assessment implications of site-specific oral relative bioavailability factors and dermal absorption fractions for polycyclic aromatic hydrocarbons in surface soils impacted by clay skeet target fragments. *Regulatory Toxicology and Pharmacology*, 113, 104649.

HAQ, A., GOODYEAR, B., AMEEN, D., JOSHI, V. & MICHNIAK-KOHN, B. 2018. Strat-M® synthetic membrane: Permeability comparison to human cadaver skin. *International Journal of Pharmaceutics*, 547, 432-437.

HARADA, Y. & INOKO, A. 1977. The oxidation products formed from: Soil organic matter by hydrogen peroxide treatment. *Soil Science and Plant Nutrition*, 23, 513-521.

HATZINGER, P. B. & ALEXANDER, M. 1995. Effect of aging of chemicals in soil on their biodegradability and extractability. *Environmental science & technology*, 29, 537-545.

HAWTHORNE, S. B., MILLER, D. J. & KREITINGER, J. P. 2006. Measurement of total polycyclic aromatic hydrocarbon concentrations in sediments and toxic units used for estimating risk to benthic invertebrates at manufactured gas plant sites. *Environmental Toxicology and Chemistry*, 25, 287-296.

HAWTHORNE, S. B., POPPENDIECK, D. G., GRABANSKI, C. B. & LOEHR, R. C. 2002. Comparing PAH Availability from Manufactured Gas Plant Soils and Sediments with Chemical and Biological Tests. 1. PAH Release during Water Desorption and Supercritical Carbon Dioxide Extraction. *Environmental Science & Technology*, 36, 4795-4803.

HETÉNYI, M., NYILAS, T. & TÓTH, T. M. 2005. Stepwise Rock-Eval pyrolysis as a tool for typing heterogeneous organic matter in soils. *Journal of Analytical and Applied Pyrolysis*, 74, 45-54.

HINDERSMANN, B. & ACHTEN, C. 2018. Urban soils impacted by tailings from coal mining: PAH source identification by 59 PAHs, BPCA and alkylated PAHs. *Environmental Pollution*, 242, 1217-1225.

HONG, L., GHOSH, U., MAHAJAN, T., ZARE, R. N. & LUTHY, R. G. 2003. PAH sorption mechanism and partitioning behavior in lampblack-impacted soils from former oil-gas plant sites. *Environmental Science & Technology*, 37, 3625-3634.

HU, J. & AITKEN, M. D. 2012. Desorption of polycyclic aromatic hydrocarbons from field-contaminated soil to a two-dimensional hydrophobic surface before and after bioremediation. *Chemosphere*, 89, 542-547.

HUANG, W., PENG, P. A., YU, Z. & FU, J. 2003. Effects of organic matter heterogeneity on sorption and desorption of organic contaminants by soils and sediments. *Applied Geochemistry*, 18, 955-972.

- HUMEL, S., SCHMIDT, S. N., SUMETZBERGER-HASINGER, M., MAYER, P. & LOIBNER, A. P. 2017. Enhanced Accessibility of Polycyclic Aromatic Hydrocarbons (PAHs) and Heterocyclic PAHs in Industrially Contaminated Soil after Passive Dosing of a Competitive Sorbate. *Environmental Science & Technology*, 51, 8017-8026.
- HWANG, S. & CUTRIGHT, T. J. 2002. Impact of clay minerals and DOM on the competitive sorption/desorption of PAHs. *Soil and Sediment Contamination*, 11, 269-291.
- HWANG, S. & CUTRIGHT, T. J. 2003. Effect of expandable clays and cometabolism on PAH biodegradability. *Environmental Science and Pollution Research*, 10, 277-280.
- HWANG, S. & CUTRIGHT, T. J. 2004. Preliminary exploration of the relationships between soil characteristics and PAH desorption and biodegradation. *Environment International*, 29, 887-894.
- INTERNATIONAL AGENCY FOR RESEARCH ON CANCER. 1965-2023. *IARC Monographs on the Identification of Carcinogenic Hazards to Humans* [Online]. International Agency for Research on Cancer (IARC),. Available: <https://monographs.iarc.fr/list-of-classifications/> [Accessed].
- INTERNATIONAL AGENCY FOR RESEARCH ON CANCER 2010. *Some non-heterocyclic polycyclic aromatic hydrocarbons and some related exposures*, World Health Organisation, Lyon, France., IARC Press, International Agency for Research on Cancer.
- JAMES, K., PETERS, R. E., CAVE, M. R., WICKSTROM, M., LAMB, E. G. & SICILIANO, S. D. 2016. Predicting polycyclic aromatic hydrocarbon bioavailability to mammals from incidentally ingested soils using partitioning and fugacity. *Environmental Science & Technology*, 50, 1338-1346.
- JAMES, K., PETERS, R. E., CAVE, M. R., WICKSTROM, M. & SICILIANO, S. D. 2018. In vitro prediction of polycyclic aromatic hydrocarbon bioavailability of 14 different incidentally ingested soils in juvenile swine. *Science of The Total Environment*, 618, 682-689.
- JAMES, K., PETERS, R. E., LAIRD, B. D., MA, W. K., WICKSTROM, M., STEPHENSON, G. L. & SICILIANO, S. D. 2011. Human Exposure Assessment: A Case Study of 8 PAH Contaminated Soils Using in Vitro Digestors and the Juvenile Swine Model. *Environmental Science & Technology*, 45, 4586-4593.
- JONES, K. D. & TILLER, C. L. 1999. Effect of Solution Chemistry on the Extent of Binding of Phenanthrene by a Soil Humic Acid: A Comparison of Dissolved and Clay Bound Humic. *Environmental Science & Technology*, 33, 580-587.

- JORAT, M. E., GODDARD, M. A., MANNING, P., LAU, H. K., NGEOW, S., SOHI, S. P. & MANNING, D. A. C. 2020. Passive CO₂ removal in urban soils: Evidence from brownfield sites. *Science of The Total Environment*, 703, 135573.
- JUHASZ, A. L., WEBER, J., STEVENSON, G., SLEE, D., GANCARZ, D., ROFE, A. & SMITH, E. 2014. In vivo measurement, in vitro estimation and fugacity prediction of PAH bioavailability in post-remediated creosote-contaminated soil. *Science of The Total Environment*, 473-474, 147-154.
- KADRY, A. M., SKOWRONSKI, G. A., TURKALL, R. M. & ABDELRAHMAN, M. S. 1995. Comparison between oral and dermal bioavailability of soil-adsorbed phenanthrene in female rats. *Toxicology Letters*, 78, 153-163.
- KANALY, R. A. & HARAYAMA, S. 2000. Biodegradation of high-molecular-weight polycyclic aromatic hydrocarbons by bacteria. *Journal of bacteriology*, 182, 2059-2067.
- KAUR, A. & FANOURLAKIS, G. C. 2018. Effect of Sodium Carbonate Concentration in Calgon on Hydrometer Analysis Results. *Periodica Polytechnica. Civil Engineering*, 62, 866.
- KAUR, L., SINGH, K., PAUL, S., SINGH, S., SINGH, S. & JAIN, S. K. 2018. A Mechanistic Study to Determine the Structural Similarities Between Artificial Membrane Strat-M™ and Biological Membranes and Its Application to Carry Out Skin Permeation Study of Amphotericin B Nanoformulations. *AAPS PharmSciTech*, 19, 1606-1624.
- KEITH, L. H. 2015. The Source of U.S. EPA's Sixteen PAH Priority Pollutants. *Polycyclic Aromatic Compounds*, 35, 147-160.
- KELSEY, J. W. & ALEXANDER, M. 1997. Declining bioavailability and inappropriate estimation of risk of persistent compounds. *Environmental Toxicology and Chemistry: An International Journal*, 16, 582-585.
- KELSEY, J. W., KOTTLER, B. D. & ALEXANDER, M. 1997. Selective Chemical Extractants To Predict Bioavailability of Soil-Aged Organic Chemicals. *Environmental Science & Technology*, 31, 214-217.
- KEMP, A. C., HORTON, B. P., NIKITINA, D., VANE, C. H., POTAPOVA, M., WEBER-BRUYA, E., CULVER, S. J., REPKINA, T. & HILL, D. F. 2017. The distribution and utility of sea-level indicators in Eurasian sub-Arctic salt marshes (White Sea, Russia). *Boreas*, 46, 562-584.
- KENNAWAY, E. 1955. The identification of a carcinogenic compound in coal-tar. *Br Med J*, 2, 749-52.
- KHAN, S., CAO, Q., LIN, A.-J. & ZHU, Y.-G. 2008. Concentrations and bioaccessibility of polycyclic aromatic hydrocarbons in wastewater-irrigated soil using in vitro gastrointestinal test. *Environmental Science and Pollution Research-International*, 15, 344-353.

- KIM, A. W., VANE, C. H., MOSS-HAYES, V. L., BERIRO, D. J., NATHANAIL, C. P., FORDYCE, F. M. & EVERETT, P. A. 2017. Polycyclic aromatic hydrocarbons (PAHs) and polychlorinated biphenyls (PCBs) in urban soils of Glasgow, UK. *Earth and Environmental Science Transactions of the Royal Society of Edinburgh*, 108, 231-247.
- KISSEL, J. C. 2011. The mismeasure of dermal absorption. *Journal of Exposure Science & Environmental Epidemiology*, 21, 302-309.
- KISSEL, J. C., RICHTER, K. Y. & FENSKE, R. A. 1996. Factors Affecting Soil Adherence to Skin in Hand-Press Trials. *Bulletin of Environmental Contamination and Toxicology*, 56, 722-728.
- KÖNITZER, S. F., STEPHENSON, M. H., DAVIES, S. J., VANE, C. H. & LENG, M. J. 2016. Significance of sedimentary organic matter input for shale gas generation potential of Mississippian Mudstones, Widmerpool Gulf, UK. *Review of Palaeobotany and Palynology*, 224, 146-168.
- KOTTLER, B. D., WHITE, J. C. & KELSEY, J. W. 2001. Influence of soil moisture on the sequestration of organic compounds in soil. *Chemosphere*, 42, 893-898.
- KUKKONEN, J. V. K., LANDRUM, P. F., MITRA, S., GOSSIAUX, D. C., GUNNARSSON, J. & WESTON, D. 2003. Sediment Characteristics Affecting Desorption Kinetics of Select PAH and PCB Congeners for Seven Laboratory Spiked Sediments. *Environmental Science & Technology*, 37, 4656-4663.
- LAFARGUE, E., MARQUIS, F. & PILLOT, D. 1998. Rock-Eval 6 applications in hydrocarbon exploration, production, and soil contamination studies. *Revue de l'institut français du pétrole*, 53, 421-437.
- LAND QUALITY MANAGEMENT LTD. 2015. *LQM/CIEH 'Suitable 4 Use Levels'* [Online]. Available: <https://www.lqm.co.uk/publications/s4ul/> [Accessed 09/01/2020 2020].
- LARSSON, M., HAGBERG, J., ROTANDER, A., VAN BAVEL, B. & ENGWALL, M. 2013. Chemical and bioanalytical characterisation of PAHs in risk assessment of remediated PAH-contaminated soils. *Environmental Science and Pollution Research*, 20, 8511-8520.
- LIMA, A. L. C., FARRINGTON, J. W. & REDDY, C. M. 2005. Combustion-derived polycyclic aromatic hydrocarbons in the environment—a review. *Environmental forensics*, 6, 109-131.
- LIN, H., MORANDI, G. D., BROWN, R. S., SNIECKUS, V., RANTANEN, T., JØRGENSEN, K. B. & HODSON, P. V. 2015. Quantitative structure–activity relationships for chronic toxicity of alkyl-chrysenes and alkyl-benz[a]anthracenes to Japanese medaka embryos (*Oryzias latipes*). *Aquatic Toxicology*, 159, 109-118.
- LORENZI, D., CAVE, M. & DEAN, J. R. 2010. An investigation into the occurrence and distribution of polycyclic aromatic hydrocarbons in two soil size

fractions at a former industrial site in NE England, UK using in situ PFE–GC–MS. *Environmental geochemistry and health*, 32, 553-565.

LORT, J. 2022. *The Measurement of the Dermal Bioavailability of Potentially Harmful Organic Soil Contaminants*. Standard, University of Nottingham.

LQM 2020. Introduction to Contaminated Land Management Training Course. Land Quality Management.

LU, Z., ZENG, F., XUE, N. & LI, F. 2012. Occurrence and distribution of polycyclic aromatic hydrocarbons in organo-mineral particles of alluvial sandy soil profiles at a petroleum-contaminated site. *Science of The Total Environment*, 433, 50-57.

LUEKING, A. D., HUANG, W., SODERSTROM-SCHWARZ, S., KIM, M. & WEBER, W. J. 2000. Relationship of Soil Organic Matter Characteristics to Organic Contaminant Sequestration and Bioavailability. *Journal of Environmental Quality*, 29, 317-323.

LUO, L., LIN, S., HUANG, H. & ZHANG, S. 2012. Relationships between aging of PAHs and soil properties. *Environmental Pollution*, 170, 177-182.

LUO, Z. & AGRANIOTIS, M. 2017. *Low-rank coals for power generation, fuel and chemical production*, Woodhead Publishing.

LUTHY, R. G., AIKEN, G. R., BRUSSEAU, M. L., CUNNINGHAM, S. D., GSCHWEND, P. M., PIGNATELLO, J. J., REINHARD, M., TRAINA, S. J., WEBER, W. J. & WESTALL, J. C. 1997. Sequestration of hydrophobic organic contaminants by geosorbents. *Environmental Science & Technology*, 31, 3341-3347.

MADER, B. T., UWE-GOSS, K. & EISENREICH, S. J. 1997. Sorption of Nonionic, Hydrophobic Organic Chemicals to Mineral Surfaces. *Environmental Science & Technology*, 31, 1079-1086.

MADRID, F., FLORIDO, M. C., RUBIO-BELLIDO, M., VILLAVERDE, J. & MORILLO, E. 2022. Dissipation of a mix of priority PAHs in soils by using availability enhancers. Effect of aging and pollutant interactions. *Science of The Total Environment*, 837, 155744.

MALOU, O. P., SEBAG, D., MOULIN, P., CHEVALLIER, T., BADIANE-NDOUR, N. Y., THIAM, A. & CHAPUIS-LARDY, L. 2020. The Rock-Eval® signature of soil organic carbon in arenosols of the Senegalese groundnut basin. How do agricultural practices matter? *Agriculture, Ecosystems & Environment*, 301, 107030.

MATHEWS, J. P. & CHAFFEE, A. L. 2012. The molecular representations of coal – A review. *Fuel*, 96, 1-14.

MCGREGOR, L. A., GAUCHOTTE-LINDSAY, C., NIC DAÉID, N., THOMAS, R. & KALIN, R. M. 2012. Multivariate Statistical Methods for the

Environmental Forensic Classification of Coal Tars from Former Manufactured Gas Plants. *Environmental Science & Technology*, 46, 3744-3752.

MEADOR, J. 2008. Polycyclic Aromatic Hydrocarbons. In: JØRGENSEN, S. E. & FATH, B. D. (eds.) *Encyclopedia of Ecology*. Oxford: Academic Press.

MENG, F., YANG, X., LUCHUN, D., NAIDU, R., NURUZZAMAN, M. & SEMPLE, K. T. 2019. Influence of pH, electrical conductivity and ageing on the extractability of benzo[a]pyrene in two contrasting soils. *Science of the Total Environment*, 690, 647-653.

MIKUTTA, R., KLEBER, M., KAISER, K. & JAHN, R. 2005. Review. *Soil Science Society of America Journal*, 69, 120-135.

MINISTRY FOR THE ENVIRONMENT NEW ZEALAND GOVERNMENT 1997. Guidelines for Assessing and Managing Contaminated Gasworks Sites in New Zealand. In: MINISTRY FOR THE ENVIRONMENT (ed.).

MINISTRY OF HOUSING COMMUNITIES AND LOCAL GOVERNMENT 2019. National Planning Policy Framework. *Department for Communities and Local Government*.

MOODY, R. P., JONCAS, J., RICHARDSON, M. & CHU, I. 2007. Contaminated Soils (I): In Vitro Dermal Absorption of Benzo[a]Pyrene in Human Skin. *Journal of Toxicology and Environmental Health, Part A*, 70, 1858-1865.

MOODY, R. P., NADEAU, B. & CHU, I. 1995. In vivo and in vitro dermal absorption of benzo[a]pyrene in rat, guinea pig, human and tissue-cultured skin. *Journal of Dermatological Science*, 9, 48-58.

MOODY, R. P., TYTCHINO, A. V., YIP, A. & PETROVIC, S. 2011. A Novel "By Difference" Method for Assessing Dermal Absorption of Polycyclic Aromatic Hydrocarbons from Soil at Federal Contaminated Sites. *Journal of Toxicology and Environmental Health, Part A*, 74, 1294-1303.

MÜLLER, S., TOTSCHKE, K. & KÖGEL-KNABNER, I. 2007. Sorption of polycyclic aromatic hydrocarbons to mineral surfaces. *European Journal of Soil Science*, 58, 918-931.

MÜLLER, S., WILCKE, W., KANCHANAKOOL, N. & ZECH, W. 2000. Polycyclic aromatic hydrocarbons (PAHs) and polychlorinated biphenyls (PCBs) in particle-size separates of urban soils in Bangkok, Thailand. *Soil Science*, 165, 412-419.

NAIDU, R., CHANNEY, R., MCCONNELL, S., JOHNSTON, N., SEMPLE, K. T., MCGRATH, S., DRIES, V., NATHANAIL, P., HARMSSEN, J. & PRUSZINSKI, A. 2015. Towards bioavailability-based soil criteria: past, present and future perspectives. *Environmental Science and Pollution Research*, 22, 8779-8785.

- NAM, K., CHUNG, N. & ALEXANDER, M. 1998. Relationship between Organic Matter Content of Soil and the Sequestration of Phenanthrene. *Environmental Science & Technology*, 32, 3785-3788.
- NATHANAIL, C. P., MCCAFFREY, C., GILLETT, A. G., OGDEN, R. C. & NATHANAIL, J. F. 2015. *The LQM/CIEH S4ULs for Human Health Risk Assessment*, Nottingham, Land Quality Press, Nottingham.
- NEWELL, A. J., VANE, C. H., SORENSEN, J. P., MOSS-HAYES, V. & GOODDY, D. C. 2016. Long-term Holocene groundwater fluctuations in a chalk catchment: evidence from Rock-Eval pyrolysis of riparian peats. *Hydrological Processes*, 30, 4556-4567.
- NIESSEN, W. M. A. 2017. MS–MS and MSn☆. In: LINDON, J. C., TRANTER, G. E. & KOPPENAAL, D. W. (eds.) *Encyclopedia of Spectroscopy and Spectrometry (Third Edition)*. Oxford: Academic Press.
- OEN, A. M., BREEDVELD, G. D., KALAITZIDIS, S., CHRISTANIS, K. & CORNELISSEN, G. 2006. How quality and quantity of organic matter affect polycyclic aromatic hydrocarbon desorption from Norwegian harbor sediments. *Environmental Toxicology and Chemistry: An International Journal*, 25, 1258-1267.
- OLIVER, L., FERBER, U., GRIMSKI, D., MILLAR, K. & NATHANAIL, P. The scale and nature of European brownfields. CABERNET 2005-International Conference on Managing Urban Land LQM Ltd, Nottingham, UK, Belfast, Northern Ireland, UK, 2005.
- OOMEN, A. G., HACK, A., MINEKUS, M., ZEIJDNER, E., CORNELIS, C., SCHOETERS, G., VERSTRAETE, W., VAN DE WIELE, T., WRAGG, J. & ROMPELBERG, C. J. 2002. Comparison of five in vitro digestion models to study the bioaccessibility of soil contaminants. *Environmental Science & Technology*, 36, 3326-3334.
- ORATA, F. 2012. Derivatization reactions and reagents for gas chromatography analysis. *Adv. Gas Chromatogr.—Prog. Agric. Biomed. Ind. Appl.*, 83-107.
- ORDOÑEZ, L., VOGEL, H., SEBAG, D., ARIZTEGUI, D., ADATTE, T., RUSSELL, J. M., KALLMEYER, J., VUILLEMIN, A., FRIESE, A., CROWE, S. A., BAUER, K. W., SIMISTER, R., HENNY, C., NOMOSATRYO, S. & BIJAKSANA, S. 2019. Empowering conventional Rock-Eval pyrolysis for organic matter characterization of the siderite-rich sediments of Lake Towuti (Indonesia) using End-Member Analysis. *Organic Geochemistry*, 134, 32-44.
- PAN, B., XING, B. S., LIU, W. X., TAO, S., LIN, X. M., ZHANG, X. M., ZHANG, Y. X., XIAO, Y., DAI, H. C. & YUAN, H. S. 2006. Distribution of sorbed phenanthrene and pyrene in different humic fractions of soils and importance of humin. *Environmental Pollution*, 143, 24-33.
- PECKHAM, T. K., SHIRAI, J. H., BUNGE, A. L., LOWNY, Y. W., RUBY, M. V. & KISSEL, J. C. 2017. Dermal absorption of benzo [a] pyrene into human

skin from soil: Effect of artificial weathering, concentration, and exposure duration. *Journal of exposure science & environmental epidemiology*, 27, 610-617.

PEHKONEN, S., YOU, J., AKKANEN, J., KUKKONEN, J. V. K. & LYDY, M. J. 2010. Influence of black carbon and chemical planarity on bioavailability of sediment-associated contaminants. *Environmental Toxicology and Chemistry*, 29, 1976-1983.

PERNOT, A., OUVRARD, S., LEGLIZE, P. & FAURE, P. 2013. Protective role of fine silts for PAH in a former industrial soil. *Environmental Pollution*, 179, 81-87.

PIATT, J. J. & BRUSSEAU, M. L. 1998. Rate-Limited Sorption of Hydrophobic Organic Compounds by Soils with Well-Characterized Organic Matter. *Environmental Science & Technology*, 32, 1604-1608.

PIES, C., HOFFMANN, B., PETROWSKY, J., YANG, Y., TERNES, T. A. & HOFMANN, T. 2008. Characterization and source identification of polycyclic aromatic hydrocarbons (PAHs) in river bank soils. *Chemosphere*, 72, 1594-1601.

PLUSKE, W., MURPHY, D. & SHEPPARD, J. 2020. *Total Organic carbon* [Online]. Available: <http://www.soilquality.org.au/factsheets/organic-carbon> [Accessed 07/05/2020 2020].

POOT, A., JONKER, M. T. O., GILLISSEN, F. & KOELMANS, A. A. 2014. Explaining PAH desorption from sediments using Rock Eval analysis. *Environmental Pollution*, 193, 247-253.

POSADA-BAQUERO, R., SEMPLE, K. T., TERNERO, M. & ORTEGA-CALVO, J.-J. 2022. Determining the bioavailability of benzo(a)pyrene through standardized desorption extraction in a certified reference contaminated soil. *Science of The Total Environment*, 150025.

PU, X., LEE, L. S., GALINSKY, R. E. & CARLSON, G. P. 2004. Evaluation of a rat model versus a physiologically based extraction test for assessing phenanthrene bioavailability from soils. *Toxicological Sciences*, 79, 10-17.

PUBLIC HEALTH ENGLAND 2017. Contaminated land information sheet: risk assessment approaches for polycyclic aromatic hydrocarbons (PAHs). London, UK.

R CORE TEAM 2023. R: A Language and Environment for Statistical Computing. Vienna, Austria: R Foundation for Statistical Computing.

RAN, Y., XIAO, B., HUANG, W., PENG, P. A., LIU, D., FU, J. & SHENG, G. 2003. Kerogen in aquifer material and its strong sorption for nonionic organic pollutants. *Journal of Environmental Quality*, 32, 1701-1709.

RANKL, F. 2023. Brownfield development and protecting the Green Belt. Available: <https://commonslibrary.parliament.uk/research-briefings/cdp-2023->

[0035/#:~:text=The%20NPPF%20sets%20out%20that,in%20%E2%80%9Cvery%20special%20circumstances%E2%80%9D.](#)

RESSLER, B., KNEIFEL, H. & WINTER, J. 1999. Bioavailability of polycyclic aromatic hydrocarbons and formation of humic acid-like residues during bacterial PAH degradation. *Applied Microbiology and Biotechnology*, 53, 85-91.

ŘEZANKA, T., PÁDROVÁ, K. & SIGLER, K. 2016. Derivatization in Gas Chromatography of Lipids. In: WENK, M. R. (ed.) *Encyclopedia of Lipidomics*. Dordrecht: Springer Netherlands.

RHODES, A. H., MCALLISTER, L. E. & SEMPLE, K. T. 2010. Linking desorption kinetics to phenanthrene biodegradation in soil. *Environmental Pollution*, 158, 1348-1353.

RHODES, A. H., RIDING, M. J., MCALLISTER, L. E., LEE, K. & SEMPLE, K. T. 2012. Influence of Activated Charcoal on Desorption Kinetics and Biodegradation of Phenanthrene in Soil. *Environmental Science & Technology*, 46, 12445-12451.

RIBEIRO, J., SILVA, T., FILHO, J. G. M. & FLORES, D. 2012. Polycyclic aromatic hydrocarbons (PAHs) in burning and non-burning coal waste piles. *Journal of Hazardous Materials*, 199-200, 105-110.

RICHTER-BROCKMANN, S. & ACHTEN, C. 2018. Analysis and toxicity of 59 PAH in petrogenic and pyrogenic environmental samples including dibenzopyrenes, 7H-benzo [c] fluorene, 5-methylchrysene and 1-methylpyrene. *Chemosphere*, 200, 495-503.

RIDING, M. J., DOICK, K. J., MARTIN, F. L., JONES, K. C. & SEMPLE, K. T. 2013. Chemical measures of bioavailability/bioaccessibility of PAHs in soil: Fundamentals to application. *Journal of Hazardous Materials*, 261, 687-700.

ROBERTS, M. S. & WALTERS, K. A. 2007. *Dermal Absorption and Toxicity Assessment*, CRC Press.

ROY, T. A., KRUEGER, A. J., TAYLOR, B. B., MAURO, D. M. & GOLDSTEIN, L. S. 1998. Studies Estimating the Dermal Bioavailability of Polynuclear Aromatic Hydrocarbons from Manufactured Gas Plant Tar-Contaminated Soils. *Environ. Sci. Technol.*, 32, 3113-3117.

ROY, T. A. & SINGH, R. 2001. Effect of Soil Loading and Soil Sequestration on Dermal Bioavailability of Polynuclear Aromatic Hydrocarbons. *Environ. Contam. Toxicol*, 67, 324-331.

RUBY, M. V., LOWNEY, Y. W., BUNGE, A. L., ROBERTS, S. M., GOMEZ-EYLES, J. L., GHOSH, U., KISSEL, J. C., TOMLINSON, P. & MENZIE, C. 2016. Oral Bioavailability, Bioaccessibility, and Dermal Absorption of PAHs from Soil—State of the Science. *Environmental Science & Technology*, 50, 2151-2164.

- SAEEDI, M., LI, L. Y. & GRACE, J. R. 2018. Desorption and mobility mechanisms of co-existing polycyclic aromatic hydrocarbons and heavy metals in clays and clay minerals. *Journal of Environmental Management*, 214, 204-214.
- SAENGER, A., CÉCILLON, L., SEBAG, D. & BRUN, J.-J. 2013. Soil organic carbon quantity, chemistry and thermal stability in a mountainous landscape: A Rock-Eval pyrolysis survey. *Organic Geochemistry*, 54, 101-114.
- SANDER, L. C. & WISE, S. A. 1997. *Polycyclic aromatic hydrocarbon structure index*, US Department of Commerce, Technology Administration, National Institute of
- SARTORELLI, P., MONTOMOLI, L., SISINNI, A. G., BUSSANI, R., CAVALLO, D. & FOÁ, V. 2001. Dermal exposure assessment of polycyclic aromatic hydrocarbons: in vitro percutaneous penetration from coal dust. *Toxicology and Industrial Health*, 17, 17-21.
- SCHEEDER, G., WENIGER, P. & BLUMENBERG, M. 2020. Geochemical implications from direct Rock-Eval pyrolysis of petroleum. *Organic Geochemistry*, 146, 104051.
- SCHMIDT, M. W., SKJEMSTAD, J. O., CZIMCZIK, C. I., GLASER, B., PRENTICE, K. M., GELINAS, Y. & KUHLBUSCH, T. A. 2001. Comparative analysis of black carbon in soils. *Global Biogeochemical Cycles*, 15, 163-167.
- SEBAG, D., DISNAR, J.-R., GUILLET, B., DI GIOVANNI, C., VERRECCHIA, E. P. & DURAND, A. 2006. Monitoring organic matter dynamics in soil profiles by 'Rock-Eval pyrolysis': bulk characterization and quantification of degradation. *European Journal of Soil Science*, 57, 344-355.
- SEBAG, D., VERRECCHIA, E. P., CÉCILLON, L., ADATTE, T., ALBRECHT, R., AUBERT, M., BUREAU, F., CAILLEAU, G., COPARD, Y., DECAENS, T., DISNAR, J. R., HETÉNYI, M., NYILAS, T. & TROMBINO, L. 2016. Dynamics of soil organic matter based on new Rock-Eval indices. *Geoderma*, 284, 185-203.
- SEMPLE, K. T., DOICK, K. J., JONES, K. C., BURAUUEL, P., CRAVEN, A. & HARMS, H. 2004. Peer reviewed: defining bioavailability and bioaccessibility of contaminated soil and sediment is complicated. ACS Publications.
- SEMPLE, K. T., RIDING, M. J., MCALLISTER, L. E., SOPENA-VAZQUEZ, F. & BENDING, G. D. 2013. Impact of black carbon on the bioaccessibility of organic contaminants in soil. *Journal of Hazardous Materials*, 261, 808-816.
- SICILIANO, S. D., LAIRD, B. D. & LEMIEUX, C. L. 2010. Polycyclic aromatic hydrocarbons are enriched but bioaccessibility reduced in brownfield soils adhered to human hands. *Chemosphere*, 80, 1101-1108.
- SIDDENS, L. K., LARKIN, A., KRUEGER, S. K., BRADFIELD, C. A., WATERS, K. M., TILTON, S. C., PEREIRA, C. B., LÖHR, C. V., ARLT, V. M., PHILLIPS, D. H., WILLIAMS, D. E. & BAIRD, W. M. 2012. Polycyclic

aromatic hydrocarbons as skin carcinogens: comparison of benzo[a]pyrene, dibenzo[def,p]chrysene and three environmental mixtures in the FVB/N mouse. *Toxicol Appl Pharmacol*, 264, 377-86.

SLEZAKOVA, K., CASTRO, D., BEGONHA, A., DELERUE-MATOS, C., ALVIM-FERRAZ, M. D. C., MORAIS, S. & PEREIRA, M. D. C. 2011. Air pollution from traffic emissions in Oporto, Portugal: Health and environmental implications. *Microchemical Journal*, 99, 51-59.

SØRENSEN, L., MEIER, S. & MJØS, S. A. 2016. Application of gas chromatography/tandem mass spectrometry to determine a wide range of petrogenic alkylated polycyclic aromatic hydrocarbons in biotic samples. *Rapid Communications in Mass Spectrometry*, 30, 2052-2058.

SPALT, E. W., KISSEL, J. C., SHIRAI, J. H. & BUNGE, A. L. 2009. Dermal absorption of environmental contaminants from soil and sediment: a critical review. *Journal of Exposure Science and Environmental Epidemiology*, 19, 119-148.

STANLEY, S., ANTONIOU, V., ASKQUITH-ELLIS, A., BALL, L. A., BENNETT, E. S., BLAKE, J. R., BOORMAN, D. B., BROOKS, M., CLARKE, M., COOPER, H. M., COWAN, N., CUMMING, A., EVANS, J. G., FARRAND, P., FRY, M., HITT, O. E., LORD, W. D., MORRISON, R., NASH, G. V., RYLETT, D., SCARLETT, P. M., SWAIN, O. D., SZCZYKULSKA, M., THORNTON, J. L., TRILL, E. J., WARWICK, A. C. & WINTERBOURN, J. B. 2021. Daily and sub-daily hydrometeorological and soil data (2013-2019) [COSMOS-UK]. NERC Environmental Information Data Centre.

STOKES, J. D., PATON, G. & SEMPLE, K. T. 2005. Behaviour and assessment of bioavailability of organic contaminants in soil: relevance for risk assessment and remediation. *Soil Use and Management*, 21, 475-486.

STOUT, S. A. & BREY, A. P. 2019. Appraisal of coal- and coke-derived wastes in soils near a former manufactured gas plant, Jacksonville, Florida. *International Journal of Coal Geology*, 213, 103265.

STOUT, S. A., EMSBO-MATTINGLY, S. D., DOUGLAS, G. S., UHLER, A. D. & MCCARTHY, K. J. 2015. Beyond 16 Priority Pollutant PAHs: A Review of PACs used in Environmental Forensic Chemistry. *Polycyclic Aromatic Compounds*, 35, 285-315.

STROO, H. F., ROY, T. A., LIBAN, C. B. & KREITINGER, J. P. 2005. Dermal bioavailability of benzo [a] pyrene on lampblack: implications for risk assessment. *Environmental Toxicology and Chemistry: An International Journal*, 24, 1568-1572.

SWARTJES, F. A. 2011. *Dealing with contaminated sites: from theory towards practical application*, Springer Science & Business Media.

- TALLEY, J. W., GHOSH, U., TUCKER, S. G., FUREY, J. S. & LUTHY, R. G. 2002. Particle-Scale Understanding of the Bioavailability of PAHs in Sediment. *Environmental Science & Technology*, 36, 477-483.
- TANG, J., LISTE, H.-H. & ALEXANDER, M. 2002. Chemical assays of availability to earthworms of polycyclic aromatic hydrocarbons in soil. *Chemosphere*, 48, 35-42.
- TAO, S., XU, F., LIU, W., CUI, Y. & COVENEY, R. M. 2006. A Chemical Extraction Method for Mimicking Bioavailability of Polycyclic Aromatic Hydrocarbons to Wheat Grown in Soils Containing Various Amounts of Organic Matter. *Environmental Science & Technology*, 40, 2219-2224.
- THAVAMANI, P., MEGHARAJ, M., KRISHNAMURTI, G. S. R., MCFARLAND, R. & NAIDU, R. 2011. Finger printing of mixed contaminants from former manufactured gas plant (MGP) site soils: Implications to bioremediation. *Environment International*, 37, 184-189.
- THAVAMANI, P., MEGHARAJ, M. & NAIDU, R. 2012. Multivariate analysis of mixed contaminants (PAHs and heavy metals) at manufactured gas plant site soils. *Environmental monitoring and assessment*, 184, 3875-3885.
- THOMAS, R. 2014. Gasworks Profile A: The History and Operation of Gasworks (Manufactured Gas Plants) in Britain. *Contaminated Land: Applications in Real Environments (CL: AIRE)*, London. 32 Bloomsbury Street, London WC1B 3QJ: Contaminated Land: Applications in Real Environments (CL:AIRE).
- THOMAS, R. 2023. *The Redevelopment and Repurposing of Historic Gas Sites, Lighting up Western Europe: Markets and Strategies in the Energy Industry, 19th to 21st centuries*, Routledge.
- THOMPSON, K. C. & NATHANAIL, P. 2003. *Chemical analysis of contaminated land*, Blackwell Publishing Ltd.
- TURKALL, R. M., ABDEL-RAHMAN, M. S. & SKOWRONSKI, G. A. Effects of soil matrix and aging on the dermal bioavailability of hydrocarbons and metals in the soil: dermal bioavailability of soil contaminants. Proceedings of the Annual International Conference on Soils, Sediments, Water and Energy, 2010. 29.
- UDESKEY, J. O., DODSON, R. E., PEROVICH, L. J. & RUDEL, R. A. 2019. Wrangling environmental exposure data: guidance for getting the best information from your laboratory measurements. *Environ Health*, 18, 99.
- UKALSKA-JARUGA, A. & SMRECZAK, B. 2020. The Impact of Organic Matter on Polycyclic Aromatic Hydrocarbon (PAH) Availability and Persistence in Soils. *Molecules*, 25, 2470.
- UKALSKA-JARUGA, A., SMRECZAK, B. & KLIMKOWICZ-PAWLAS, A. 2019. Soil organic matter composition as a factor affecting the accumulation of

polycyclic aromatic hydrocarbons. *Journal of Soils and Sediments*, 19, 1890–1900.

UMEH, A. C., DUAN, L., NAIDU, R., ESPOSITO, M. & SEMPLE, K. T. 2019a. In vitro gastrointestinal mobilization and oral bioaccessibility of PAHs in contrasting soils and associated cancer risks: Focus on PAH nonextractable residues. *Environment International*, 133, 105186.

UMEH, A. C., DUAN, L., NAIDU, R. & SEMPLE, K. T. 2018. Time-Dependent Remobilization of Nonextractable Benzo[a]pyrene Residues in Contrasting Soils: Effects of Aging, Spiked Concentration, and Soil Properties. *Environmental Science & Technology*, 52, 12295-12305.

UMEH, A. C., DUAN, L., NAIDU, R. & SEMPLE, K. T. 2019b. Extremely small amounts of B[a]P residues remobilised in long-term contaminated soils: A strong case for greater focus on readily available and not total-extractable fractions in risk assessment. *Journal of Hazardous Materials*, 368, 72-80.

UNITED STATES ENVIRONMENTAL PROTECTION AGENCY (EPA). 2012. *Vocabulary Catalog* [Online]. Available: https://ofmpub.epa.gov/sor_internet/registry/termreg/searchandretrieve/glossariesandkeywordlists/search.do;jsessionid=N4W3MnFreRP0auhepd8DFLmZLaL70fZeqlkGgihJMotaL7ap7uj!-1405441119?details=&vocabName=Eco%20Risk%20Assessment%20Glossary&filterTerm=contaminant&checkedAcronym=false&checkedTerm=false&hasDefinitions=false&filterTerm=contaminant&filterMatchCriteria=Contains [Accessed 15/06/2020 2020].

UPTON, A., VANE, C. H., GIRKIN, N., TURNER, B. L. & SJÖGERSTEN, S. 2018. Does litter input determine carbon storage and peat organic chemistry in tropical peatlands? *Geoderma*, 326, 76-87.

UYTTEBROEK, M., BREUGELMANS, P., JANSSEN, M., WATTIAU, P., JOFFE, B., KARLSON, U., ORTEGA-CALVO, J. J., BASTIAENS, L., RYNGAERT, A. & HAUSNER, M. 2006. Distribution of the Mycobacterium community and polycyclic aromatic hydrocarbons (PAHs) among different size fractions of a long-term PAH-contaminated soil. *Environmental Microbiology*, 8, 836-847.

VANE, C., KIM, A., BERIRO, D., CAVE, M., LOWE, S., LOPES DOS SANTOS, R., FERREIRA, A. & COLLINS, C. 2021. Persistent Organic Pollutants in Urban Soils of Central London, England, UK: Measurement and Spatial Modelling of Black Carbon (BC), Petroleum Hydrocarbons (TPH), Polycyclic Aromatic Hydrocarbons (PAH) and Polychlorinated Biphenyls (PCB). *Advances in Environmental and Engineering Research*, 02, 012.

VANE, C. H., KIM, A. W., BERIRO, D. J., CAVE, M. R., KNIGHTS, K., MOSS-HAYES, V. & NATHANAIL, P. C. 2014. Polycyclic aromatic hydrocarbons (PAH) and polychlorinated biphenyls (PCB) in urban soils of Greater London, UK. *Applied Geochemistry*, 51, 303-314.

- VANE, C. H., KIM, A. W., EMMINGS, J. F., TURNER, G. H., MOSS-HAYES, V., LORT, J. A. & WILLIAMS, P. J. 2020. Grain size and organic carbon controls polyaromatic hydrocarbons (PAH), mercury (Hg) and toxicity of surface sediments in the River Conwy Estuary, Wales, UK. *Marine Pollution Bulletin*, 158, 111412.
- VANE, C. H., KIM, A. W., LOPES DOS SANTOS, R. A. & MOSS-HAYES, V. 2022. Contrasting sewage, emerging and persistent organic pollutants in sediment cores from the river Thames estuary, London, England, UK. *Marine Pollution Bulletin*, 175, 113340.
- WANG, S., NI, H.-G., SUN, J.-L., JING, X., HE, J.-S. & ZENG, H. 2013. Polycyclic aromatic hydrocarbons in soils from the Tibetan Plateau, China: distribution and influence of environmental factors. *Environmental Science: Processes & Impacts*, 15, 661-667.
- WANG, W., QU, X., LIN, D. & YANG, K. 2021. Octanol-water partition coefficient (logK_{ow}) dependent movement and time lagging of polycyclic aromatic hydrocarbons (PAHs) from emission sources to lake sediments: A case study of Taihu Lake, China. *Environmental Pollution*, 288, 117709.
- WASSENAAR, P. N. H. & VERBRUGGEN, E. M. J. 2021. Persistence, bioaccumulation and toxicity-assessment of petroleum UVCBs: A case study on alkylated three-ring PAHs. *Chemosphere*, 276, 130113.
- WATERS, C. N., VANE, C. H., KEMP, S. J., HASLAM, R. B., HOUGH, E. & MOSS-HAYES, V. L. 2020. Lithological and chemostratigraphic discrimination of facies within the Bowland Shale Formation within the Craven and Edale basins, UK. *Petroleum Geoscience*, 26, 325-345.
- WESTER, R. C., MAIBACH, H. I., BUCKS, D. A. W., SEDIK, L., MELENDRES, J., LIAO, C. & DIZIO, S. 1990. Percutaneous absorption of [¹⁴C]DDT and [¹⁴C]Benzo[a]pyrene from soil. *Toxicological Sciences*, 15, 510-516.
- WHITE, J. C. & ALEXANDER, M. 1996. Reduced biodegradability of desorption-resistant fractions of polycyclic aromatic hydrocarbons in soil and aquifer solids. *Environmental Toxicology and Chemistry: An International Journal*, 15, 1973-1978.
- WHITE, J. C., KELSEY, J. W., HATZINGER, P. B. & ALEXANDER, M. 1997. Factors affecting sequestration and bioavailability of phenanthrene in soils. *Environmental Toxicology and Chemistry: An International Journal*, 16, 2040-2045.
- WHITE, J. C. & PIGNATELLO, J. J. 1999. Influence of Bisolute Competition on the Desorption Kinetics of Polycyclic Aromatic Hydrocarbons in Soil. *Environmental Science & Technology*, 33, 4292-4298.
- WILLIAMS-CLAYSON, A. M., VANE, C. H., JONES, M. D., THOMAS, R., KIM, A. W., TAYLOR, C. & BERIRO, D. J. 2023. Characterisation of former

manufactured gas plant soils using parent and alkylated polycyclic aromatic hydrocarbons and Rock-Eval(6) pyrolysis. *Environmental Pollution*, 122658.

WRAGG, J., CAVE, M., BASTA, N., BRANDON, E., CASTEEL, S., DENYS, S., GRON, C., OOMEN, A., REIMER, K., TACK, K. & VAN DE WIELE, T. 2011. An inter-laboratory trial of the unified BARGE bioaccessibility method for arsenic, cadmium and lead in soil. *Science of the Total Environment*, 409, 4016-4030.

WU, F., XU, L., SUN, Y., LIAO, H., ZHAO, X. & GUO, J. 2012. Exploring the relationship between polycyclic aromatic hydrocarbons and sedimentary organic carbon in three Chinese lakes. *Journal of Soils and Sediments*, 12, 774-783.

WU, S. C. & GSCHWEND, P. M. 1986. Sorption kinetics of hydrophobic organic compounds to natural sediments and soils. *Environmental Science & Technology*, 20, 717-725.

XIA, H., GOMEZ-EYLES, J. L. & GHOSH, U. 2016. Effect of Polycyclic Aromatic Hydrocarbon Source Materials and Soil Components on Partitioning and Dermal Uptake. *Environmental Science & Technology*, 50, 3444-3452.

XING, B. 1997. The effect of the quality of soil organic matter on sorption of naphthalene. *Chemosphere*, 35, 633-642.

XING, B. 2001. Sorption of naphthalene and phenanthrene by soil humic acids. *Environmental Pollution*, 111, 303-309.

XING, B. & PIGNATELLO, J. J. 1997. Dual-Mode Sorption of Low-Polarity Compounds in Glassy Poly(Vinyl Chloride) and Soil Organic Matter. *Environmental Science & Technology*, 31, 792-799.

YAN, L., BAI, Y., ZHAO, R., LI, F. & XIE, K. 2015. Correlation between coal structure and release of the two organic compounds during pyrolysis. *Fuel*, 145, 12-17.

YANG, J. J., ROY, T. A., KRUEGER, A. J., NEIL, W. & MACKERER, C. R. 1989. In vitro and in vivo percutaneous absorption of benzo [a] pyrene from petroleum crude-fortified soil in the rat. *Bulletin of environmental contamination and toxicology*, 43, 207-214.

YANG, Y., TAO, S., ZHANG, N., ZHANG, D. Y. & LI, X. Q. 2010. The effect of soil organic matter on fate of polycyclic aromatic hydrocarbons in soil: A microcosm study. *Environmental Pollution*, 158, 1768-1774.

YAO, X., MCSHANE, A. J. & CASTILLO, M. J. 2013. Chapter 17 - Quantitative Proteomics in Development of Disease Protein Biomarkers. In: ISSAQ, H. J. & VEENSTRA, T. D. (eds.) *Proteomic and Metabolomic Approaches to Biomarker Discovery*. Boston: Academic Press.

YU, L., DUAN, L., NAIDU, R. & SEMPLE, K. T. 2018. Abiotic factors controlling bioavailability and bioaccessibility of polycyclic aromatic

hydrocarbons in soil: Putting together a bigger picture. *Science of The Total Environment*, 613-614, 1140-1153.

YUNKER, M. B., MACDONALD, R. W., VINGARZAN, R., MITCHELL, R. H., GOYETTE, D. & SYLVESTRE, S. 2002. PAHs in the Fraser River basin: a critical appraisal of PAH ratios as indicators of PAH source and composition. *Organic Geochemistry*, 33, 489-515.

Appendix A

Table S1 List of highlighted research papers investigating the influence of soil properties on the PAH fate in soils for the literature review in Chapter 2 Literature Review.

Paper	No. Soils	No. PAHs	Spiked vs field-contaminated	Method	Results	PAH release correlation with soil parameters		
						Negative	Positive	None
<i>Chung and Alexander (2002)</i>	16	1	Spiked	Biodegradation Extractability	% Decrease in biodegradation = $10.35 + 1.123 \text{ OC} + 0.131 \text{ silt}$ ($R^2 = 0.532$) % Decrease in extractability = $19.94 - 4.43 \log \text{ OC} - 0.360 \text{ clay} + 0.798 \text{ CEC}$ ($R^2 = 0.479, p < 0.15$)	OC, nanopore volume		
<i>Nam et al. (1998)</i>	5	1	Spiked	Biodegradation Extractability	>2.0% OC for sequestration to occur. Phenanthrene remaining highest in >2.0% OC and lowest in sand. Greatest sequestration in soils with largest nanopore volume and surface area.	OC, nanopore volume, surface area		
<i>Bogan and Sullivan (2003)</i>	6	2	Spiked	Mycobacterial biodegradation	TOC content most important parameter ($R^2=0.941$).	TOC		

				Extractability	Pore volume & surface area inversely correlated with TOC, so not a main parameter. Sequestration was strongly TOC-dependent; but no correlation between n-butanol extractability and mycobacterial PAH mineralisation.		
<i>Carmichael et al. (1997)</i>	2	2	Spiked	Biodegradation, desorption kinetics	Sorption & desorption equilibria more rapid in lower OC soil.	OC	
<i>Rhodes et al. (2010)</i>	4	1	Spiked	Biodegradation, desorption kinetics	Soils with higher TOC contents had lower F_{rap} , and higher F_{slow} and $F_{very\ slow}$.	TOC	
<i>Pu et al. (2004)</i>	4	1	Spiked	Blood AUC in rats after oral dosing, PBET assay	Lower bioavailability with higher OC and with higher clay content.	OC, clay	
<i>Tao et al. (2006)</i>	7	4	Spiked	Plant root accumulation, sequential extraction	Total OM (TOM) negatively correlated with PAH recoveries and accumulation. DOM positively correlated with PAH recoveries and accumulation.	TOM	DOM
<i>Duan et al. (2014)</i>	8	1	Spiked	Blood AUC in swine after oral dosing	No significant relationship between extractability and TOC.	FRAC (slit + clay)/TOC,	TOC and clay

				Extractability	No direct correlation between relative bioavailability (RB) and specific soil properties such as TOC and clay content. RB significantly reduced after ageing apart from very sandy soil. Expandable clay significantly decreased bioavailability. Strong relationship between RB and FPAC and PF <6 nm.	TOC, PF <6 nm	
<i>Duan et al. (2015)</i>	4	1	Spiked	Extractability	No significant relationships for BaP extractability as a function of TOC. Negative trend in extractability by harsher solvents (DCM/Ace and BuOH) with clay contents. Rapid decrease of the dissolvable fraction with higher sand content and number of pores <6 nm.	Clay, pores <6nm	TOC
<i>Luo et al. (2012)</i>	7	3	Spiked	Desorption kinetics	$k_{rap} = -0.456[PF6nm] - 0.003[TOC] + 0.436$ ($r^2 = 0.793$, $p < 0.05$) $k_{slow} = -3.3 \times 10^{-4}[\text{hard OC}] - 4.7 \times 10^{-6}[PF6nm] + 7.1 \times 10^{-5}$ ($r^2 = 0.923$, $p < 0.05$)	PF <6 nm, TOC, hard OC	
<i>Doick et al. (2005)</i>	1 and 3 size fractions	2	Spiked	Sample oxidation and ^{14}C liquid scintillation	HN had the highest amount of PAH nonextractable residues (NER) compared to HA and FA fractions.	Humins, silt and clay	

					PAHs decreased in the order: medium and fine silt (20-2 μm) \approx clay (<2 μm) > sand plus coarse (>20 μm).		
Chen et al. (2007)	1 +HA, HN + deashed HN	2	Spiked	Sorption Equilibrium	Highest sorption capability when no minerals associated, strongest nonlinearity observed when minerals present. SOM aliphatic components contributed greatly to sorption.	Aliphaticity, humin	Mineral association
Pan et al. (2006)	4 + humic fractions	2	Spiked	Sorption equilibrium	HN is the main region for slow sorption. 55-76% Phe and 49-78% Pyr residing in HN.	Humin	
Xing (2001)	1 soil at different depths & HSs	2	Spiked	Sorption equilibrium	Increasing aromaticity with soil depth, sorption increased.	Aromaticity	
Xing (1997)	5	1	Spiked	Sorption equilibrium	Increase aromaticity increases sorption. Aromaticity correlated to K_{oc} $r^2 = 0.994$. Decrease polarity increases sorption. Effective polarity correlated with K_{oc} $r^2 = 0.962$.	Aromaticity	Polarity
Hwang and Cutright (2002)	1 soil & separated SOM &	2	Spiked	Sorption and desorption equilibrium	Removal of clay leads to significant amount of desorption, SOM surfaces easily desorbed (weak binding forces).	Clay association, DOM	

	mineral fractions				Decreased desorption amount by the DOM addition.		
Hwang and Cutright (2003)	3	1	Spiked	Hexane desorption	Increase in expandable clay minerals decreased desorption. Neither dissolved organic matter (DOM) nor total clay amounts made a good desorption prediction.	Expandable clay	
Jones and Tiller (1999)	Kaolinite and illite	1	Spiked	Fluorescence quenching	PAH binding: Bulk humic > mineral bound humic. Low pH lowered K _{OC} , sites became inaccessible.		Low pH, mineral association
Bonin and Simpson (2007)	4 soils + humic fractions	1	Spiked	Sorption equilibrium	K _{OC} : Humic > origin soil. K _{OC} : mineral removed humin > humin. Mineral associated to humin changed humins conformation.	Humin	Mineral association
Ahangar et al. (2008)	Agricultural soils and their SOM	1	Spiked	Sorption equilibrium	Removal of minerals increased K _{OC} (r ² = 0.43). Correlation of K _{OC} and C type only after mineral removal.	Aryl-C and carbonyl C	Mineral association, O-alkyl C
Duan and Naidu (2013)	32	1	Spiked	Sorption equilibrium	TOC accounts for ~68% of variation in partition coefficient (K _f). logK _{OC} = 3.430(±0.183)-0.421(±0.082) log TOC -0.011(±0.003)	TOC, clay	

					Clay+0.218(±0.086) log DOC (R ² =0.714 P<0.001).			
<i>Pernot et al. (2013)</i>	1	16	Field-contaminated	Tenax extraction	Lowest availability from fine silts, assumption of silts protective role for OM and PAH release.	Silt		
<i>Amellal et al. (2001)</i>	1 soil and size fractions	8	Spiked	Year of PAH degradable bacteria (Soxhlet extraction)	PAH concentration: clay > fine silt > coarse silt > soil > sand. High concentration in finer soil fractions, due to OM.	Clay, silt	Sand	
<i>Siciliano et al. (2010)</i>	18	11	Field-contaminated	SHIME model	Highest PAH concentration but lowest released in <45 µm size fraction.	<45 µm size fraction		
<i>Bartolomé et al. (2018)</i>	35	16	Field-contaminated	Passive equilibrium	K _{oc} values: Skeet > pyrogenic > petrogenic. f _{bioac} : skeet < pyrogenic < petrogenic rural/forest. Petrogenic polluted soil had the highest bioaccessible fractions (71% on average). TOC & BC had no influence on K _{oc} .	Skeet, pyrogenic	Petrogenic	TOC, BC
<i>Rhodes et al. (2012)</i>	4	1	Spiked	Extractability	Addition of activated carbon (AC) decreased %F _{rapid} , increased %F _{slow} .	AC		
<i>Xia et al. (2016)</i>	30	12	Constructed soil of contaminated	Sorption equilibrium	PAH source most dominant role. Partition coefficient (KD: skeet > soot > fuel oil > solvent).	Skeet, soot, OM, charcoal		

			PAH sources and spiking		Minerals showed weakest sorption to PAHs compared to OM. Addition of charcoal increased partitioning.			
<i>Chung and Alexander (1998)</i>	16	1	Spiked	Extractability	Decrease in extraction when OC > 1.0%, negative correlation. No correlation with extraction and the field capacity, clay, sand and silt fractions.	OC		Clay, silt, sand, field capacity
<i>Umeh et al. (2018)</i>	4	1	Spiked	Extractability	Hard OC and clay had negative correlations with BaP extractability, and none with soft OC. Larger extractabilities with sandy soils.	Hard OC, clay	Sand	Soft OC,
<i>De Jonge et al. (2008)</i>	8	2	Spiked	Sorption equilibrium	Sorption cannot be based on SOC contents alone. K _{OC} negatively correlate to clay, CEC, pH.	Clay, CEC, pH		
<i>Barnier et al. (2014)</i>	3	16	Field-contaminated	Extractability	Increased OC content increased available fraction – suggesting quantity not as important as quality – sorption varied between OM types. No direct link to BC and extractability. MGP soil had higher proportion of fine fractions and less available PAHs. Lightest PAHs had highest extractability.	OM quality, fine fractions		BC

<i>James et al. (2018)</i>	14	14	Field-contaminated	<i>In vitro</i> ingestion	No soil physicochemical properties predicted PAH bioavailability/bioaccessibility.		pH, OC, particle size
<i>White et al. (1997)</i>	7	1	Spiked	Earthworm uptake Extractability	Higher uptake in soils with lower OM (1.1%), but no variance in uptake with OM at higher concentrations (4.5%, 8.5% and 13.0%). Uptake increased with clay, decreased by leaching. Decreased extractability with increase clay.	OM, clay (extracted) leaching	Clay (uptake)
<i>White and Alexander (1996)</i>	3	1	Spiked	Mineralisation	Mineralisation higher in lower organic soils.	OM	
<i>Talley et al. (2002)</i>	1 sediment size fractions	17	Field-contaminated	Desorption equilibrium	Coal-derived fraction strongly bonded to PAHs. PAHs in the <63 µm clay/silt fractions are largely available for biodegradation.	Coal	<63 µm clay/silt fractions
<i>Hatzinger and Alexander (1995)</i>	3	1	Spiked	Biodegradability Mineralisation	OM decreased mineralisation rate.	OM	
<i>Tang et al. (2002)</i>	6	4	Spiked	Earthworm uptake	Uptake greater in lowest OM soils, but no link between OM %.	OM	
<i>Saeedi et al. (2018)</i>	3 artificially made soils	3	Spiked	Sorption equilibrium	Increasing HA decreased release. Clay content intensifies OM effects on	OM-clay, HA,	

					decreasing PAH removal. More kaolinite soils had higher HA sorption capacities. Presence of heavy metals in clay mineral mixtures decreases PAHs mobility and removal.	kaolinite, heavy metals	
<i>Piatt and Brusseau (1998)</i>	2	3	Spiked	Sorption equilibrium	HA stronger sorption than FA.	HA	
<i>Brändli et al. (2008)</i>	2	14	Field-contaminated	Sorption equilibrium	Increased sorption with BC. Powdered activated carbon (PAC) more sorption than granulated AC.	BC, smaller size	
<i>Ran et al. (2003)</i>	2	1	Spiked	Sorption equilibrium	Kerogen larger sorption capacity than sand.	Kerogen	
<i>Müller et al. (2007)</i>	3	2	Spiked	Sorption equilibrium	Quartz-montmorillonite mixture had weakest affinity, due to being outcompeted by water.	Quartz-montmorillonite mixture	
<i>Umeh et al. (2019a)</i>	8	10	4 spiked and 4 MGP soils	Extractability	Decreased extractability with increasing ageing, especially in sandy-loam soil.	Sand	
<i>Mader et al. (1997)</i>	2 minerals corundum's (α -Al ₂ O ₃ and α -Fe ₂ O ₃)	6	Spiked	Sorption equilibrium	Sorption coefficients still high with limited OC, shows minerals ability to sorb to PAHs. Neither solution pH or the sorbents surface charge sign or magnitude affected sorption.	Mineral surface	pH or surfaces charge

<i>Meng et al. (2019)</i>	2	1	Spiked	Extractability	pH and EC changes had a greater effect on sandy soils, due to lower TOC and clay content. High pH creates negative charges which repel hydrophobic PAHs.		High pH and EC (especially in sand)
<i>Hu and Aitken (2012)</i>	1	7	Field-contaminated	Desorption equilibrium	Increase soil moisture content (SMC) decreases desorption.	SMC	
<i>Enell et al. (2005)</i>	1	5	Field-contaminated	Desorption equilibrium	Decrease temperature decreases PAH desorption rates, the desorption process is related to the activation energy.		Temperature
<i>Uytbroek et al. (2006)</i>	1 soil + size fractions	1	Field-contaminated	Mineralisation	Lowest release from soil with expandable layer.	Expandable clay	

Table S2. GC-MS/MS analyte quantifier ions and collision energies used in study, compiled by other literature (Ghetu et al., 2021, Sørensen et al., 2016).

Analyte	Retention Time (min)	Window (min)	Quantifier Precursor Ion	Quantifier Product Ion	Collision Energy (V)
Nap	8.4	0.5	128.1	77.1	30
Nap	8.4	0.5	128.1	102	20
Nap	8.4	0.5	128.1	128.1	25
2-mNap	9.9	0.6	142	115	40
2-mNap	9.9	0.6	142	141	20
1-mNap	10.3	0.6	142	115	40
1-mNap	10.3	0.6	142	141	20
C2-Nap	11.6	4	156	141	20
C2-Flu	11.8	4.5	194	165	30
C2-Flu	11.8	4.5	194	179	20
Acy	12.6	0.5	152	150	35
Acy	12.6	0.5	152	151	25
Acy	12.6	0.5	152	152	25
C3-Nap	12.8	3	170	141	20
C3-Nap	12.8	3	170	155	15
Ace	12.9	0.5	153.07	151.07	40
Ace	12.9	0.5	154	152	25
Ace	12.9	0.5	154	153	20
C4-Nap	13	3	184	141	20
C3-Nap	13.5	3.5	170	141	20
C3-Nap	13.5	3.5	170	155	15
C1-Flu	14	4.5	180	165	20
C1-Flu	14	4.5	180	179	30
C2-Flu	14	4.5	194	165	30
C2-Flu	14	4.5	194	179	20
Flu-d10	14.2	0.5	174.1	170.1	30
Flu-d10	14.2	0.5	176	174	25
Flu	14.3	0.5	165.1	139	30
Flu	14.3	0.5	165.1	163.1	30
Flu	14.3	0.5	166	165	25
C3-Nap	14.8	3	170	141	20
C3-Nap	15.0	3.5	170	141	20
C3-Nap	15.0	3.5	170	155	15
C3-Nap	15.8	3	170	141	20
C3-Nap	15.8	3	170	155	15
C1-Flu	16	4.5	180	165	20
C1-Flu	16	4.5	180	179	30
C4-Nap	16	3	184	141	20
C2-Flu	17	4.5	194	165	30
C2-Flu	17	4.5	194	179	20

DBT	17.6	0.5	184	139	45
DBT	17.6	0.5	184	152	30
Phen-d10	17.9	0.5	188	158	30
Phen-d10	17.9	0.5	188	160	30
C3-Flu	18	8	208	179	30
C3-Flu	18	8	208	193	30
C3-Flu	18	8	208	193	20
C1-Flu	18	4.5	180	165	20
C1-Flu	18	4.5	180	179	30
C4-Nap	18	3	184	141	20
Phen	18	0.5	178.1	152.1	25
Phen	18	0.5	178.1	176.1	20
An	18.3	0.5	178.1	152.1	25
An	18.3	0.5	178.1	176.1	20
C2-Flu	19	4.5	194	165	30
C2-Flu	19	4.5	194	179	20
C1-DBT	19.7	4	198	197	20
C1-DBT	19.7	4	198	197	5
C2-Phen/An	20	4.5	206	191	20
C1-Phen/An	20.7	4	192	191	20
C2-DBT	21	4.5	212	197	20
C2-DBT	21	4.5	212	211	20
C2-DBT	21	4.5	212	211	5
C2-Flu/Pyr	21.7	5	230	215	20
C2-Flu	21.7	4.5	194	165	30
C2-Flu	21.7	4.5	194	179	20
C3-Flu	22	8	208	179	30
C3-Flu	22	8	208	193	30
C3-Flu	22	8	208	193	20
C3-Phen/An	22	6	220	191	25
C3-Phen/An	22	6	220	205	20
C2-Phen/An	22.9	4.5	206	191	20
C2-Fla/Pyr	23.7	5	230	215	20
Fla-d10	23.7	0.5	212	184	25
Fla-d10	23.7	0.5	212	208	35
Fla-d10	23.7	0.5	212	212	50
C3-DBT	23.8	5	226	197	20
C3-DBT	23.8	5	226	221	20
C3-DBT	23.8	5	226	225	5
Fla	23.9	0.5	202.1	176.1	35
Fla	23.9	0.5	202.1	200.1	30
Fla	23.9	0.5	202.1	202.1	50
C3-Phen/An	25.1	6	220	191	25
C3-Phen/An	25.1	6	220	205	20

Pyr-d10	25.2	0.5	212	184	25
Pyr-d10	25.2	0.5	212	208	30
Pyr-d10	25.2	0.5	212	210	30
Pyr	25.3	0.5	202.1	176.1	25
Pyr	25.3	0.5	202.1	200.1	30
Pyr	25.3	0.5	202.1	201.1	30
C2-Fla/Py	25.6	5	230	215	20
C3-Flu	26	8	208	179	30
C3-Flu	26	8	208	193	30
C3-Flu	26	8	208	193	20
C4-Phen/An	26	8	234	191	25
C4-Phen/An	26	8	234	205	20
C4-Phen/An	26	8	234	219	20
C1-Fla/Py	27.1	6	216	215	30
BaFlu	27.4	4	215	213	39
BaFlu	27.4	4	216	215	28
BaFlu	27.4	4	216	216	50
BcFlu	27.5	4	215	213	39
BcFlu	27.5	4	216	215	28
BcFlu	27.5	4	216	216	50
BbFlu	27.6	4	216	213	39
BbFlu	27.6	4	216	215	28
BbFlu	27.6	4	216	216	50
BbFlu	27.6	4	217	202	35
BbFlu	27.6	4	217	215	35
C3-Fla/Pyr	28	10.3	215	189	30
C3-Fla/Pyr	28	10.3	244	215	30
C4-Phen/An	30	8	234	191	25
C4-Phen/An	30	8	234	205	20
C4-Phen/An	30	8	234	219	20
C1-BaA/Chry/TPh	30	6	242	226	35
C1-BaA/Chry/TPh	30	6	242	241	20
C1-BaA/Chry/TPh	30	6	243	227	30
C1-BaA/Chry/TPh	30	6	243	228	30
C2-BaA/Chry/TPh	30	6	256	241	20
C2-BaA/Chry/TPh	30	6	256	241	15
BcPhen	30.4	0.7	228	226.1	40
BcPhen	30.4	0.7	229	227	30
BcPhen	30.4	0.7	229	228	30
BaA	32.3	0.5	228.1	202.1	35
BaA	32.3	0.5	228.1	226.1	30
BaA	32.3	0.5	228.1	228.1	50
C2-Fla/Pyr	32.6	10	230	215	20
CPP	32.7	0.5	226	224	45

CPP	32.7	0.5	226	225	25
CPP	32.7	0.5	226	226	50
TPh	32.7	0.5	226	224	45
TPh	32.7	0.5	228	226	40
TPh	32.7	0.5	228	228	50
Chry	32.8	0.5	228.1	202.1	35
Chry	32.8	0.5	228.1	226.1	30
Chry	32.8	0.5	228.1	228.1	50
C1-BaA/Chry/TPh	34.2	6	242	226	35
C1-BaA/Chry/TPh	34.2	6	242	241	20
C1-BaA/Chry/TPh	34.2	6	243	227	30
C1-BaA/Chry/TPh	34.2	6	243	228	30
C4-Phen/An	35	8	234	191	25
C4-Phen/An	35	8	234	205	20
C4-Phen/An	35	8	234	219	20
C3-Fla/Pyr	36.4	10.3	215	189	30
C3-Fla/Pyr	36.4	10.3	244	215	30
C1-BaA/Chry/TPh	36.6	6	242	226	35
C1-BaA/Chry/TPh	36.6	6	242	241	20
C1-BaA/Chry/TPh	36.6	6	243	227	30
C1-BaA/Chry/TPh	36.6	6	243	228	30
C2-BaA/Chry/TPh	37.5	6	256	241	20
C2-BaA/Chry/TPh	37.5	6	256	241	15
C1-BaA/Chry/TPh	38.6	6	242	226	35
C1-BaA/Chry/TPh	38.6	6	242	241	20
C1-BaA/Chry/TPh	38.6	6	243	227	30
C1-BaA/Chry/TPh	38.6	6	243	228	30
BbF-d12	38.6	1	264	230	30
BbF-d13	38.6	1	264	260	30
BbF-d14	38.6	1	264	262	50
BbF-d15	38.6	1	264	264	50
BbF	38.7	1.5	252.1	226.1	35
BbF	38.7	1.5	252.1	250.1	30
BbF	38.7	1.5	252.1	252.1	50
BkF	38.9	1.5	252.1	226.1	35
BkF	38.9	1.5	252.1	250.1	30
BkF	38.9	1.5	252.1	252.1	50
BjF	39.0	1.5	252	225	45
BjF	39.0	1.5	252	250	45
BjF	39.0	1.5	252	252	50
BaF	39.5	1.5	252.09	226.08	35
BaF	39.5	1.5	252.09	250.09	30
BaF	39.5	1.5	253	251	40
BaF	39.5	1.5	253	252	40

C3-BaA/Chry/TPh	39.5	8	270	241	20
C3-BaA/Chry/TPh	39.5	8	270	255	20
C4-BaA/Chry/TPh	40	10	284	241	20
C4-BaA/Chry/TPh	40	10	284	255	20
C4-BaA/Chry/TPh	40	10	284	269	20
Benzo[E/Py	40.5	0.5	252	225	45
BeP	40.5	0.5	252	250	45
BeP	40.5	0.5	252	252	50
BaP	40.8	0.5	252	226	35
BaP	40.8	0.5	252	250	30
BaP	40.8	0.5	252	252	50
BaP-d12	40.8	0.5	264	230	30
BaP-d12	40.8	0.5	264	260	30
BaP-d12	40.8	0.5	264	262	50
BaP-d12	40.8	0.5	264	264	50
Per-d12	41.4	0.5	264	230	30
Per-d12	41.4	0.5	264	260	30
Per-d12	41.4	0.5	264	262	50
Per-d12	41.4	0.5	264	264	50
Per	41.6	0.5	252	226	35
Per	41.6	0.5	252	250	30
Per	41.6	0.5	252	252	50
DacA	44.7	1.5	276	274	40
DacA	44.7	1.5	278	276	40
DacA	44.7	1.5	279	276	40
DacA	44.7	1.5	279	277	40
IcdP	46.1	0.9	276.1	272.1	60
IcdP	46.1	0.9	276.1	274.1	40
IcdP	46.1	0.9	276.1	276.1	50
IcdP-d12	46.3	0.9	288	286	50
IcdP-d13	46.3	0.9	288	288	50
DahA	46.4	0.5	278.1	274.1	60
DahA	46.4	0.5	278.1	276.1	30
DahA	46.4	0.5	278.1	278.1	50
BghiP-d12	47.6	0.5	288	286	50
BghiP-d12	47.6	0.5	288	288	50
BghiP	47.8	0.5	276.1	272.1	60
BghiP	47.8	0.5	276.1	276.1	40
C4-BaA/Chry/TPh	50	10	284	241	20
C4-BaA/Chry/TPh	50	10	284	255	20
C4-BaA/Chry/TPh	50	10	284	269	20
DaeF	51.6	2.1	303	301	40
DaeF	51.6	2.1	303	302	40
DaiP/DaeP/ DaiP/ DahP	53.5	6	300	298	45

DalP/DaeP/ DaiP/ DahP	53.5	6	302	300	45
DalP/DaeP/ DaiP/ DahP	53.5	6	302	302	50

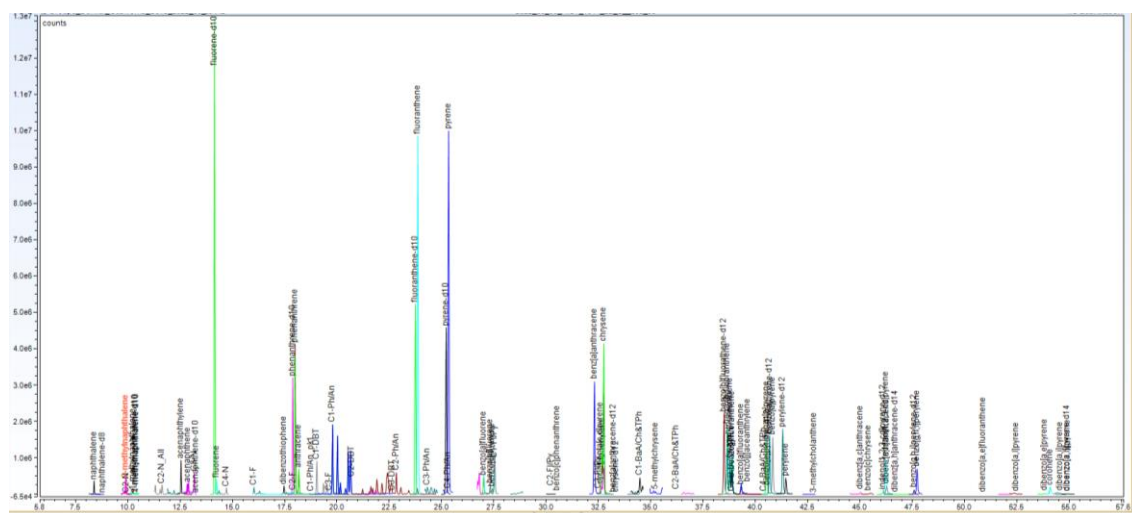
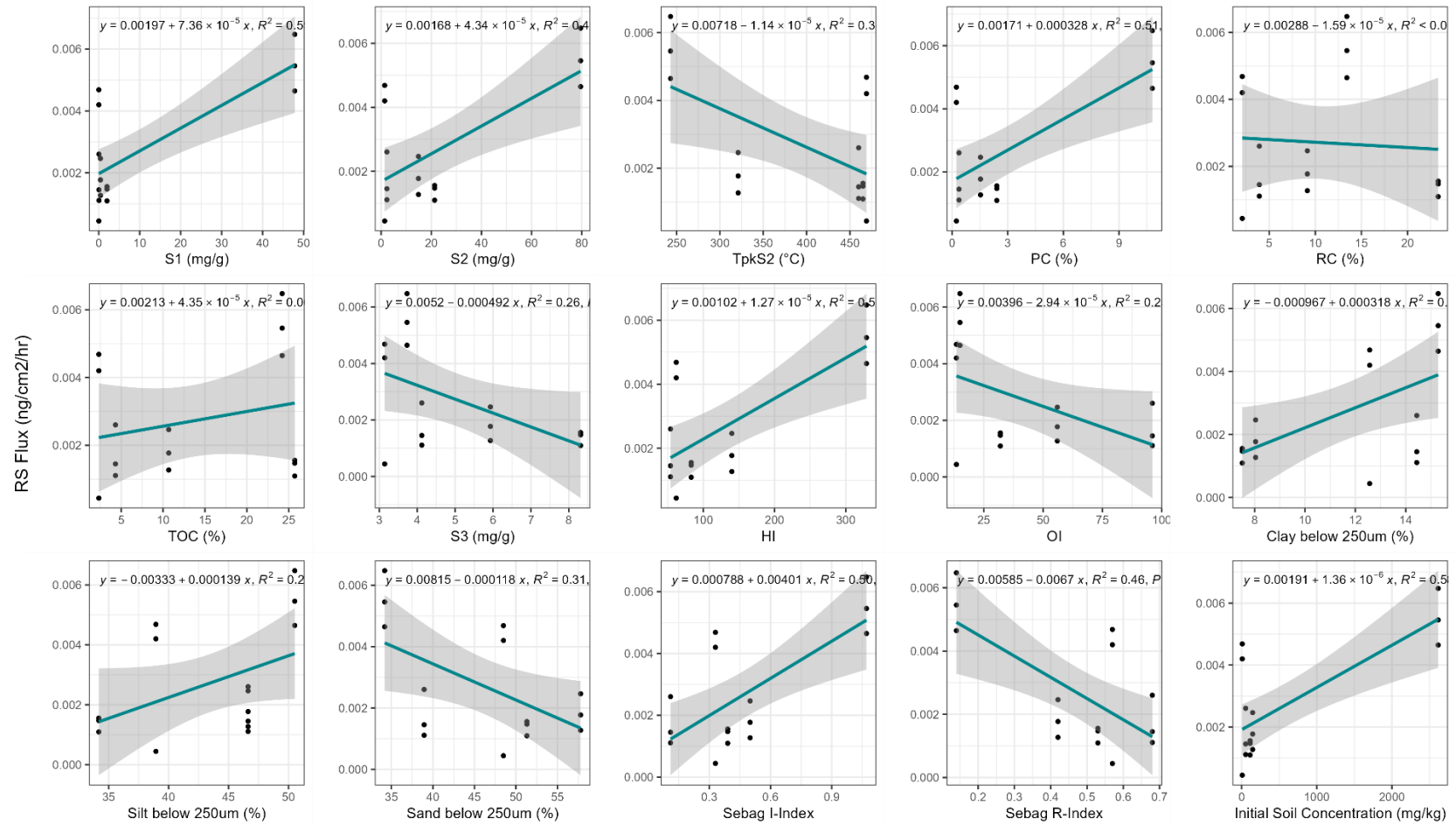
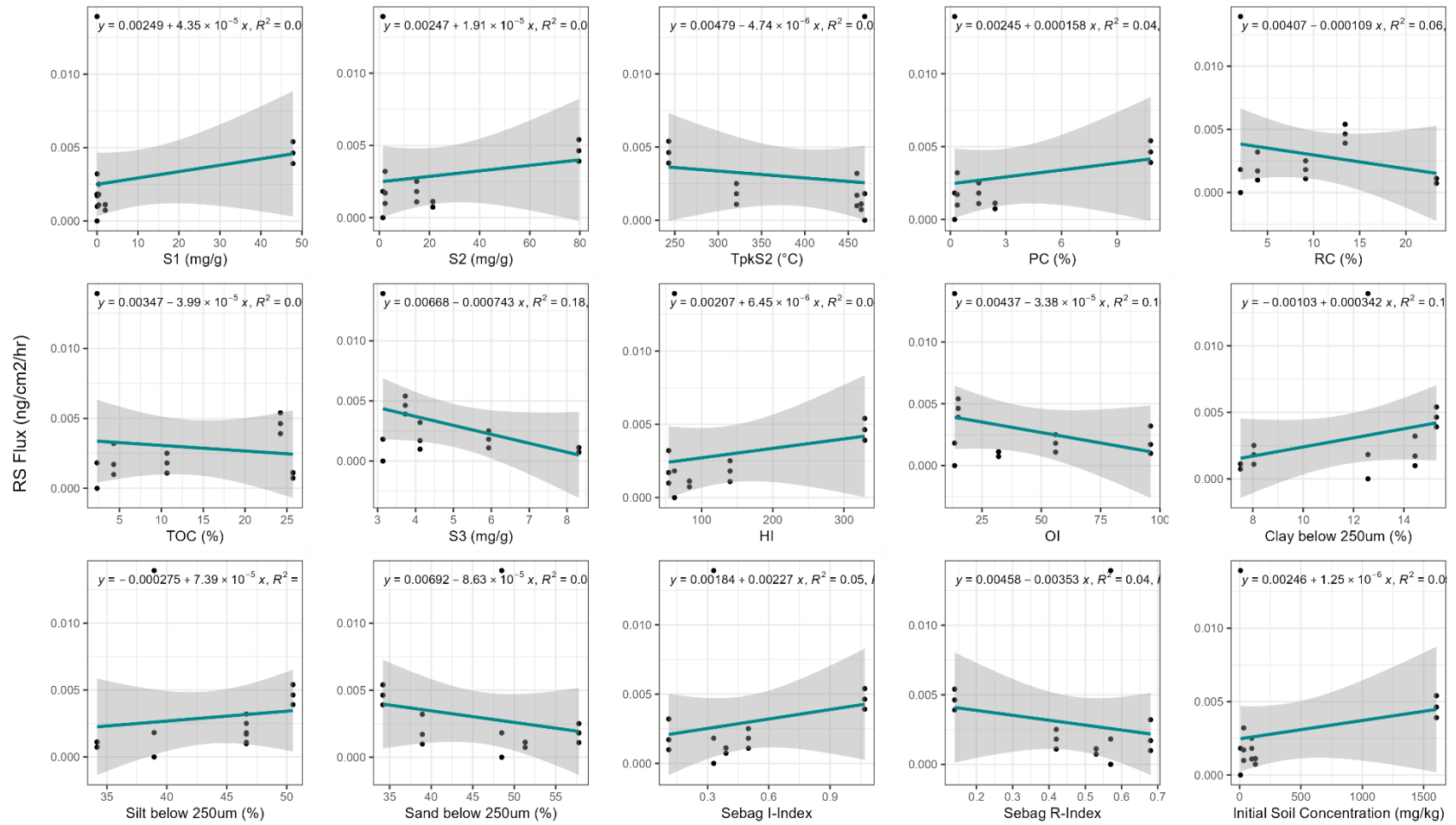


Figure S1. GC-MS/MS chromatogram for the CRM NIST-1944.

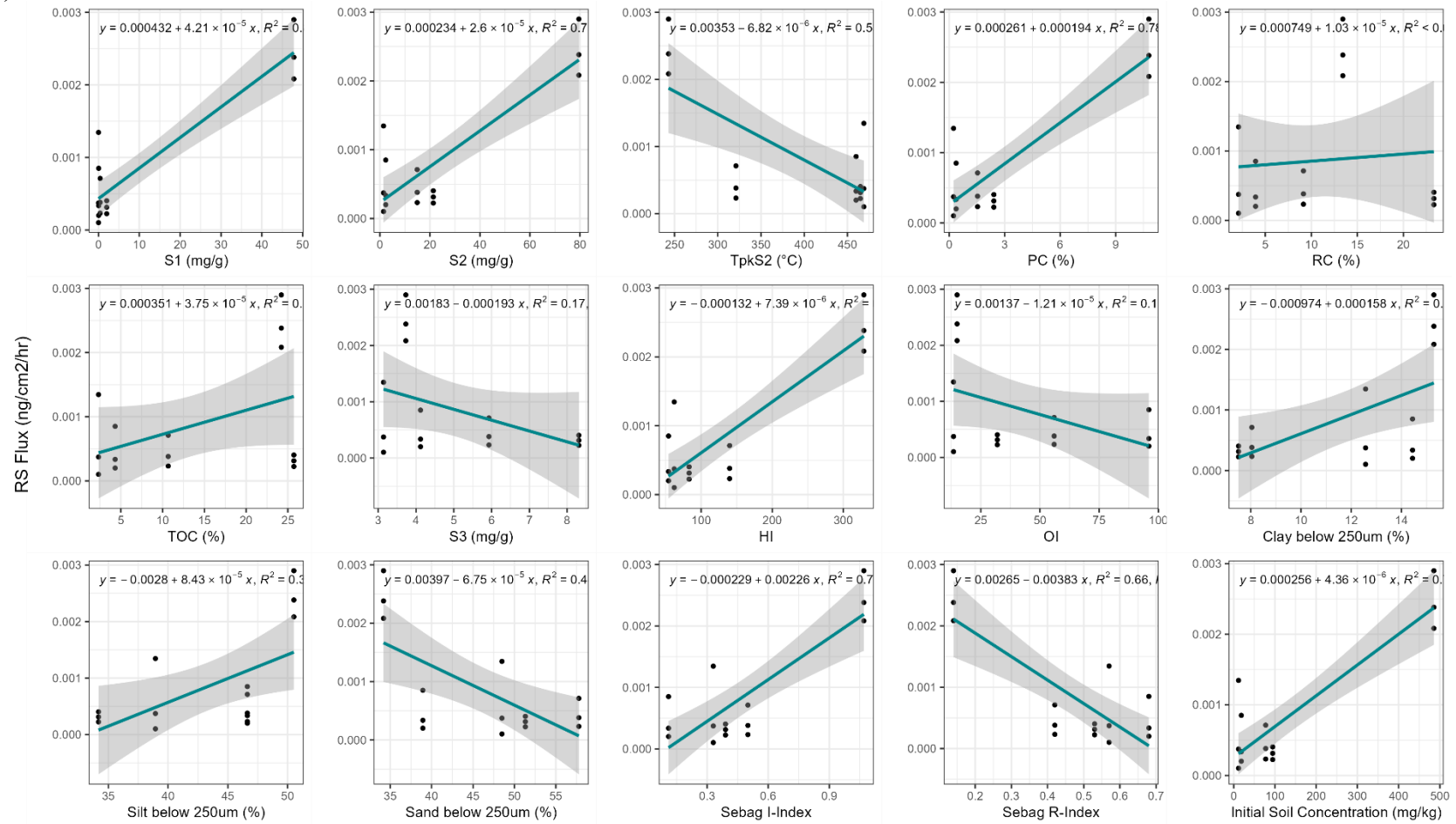
(a)



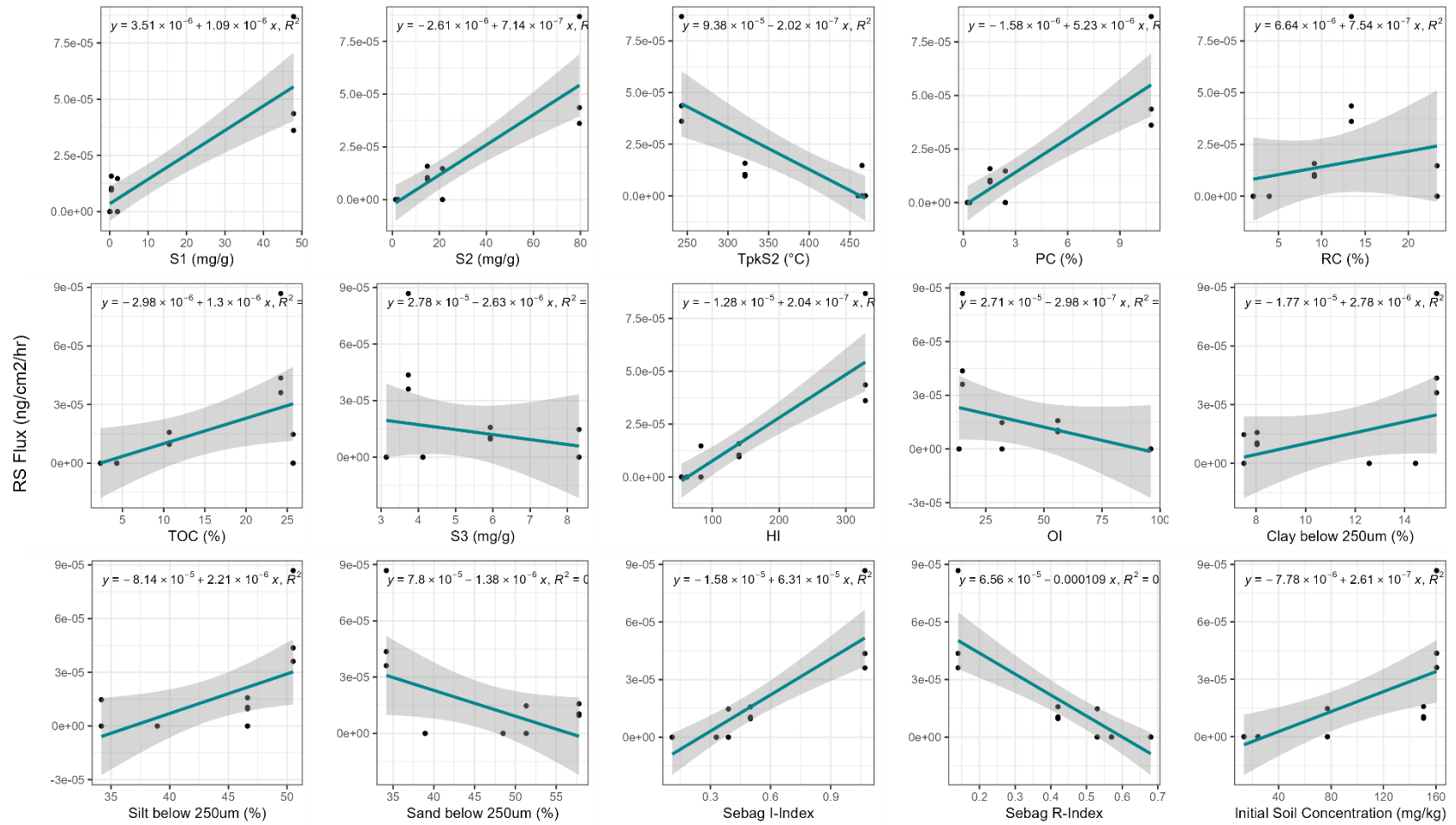
(b)



(c)



(d)



(e)

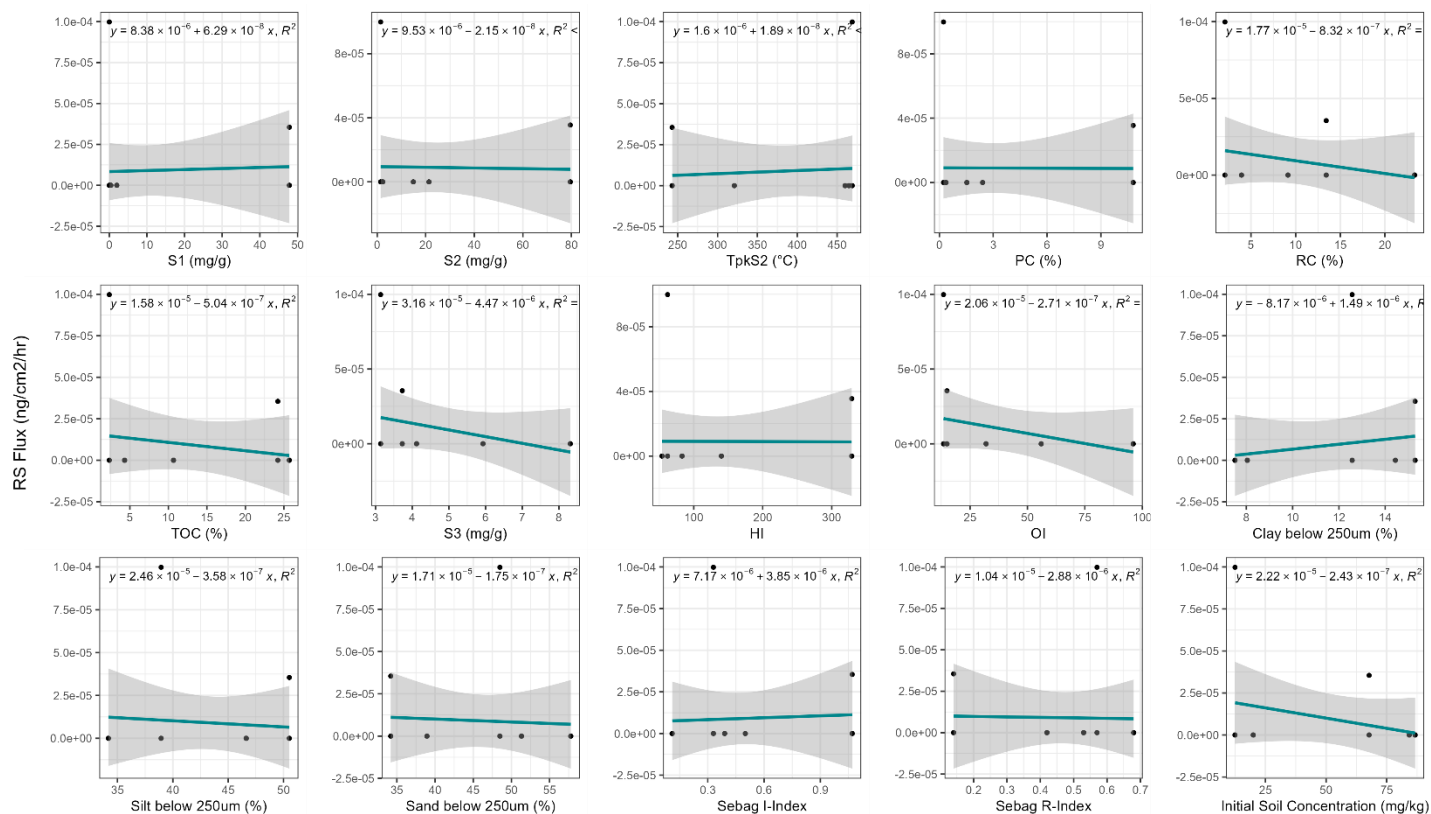


Figure S3 Simple linear regression between the normalised RS flux by the initial soil concentration and the RE parameters for the HMW PAHs: (a) Fla, (b) Pyr, (c) C1-Fla/Pyr, (d) BaP and (e) BghiP. (Points are each experiment taken for the 5 MGP soils).

APPENDIX B-C

CHAPTER 5 & 6 SI

The SI for Chapter 5 research paper – “Characterisation of former Manufactured Gas Plant soils using parent and alkylated Polycyclic Aromatic Hydrocarbons and Rock-Eval(6) Pyrolysis” can be found at:

<https://doi.org/10.1016/j.envpol.2023.122658>

The SI for Chapter 6 research paper – “Dermal absorption of high molecular weight parent and alkylated polycyclic aromatic hydrocarbons from manufactured gas plant soils using *in vitro* assessment” can be found at:

<https://doi.org/10.1016/j.jhazmat.2024.133858>

APPENDIX D

Chapter 7 SI

This present section includes the SI created for Chapter 7 research paper.

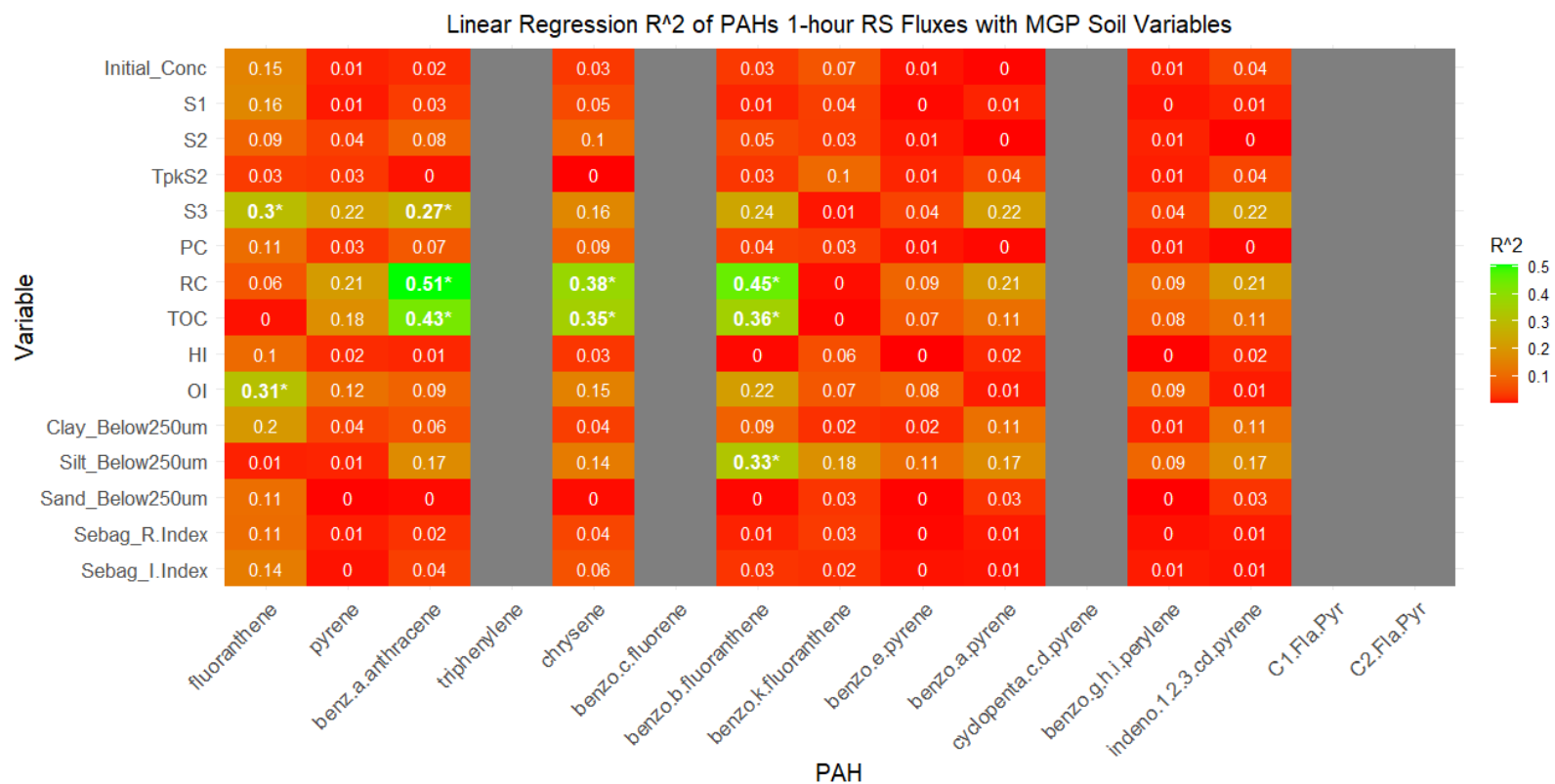


Figure S12. R² values from linear regression on MGP samples soil properties vs RS flux (triplicate dermal experiments results) at the 1-hour timestep for each HMW PAH.GP samples. Brighter green tiles signify a higher R² values (higher percentage of variation explained by soil property), and brighter red colours are associated to lower R² values. * Indicates significant correlation with a p-value < 0.05.

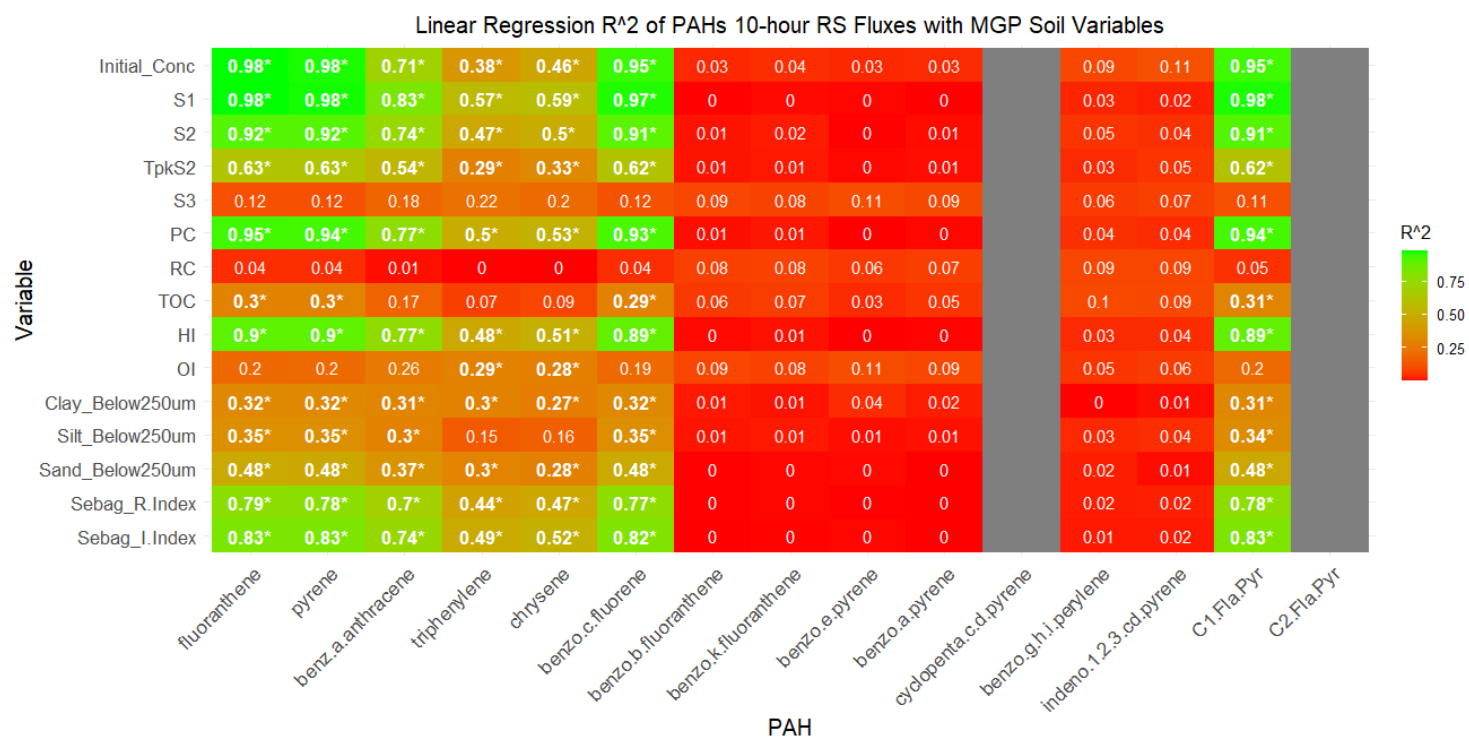
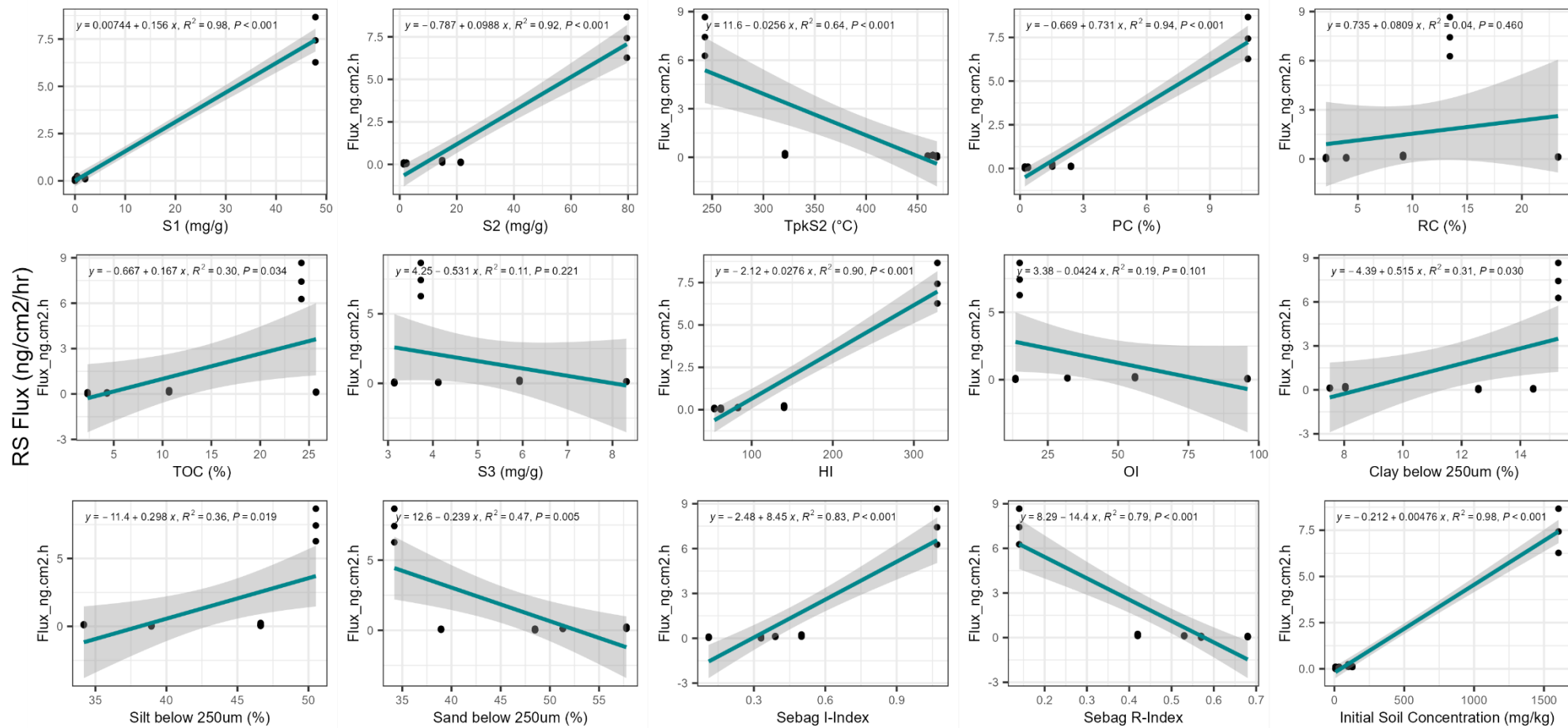
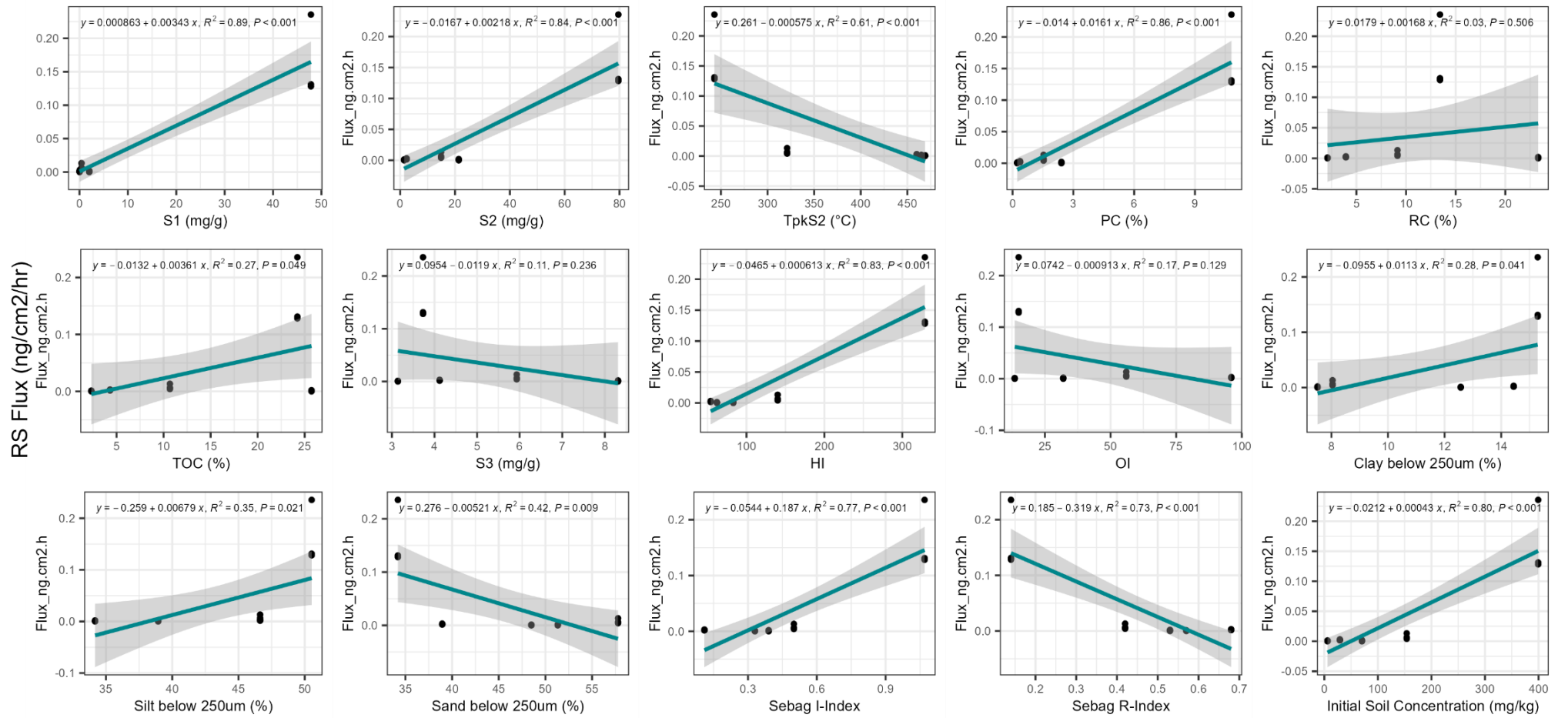


Figure S13. Linear regression r^2 values from MGP samples soil properties vs RS flux (triplicate dermal experiments results) at the 10-hour timestep for each HMW PAH.GP samples. Brighter green tiles signify a higher R^2 values (higher percentage of variation explained by soil property), and brighter red colours are associated to lower R^2 values. * Indicates significant correlation with a p-value < 0.05.

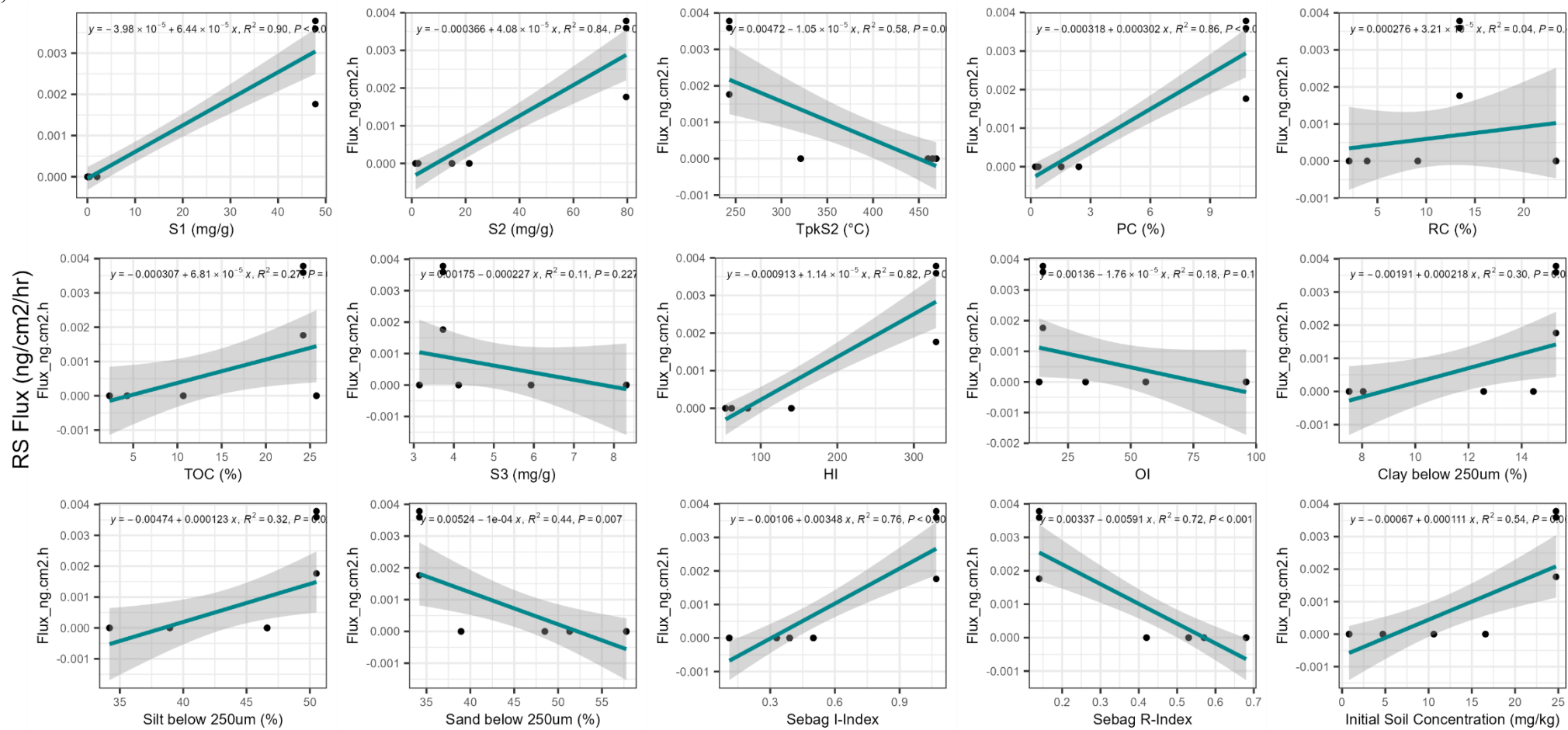
(a)



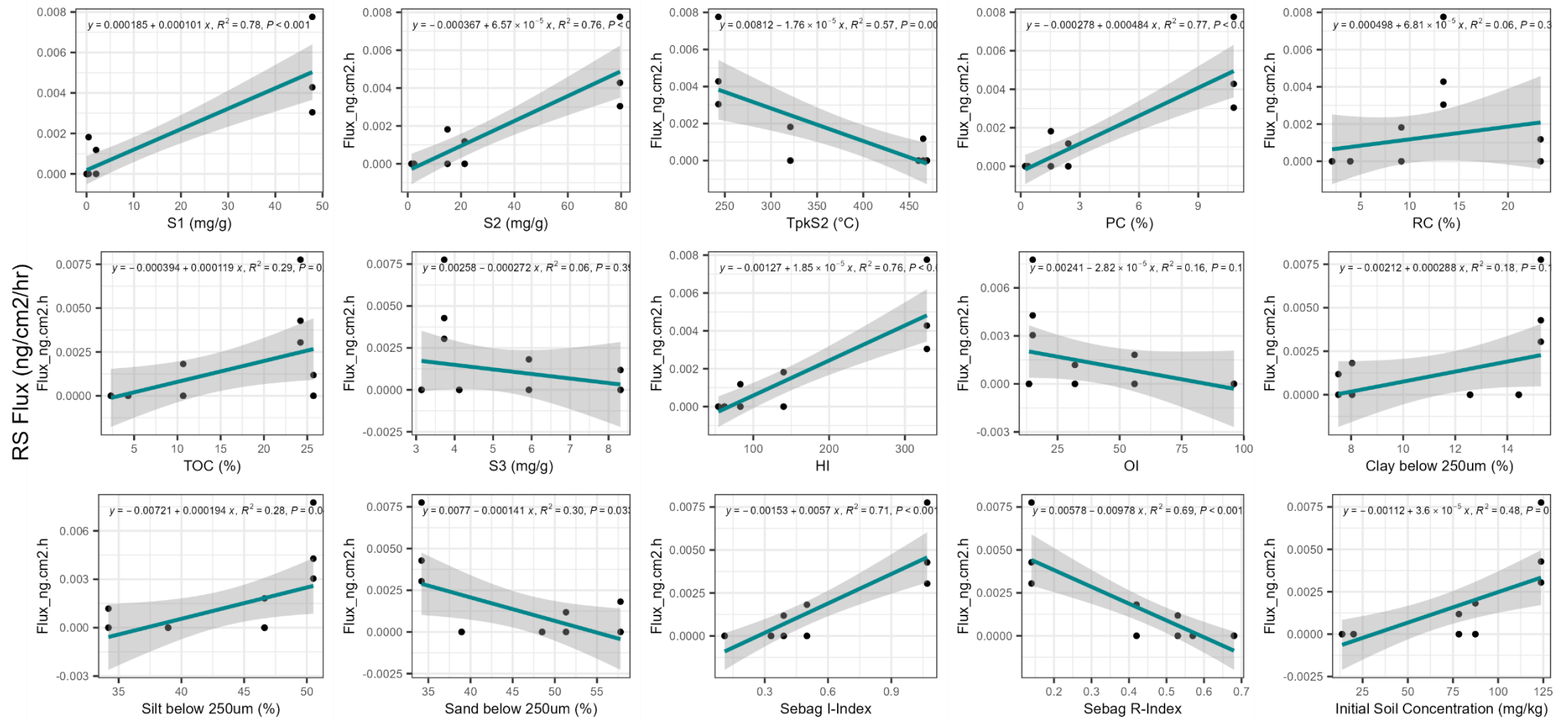
(b)



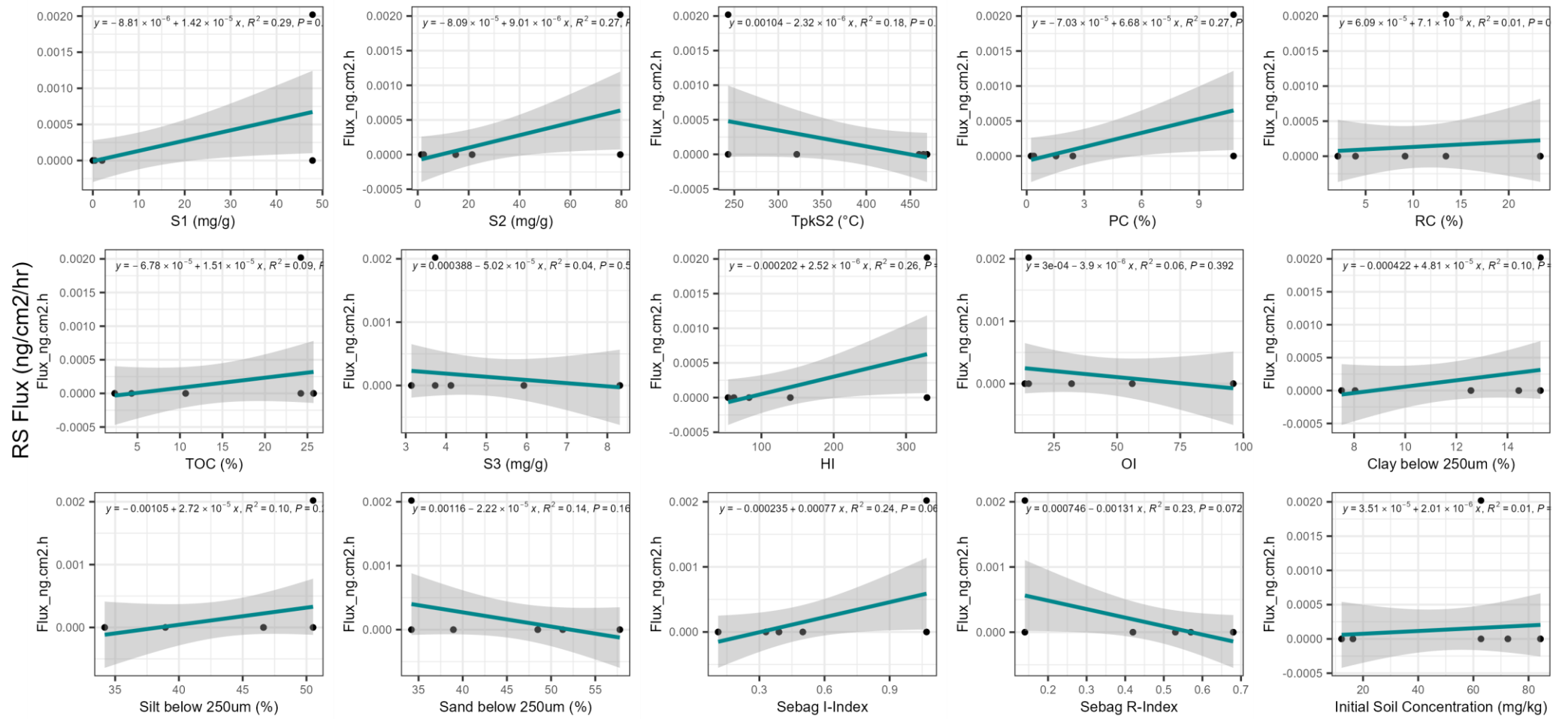
(c)



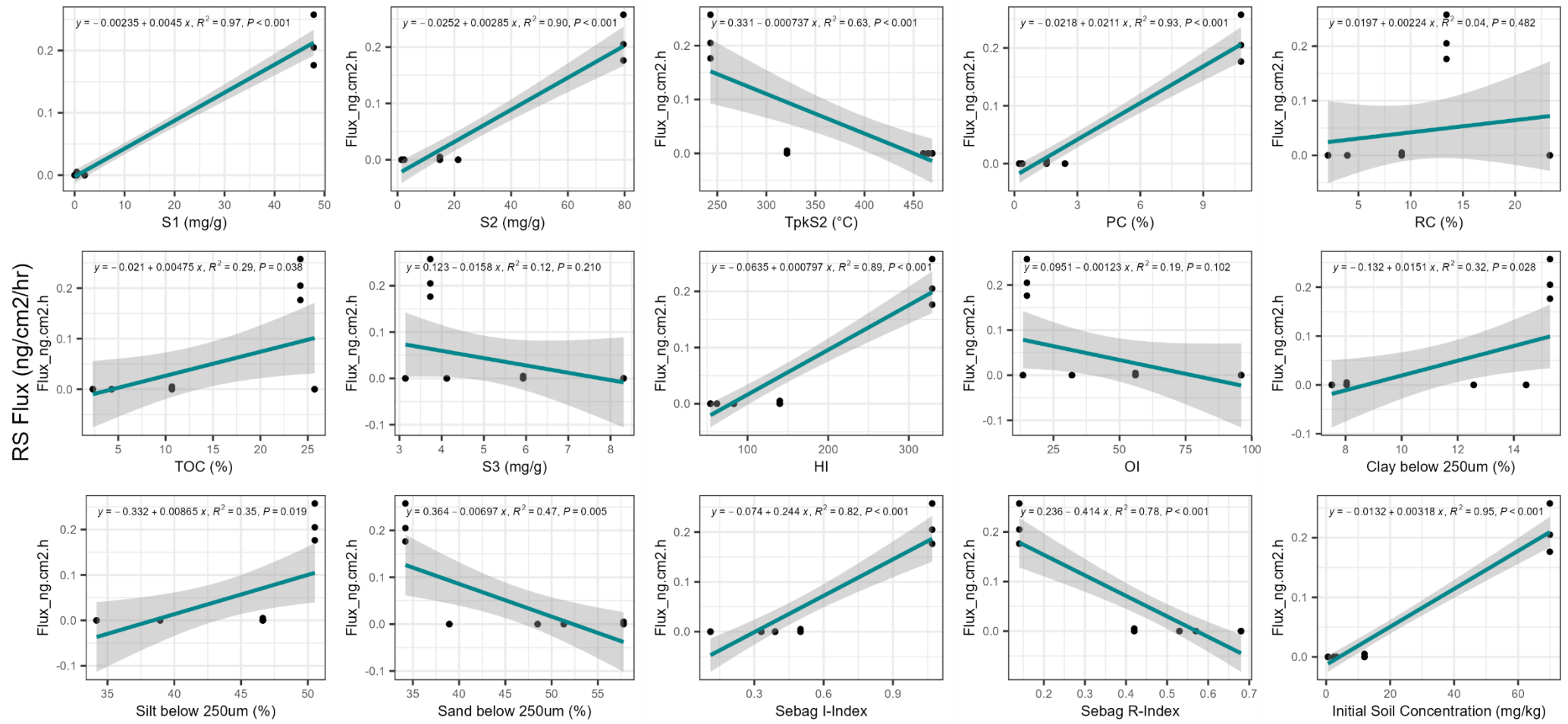
(h)



(j)



(1)



(n)

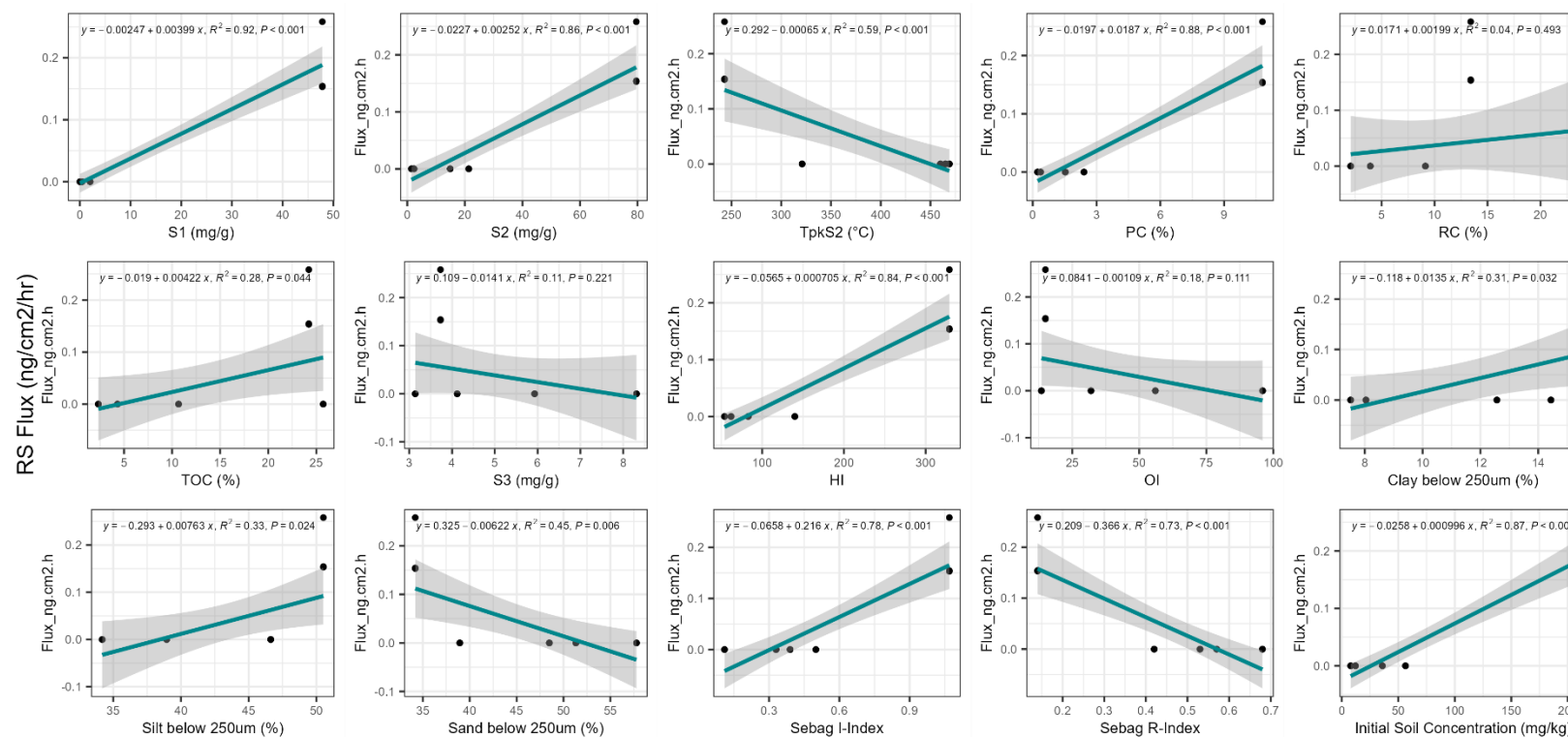
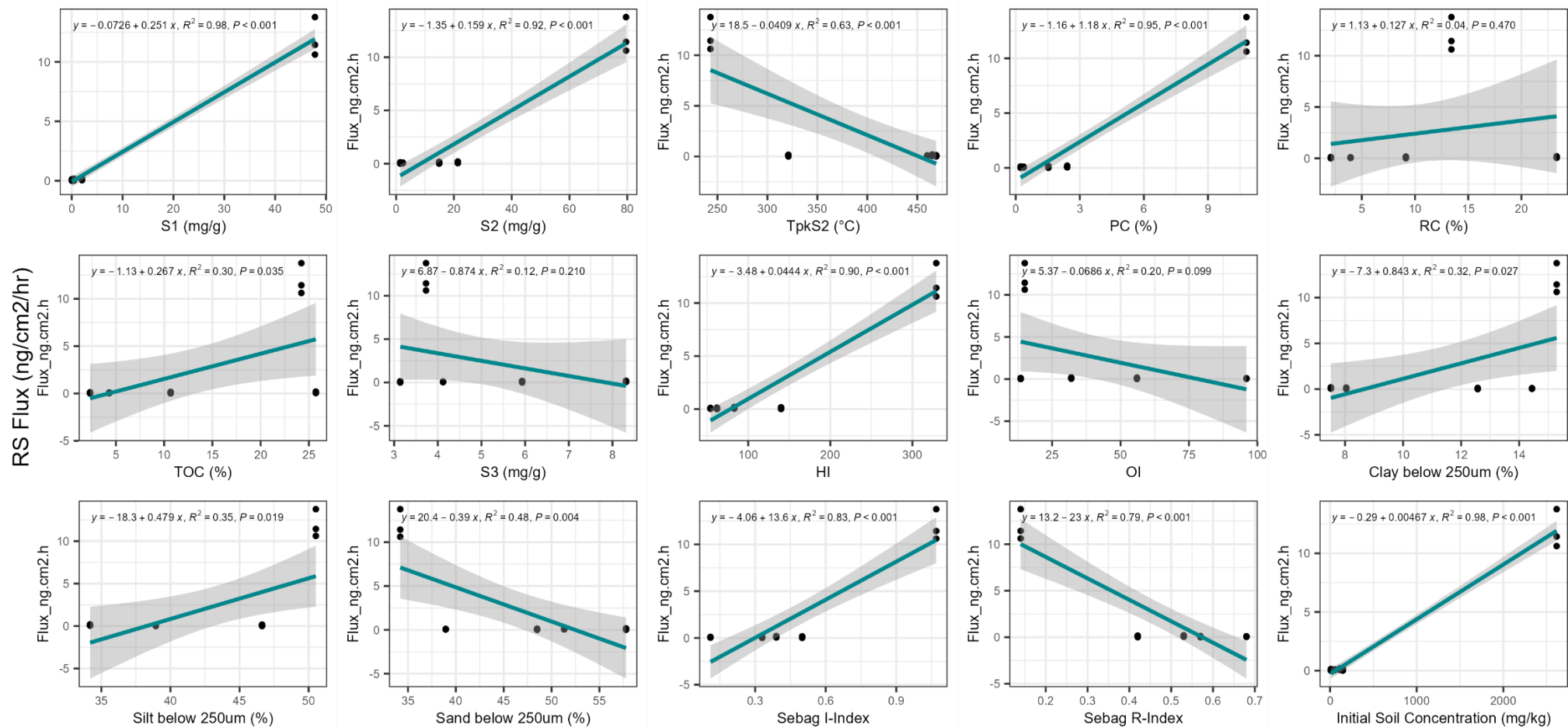
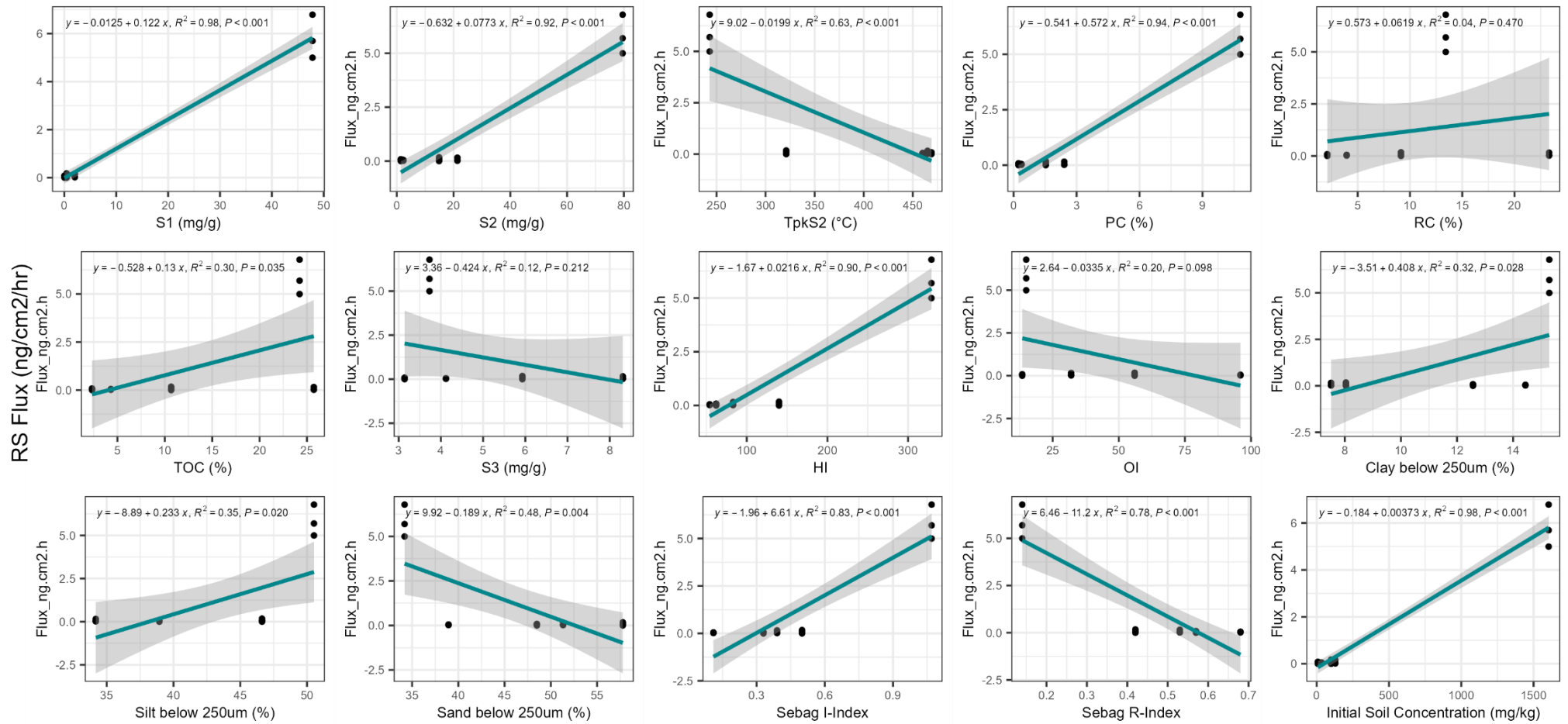


Figure S14. Linear regression on MGP samples soil properties vs RS flux (triplicate dermal experiments results) at 24-h for each HMW PAH, (a) Pyr, (b) BaA, (c) CCP, (d) TPh, (e) Chry, (f) BbF, (g) BkF, (h) BeP, (i) BaP, (j) IcdP, (k) BghiP, (l) BcFlu, (m) C1-Fla/Pyr and (n) C2-Fla/Pyr. PAHs correlation plots not displayed for PAHs not detected in the RS included: BjF, Per, DahA, DaeP, DahP, DaiP, DalP, C3-Fla/Pyr, C1-BaA/Chry/TPh, C2-BaA/Chry/TPh, C3-BaA/Chry/TPh and C4-BaA/Chry/TPh.

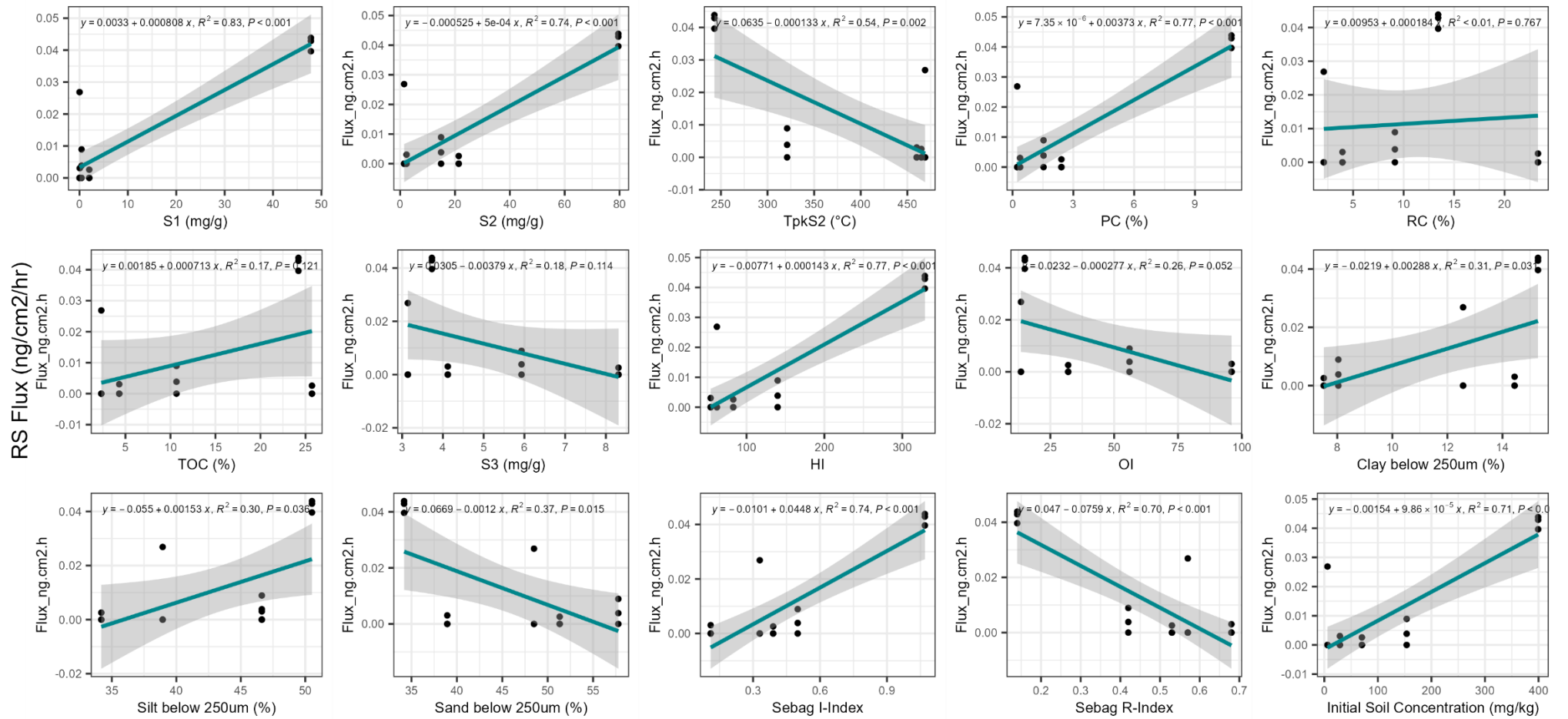
(a)



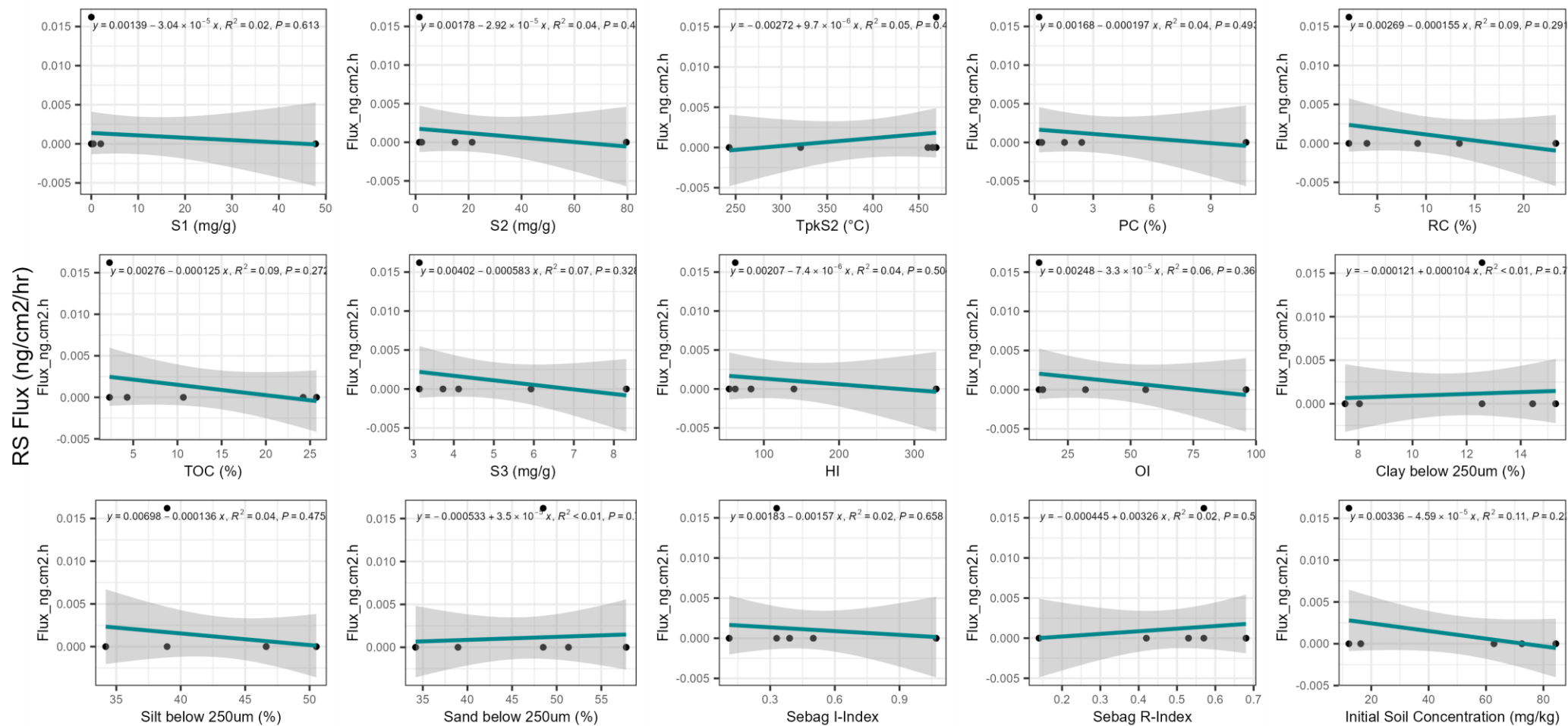
(b)



(d)



(i)



(j)

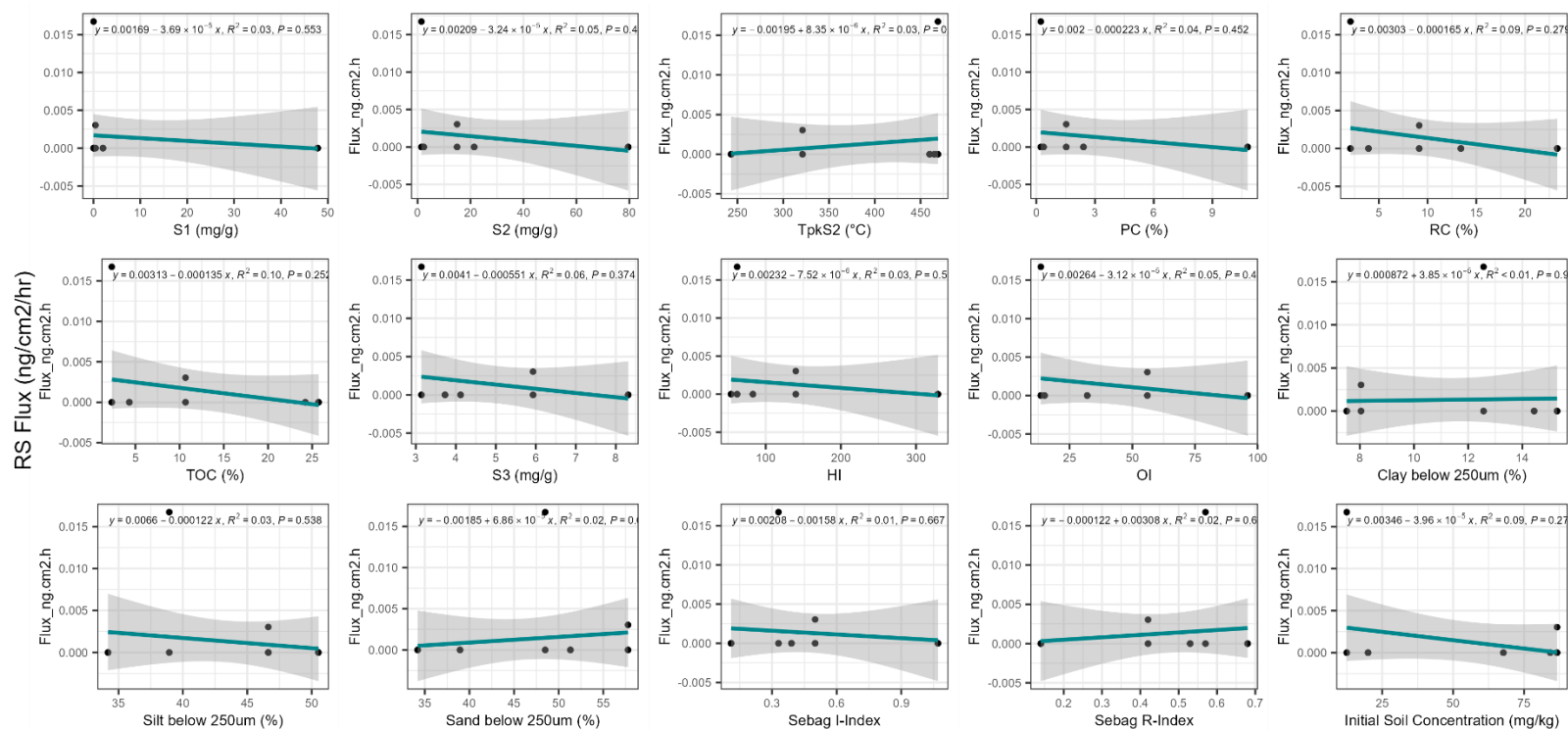
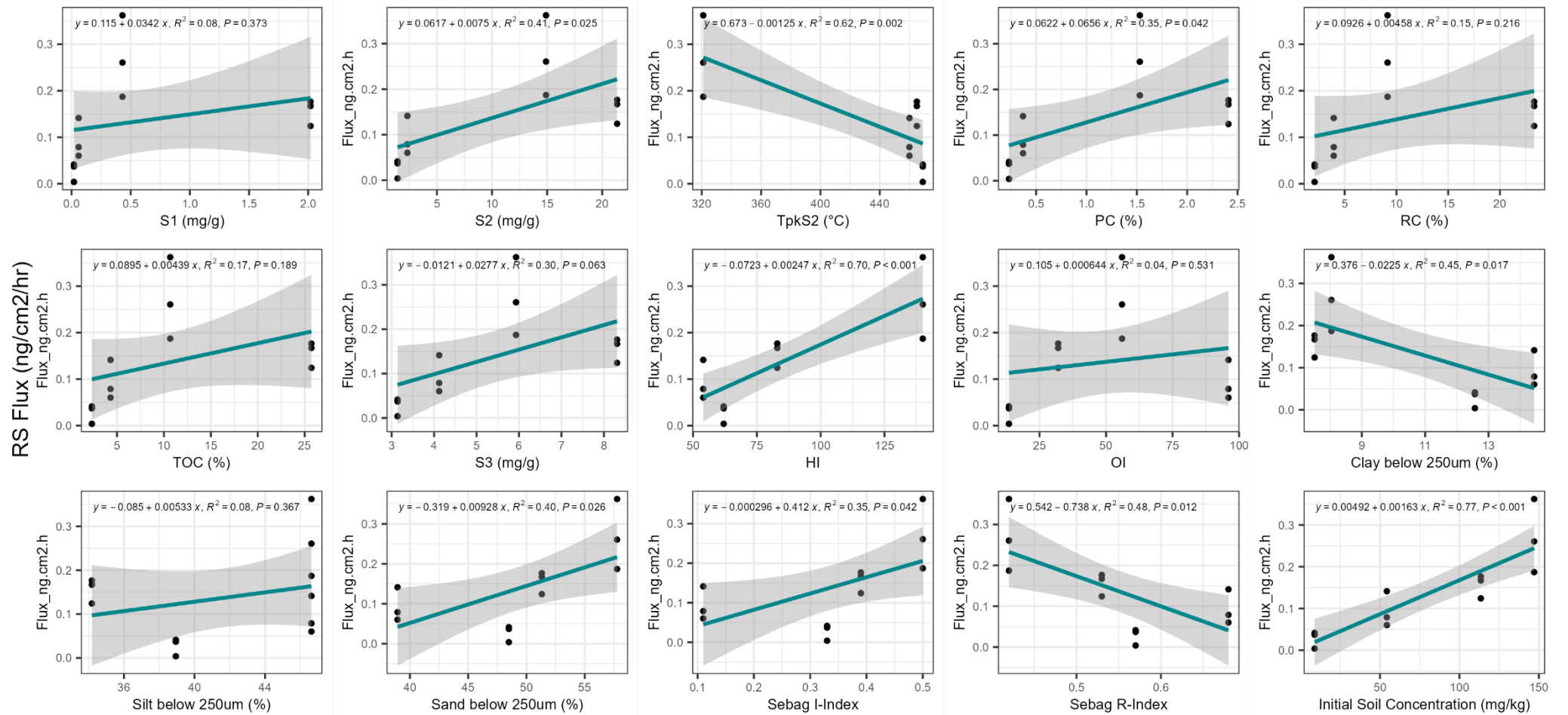
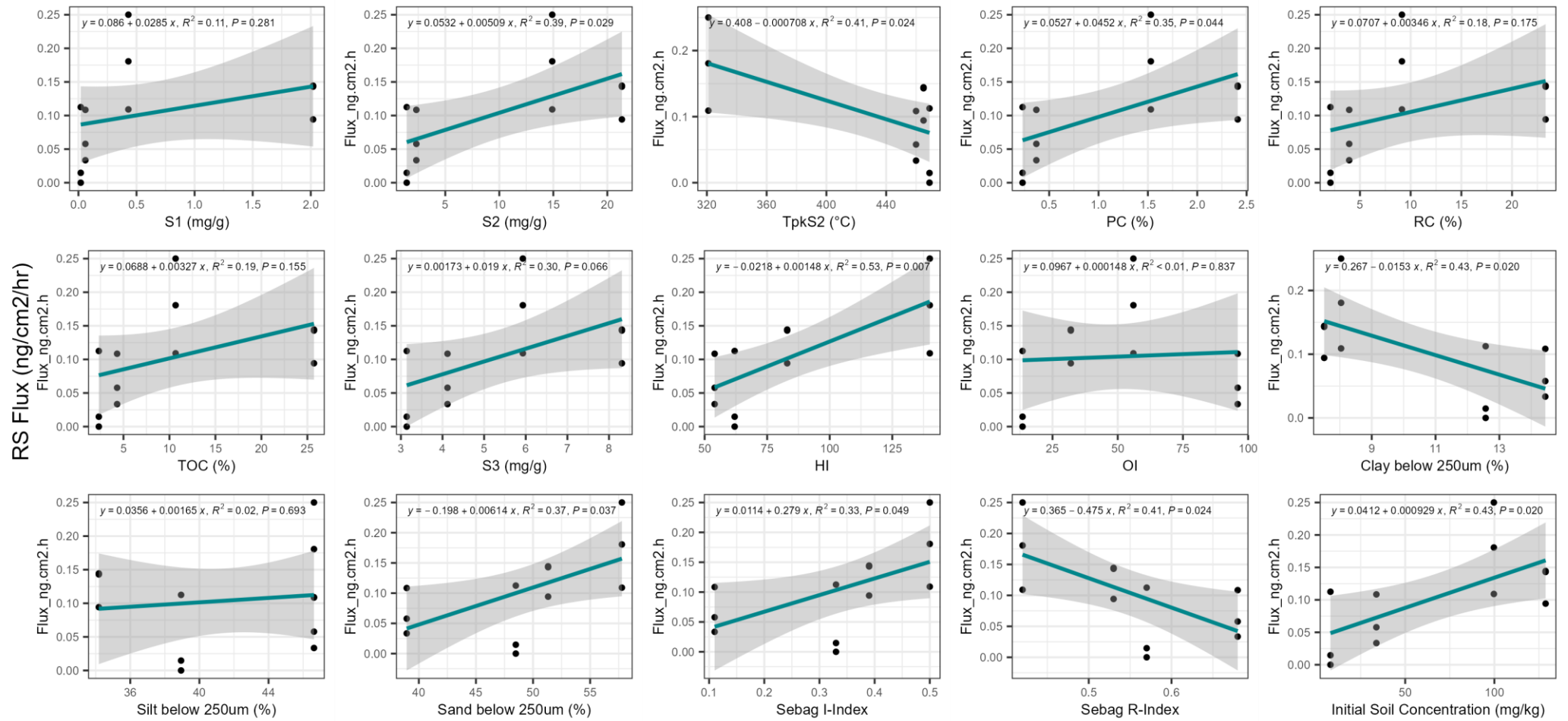


Figure S15. Linear regression on MGP samples soil properties vs RS flux (triplicate dermal experiments results) at 1-h for each HMW PAH, (a) Fla, (b) Pyr, (c) BaA, (d) Chry, (e) BbF, (f) BkF, (g) BeP, (h) BaP, (i) IcdP and (j) BghiP. PAHs correlation plots not displayed for PAHs not detected in the RS included: CCP, TPh, BjF, BcFlu, Per, DahA, DaeP, DahP, DaiP, DalP, C1-Fla/Pyr, C2-Fla/Pyr, C3-Fla/Pyr, C1-BaA/Chry/TPh, C2-BaA/Chry/TPh, C3-BaA/Chry/TPh and C4-BaA/Chry/TPh.

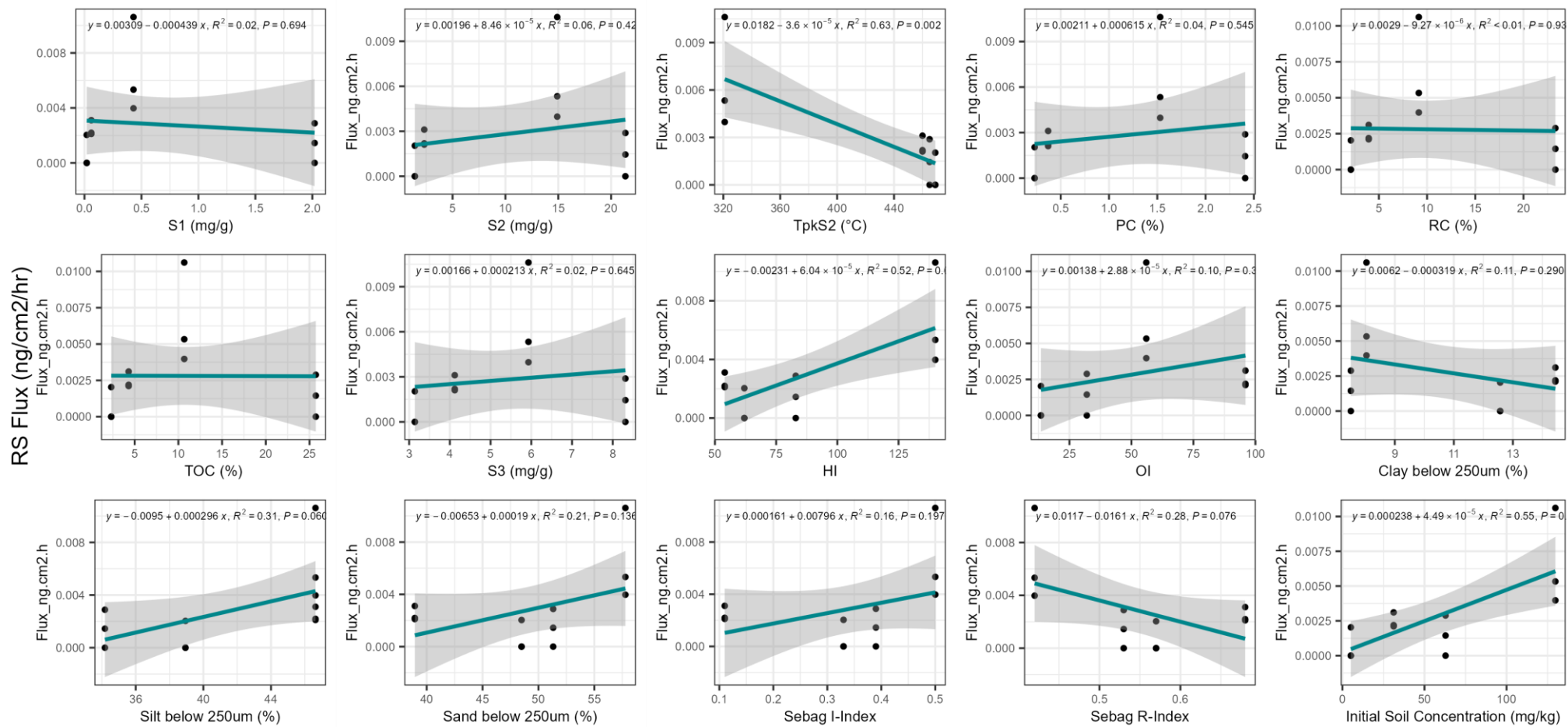
(a)



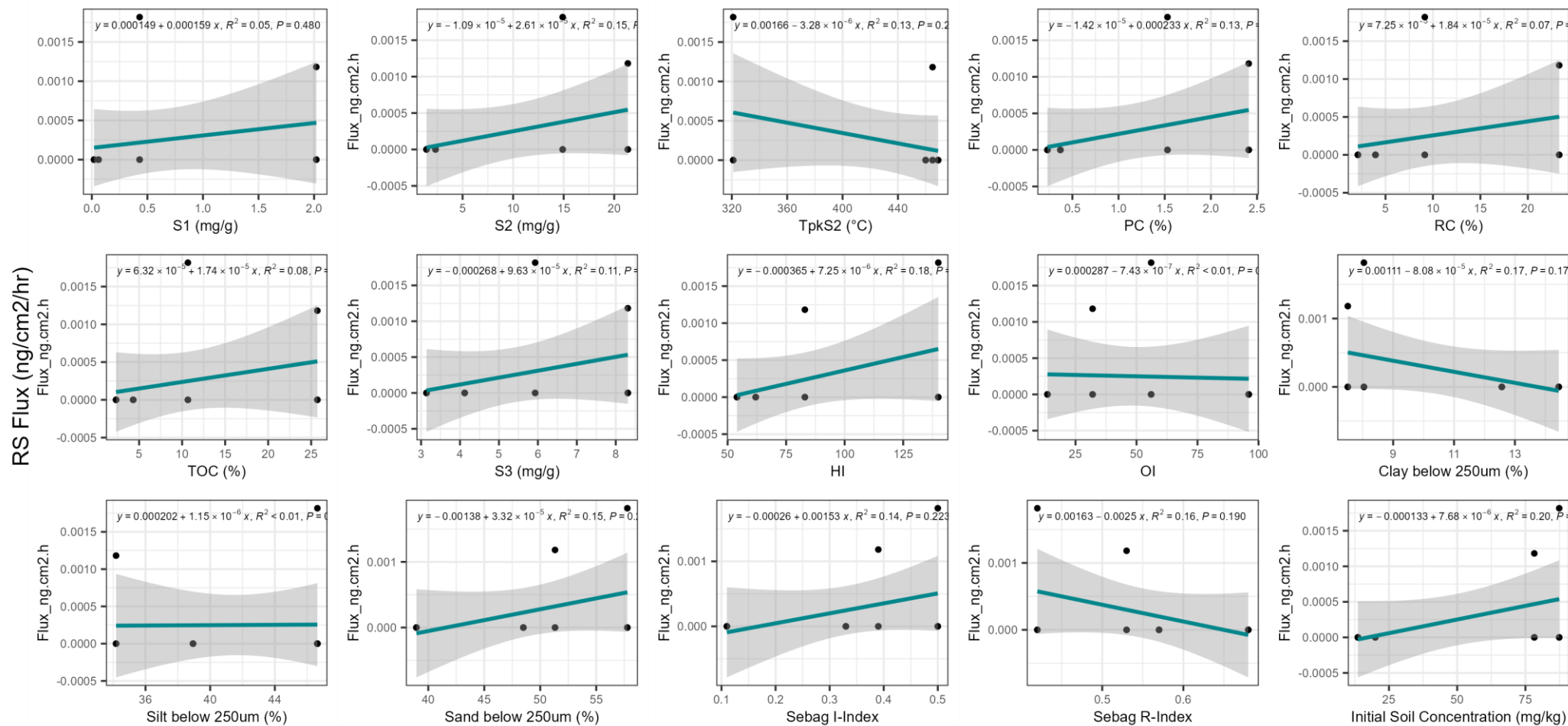
(b)



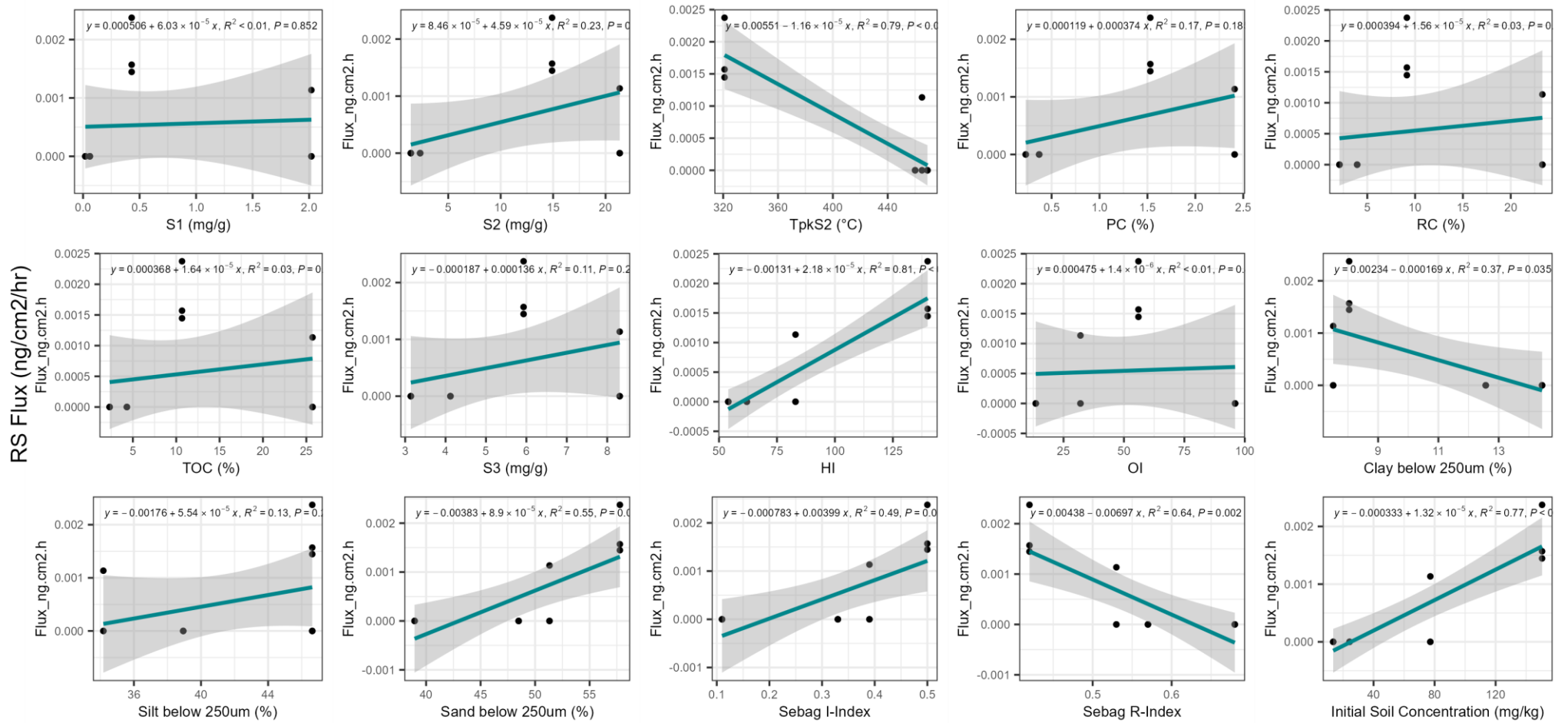
(e)



(g)



(h)



(k)

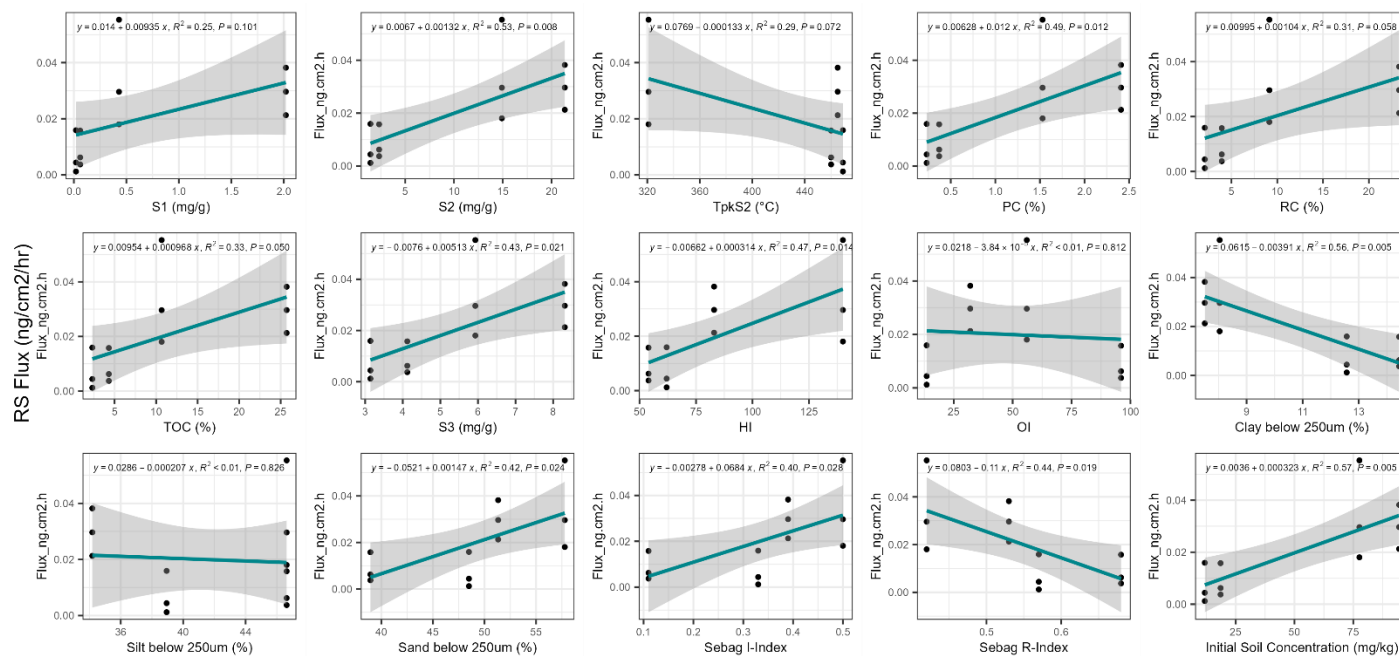


Figure S16. Linear regression on MGP samples excluding the highest concentrated soil sample E1.5 soil properties vs RS flux (triplicate dermal experiments results) at 24-h for each HMW PAH, (a)Fla, (b) Pyr, (c) BaA, (d) TPh, (e) Chry, (f) BbF, (g) BeP, (h) BaP, (i) BghiP, (j) BcFlu, and (k) C1-Fla/Pyr. PAHs correlation plots not displayed for PAHs not detected in the RS for the four MGP soils included: CCP, TPh, BkF, BjF, IcdP, BcFlu, Per, DahA, DaeP, DahP, DaiP, DalP, C2-Fla/Pyr, C3-Fla/Pyr, C1-BaA/Chry/TPh, C2-BaA/Chry/TPh, C3-BaA/Chry/TPh and C4-BaA/Chry/TPh.